TECHNISCHE UNIVERSITÄT MÜNCHEN

Wissenschaftszentrum Weihenstephan für Ernährung, Landnutzung und Umwelt

Lehrstuhl für Molekulare Ernährungsmedizin

Novel non-adrenergic, endocrine mediators of brown adipose tissue thermogenesis

Katharina Schnabl

Vollständiger Abdruck der von der Fakultät Wissenschaftszentrum Weihenstephan für Ernährung, Landnutzung und Umwelt der Technischen Universität München zur Erlangung des akademischen Grades eines

Doktors der Naturwissenschaften

genehmigten Dissertation.

Vorsitzender:	Prof. Dr. Harald Luksch
Prüfer der Dissertation:	1. Prof. Dr. Martin Klingenspor
	2. Prof. Dr. Hannelore Daniel
	3. Prof. Dr. Jakob Linseisen

Die Dissertation wurde am 01.07.2019 bei der Technischen Universität München eingereicht und durch die Fakultät Wissenschaftszentrum Weihenstephan für Ernährung und Umwelt am 28.01.2020 angenommen.

TABLE OF CONTENTS

ABBREVIATIONS

ACTH	adrenocorticotropic hormone
ANOVA	analysis of variance
ANP	atrial natriuretic peptide
AR	adrenergic receptor
ATGL	adipose triglyceride lipase
ATP	adenosine triphosphate
BAT	brown adipose tissue
BMR	basal metabolic rate
BSA	bovine serum albumin
BW	body weight
cAMP	cyclic adenosine monophosphate
CCK	cholecystokinin
CT	computed tomography
DIO	diet-induced obese
DMEM	Dulbecco's modified eagle's medium
ELISA	emzyme-linked immunosorbent assay
FBS	fetal bovine serum
FCCP	Carbonyl cyanide-p-trifluoromethoxyphenylhydrazon
FDG	fluorodeoxyglucose
FFA	free fatty acid
GLP1	glucagon-like peptide 1
GPCR	G-protein coupled receptor
Hb	hemoglobin
HbO_2	oxygenated hemoglobin
HBSS	Hank's buffered salt solution
HSL	hormone-sensitive lipase
i.p.	intraperitoneal
iBAT	interscapular brown adipose tissue
iWAT	inguinal white adipose tissue
gWAT	gonadal white adipose tissue
MAPK	mitogen-activated protein kinase
MC2R	melanocortin 2 receptor
MSOT	multi spectral optoacoustic tomography
NE	norepinephrine
NST	non-shivering thermogenesis
PET	positron emission tomography
PKA	protein kinase A
PLUC	Photinus luciferase
PYY	peptide YY
RIPA	radioimmunnoprecipitation assay buffer
RLUC	Renilla luciferase
SCTR	secretin receptor
SNS	sympathetic nervous system
SO_2	oxygen saturation
TBV	total blood volume
UCP1	uncoupling protein 1
WAT	white adipose tissue
WHO	world health organization

ABSTRACT

Brown adipose tissue (BAT) is a heater organ that is activated in the cold to defend body temperature. Non-shivering thermogenesis (NST) is facilitated by a protein exclusively expressed in the inner mitochondrial membrane of brown and brite adipocytes, uncoupling protein 1 (UCP1). Due to its ability to metabolize stored chemical energy and thereby effectively dissipate it, BAT is an enticing target to develop new therapies for common metabolic diseases such as obesity, diabetes and dyslipidemia. The aim of the present thesis was to identify and characterize novel activators of BAT-mediated NST.

The activation of UCP1 as a crucial event in triggering non-shivering thermogenesis has previously been attributed to a rise in free fatty acids alone. Thus, activating lipolysis is an essential step to induce brown fat thermogenesis. Besides the classical cAMP-PKA signaling cascades, additional sources of free fatty acids as well as receptor-independent pro-lipolytic effectors have to be considered. Nevertheless, initiation of the signaling cascade downstream of any G_s-protein coupled receptor seems to be a promising strategy to induce UCP1-dependent respiration. In addition to adrenergic receptors, murine brown adipocytes express a variety of other G_s-coupled receptors. The identification of 12 abundantly expressed G_s-coupled receptors and a subsequent screening approach for the respective ligands concerning their ability to recruit and activate UCP1, revealed adrenocorticotropic hormone as a potent non-adrenergic activator of brown adipocyte thermogenesis, initiating the canonical cAMP-PKA-lipolysis pathway via its receptor, melanocortin 2 receptor (MC2R). Besides the MC2R, the secretin receptor is highly expressed in BAT. Indeed, the gut hormone secretin, classically known to stimulate pancreatic water and bicarbonate secretion upon food intake, potently activated UCP1-dependent respiration in brown adipocytes and BAT thermogenesis *in vivo*. Furthermore, secretin reduced food intake in fasted mice depending on the presence of UCP1. In mice, endogenous secretin mediated a transient increase in BAT temperature associated with food intake in mice and neutralization of endogenous secretin led to acute overeating. Interferences in both secretin and intact BAT significantly changed meal patterns, while total daily energy intake remained unaltered. Thus, secretin-induced BAT activation regulates meal termination and satiation, rather than long-term energy balance and satiety. Assembled into a regulatory feedback system, secretin mediates a gut-BAT-brain axis to promote satiation through meal-associated thermogenesis. It is crucial that the discovery of BAT as a peripheral component of the regulation of food intake transforms any means of its activation into a two-track intervention targeting both components of the energy balance - energy expenditure and energy intake. Furthermore, first indications of the presence of this physiological mechanism in humans make it an even more attractive target for the treatment of obesity. Especially from the point of view that clear evidence of active BAT in humans has been reported by a number of milestone publications.

ZUSAMMENFASSUNG

Braunes Fettgewebe (BAT) ist ein Heizorgan, welches in Kälte zur Aufrechterhaltung der Körpertemperatur aktiviert wird. Zitterfreie Thermogenese wird durch ein Protein ermöglicht, welches ausschließlich in der inneren Mitochondrienmembran von braunen und beigen Adipozyten vorkommt – das Entkopplerprotein 1 (UCP1). Aufgrund seiner Fähigkeit, gespeicherte chemische Energie umzusetzen/ zu „verschwenden“, ist BAT ein attraktives Ziel, um neue Therapien für häufige Stoffwechselerkrankungen wie Fettleibigkeit, Diabetes und Dyslipidämien zu entwickeln. Das Ziel der vorliegenden Arbeit war es, neue Aktivatoren der durch braunes Fett vermittelten zitterfreien Thermogenese zu identifizieren und zu charakterisieren.

Die Aktivierung von UCP1 als entscheidendes Ereignis zum Anschalten der zitterfreien Thermogenese wird auf einen Anstieg der freien Fettsäuren zurückgeführt. Die Manipulation der Lipolyse ist daher ein entscheidender Schritt, um die Thermogenese des Braunfetts zu induzieren. Neben den klassischen cAMP-PKA-Signalkaskaden, sind zusätzliche Quellen für freie Fettsäuren sowie rezeptorunabhängige pro-lipolytische Effektoren zu berücksichtigen. Trotz allem scheint die Aktivierung von G_s-Protein-gekoppelten Rezeptoren und nachgeschalteter cAMP-PKA Signalkaskade eine vielversprechende Strategie zur Induktion der UCP1-abhängigen Atmung zu sein. Neben den adrenergen Rezeptoren exprimieren murine braune Adipozyten eine Vielzahl anderer G_s-gekoppelter Rezeptoren. Die Identifizierung von zwölf hoch exprimierten G_s-gekoppelten Rezeptoren und ein anschließender Screening-Ansatz für die jeweiligen Liganden hinsichtlich ihrer Fähigkeit, UCP1 zu rekrutieren und zu aktivieren, zeigte, dass das adrenokortikotrope Hormone ein potenter nicht-adrenerger Aktivator von braunen Adipozyten ist. Neben dem Melanocortin-2-Rezeptor ist der Sekretin-Rezeptor in BAT stark exprimiert. Tatsächlich aktivierte das Darmhormon Sekretin, welches klassischerweise dafür bekannt ist, die Wasser- und Bikarbonat-Sekretion der Bauchspeicheldrüse zu stimulieren, die UCP1-abhängige Atmung in braunen Adipozyten und die BAT-Thermogenese *in vivo*. Darüber hinaus reduzierte Sekretin die Nahrungsaufnahme in gefasteten Mäusen in Abhängigkeit von UCP1. Endogenes Sekretin vermittelte einen vorübergehenden, Nahrungsaufnahme-assoziierten Anstieg der BAT-Temperatur und die Neutralisierung von endogenem Sekretin führte zu einer akuten, übermäßigen Nahrungsaufnahme. Sowohl eine Manipulation des Sekretinspiegels als auch von braunem Fett veränderten das Fressverhalten/Mahlzeitenhäufigkeit der Mäuse signifikant, während die absolute tägliche Energiezufuhr unverändert blieb. Schlussfolgernd kann festgehalten werden, dass die Sekretin-induzierte BAT-Aktivierung die Beendigung einer Mahlzeit initiiert und somit Sättigung reguliert, jedoch keinen Einfluss auf die langfristige Energiebilanz hat. Das heißt, Sekretin ist der Mediator einer Darm-BAT-Hirnachse, die Sättigung durch die mit einer Mahlzeit assoziierten Thermogenese herbeiführt. Aktiviertes BAT

setzt also an beiden Seiten der Energiebilanz an. Es erhöht den Energieumsatz und reduziert die Energieaufnahme. Darüber hinaus, machen erste Hinweise auf das Vorhandensein dieses physiologischen Mechanismus beim Menschen, diesen zu einem noch attraktiveren Ziel in der Behandlung von Übergewicht. Vor allem unter dem Gesichtspunkt, dass eindeutige Beweise für aktives braunes Fettgewebe beim Menschen in einer Reihe von Meilenstein-Publikationen gezeigt wurden.

1 INTRODUCTION

We are about to experience a global epidemic of obesity, a major risk factor for the development of noncommunicable diseases such as diabetes mellitus, dyslipidemias, fatty liver, hypertension, and arteriosclerosis.

The global burden of obesity

Overweight and obesity are defined as abnormal and excessive accumulation of energy-rich triglycerides in white adipose tissues (WAT) caused by a chronic positive energy balance. Energy balance is the relation between energy intake and energy expenditure. If both parameters are in equilibrium, body weight is maintained. Positive energy balance is the result of energy intake being higher than energy expenditure and causes weight gain, while vice versa leads to weight loss. In 2016, 1.9 billion adults aged 18 and over were overweight, 650 million of whom were obese, almost tripling the prevalence of obesity since 1975 (WHO, 2018). Even more alarming are the numbers for children. 41 million children under the age of five were classified as overweight or obese in 2016. Although there is a genetic component, obesity and related noncommunicable diseases are largely preventable in most cases. Since energy balance is influenced by both energy intake and energy expenditure, regular physical activity and limited calorie intake seems to be the easiest way to combat obesity at an individual level. On this basis, the present PhD project was initiated to investigate non-adrenergic, endocrine effectors of brown adipocyte function that may trigger a negative energy balance.

The adipose organ – white, brite and brown

In mammals, there are two types of adipose tissue: white and brown adipose tissue (BAT). While WAT is the primary energy storage for excessive calories, brown adipose tissue is specialized for energy expenditure in form of heat production. In contrast to WAT brown fat is densely vascularized which ensures a sufficient supply of oxygen and metabolic substrates. In addition, it is densely innervated by the sympathetic nervous system. Brown adipocytes store triglycerides in multilocular lipid droplets and are rich in mitochondria equipped with a high respiratory capacity. Similarly to WAT, brown adipose tissue resides in different locations. Rodents, which are subject of brown fat research for more than 50 years, possess significant amounts of visceral and subcutaneous BAT in the mediastinic and perirenal region as well as the cervical, axillary, subscapular and interscapular region, respectively (Cinti, 2005). The interscapular depot represents the largest among all murine depots. Drainage of this tissue by a large blood vessel, the Sulzer's vein, allows the transfer of locally produced heat to the blood circulation and thus ensures heat distribution throughout the body (Rauch and Hayward, 1969). From this point of view, it is interesting that the anatomical arrangement of all BAT depots resembles a thoracic heating cuff under the fur (Heldmaier and Neuweiler, 2004).

In endothermic animals, body temperature is rather constant independent of environmental conditions by means of physiological mechanisms that provide heat production or changes in heat loss. To maintain body temperature in the cold, adaptive heat production is necessary which is composed of shivering and non-shivering thermogenesis (NST). Shivering is an involuntary process, characterized by repeated contractions of skeletal muscle driven by hydrolysis of adenosine triphosphate (ATP) without physical work. The energy turn over leads to heat dissipation. Shivering occurs when NST, which is mediated by BAT, is not sufficient to fully compensate heat loss (Cannon and Nedergaard, 2004). In small mammals, the activation of NST is essential to survive.

The cold-induced activation of BAT is mediated by the sympathetic nervous system (SNS) (Wirsen C, 1964; Bargmann W, 1968). In response to cold exposure, the SNS neurotransmitter norepinephrine is released from the SNS and binds to adrenergic receptors (AR) in brown adipocytes. Of note, physiological range of circulating catecholamine levels in the blood are insufficient to activate brown fat thermogenesis (Girardier and Seydoux, 1986). Mature adipocytes express a large variety of α- and β-ARs, which belong to the family of G-protein coupled receptors (GPCRs) coupling to G_s, G_i and G_q-dependent intracellular signaling modules. Although NE has a greater affinity to α- than to β-ARs, the receptor abundance largely determines which signaling modules are activated. In rodent adipocytes, the G_s-coupled β_3-AR is predominantly expressed. Upon ligand binding, the cAMP-dependent lipolytic signaling cascade is initiated. In detail, adenylyl cyclase is activated leading to a rise in cAMP levels, which in turns activates protein kinase A (PKA). Activated PKA phosphorylates perilipin (Chaudhry and Granneman, 1999) and hormone-sensitive lipase (HSL) (Shih and Taberner, 1995) leading together with PKA-independent pathways involving

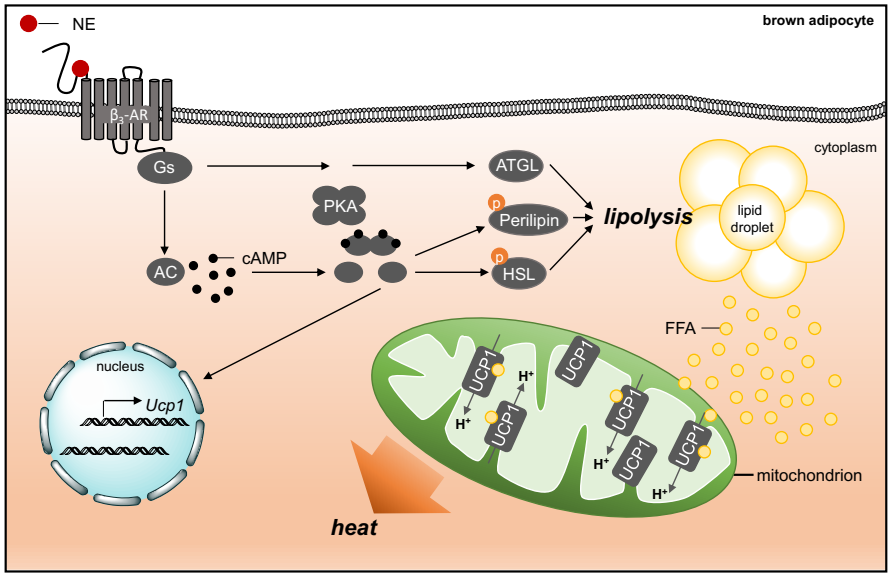

Figure 1:Cold-induced activation of brown adipocytes.
Binding of norepinephrine (NE) to the G_s-protein coupled β3-adrenergic receptor leads to the activation of adenyl cyclase (AC) and a rise in cyclic adenosine monophosphate (cAMP) levels, which in turns acitvates protein kinase A (PKA). Activated PKA phosphorylates perilipin and hormone-sensitive lipase (HSL) leading to lipolysis and the release of free fatty acids (FFA) from lipid droplets. As fuel and as activators of the uncoupling protein 1 (UCP1), these fatty acids are the final effectors inducing non-shivering thermogenesis. Additionally, the recruitment of thermogenic capacity is initiated by norepinephrine (modified from Braun et al., 2018).

adipose triglyceride lipase (ATGL) to lipolysis (Robidoux et al., 2006; Zimmermann et al., 2004). Free fatty acids serve both as fuel for mitochondrial β-oxidation and as activators of the uncoupling protein1 (UCP1) within the inner mitochondrial membrane. UCP1 is a unique feature of brown and brite adipocytes and its activation leads to the dissipation of the chemical energy of nutrients by uncoupling ATP synthesis from oxygen consumption. Thereby, electron transport is stimulated and respiration is enhanced (**Fig. 1**). Heat is generated from the combustion of available substrates and is distributed in the body through circulation (Klingenspor, 2003).

In addition to the activation of UCP1, it should be noted that cold exposure also induces the thermogenic gene expression program and thus recruits thermogenic capacity in brown fat (Cannon and Nedergaard, 2004). Moreover, brown-like adipocytes also known as inducible brown fat cells, beige (Ishibashi and Seale, 2010) or brite (brown-in-white) (Petrovic et al., 2010) adipocytes can be found scattered in white adipose tissue (Li et al., 2014a; Young et al., 1984). These UCP1-expressing brite adipocytes appear in WAT, in response to cold exposure, adrenergic stimulation, peroxisome proliferator-activated receptor gamma (PPARγ) agonist treatment or during postnatal development. This process is termed browning (Cousin et al., 1992; Galmozzi et al., 2014; Guerra et al., 1998; Himms-Hagen et al., 2000; Lasar et al., 2013; Maurer et al., 2015; Young et al., 1984) (**Fig. 1**).

Brown adipose tissue in humans

As already mentioned, almost all views on BAT thermogenesis come from studies with small rodents such as mice, rats and hamsters. In humans, newborns have significant amounts of BAT which support the regulation of body temperature during neonatal life, probably in the same way as for small rodents. Brown adipose tissue was thought to rapidly disappear postpartum and consequentially to play a negligible role in adult humans (Cinti, 2006; Del Mar Gonzalez-Barroso et al., 2000; Himms-Hagen, 2001). Thus, for a long time the occurrence of active BAT was believed to be restricted to these small mammals, hibernators and human newborns. The detection of metabolically active BAT in adult humans around ten years ago reopened the field of brown fat research. In clinical studies with fluorodeoxyglucose (FDG) positron emission tomography (PET) a symmetrical FDG uptake in the shoulder and thoracic spine regions was detected. Simultaneous PET and X-ray computed tomography (CT) examinations identified the site of FDG uptake as adipose tissue rather than musculature (Hany et al., 2002). This FDG uptake was increased at lower environmental temperatures (Christensen et al., 2006; Cohade et al., 2003; Garcia et al., 2006) and was reduced by pretreatment with adrenergic blockers (Parysow et al., 2007; Soderlund et al., 2007). These findings suggested metabolically active BAT (Nedergaard et al., 2007) and initiated further focused human studies either by FDG PET scans on a small number of healthy adult volunteers (Saito et al., 2009; van Marken Lichtenbelt et al., 2009; Virtanen et al., 2009) or by

retrospective analyses of a large number of clinical scans which have been performed on patients for various diagnostic reasons (Au-Yong et al., 2009; Cypess et al., 2009; Gerngross et al., 2017). All these studies detected substantial depots of brown adipose tissue in adult humans mainly observed in the supraclavicular, suprarenal, paravertebral and neck region (**Fig. 2**). Importantly, cold-induced BAT activity is strongly reduced in obese patients (Saito et al., 2009) as well as with age (Cypess et al., 2009) and can be recovered by cold acclimation (van Marken Lichtenbelt et al., 2009). Acute mild cold exposure led to a 12-fold increase in glucose uptake, an increase in energy expenditure and improved insulin sensitivity (Chondronikola et al., 2014), while chronic mild cold acclimation resulted in a significant recruitment of BAT, with a consequent elevation of cold-induced BAT thermogenesis and a decrease in body fat which was proportional to BAT activity (van der Lans et al., 2013; Yoneshiro et al., 2013).

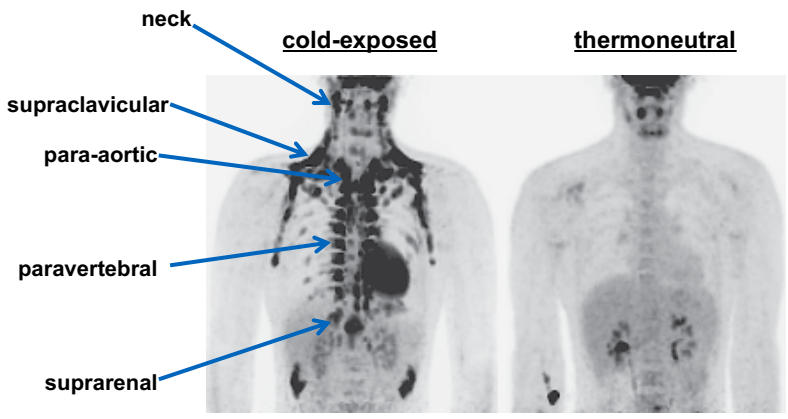

Figure 2: Brown adipose tissue in humans.
In humans, brown adipose tissue depots are found in the neck, supraclavicular, para-aortic, paravertebral and suprarenal region. In comparison of FDG-PET scans taken after cold exposure and in thermoneutral environment the localization of active brown adipose tissue is evident (depicted and modified from van Marken Lichtenbelt et al., 2009).

The overall conclusion of these studies is that BAT is present and can be activated in most adult humans and that total BAT activity is inversely associated with adiposity and indexes of the metabolic syndrome suggesting that increasing BAT mass and activity may be a target for pharmacologic and nutritional interventions that modulate energy expenditure to treat obesity (Celi, 2009). Obviously, the question arises whether energy expenditure due to metabolic activity of brown adipose tissue significantly influences the regulation of energy balance in humans. In principle, total brown fat mass in humans which is currently estimated to account for more than 300 g, could significantly contribute to a negative energy balance, if permanently active (Gerngross et al., 2017). For therapeutic success, it is of enormous importance to take into account that UCP1 is constitutively inactive. Indeed, recruiting thermogenic capacity is required, but not sufficient in the attempt to reduce weight by increasing energy expenditure. That means, to achieve an increase in energy expenditure mediated by BAT, the activation of UCP1 is inevitable.

However, our lifestyle in a thermoneutral environment due to unrestricted access to heaters and warm clothing, generally excludes cold-induced activation of brown fat. Freezing is unpleasant and would not be tolerated by the majority of people, although it is a natural and

non-invasive method to activate brown fat. Thus, there is need for a feasible pharmacological recruitment and activation of BAT.

Dangers and risks of pharmacological agonists of the β-adrenergic receptors

Since cold-induced activation of BAT is mediated by norepinephrine from the sympathetic nervous system, sympathomimetic drugs were engaged in the first attempt for pharmacological BAT activation. Unfortunately, nonspecific sympathomimetic drugs cannot stimulate human BAT without marked effects on the cardiovascular system (Carey et al., 2013; Cypess et al., 2012; Vosselman et al., 2012). Therefore, selective agonists of the relatively fat-specific β_3-AR have been developed, but had only little success in humans (Arch, 2008; Larsen et al., 2002; Redman et al., 2007; Weyer et al., 1998). In humans, the β_3-AR is expressed on the surface of brown and white adipocytes, urinary bladder, and potential other tissues (Cypess et al., 2013; Ursino et al., 2009; Virtanen et al., 2009). The β_3-AR agonist, mirabegron was approved for treatment of overactive bladder. In addition to having satisfactory bioavailability (Malik et al., 2012), mirabegron has a higher *in vitro* binding affinity for the human β_3-AR compared to other members of the class of β_3-AR agonists (Takasu et al., 2007). Indeed, 200 mg of oral mirabegron was effective in acutely stimulating human BAT thermogenesis and in increasing resting metabolic rate (Cypess et al., 2015). However, this activation was associated with tachycardia and elevated systolic blood pressure. Thus, the application of sympathomimetic drugs as BAT activators is problematic due to unwanted detrimental cardiovascular effects. Conclusively, the identification of druggable non-adrenergic regulators of BAT are an essential step towards the modulation of the heating organ as a regulator of energy expenditure and body fat in humans.

Non-adrenergic regulators of brown adipose tissue

In addition to the adrenergic induction of thermogenesis and recruitment of thermogenic capacity, a number of alternative factors have been identified that are capable of activating BAT. Among these, adenosine, atrial natriuretic peptide (ANP), and bile acids can be named as example. High expression levels of their respective target receptors in brown adipocytes support their putative role in BAT regulation.

In detail, adenosine, a purine nucleoside, increases NE-induced lipolysis and expression of thermogenic marker genes in murine and humane brown adipocytes via the GPCR ADORA2A. Interestingly, ADORA2A-ablated newborn mice exhibit reduced BAT thermogenesis, which confirms a physiological role of adenosine in BAT function (Gnad et al., 2014).

Induction of lipolysis and thermogenesis by ANP in brown adipocytes is mediated by a pathway involving intracellular cyclic guanosine monophosphate-dependent protein kinase (cGMP) and p38 mitogen-activated protein kinase (MAPK) (Bordicchia et al., 2012). Of note, the lipolytic action is detected only in primate adipocytes, but not in those of rodents, rabbits and dogs

(Sengenes et al., 2000). In rodents, a relatively high receptor-mediated clearance suppresses ANP activity (Sengenes et al., 2002).

Upon binding of bile acids to the GPCR TGR5 in brown adipocytes thyroid hormone signaling is stimulated which leads to an increase in thermogenic capacity. Bile acid supplementation elevates the expression of the thermogenic machinery accompanied by an increased energy expenditure and resistance to diet-induced obesity in mice (Watanabe et al., 2006). TGR5-specific bile acids increase lipolysis resulting in the release of free fatty acids that not only fuels β-oxidation, but also promotes UCP1-dependent thermogenesis (Velazquez-Villegas et al., 2018).

This exemplary excerpt of non-adrenergic modulators of BAT illustrates how versatile thermogenic activation can be in terms of signaling. It opens a broad field of starting points in the search of druggable activators of brown fat. However, all of these compounds share a lipolytic property. Lipolysis plays a crucial role and is an essential requirement for UCP1 activation. Indeed, pharmacological inhibition of ATGL and HSL, the two lipases that catalyze the first two steps in the hydrolysis of triglycerides, completely diminishes adrenergic stimulation of UCP1-dependent respiration (Li et al., 2014b). As a working hypothesis, any stimulus affecting the balance of lipolysis and re-esterification potentially activates or attenuates thermogenesis in brown and brite adipocytes (Li et al., 2017).

G-protein coupled receptors as targets for brown fat activation

One approach to manipulate this balance would be the targeted activation of G-protein coupled receptors in brown adipocytes. In addition to β-adrenergic receptors, mature brown adipocytes express a broad set of around 230 other G-protein-coupled receptors (Klepac et al., 2016). GPCR's are a large family of seven transmembrane proteins (Kobilka, 2011; Lefkowitz, 2007) that regulate important biological processes in different tissues, including adipose tissues (Latek et al., 2012; Wettschureck and Offermanns, 2005). Their enormously important role in disease and therapy is illustrated by the fact that approximately 30% of all approved drugs target GPCRs (Hauser et al., 2017; Santos et al., 2017). The heterotrimeric guanine nucleotide-binding protein (G-protein) which is coupled to these receptors consists of α-, β- and γ-subunits. Ligand binding and the associated activation of GPCRs leads to the dissociation of Gα from the Gβγ-dimer, which enables the binding and regulation of signal transducers. The G-protein coupling party determines the downstream signaling of GPCRs (Neves et al., 2002). There exist four main subclasses of Gα: G_s, G_i, G_q and $G_{12/13}$. The activation of G_s and G_i leads to the stimulation or inhibition of cyclic adenosine monophosphate (cAMP), respectively, while G_q activates phospholipase C which consequently leads to a rise in inositoltriphosphate. $G_{12/13}$ activates the small GTPase Rho, a pathway known to be modulated by proteins of the G_q family (Buhl et al., 1995; Wang et al., 2013). Due to the cAMP-PKA activating properties, the analysis of BAT GPCRs focused mainly on G_s-coupled

receptors, like the β-ARs (Cannon and Nedergaard, 2004) and adenosine receptors (Gnad et al., 2014) as they have the ability to stimulate lipolysis and activate UCP1-dependent thermogenesis. Taken together, stimulation of G_s-coupled receptors triggers the same canonical adenylyl cyclase – cAMP – PKA pathway like norepinephrine from the sympathetic nervous system in cold-induced BAT thermogenesis. As this pathway stimulates lipolysis which is an essential prerequisite for the activation of UCP1, and therefore induces non-shivering thermogenesis (Klingenspor et al., 2017), the identification of highly expressed G_sPCR in brown adipocytes and a subsequent analysis of the respective ligands for their potential to activate and recruit thermogenic capacity, constitutes a promising approach in the finding of non-adrenergic activators of brown adipose tissue, which was the major objective of this present thesis.

Meal-associated brown fat thermogenesis

It has to be mentioned that besides cold-induced thermogenesis BAT also contributes to meal-associated thermogenesis (Glick et al., 1981; Saito and Yoneshiro, 2013; U Din et al., 2018; Vosselman et al., 2013) and long-term diet-induced thermogenesis (Rothwell and Stock, 1979). In this context, brown fat has been linked to the hypothesis of thermoregulatory feeding which says that heat production in response to feeding may serve as a feedback signal for satiety which is involved in the control of meal initiation and termination (Brobeck, 1948; Himms-Hagen, 1995). Thus, aside from the mere capacity to burn excess glucose and fatty acids, BAT has also been suggested to play a role in the control of food intake (Glick, 1982; Himms-Hagen, 1995). In rats, BAT temperature increases about 15 min prior to meal initiation, and drops upon meal termination (Blessing et al., 2013). An increased periprandial tone of the SNS is thought to activate BAT thermogenesis by the release of NE from the sympathetic nerves in BAT. In fact, acute pharmacological activation of BAT in fasted mice with a β_3-AR agonist reduces cumulative food intake during refeeding (Grujic et al., 1997; Susulic et al., 1995). Pertaining to nutritional neurophysiology, all macronutrients elicit meal-associated thermogenesis, but only carbohydrates activate the SNS (Glick, 1982; Himms-Hagen, 1995; Welle et al., 1981). Therefore, although the SNS is likely to be involved, other so far unknown triggers may contribute. As the release of gastrointestinal peptides is one of the first physiological responses to eating, periprandially secreted gut hormones may be potential evokers of meal-associated BAT thermogenesis. All along the gastrointestinal tract, specialized endocrine cells produce peptide hormones, making the gut one of the largest endocrine organs in the body (Coate et al., 2014). During a meal, secretion of gut hormones initiates complex neuroendocrine responses encoding information on the nutritional status (Cummings and Overduin, 2007). Gut hormones not only act locally to orchestrate motility, secretion, digestion and nutrient absorption, but also promote the central perception of satiation via central neuronal circuits in the brain controlling food intake and limiting meal size (Chaudhri et al., 2006). Most prominently, glucagon-like peptide (GLP-1), cholecystokinin

(CCK), oxyntomodulin, peptide YY (PYY), and secretin promote satiation and inhibit food intake as demonstrated in animal experiments, whereas ghrelin promotes hunger (Chaudhri et al., 2006; Cheng et al., 2011). Indeed, some of these gut hormones activate BAT through their central effects on efferent SNS tone, such as CCK and GLP-1 (Beiroa et al., 2014; Blouet and Schwartz, 2012). Notably, some of these gut hormones also modulate fat metabolism in white adipocytes. For example, PYY inhibits lipolysis via Y2R coupling to G_i signaling (Valet et al., 1990), and secretin stimulates lipolysis through the secretin receptor (SCTR) coupling to G_s in white adipocytes (Butcher and Carlson, 1970; Miegueu et al., 2013; Rudman and Del Rio, 1969; Sekar and Chow, 2014). As already mentioned, lipolysis is an essential prerequisite of BAT activation. Thus, the identification and investigation of gut hormones that directly activate meal-associated thermogenesis in BAT and control satiation seems reasonable to reveal functional significance of meal-associated BAT thermogenesis as well as the molecular mediators. With regard to the pharmacological activation of BAT a better understanding of its contribution to meal-associated thermogenesis is fundamental, since the regulation of energy intake together with an increase of energy expenditure makes it an even more attractive target to treat obesity.

Aims of the thesis

Due to its capacity to increase metabolic rate, BAT is a promising target for the prevention and therapy of overweight and obesity. Since adrenergic effectors were not capable to induce BAT activation without severe unwanted effects on the cardiovascular system, the primary aim of this study was the identification of novel non-adrenergic activator of brown fat. Therefore, the following research questions and goals were addressed:

(1) **CHAPTER I – Discussion of adrenergic and non-adrenergic mechanisms controlling lipolysis and thermogenesis in adipocytes and a comprehensive overview of pro- and anti-lipolytic mediators**

In contrast to sympathomimetics, non-adrenergic activators could provide the possibility to regulate BAT function bypassing severe cardiovascular side effects. The aim was to assemble a collection of non-adrenergic biomolecules that have been identified to effect lipolysis in white and brown adipocytes as any pro-lipolytic stimulus potentially activates thermogenesis in these cells.

(2) CHAPTER II – *In vitro* screening approach to identify novel non-adrenergic activators and recruiters of brown adipocyte thermogenic capacity

Activation of G_s-protein coupled receptors leads to the stimulation of the second messenger cAMP and the initiation of the subsequent PKA-dependent signaling, which is common to the canonical adrenergic activation of BAT. Therefore, the aim was to investigate a selection of non-adrenergic G_s-coupled GPCRs in the light of their ability to activate and recruit UCP1-mediated thermogenesis in brown adipocytes.

(3) **CHAPTER III – Deciphering the contribution of BAT to meal-associated thermogenesis as well as identification of its molecular mediator**

Cold-induced BAT thermogenesis is well established, while the role of BAT for meal-associated thermogenesis remains elusive. Gut hormones released during eating are potential endocrine mediators of BAT thermogenesis. Therefore, the aim was to investigate the role of gut hormones in meal-associated BAT thermogenesis and food intake.

2 METHODS[1]

2.1 ANIMALS

Unless stated otherwise, all animal breeding and experimentations were conducted within the SPF facility of the Technical University of Munich registered at the local authorities according to §11 of the German Animal Welfare Act (AZ32-568, 01/22/2015). Mice were group-housed in individual ventilated cages at 23°C with *ad libitum* access to chow food and water prior to the experiments. Housing of mice at thermoneutrality (30°C) during experiments was conducted in constant climate cabinets (HPP750life, Memmert) at 55-65% relative humidity and 12/12 hours light/dark cycle (5:00 am/pm CET). Mouse husbandry inside climate cabinets was conducted in an open cage system using type II cages (for 1-3 mice, 370 cm²). All animal experimentation was conducted in accordance with the German animal welfare law.

Male 129S6/SvEvTac, 129S1/SvEvTac mice (UCP1$^{-/-}$ mice and wild-type littermates UCP1$^{+/+}$) and heterozygous C57BL/6N *Ucp1* dual-reporter gene mice (C57BL/6NTac-Ucp1tm3588 $^{(Luciferase\text{-}T2A\text{-}iRFP\text{-}T2A\text{-}Ucp1)Arte}$), aged 5–6 weeks, were used to prepare primary cultures of brown and white adipocytes. The latter simultaneously express firefly luciferase and near-infrared fluorescent protein 713 (iRFP713). The *Luciferase-T2A-iRFP713-T2A* sequence was introduced into the 5′-untranslated region of the endogenous *Ucp1* gene (Wang et al., 2019).

Male C57BL/6J, male 129S6/SvEvTac, and male 129S1/SvEvTac mice (UCP1$^{-/-}$ mice and wild-type littermates UCP1$^{+/+}$) were used for the in vivo experiments (approval number: 55.2-1-54-2532-34-2016).

Athymic female Nude-Foxn1^{nu} mice, aged 13 weeks at the beginning of MSOT experiments, (approval number: 55.2-1-54-2532-123-2013) were obtained from Envigo and kept at 24±1°C with ad libitum access to food and water at the Helmholtz Zentrum München.

Diet-induced obese (DIO) male C57BL/6N mice were obtained from Taconic Biosciences (Cambridge City, IN) at the age of 10 to 31 weeks and kept at Eli Lilly on a calorie rich diet (TD95217; Teklad, Madison, WI).

2.2 *IN VITRO* ANALYSES OF THE RECRUITMENT AND ACTIVATION OF THERMOGENIC CAPACITY

2.2.1 Primary cell culture

Primary cell isolation

The interscapular brown adipose tissue (iBAT) or the inguinal white adipose tissue (iWAT) of four to six weeks old mice was dissected and placed into prewarmed phosphate buffered saline

[1] Detailed resource table in appendix 6.3

(PBS) supplemented with Gentamycin and Penicillin/Streptomycin (40 µg/ml). To improve cell yield, fat depots from 2-3 mice were pooled. The tissues were minced using surgical scissors and digested in collagenase-containing isolation medium (Hank's Buffered Salt Solution (HBSS) containing 1 mg/ml collagenase, 3.5 % Bovine Serum Albumin (BSA) and 0.55 mM glucose) for 45 min at 37°C in an orbital shaker incubator at 120 rpm with additional 1-min-intervals at 160 rpm every 10 min to improve digestion yield. Subsequently, the cell suspension was filtered through a sterilized 250 µm pore-size nylon mesh and centrifuged at 250 *g* at room temperature for 5 min to separate stromal vascular fraction from mature adipocytes. To complete the separation of the stromal cells from the floating mature adipocytes, tubes were shaken vigorously to thoroughly disrupt the floating fraction. After another centrifugation at 250 *g* for 5 min the supernatant with the mature adipocytes was discarded without disturbing the pellet. The SVF pellet was re-suspended in 7 ml washing buffer (HBSS containing 3 % BSA) and again centrifuged at 500 *g* for 5 min. After removal of the supernatant, the pellet was re-suspended in 1 ml pre-warmed culture medium w/Amphotericin B (see below), passed through a 40 µm cell strainer to obtain single cell suspensions, diluted in an appropriate volume of culture medium and seeded into either 12-well culture plates or XF96 V3-PS cell culture microplates.

Primary cell cultivation

The day after seeding, culture medium was removed and cells were washed with pre-warmed PBS to remove dead cells and cell debris. Attached cells were cultured with culture medium (high-glucose DMEM containing 20 % fetal bovine serum (FBS) and antibiotics (Gentamycin and Penicillin/Streptomycin, each 40 µg/ml)) until confluence with medium change every second day. At the stage of confluence, differentiation was initiated with induction medium containing 10 % FBS, 40 µg/ml Gentamycin and Penicillin/Streptomycin, 500 µM isobutylmethylxanthine, 125 µM indomethacin, 1 µM dexamethasone, 850 nM insulin and 1 nM triiodothyronine (T3) for 48 hours. After two days of induction, cells were maintained in differentiation medium (10 % FBS, 40 µg/ml Gentamycin and Penicillin/Streptomycin, 850 nM insulin and 1 nM T3). Measurements were conducted after seven days of differentiation when cells were fully differentiated.

2.2.2 Microplate-based respirometry for the assessment of UCP1 activation

Oxygen consumption is the key-readout for UCP1 activity. Thus, oxygen consumption of fully differentiated primary brown adipocytes was measured using microplate-based respirometry (*XF96* Extracellular Flux Analyzer, Seahorse Bioscience) as described previously (Li et al., 2014b). Based on a 96 well microplate-cartridge system, this technique enables the measurement of oxygen consumption of adherent cells via fluorescent sensors.

Sensor cartridges were hydrated overnight with 200 µl of *XF96* Calibrant buffer at 37°C in a non-CO2 incubator. At day 7 of differentiation, cells were washed with pre-warmed, unbuffered assay medium (DMEM basal medium supplemented with 25 mM glucose, 2 mM sodium pyruvate, 31 mM NaCl, 2 mM GlutaMax and 15 mg/l phenol red, pH 7.4). Next, medium was replaced with fresh assay medium containing 1% essentially fatty acid free BSA and cells were incubated at 37°C in the non-CO2 incubator for 1 h. Meanwhile, the drug injection ports of the sensor cartridges were loaded with assay reagents at 10X concentrations in basal assay medium (no BSA). Measurements were performed in 8 technical replicates. First, basal adipocyte respiration was measured in untreated cells. Next, ATP-Synthase was blocked by addition of oligomycin (5 µM) in order to determine basal leak respiration. Subsequently, effector was added to investigate UCP1-dependent uncoupled respiration. Isoproterenol, a non-selective β-adrenergic receptor agonist was used as a positive control. By the addition of FCCP (1 µM), maximal respiratory capacity was assessed. Finally, mitochondrial respiration was blocked by antimycin A (5 µM) and the residual oxygen consumption was considered as non-mitochondrial respiration and subtracted from all other values (**Fig. 3**)[2]. Oxygen consumption rates were calculated by plotting oxygen concentration (nmoles O2) versus time (min), using the original fixed algorithm of the *XF* Software. Stimulated respiration was calculated as fold increase over basal leak respiration (mean UCP1-dependent uncoupled effector-mediated respiration/ minimal basal leak respiration).

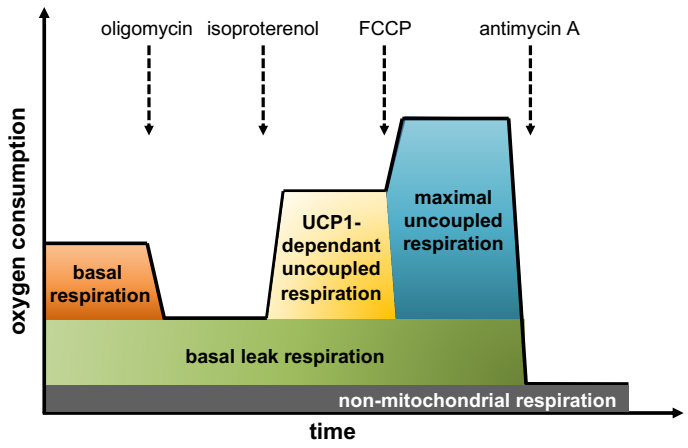

Figure 3: Bioenergetic profile of brown adipocytes including basal, basal leak, UCP1-dependent uncoupled and maximal uncoupled respiration, as well as non-mitochondrial respiration as background control.

For some experiments, cells were pretreated for 1 h with 50 µM H89 (protein kinase A inhibitor), 1-100 µM propranolol (β-adrenergic receptor antagonist), 100 nM and 750 nM GPS1573 (MC2R antagonist), 40 µM Atglistatin (ATGL inhibitor) and 40 µM Hi76-0079 (HSL inhibitor) 1 h prior to the measurement. Furthermore, primary brown adipocytes were reverse transfected with small interfering RNAs (siRNAs) targeting *SctR* and non-targeting control siRNA as described previously (Li et al., 2017).

[2] Entire protocol in appendix 6.4

2.2.3 Cytosolic cAMP quantification

Changes in cytosolic cyclic adenosine monophosphate (cAMP) levels in response to agonistic stimulation of G-protein coupled receptors (GPCRs) were analyzed using the commercially available kit system cAMP-Glo Assay (Promega). Increasing cAMP levels stimulate enzyme activity of protein kinase A (PKA), which subsequently catalyzes ATP-dependent phosphorylation of its substrate. Decreased availability of ATP can finally be monitored as reduced bioluminescent light production in a coupled photinus luciferase (PLUC) reaction. PKA enzyme, PKA substrate, ATP, luciferase and its substrate luciferin are thereby provided by the kit system.

The assay was performed with differentiated primary brown adipocytes in a 96-well format. Cells were stimulated for 30 min at 37°C with their respective effector diluted in cAMP induction medium (PBS) containing the broad-range phosphodiesterase inhibitors IBMX (500 µM, Sigma-Aldrich) and RO 20-1724 (100 µM, Sigma-Aldrich) to avoid rapid cAMP hydrolysis. Subsequently, the treated cells were lysed wit 20 µl/well of cAMP-Glo™ Lysis Buffer for 15 min to release cytosolic cAMP for detection. PKA enzyme and substrate were added within the cAMP-Glo™ Detection Solution (40 µl/well) and the cells were incubated for 20 min to enable ATP-dependent substrate phosphorylation by PKA. Thereafter, luciferase and its substrate luciferin were provided in the prepared Kinase-Glo™ Reagent (80 µl/well). After an incubation time of 10 min, the reaction mix was transferred to a glass tube, and bioluminescence was measured in a tube luminometer (delay time: 10 s, measurement time: 10 s; Single Tube Luminometer, Titertek-Berthold GmbH). In the given assay, increasing effector-induced cAMP levels were detected as decreasing luminescence values. Delta photinus luciferase light units were calculated by subtracting the PLUC value of each treated sample form the PLUC value of an untreated control sample, to allow more comprehensive date presentation. The measured luminescence values were normalized to protein content per well.

2.2.4 Luciferase reporter assay for UCP1 expression

After overnight stimulation of primary brown adipocytes of transgenic mice expressing firefly luciferase (*Pluc*) under the control of the *Ucp1* promotor, luciferase activity was assayed using a commercial kit system (Luciferase Assay System Freezer Pack E4030, Promega GmbH). Primary cells were lysed in 1x reporter lysis buffer by shaking for 20 min at room temperature. 10 µl lysate was mixed with 50 µl luciferase assay substrate solution, and the mixture was measured by FB12 in a luminometer (Single Tube Luminometer, Titertek-Berthold GmbH). Bioluminescence readouts were normalized to total protein content.

2.2.5 Gene expression analysis

RNA isolation

Ribonucleic acid (RNA) isolation was performed with a commercial kit (SV Total RNA Isolation System, Promega), according to the manufacturer's instructions with some modifications. Deep-frozen tissue samples (inguinal white adipose tissue (iWAT), gonadal WAT (gWAT) and interscapular brown adipose tissue (iBAT)) were homogenized in 1 ml TRIsure (Bioline) using a dispersing instrument (Ultra-Turrax D-1, Miccra GmbH). For cells cultured in 12-well plates 400 µl/well of TRIsure were used. Lysates were further mixed with 200 µl (12-well: 80 µl) of Chloroform (TRIsure:Chloroform; 5:1), vortexed and incubated at room temperature (RT) for 2-3 min followed by a centrifugation step at 12000 *g* at 4°C for 15 min to achieve phase separation. RNA remains exclusively in the colorless upper aqueous phase, whereas DNA and proteins are sequestered into the interphase and green-colored phenol-chloroform organic phase. The upper, clear phase was added to 500 µl EtOH (75% in DEPC treated water) (12-well: 200 µl) and mixed well. Samples were transferred to spin columns of the RNA isolation kit and processed referring to the manufacturer's protocol. After attaching RNA to the columns, degradation of genomic DNA by DNase and washing with EtOH containing buffer, RNA was eluted in 50 µl nuclease-free water. Following isolation, RNA concentration was determined spectrophotometrically using the InfiniteM200 NanoQuant (Tecan). Eluted RNA was stored at -80°C.

cDNA synthesis

RNA was reverse transcribed to complementary deoxyribonucleic acid (cDNA) by viral enzyme reverse transcriptase, using commercial QuantiTect® Reverse Transcription kit (Qiagen, Germany) according to the manufacturer's protocol. 500 ng template RNA were used for cDNA synthesis in a final reaction volume of 10 µl containing poly deoxythymidine oligonucleotide, random hexamer primers and reverse transcriptase (primer annealing: 25°C, 10 min; reverse transcription: 42°C, 15 min; inactivation: 85°C, 5 min; 4°C hold). cDNA was stored at -20°C.

Quantitative polymerase chain reaction (qPCR)

Measurement of expression of genes of interest was performed by quantitative real-time PCR. This method uses a high-sensitive optical detection technology. Briefly, SybrGreen intercalates into double-stranded DNA (dsDNA), leading to a photometrically detectable fluorescent signal. With ongoing amplification of DNA templates during every reaction cycle, the fluorometric signal increases until it exceeds background fluorescence (=cycle threshold, Ct-value). The Ct-value gives information about the relative amount of target template when compared to a standard curve. For the generation of the standard curve 2 µl of each sample were pooled and serial diluted 2^n in eight steps. qPCR was performed in 384-well plates (4titude) using 1 µl of cDNA (1:10) in a 12.5 µl reaction containing 6.25 µl of 2x SensiMix SYBR Master Mix No-ROX

(Bioline) 0.3125 µl of 10 µM forward and reverse primers, and 5.19 µl nuclease-free water. Thermal cycling and fluorescence detection were performed using Lightcycler 480 II (Roche). Reactions for cDNA samples were performed in triplicates, standard reactions were performed in duplicates. Cycling parameters were as follows: 95°C for 6 min, 45 cycles of 97°C for 10 sec, 52°C for 15 sec and 72°C for 20 sec. After cycling, a melting curve analysis was performed to verify that a single product was generated in each reaction. To correct for inter-individual differences, the expression of each gene was normalized to the abundance of a housekeeping gene (*general transcription factor 2b, Gtf2b*).

2.2.6 Immunoblot analysis

To analyze protein expression a sodium dodecyl sulfate polyacrylamide gel electrophoresis (SDS-PAGE) is used to separate proteins in an electric field according to their size. Following, the proteins are transferred from the gel to a membrane. The specific primary antibody detects the protein of interest on the membrane, whereas the fluorescently-labeled secondary antibody detects the species of the primary antibody.

Protein extraction

Frozen cells were lysed in Radioimmunoprecipitation assay (RIPA) buffer (150 mM Nacl, 50 mM Tris-HCl, 1 mM EDTA, 1% NP-40, 0.25% NA-deoxycholat). Cell lysis was achieved by shaking of the cells at 4°C for 15 min. Solubilized proteins were separated from cell nuclei and cellular debris by centrifugation at 14,000 *g* at 4°C for 15 min. The supernatant was collected and protein concentration was determined with the bicinchoninic acid method in a 96-well format using a commercial microplate kit (Pierce™ BCA Protein Assay Kit, Thermo Fisher Scientific) according to the manufacturer's instruction.

Western blotting

30 mg of proteins were supplied with an appropriate volume of 2x sample buffer with 5% mercaptoethanol and heated up to 95°C for 5 min in order to achieve protein denaturation. Lysates were resolved by 12.5% SDS-PAGE, electroblotted onto a PVDF membrane (Millipore) by using a Trans-Blot Semi-Dry Transfer Cell (Bio-Rad) and probed with either rabbit anti-UCP1 antibody (1:10000) or mouse anti-Actin antibody (1:10000). Secondary antibodies conjugated to IRDye™ 680 or IRDye™ 800 (Licor Biosciences) were incubated at a

2.3 DUAL LUCIFERASE REPORTER ASSAY FOR THE MEASUREMENT OF SECRETIN RECEPTOR ACTIVATION

In vitro characterization of anti-secretin antibody was performed in a dual luciferase HEK293 cell system. The evaluation is based on the determination of secretin receptor activation in response to varying combinations of secretin and its antibody. The method relies on the simultaneous expression and measurement of two reporter enzymes, the firefly (*Photinus*

pyralis) and the renilla (*Renilla reniformis*) luciferase, within the same system, the secretin receptor expressing HEK293 cell.

Expression of the firefly luciferase, presenting the experimental reporter enzyme, thereby reflects secretin receptor activation. Stimulation of the G-protein coupled secretin receptor results in the accumulation of cytosolic cAMP and subsequent PKA activation. PKA phosphorylates the transcription factor cAMP response element binding protein (CREB), which in turn activates expression of *PLuc* gene under the control of the cAMP response element (CRE). Expression of *PLuc* is proportional to secretin receptor activation. In contrast, *renilla luciferase* (*RLuc*), presenting the control reporter, is constitutively expressed to monitor baseline response. PLUC and RLUC expression is measured sequentially in the lysed cells by providing their respective substrates and measurement of bioluminescence (**Fig. 4**). By normalization of the experimental reporter (PLUC) to that of the internal standard (RLUC), experimental variability, caused by varying cell number or viability, transfection or cell lysis efficiency, shall be minimized. For generation of the dual luciferase-secretin receptor reporter HEK293 cell system, cells were transiently transfected by calcium phosphate precipitation with vectors carrying *PLuc* (pAD-Cre-Luc), *RLuc* (phRG-B) and the murine *secretin receptor* (sctr-pcDNA3.1) genes. The day preceding the transfection, cells were seeded on a 10-cm cell culture plate. Transfection was performed at a 40-60% confluence stage. Two hours before transfection, medium was changed. Plasmid DNAs (5 µg each) were mixed with 62 µl $CaCl_2$ (2.5 M) and replenished with water to 500 µl. The mixture was added to 2xHBSS buffer under vortex mixing, followed by 15 min incubation to allow DNA-calcium phosphate precipitate formation. Finally, the transfection solution was slowly dropped onto the cells. On the day after the transfection, cells were transferred to a poly-D-lysine coated 96-well plate. The next day, cells were stimulated with secretin, anti-secretin antibody or different combinations of both for 6 h, then washed with PBS and frozen at -20°C until

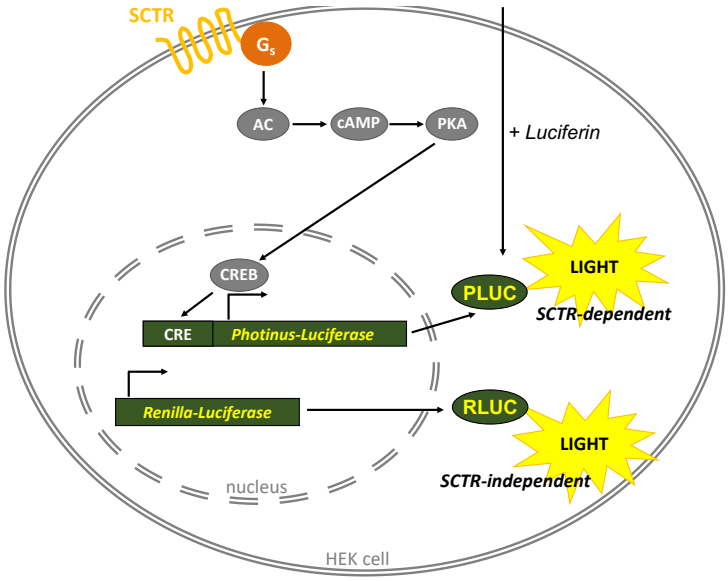

Figure 4: Dual luciferase reporter assay for the measurement of secretin receptor activation.
HEK293 cells were transiently transfected with vectors for the secretin receptor (SCTR), Photinus luciferase (PLUC) and renilla luciferase (RLUC). SCTR activation initiates adenylyl cyclase (AC) leading to a rise in cyclic adenosine monophosphate (cAMP) and the activation of protein kinase A (PKA). The latter phosphorylates cAMP response element binding protein (CREB) and leads to a subsequent expression of PLUC. PLUC and RLUC activity is determined by the addition of luciferin and bioluminescence measurements.

luciferase analysis (Dual luciferase reporter assay, Promega). Secretin receptor activity was quantified as the ratio of bioluminescence of firefly (PLUC) and renilla (RLUC) luciferase.

2.4 *IN VIVO* METABOLIC PHENOTYPING

Food intake and BAT activity are two crucial parameters for the investigation of meal-associated thermogenesis and thermoregulatory feeding. For a better understanding of physiological control mechanisms, the following different mouse models were scrutinized concerning food intake and BAT activity. In all experiments, intraperitoneally injected secretin (5 nmol/mouse) was tested against a PBS control. Moreover, mice were accustomed to the injections by being injected with PBS on 3 consecutive days prior to the experiments.

- To test for BAT-specific effects: UCP1KO mice
- To test for SNS effects: Pretreatment with propranolol (10 mg/kg body weight (BW)), a non-selective beta-blocker, 20 min prior to the experiment
- To block endogenous secretin activity: Pretreatment with either anti-secretin or GFP-antibody by subcutaneous injections at the time when food was removed the day prior to the experiment. Postprandial secretin serum levels as well as in vitro testing results for blocking efficiency of the anti-secretin antibody were used to estimate the appropriate concentration of the antibody to block endogenous secretin activity during refeeding. Assuming a total blood volume of 2 ml/mouse, 400 pmol anti-secretin antibody were injected per mouse.
- To compare and evaluate the effect size of secretin: Including BAT activating agents: CL-316243 (0.2 mg/kg BW) and norepinephrine (1 mg/kg BW)
- To obtain maximal secretin- or NE-induced thermogenic effect: Pre-acclimatization to 30°C for one week, as BAT is already activated at room temperature. 30°C is the thermoneutral zone of mammals in which no thermoregulation occurs.

2.4.1 Assessment of food intake – satiation vs. satiety

Monitoring of food intake

Food intake of individually housed mice was recorded using an automated monitoring system (TSE LabMaster Home Cage Activity). The food baskets were connected to high precision balances to record cumulative food intake. Food basket weights were averaged in 5 min intervals. The day prior to the refeeding experiments, food was removed from the cages at 5 pm and mice were fasted overnight. After refeeding cumulative food intake was monitored during the following 72 h.

Analysis of food intake patterns

For meal pattern analyses, food intake was calculated as first derivative of cumulative food intake obtained from the automated monitoring system (see above). Food intake greater than 0.005 g and separated by intermeal bouts greater or equal than 15 min was defined as meal. Mean meal duration and mean intermeal bout length were calculated as mean of individual values per mouse. Data from one dark phase were evaluated. It was ensured that no confounders like fasting could exert any influence on food intake.

2.4.2 Hypothalamic neuropeptide gene expression analysis

Regardless of the causal trigger, the reduction/termination of food intake is a behavior that requires the contribution of the brain. To confirm this and to further investigate the role of BAT in it, hypothalamic neuropeptide gene expression was analyzed in both overnight-fasted UCP1 WT and KO (129S1/SvImJ) mice subsequent to either secretin or PBS injection. 4 h after treatment, hypothalamic tissue was dissected. In a second experiment, WT mice (129S6/SvEv) were exposed to room temperature or moderate heat for 4 h following overnight-fasting. In case of the heat exposure, environmental temperature was gradually increased from 34°C to 37°C (1 degree per hour), to facilitate heat loss and acclimatization. Afterwards, hypothalamic tissue and preoptical region were separately dissected. Tissues were snap-frozen and later subjected to RNA extraction and gene expression analysis.

2.4.3 Detection of brown fat activity in mice and humans

In research on brown adipose tissue, it is of vital importance to be able to detect presence, abundance and thermogenic activity of this tissue, ideally in a non-invasive manner allowing for repeated measures.

Indirect calorimetry and norepinephrine tests

In rodents, the gold standard for the determination of maximal thermogenic capacity and current thermogenic activity is indirect calorimetry during different ambient temperature regimes or in response to norepinephrine (NE) injection (Cannon and Nedergaard, 2004; Virtue and Vidal-Puig, 2013). The NE-test is based on the activation of the β_3-adrenergic receptor, which is highly expressed in murine BAT. Injection of NE in high dose (1mg/kg BW) leads to acute and maximal stimulation of UCP1-dependent mitochondrial respiration and thus heat production in brown adipose tissue. Thermogenic BAT activity is reflected in the oxygen consumption of the animal, which is recorded via indirect calorimetry. As these metabolic measures lack information on specific localization of oxygen consumption, UCP1KO mice were included in the test to check to what extend BAT accounts for an increase in metabolic rate.

In the morning of the test day, body mass was determined and mice were placed in metabolic cages (3-liter volume) without food and water. The cages were connected to the indirect

calorimetry setup (LabMaster, TSE Systems) inside a climate cabinet (TPK 600, Feutron) preconditioned to 31°C. Oxygen consumption and carbon dioxide production of the mice was recorded over a period of 4 hours (8:00 am – 12 am) to determine basal metabolic rate (BMR). The air of the cages was extracted with a flow rate of 33 l/h over a period of 1 min every 5 min, dried in a cooling trap and analyzed for oxygen and carbon dioxide content. Oxygen consumption and carbon dioxide production were determined by comparison of air from the cages with an empty reference cage. The BMR was calculated as the lowest mean of three consecutive oxygen consumption values, which had a coefficient of variation less than 5 %.

After BMR measurement, cabinet temperature was reduced to 27°C to facilitate heat loss to the environment produced in response to injection to avoid hyperthermic reactions. Mice were injected intraperitoneally (i.p.) either with 1mg/kg NE (Arterenol 1 mg/kg, Sanofi), 5 nmol secretin (Tocris) or equal volume of PBS and immediately reconnected to the indirect calorimetry setup. Oxygen consumption and carbon dioxide production was recorded in 3 min intervals for about one hour. Metabolic rates were converted into heat production via the following formula: HP (mW) = (4.44+1.43*respiratory exchange rate)*oxygen consumption (ml/h).

Surgical implantation of telemetry transmitters and monitoring of iBAT temperature

Tissue temperature is a surrogate measure for brown fat activity. Therefore, telemetry transmitters (G2 E-Mitter, Starr Life Science Corp., Oakmont, PA, USA) were implanted above the interscapular BAT into 10-weeks-old 129S6/SvEv mice to continuously monitor tissue temperature. Implantation was performed subsequent to a combined i.p. anesthesia of medetomidinehydrochlorid (0.5 mg/kg; Dorbene vet, Zoetis), midazolam (5 mg/kg; Dormicum, Roche) and fentanyl (0.05 mg/kg; Fentadon, Albrecht). The intersacpular region was opened by a small incision and the transmitter was placed above the interscapular BAT depot. Surgical adhesive was used to close the incision and anesthesia was terminated by a subcutaneous injection of atipamezolhydrochlorid (2.5 mg/kg; Atipazole, Prodivet Pharmaceuticals), flumazenil (0.5 mg/kg; Flumazentil, Hexal) and naloxonhydrochloride (1.2 mk/kg; Naloxon, Ratiopharm). In addition mice received carprofen (10 mg/kg; Rimadyl, Zoetis) and were single housed in the post-operative recovery period for 4-5 days. 2 weeks after surgery, when the fur had completely returned and the wound had healed, brown fat temperature (T_{iBAT}) signals were continuously recorded by a receiver plate (ER4000 Energizer/Receiver, Oakmont, PA, USA) underneath the cage.

Macroscopic multi-spectral optoacoustic tomography (MSOT) combined with indirect calorimetry

For further visualization of BAT activity, indirect calorimetry combined with real-time multi-spectral optoacoustic tomography (MSOT) was performed in anaesthetized nude mice using an MSOT small animal imaging system (in Vision 256-TF, iThera Medical GmbH) in

cooperation with the Institute of Biological and Medical Imaging (Helmholtz Zentrum München). This technique is based on optoacoustic effects and allows a real time analysis of interscapular BAT activation *in vivo*.

The tissue's energy absorption of light pulses generates acoustic waves, which is detected by ultrasound detectors. In detail, brown adipose tissue is illuminated through pulses of different wavelength (near-infrared). The absorption of this energy leads to a thermoelastic dilatation of the tissue which results in the generation of acoustic waves, which can then be detected. With MSOT the spectra of oxygenated and deoxygenated hemoglobin are analyzed in high resolution deep in tissues and blood vessels (Reber et al., 2018).

The analysis of the present study was performed on the Sulzer's vein, the only venous drainage of iBAT. Therefore total blood volume (TBV = oxygenated hemoglobin (HbO_2) + deoxygenated hemoglobin (Hb)) and oxygen saturation (SO_2 = HbO_2/TBV) were calculated. In parallel O_2 consumption and CO_2 production were analyzed in 1 sec intervals using a transportable indirect calorimetry system (FoxBox, Sable Systems International, USA) allowing the comparison of energy expenditure and activation state of BAT. Metabolic rates from indirect calorimetry data were again calculated as HP.

Positron Emission Tomography – Computed Tomography (PET/CT)

A direct consequence of BAT activation is the uptake of fuels, like glucose and fatty acids or oxygen consumption of this tissue. Thus, the measurement of radiotracer uptake (like 2-deoxy-2-^{18}F-fluoro-D-glucose (^{18}F-FDG)-, ^{18}F-fluoro-6-thai-heptadecanoic acid (^{18}F-FTHA)- or ^{15}O-O_2) by positron-emission tomography (PET) is a common method for the metabolic imaging of BAT. For anatomical localization purposes, PET is combined with computed tomography (CT).

PET-CT scans on human subjects have been performed in two separate cohorts in Turku PET Centre in Finland. The ethical committee of South-Western Finland Hospital District evaluated and approved the studies, and all participants gave their written informed consent before any study procedure (Clinical trial number: NCT03290846).

In summary, two parameters were determined in the two distinct studies. First, postprandial BAT activation was determined in the supraclavicular and upper thoracic region by measuring oxygen and fatty acid uptake and subsequently correlated to the rise in circulating secretin level. Blood samples for secretin measurements were drawn at baseline (overnight fasting) and 30- 40 min after completing a mixed meal consisting of 542 kcal (58% carbohydrates, 25% fat, and 17% protein). Second, effects of secretin on BAT glucose metabolism was evaluated in a single-blinded randomized cross-over study. Dynamic PET-CT scans of the neck area using 18F-FDG were performed subsequent to two short intravenous infusions of secretin hydrochloride (Secrelux, 1IU/kg each) or saline (placebo). Scans were done and analyzed as described earlier (Virtanen et al., 2009).

2.4.4 Diet-induced obese mice study

All studies on diet-induced obese (DIO) mice have been approved by Eli Lilly and company's Institutional Animal Care and Use Committee.

Human secretin (1-27 amide: HSDGTFTSELSRLREGARLQRLLQGLV-amide; native secretin) and modified human secretin analog (1-27 amide: HSDGTFTSELSRLREE*ARLK*RLLQGLV-amide, modified secretin) (Dong et al., 2011) that contains a lactam bridge between side chains of Glu16 and Lys20 were synthesized by solid-phase peptide synthesis using established chemical protocols. After cleavage from the solid support and purification using reversed-phase chromatography, the lyophilized powders as trifluoroacetate salts were formulated in aqueous buffer.

DIO mice at the age of 30 to 31 weeks, were maintained on a calorie rich diet since arrival at Lilly (TD95217; Teklad, Madison, WI). Mice were individually housed in a temperature-controlled facility (24°C) with 12/12 hours light/dark cycle (lights on 10 pm) and free access to food and water. Mice were randomized according to their body weight after acclimation to the facility (minimum 2 weeks). The body weights ranged from 46 to 54 g. Vehicle (20 mM citrate at pH 5.5), native secretin (166 nmol/kg/day) or modified secretin (163 nmol/kg/day) dissolved in vehicle was administered by s.c. mini-osmotic pump (Alzet, Model 2002, Durect Corporatoin, Cupertino, CA) as an infusion (12 µl/mouse/day) to ad libitum fed DIO mice throughout the study period. Body weight and food intake was monitored daily. Absolute changes in body weight were calculated by subtracting the body weight of the same animal on the first day of the treatment. On Days 1 and 14, total fat mass and total water mass were measured by quantitative nuclear magnetic resonance (QNMR) using an Echo Medical System (Houston, TX) instrument. Fat-free mass was calculated as body weight – fat mass. For the thermoneutral experiment, mice were acclimatized to 30°C one week before the experiment started. Apart from the dosage, all other study conditions were kept (native secretin: 996 nmol/kg/day; modified secretin: 326 nmol/kg/day). Additionally, oxygen consumption was measured.

2.4.5 Quantification of secretin serum level

For the quantitative measurement of both human and murine serum secretin levels a commercially available enzyme-linked immunosorbent assay (ELISA) kit (Cloud-Clone Corp) was used. This kit employs the competitive ELISA principle. The central event of competitive ELISA is a competitive binding process executed by the sample antigen.

A monoclonal antibody specific to secretin is pre-coated onto a microplate. A competitive inhibition reaction is launched between biotin labeled secretin and unlabeled secretin (standards or samples) with the pre-coated antibody specific to secretin. After incubation the unbound conjugate is washed off. Next, avidin conjugated to Horseradish Peroxidase (HRP) is added to each microplate well and incubated. The amount of bound HRP conjugate is

reverse proportional to the concentration of secretin in the sample. After addition of the substrate solution, the intensity of the color developed is reverse proportional to the concentration of secretin in the sample. Secretin concentrations were calculated using a standard curve generated by secretin standards included in the kit.

2.5 STATISTICAL ANALYSIS

Significant differences for single comparisons were assessed by two-tailed Student's *t* tests. Analysis of variance (ANOVA) with Tukey's *post hoc* tests were used for multiple comparison. PET/CT analysis was analyzed using paired one-tailed t test. P-values below 0.05 were considered significant. Statistical analysis was performed with GraphPad prism 6 software. All data are presented as mean ± SD.

The linear mixed effect models in Chapter III were calculated with *fitlme* function of MATLAB R2016b (Mathworks). In detail, cumulative food intake was analyzed by means of linear mixed effect models with fixed effects 'time' and 'treatment group', their interaction, and 'individual' as random effect. Additionally, we applied a more sophisticated model to specifically detect an effect of secretin on metabolic rate from cumulative food intake data by including the additional random factors 'initial body mass' (to capture the metabolic requirements of the mouse) and 'overall change in body mass' (to capture the alternate fate of food, i.e. fat deposition/loss).

2.6 DATA AND SOFTWARE AVAILABILITY

The accession number for the RNA-Seq data presented in Chapter II and Chapter III is GEO: GSE119452.

3 PUBLICATIONS[3]

CHAPTER I – "NON-ADRENERGIC CONTROL OF LIPOLYSIS AND THERMOGENESIS IN ADIPOSE TISSUE"

Katharina Braun, Josef Oeckl, Julia Westermeier, Yongguo Li, Martin Klingenspor

Journal of Experimental Biology, 2018 Mar; 221(Pt Suppl 1)

Personal contribution: Katharina Schnabl prepared the figures and contributed 6 out of 12 sections of this review article.

CHAPTER II – "OPPOSING ACTIONS OF ADRENOCORTICOTROPIC HORMONE AND GLUCOCORTICOIDS ON UCP1-MEDIATED RESPIRATION IN BROWN ADIPOCYTES"

Katharina Schnabl, Julia Westermeier, Yongguo Li, Martin Klingenspor

Frontiers in Physiology, 2019 Jan; 9:1931

Personal contribution: Katharina Schnabl designed the study, performed the experiments, analyzed the data, prepared the figures, and wrote and revised the manuscript.

CHAPTER III – "SECRETIN-ACTIVATED BROWN FAT MEDIATES PRANDIAL THERMOGENESIS TO INDUCE SATIATION"

Yongguo Li*, **Katharina Schnabl***, Sarah-Madeleine Gabler, Monja Willershäuser, Josefine Reber, Angelos Karlas, Sanna Laurila, Minna Lahesmaa, Mueez U Din, Andrea Bast-Habersbrunner, Kirsi A. Virtanen, Tobias Fromme, Florian Bolze, Libbey S. O'Farrell, Jorge Alsina-Fernandez, Tamer Coskun, Vasilis Ntziachristos, Pirijo Nuutila, Martin Klingenspor (*These authors contributed equally)

Cell, 2018 Nov;175(6):1561-1574

Personal contribution: Katharina Schnabl contributed substantially to the design of the study. She established methods, wrote the required animal ethics applications, conducted all mouse experiments (apart from DIO and MSOT), took responsibility for communication with external partners, and performed the *in vitro* characterization of the secretin antibody, the detailed analysis of food intake, and most of the microplate-based respirometry measurements. She analyzed the data, prepared the figures, and contributed substantially to writing and revising of the manuscript. For detailed description, see author contributions.

Univ. Prof. Dr. Martin Klingenspor (Supervisor)
Chair for Molecular Nutritional Medicine

[3]Original publications are shown in 6.1; Letters of approval are shown in appendix 6.2

CHAPTER I – "NON-ADRENERGIC CONTROL OF LIPOLYSIS AND THERMOGENESIS IN ADIPOSE TISSUE"

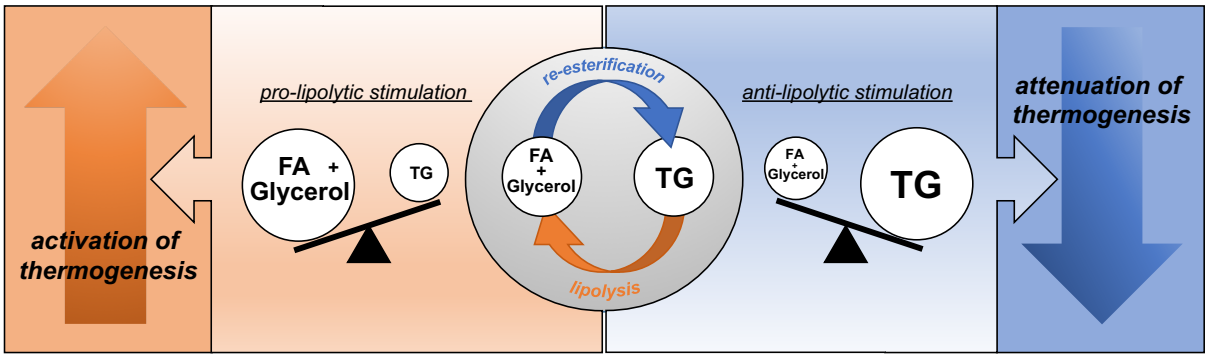

Highlights

- Lipolysis and re-esterification - Storage, mobilization and combustion of free fatty acids
- Dual role of catecholamines in the adrenergic control of lipolysis
- Anti-and pro-lipolytic effectors of adipocyte function
- Species-specific differences in the regulation of lipolysis
- Modulating lipolysis to control brown adipocyte thermogenesis

The activation of BAT, more specifically of UCP1, is essential in order to achieve an increase in energy expenditure. As thermogenic activity of UCP1 is controlled by the regulation of free fatty acid levels, the goal of the present review was to provide a comprehensive overview of pro- and anti-lipolytic agents, which can be regarded as a list of potential pro- and anti-thermogenic modulators.

In energy balance, lipolysis of triacylglyerols and re-esterification of free fatty acids are opposing processes operating in parallel at identical rates. This enables a highly dynamic transition from anabolism to catabolism and vice versa and thereby allows a rapid adaptation to changing physiological states of energy demand. Efficient mobilization or storage of energy is achieved by one process dominating the other. This enormous plasticity of adipose tissue is under neuronal and endocrine control. As storage, mobilization and dissipation of energy are essential for survival, it is not surprising that key functions in lipolysis and re-esterification are controlled by multiple redundant pathways.

The catecholamines epinephrine and norepinephrine, for example, play a dual role in the adrenergic control of lipolysis. Both neurotransmitters elicit distinct adrenergic signaling pathways in adipocytes by activating a large family of α- and β-adrenergic receptors (AR). Thus, the receptor abundance largely determines which signaling modules are activated. In rodent adipocytes the β_3-AR ARDB3 is the predominant AR paralog. Its activation by norepinephrine released as neurotransmitter from sympathetic nerves is the prime driver of lipolysis in adipose tissue by initiating the classical adenylyl cyclase-cAMP-PKA pathway. Furthermore, the purine nucleoside adenosine is presented as an anti-lipolytic effector, as the activation of one of the two adenosine receptor paralogs (ADORA1) inhibits adenylyl cyclase through G_i. Melanocortins, glucocorticoids, natriuretic peptides, bile acids, parathyroid hormone and secretin have been repeatedly shown to exhibit pro-lipolytic effects in white adipocytes. This list of pro-lipolytic modulators is extended by receptor-independent effectors like α-β hydrolase domain-containing protein 5, as well as compounds categorized as protein, small molecules and plant extracts. In addition, sources of fatty acids other than hydrolysis of triacylglycerol in lipid droplets via the classical lipolytic pathway have to be taken into account. Examples are (I) the mitochondrial phospholipase 2, which provides long-chain fatty acids within the inner mitochondrial membrane and (II) lipophagy, which is a form of macroautophagy contributing to the hydrolysis of triacylglycerols stored in lipid droplets.

For most of these molecules, our knowledge about their impact on lipid metabolism is mostly limited to white adipocytes cultured *in vitro*, with little or no insights available on their physiological function *in vivo*. Moreover, to date, only few of these modulators have been studied for their effects on lipolysis in brown and brite adipocytes. Coming back to lipolysis as an essential prerequisite for the activation of UCP1-mediated thermogenesis, pro-lipolytic effectors working through the cAMP-PKA pathway are very likely to recruit and activate thermogenic capacity.

CHAPTER II – "OPPOSING ACTIONS OF ADRENOCORTICOTROPIC HORMONE AND GLUCOCORTICOIDS ON UCP1-MEDIATED RESPIRATION IN BROWN ADIPOCYTES"

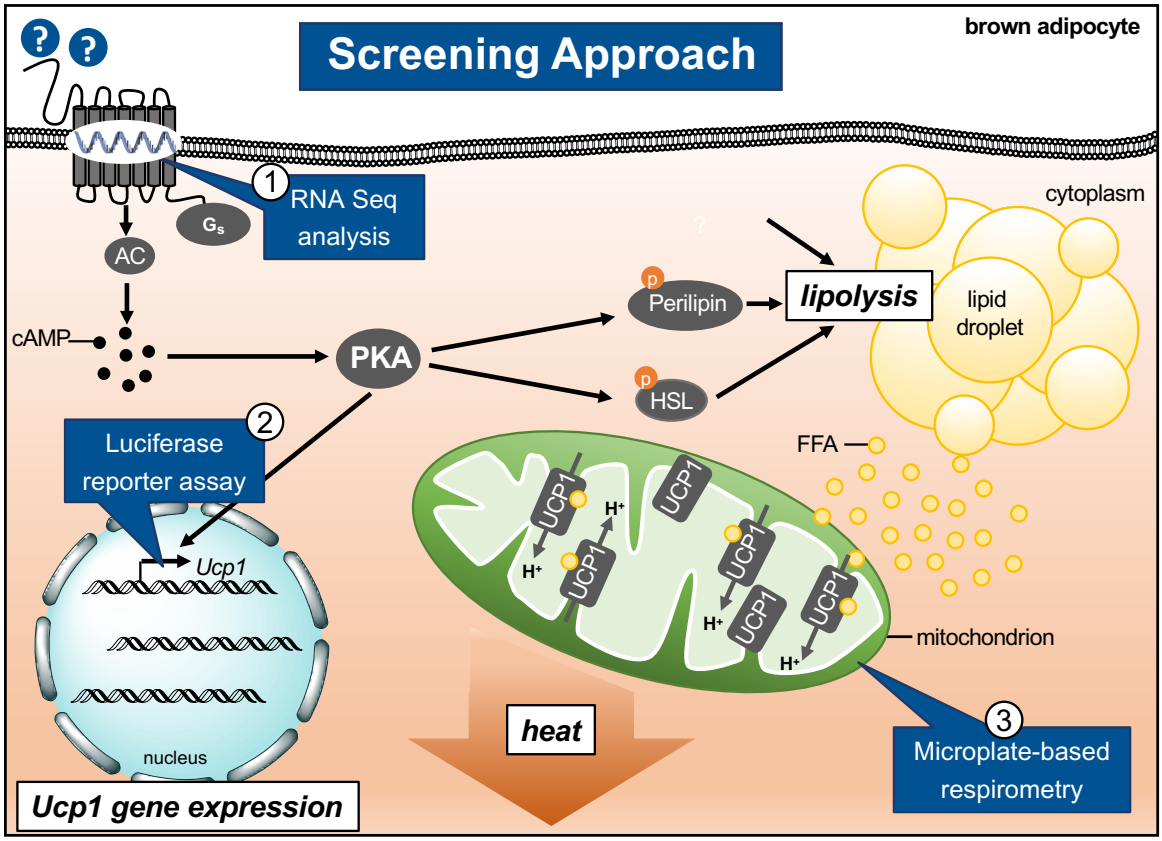

Highlights

- Identification of 12 non-adrenergic G_s-protein coupled receptors abundantly expressed in murine brown adipose tissue
- Reporter-assay and cellular respirometry screening of G_s-protein coupled receptor ligands for UCP1 activation and regulation
- The stress hormone ACTH activates thermogenesis via the canonical MC2R-cAMP-PKA-lipolysis-UCP1 pathway in primary brown adipocytes
- ACTH increases *Ucp1* expression in primary white and brown adipocytes
- A synthetic ACTH fragment slightly stimulates respiration and increases *Ucp1*
- Acute glucocorticoid treatment attenuates β_3-adrenergic signaling

Classical, non-shivering thermogenesis in BAT is under the control of the sympathetic nervous system. The second messenger cascade downstream of the receptor that finally causes lipolysis is composed of the typical steps shared by all G_s-coupled receptors, namely adenylyl cyclase, cyclic adenosine monophosphate (cAMP) and protein kinase A. Thus, initiation of this signaling cascade by any G_s-coupled receptors seemed a plausible approach to activate BAT in a non-adrenergic fashion. Indeed, besides the β-AR brown adipocytes express a large variety of G-protein coupled receptors. Therefore, the aim of the present study was to identify highly expressed G_s-coupled receptors by the analysis of RNA Seq data of murine brown adipose tissue and subsequently to screen ligands for these receptors concerning their potential to recruit and activate thermogenic capacity in brown adipocytes. First, luciferase activity (FLUC) measurements in primary brown adipocytes of transgenic mice expressing *Fluc* driven by the *Ucp1* promotor were applied to determine the effect of the G_sPCR ligands on *Ucp1* expression. Second, microplate-based cellular respirometry was performed to determine UCP1-activating properties of the respective receptor ligands.

The analysis revealed 12 G_s-coupled receptors abundantly expressed in murine BAT. Among all ligands for these receptors, adrenocorticotropic hormone (ACTH) and secretin turned out to be the most potent activators of UCP1. ACTH is the glandotropic hormone of the endocrine hypothalamic-pituitary-adrenal-axis stimulating the release of glucocorticoids from the adrenals in response to stress. In primary brown adipocytes ACTH increases UCP1-dependent respiration in a non-adrenergic fashion via the melanocortin 2 receptor (MC2R). This has been verified by the use of cells from UCP1KO mice as well as by pretreatment with propranolol, a non-selective β-blocker and GPS1573, a MC2R antagonist. Inhibitor-based studies showed that the thermogenic effect of ACTH is dependent on protein kinase A and lipolysis, compatible with a rise in cAMP.

To further characterize ACTH's impact on brown fat, thermogenic effects of both, a mutant and a natural ACTH fragment (heptapeptide $ACTH_{(4-10)}$), which have been reported to bind and activate MC2R were determined. While the natural ACTH fragment had no effect on uncoupled respiration, the mutant analog with an amino acid exchange from Arg to His slightly increased UCP1-mediated respiration.

In addition, the interplay of ACTH and dexamethasone was investigated in this study, as the stress hormone triggers the release of glucocorticoids which have been reported to negatively regulate *Ucp1* expression. Interestingly, dexamethasone attenuated isoproterenol-induced respiration in a time-dependent manner (0-4 h), whereas ACTH effects have not been influenced.

Thus, ACTH is a non-adrenergic activator of primary brown adipocytes, initiating the same canonical cAMP-PKA-lipolysis-UCP1 pathway like norepinephrine. Furthermore, it possibly limits cold-/ stress-induced BAT thermogenesis by causing the release of glucocorticoids.

CHAPTER III – "SECRETIN-ACTIVATED BROWN FAT MEDIATES PRANDIAL THERMOGENESIS TO INDUCE SATIATION"

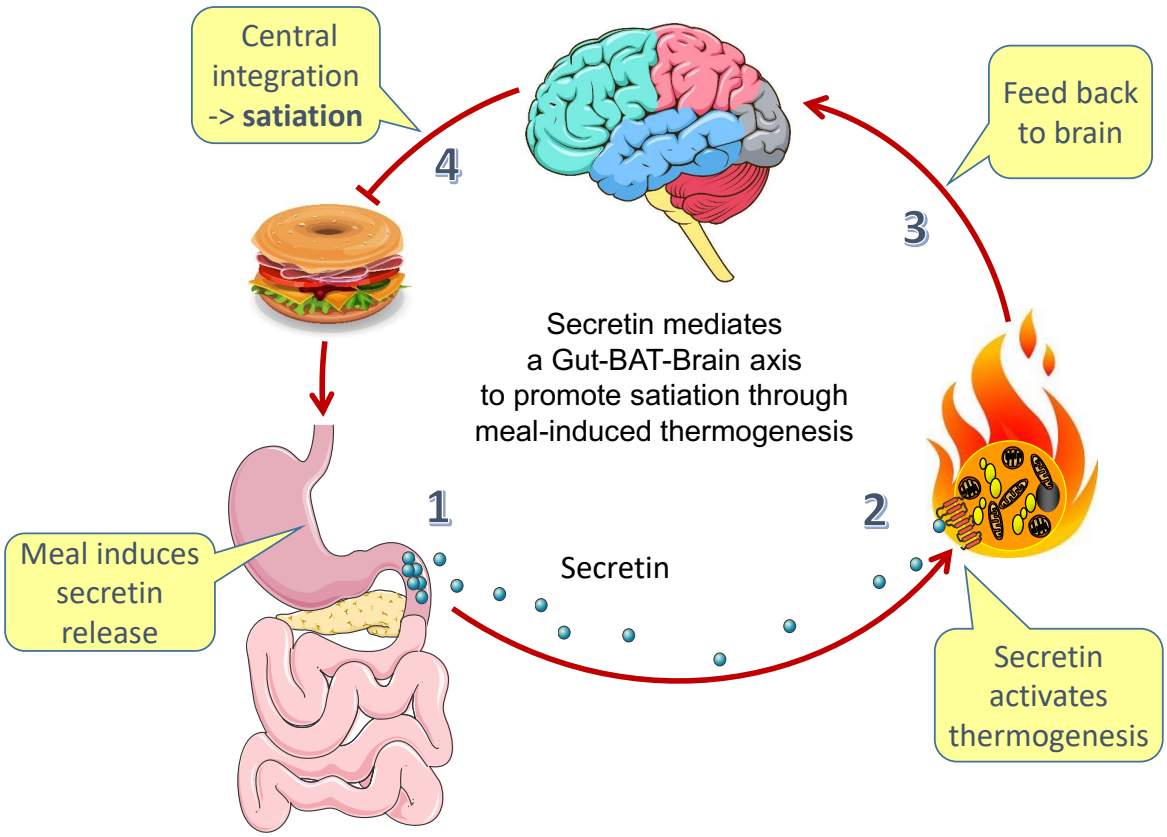

Depicted from Li, Schnabl et al., 2018.

Highlights

- Abundant expression of the secretin receptor in brown adipocytes
- Secretin activates BAT thermogenesis through SCTR-PKA-lipolysis pathway
- Secretin-activated BAT induces satiation
- Neutralizing prandial secretin activity attenuates meal-associated thermogenesis and increases food intake
- Both, secretin and intact BAT are required for the regulation of feeding patterns
- Secretin infusion transiently elevates energy expenditure in diet-induced obese mice
- Secretin activates human BAT

Brown adipose tissue has been repeatedly reported to contribute to meal-associated or long-term diet-induced thermogenesis. However, the molecular mediator and the functional significance of meal-associated BAT thermogenesis remained elusive so far. As the release of gastrointestinal peptides, like GLP1, PYY and ghrelin, is the initial physiological response to food intake, these endocrine factors seem to harbor a high potential to mediate meal-associated BAT thermogenesis. RNA Seq analysis of murine BAT revealed that the secretin receptor (SCTR) is abundantly expressed, while receptors for other gastrointestinal peptides are rather absent. Secretin is a gut hormone that is classically known to stimulate pancreatic water and bicarbonate secretion upon food intake, but has also been reported to induce lipolysis in adipocytes, which is an essential prerequisite for the activation of UCP1.

Indeed, in primary brown adipocytes secretin increased UCP1-dependent respiration. Further detailed *in vitro* analysis revealed that secretin initiates the canonical SCTR-cAMP-PKA-lipolysis-UCP1 pathway. *In vivo*, its thermogenic effect was assessed by indirect calorimetry and multi-spectral optoacoustic tomography in three different mouse models. The thermogenic effect was (I) UCP1-dependent, (II) comparable to norepinephrine, (III) significantly present at room temperature and thermoneutrality and (IV) was accompanied by a rise in iBAT temperature (T_{iBAT}). In addition, plasma secretin levels were decreased by fasting and increased significantly within one hour after refeeding, which was congruent with changes in T_{iBAT}. Furthermore, a single secretin injection into fasted mice reduced food intake in a UCP1-dependent manner, which was reflected by the regulation of anorexigenic and orexigenic hypothalamic peptides in wildtype but not UCP1KO mice. This effect on food intake was induced by a direct activation of BAT independent from the SNS, assessed by the pretreatment with the non-selective β-blocker propranolol. An antibody-based neutralization of endogenous secretin activity resulted in increased food intake in refed mice as well as an attenuation of the meal-induced rise in T_{iBAT}. Importantly, food intake and T_{iBAT} were negatively correlated. Meal-pattern analyses revealed that the interplay of secretin and BAT regulates food intake in mice. Although total food intake was not altered in the absence of either secretin or intact BAT, the number of meals per night as well as intermeal bout length were decreased, while meal size and meal duration were increased.

To clarify a potential therapeutic use, diet-induced obese mice were chronically infused with a modified secretin analog. At room temperature, the modified secretin caused a transient reduction in food intake and body weight, which was complemented by a transient elevation of energy expenditure determined at thermoneutrality. In humans, postprandial secretin positively correlated with oxygen and fatty acid uptake rates into BAT. Direct evidence for the thermogenic action of secretin in BAT was obtained by FDG-PET-CT scans demonstrating that two secretin infusions significantly increased glucose uptake into human BAT. Conclusively, targeting this secretin-BAT-brain axis might hold promise for developing novel obesity therapies as it promotes negative energy balance through both increasing energy expenditure and decreasing energy intake.

4 DISCUSSION

The high prevalence of obesity in our modern societies represents a serious threat to human health and well-being. People with obesity suffer from stigmatization and a severely compromised quality of life. Obesity strongly clusters with other comorbidities, in particular type 2 diabetes, arterial hypertension and dyslipidemia. Current therapeutic strategies to achieve a negative energy balance and thus weight loss are lifestyle changes in combination with pharmacotherapies targeting energy intake in severe cases of obesity. Examples for drug treatment are (I) ***Orlistat***, which binds dietary fat in the stomach and in the intestinal tract and thus inhibits the fat absorption, (II) the anti-diabetic drug ***Liraglutid***, which promotes the feeling of satiety, reduces appetite and thereby also food intake (Pilitsi et al., 2019) and (III) the combination therapy of ***Naltrexon*** and ***Buproprion***, which inhibits appetite and affects the reward system (Khera et al., 2016). In the context of restoring obesity-causing energy imbalance, brown adipose tissue received great attention due to its energy dissipation properties (Tseng et al., 2010). In addition to positive effects on energy balance, chronic activation of BAT leads to improved glucose tolerance and the release of batokines that beneficially regulate metabolism in rodent models (Bartelt et al., 2011; Hondares et al., 2011). The development of successful BAT-based therapeutic strategies to treat and/or prevent obesity relies on a good understanding of its basic biology. This includes the identification of non-adrenergic activators of BAT to be able to circumvent the adverse effects of sympathomimetics. In this dissertation the major goals were to identify potent non-adrenergic activators of BAT as well as novel functions of the heating organ in energy balance regulation. BAT has been proposed to mediate both cold-induced and meal-associated thermogenesis. The molecular mediator and functional significance of meal-associated brown fat thermogenesis, however, remained elusive so far and was therefore examined more detailed in this work.

UCP1 is constitutively inactive

Several novel molecular mediators for the recruitment of BAT and/or the browning of WAT have been identified (Bartelt and Heeren, 2014), but so far only few direct activators of respiration in brown adipocytes have been reported (Braun et al., 2018). The latter are mostly adrenergic receptor agonists which exhibit unwanted systemic side effects (Carey and Kingwell, 2013; Cypess et al., 2012; Cypess et al., 2015; Vosselman et al., 2012). The mere augmentation of thermogenic capacity, however, is useless in terms of a targeting BAT for therapeutic purposes in obesity prevention and treatment. That means the activation of UCP1 is crucial in terms of increasing energy expenditure, since it is inherently inactive (Li et al., 2014b). This prerequisite becomes even more important when reflecting that humans live in a thermoneutral environment with heaters and warm clothing, as this normally precludes cold-induced brown fat activation. Therefore, the aim of this thesis was to identify novel non-

adrenergic activators of brown adipocytes. A screen for G_sPCRs expressed in mature murine adipocytes was performed first, as the activation of cAMP-PKA signaling cascade leads to increased lipolysis providing FFAs that are essential for the activation of UCP1-dependent respiration. As oxygen consumption is the key readout for UCP1 activity, cellular respirometry is an appropriate tool in the search for activators of brown adipocytes *in vitro*. It is crucial to prevent unspecific UCP1-independent uncoupling activity induced by uncontrolled high FFA levels (Li et al., 2014b). To ascertain UCP1 specificity, cells of UCP1KO mice have been investigated. This screening approach identified six peptidergic ligands of non-adrenergic G_sPCRs which acutely activated UCP1-mediated respiration in cultured adipocytes. Among these, the glandotropic stress hormone ACTH and the gut hormone secretin were the most potent activators of the canonical cAMP-PKA-lipolysis-UCP1 pathway inducing brown adipocyte respiration.

Qualification of ACTH as BAT stimulating agent

The lipolytic activity of ACTH in rodent adipocytes has already been reported in 1958 (White and Engel, 1958). The stress hormone is known to be elevated in response to cold exposure (van den Beukel et al., 2014). It enhances BAT function in obese rats (York and Al-Baker, 1984) and increases glucose transport and respiration in isolated brown adipocytes (Marette and Bukowiecki, 1990) via fatty acid activation of mitochondrial uncoupled respiration. Nevertheless, the effective concentrations in cell culture are approximately 1,000-fold higher than the maximal physiological ACTH levels in response to restraint stress or cold exposure (Heinzmann et al., 2010; van den Beukel et al., 2014). In a physiological context, it has to be taken into account that the sensitivity and affinity of the MC2R might be different, or even increased by certain stimuli such as cold (Rochon and Bukowiecki, 1990). Nevertheless, when considering ACTH as a BAT stimulating agent, it should not be neglected, that pathophysiological chronic exposure to excessive concentrations of ACTH results in elevated glucocorticoid levels, as known for Cushing's syndrome, with symptoms like visceral obesity, growth retardation, hirsutism, acne and hypertension (Bista and Beck, 2014; Lacroix et al., 2015). Pertaining to the physiological relevance, it remains to be clarified whether the rise in ACTH plasma levels (van den Beukel et al., 2014) is sufficient to transiently activate BAT thermogenesis and to contribute to the initial defense of body temperature in the cold. It is conceivable that lipolytic activity in white adipose tissue may also indirectly supply fuels for BAT in the cold by augmenting the release of fatty acids into circulation. As MC2R is downregulated in BAT during chronic cold exposure, it seems less likely, that ACTH is involved in long-term stimulation and maintenance of cold-induced thermogenesis. Further studies *in vivo* are required to elucidate the effects of cold- and stress-induced ACTH levels on BAT thermogenesis.

Revealing a physiological mechanism controlling satiation

Besides ACTH, the gut hormone secretin was the strongest activator of UCP1-mediated uncoupled respiration in our screening approach. Although secretin was discovered already in 1902 (Bayliss and Starling, 1902), only little is known about its degradation, etc. Beyond its well characterized gastrointestinal functions, it was reported to stimulate lipolysis in white adipocytes (Butcher and Carlson, 1970) and to inhibit food intake via vagal sensory nerves and melanocortin signaling in the brain (Cheng et al., 2011; Chu et al., 2013). The present study demonstrates that secretin upon prandial release directly activates BAT thermogenesis by an endocrine route independent of the central nervous system. The acute satiation effect of secretin requires functional BAT, and is proportional to the meal-associated rise in iBAT temperature. Manipulating secretin or BAT results in an enormous alteration in feeding behavior, although daily energy intake is unchanged. Secretin is thereby identified as a key hormone stimulating meal-associated BAT thermogenesis, which plays a physiological role in the control of hunger and satiation. Essentially, the present work delivers proof that this mechanism is also relevant in humans. These findings establish a so far unknown endocrine gut – secretin – brown fat – brain axis with major implications for integrative energy balance physiology.

In addition to the importance of elucidating a novel mechanism of satiation, these findings yield a number of interesting implications. First, they may explain the presence of BAT in large species such as humans, in which allometric models of thermoregulation conclude non-shivering thermogenesis to be of minor importance. In larger mammals such as humans, this heat may serve a regulatory, rather than a homeostatic purpose. The rate of heat loss is related to the surface-to-volume ratio that decreases with increasing size of the animal. That means NST plays a subordinated role in thermoregulation of large animals compared to smaller animals. In fact, the contribution to overall thermogenic capacity in humans seems to be less than 10-15% (van der Lans et al., 2013) compared to rodents where NST ranges from 30-80 % depending on acclimation temperatures (Meyer et al., 2010). Second, these findings qualify BAT as an even more attractive therapeutic target that not only increases energy expenditure but also reduces energy intake at the same time. Based on the findings of this study one may hypothesize that any stimulus that activates BAT could potentially induce satiation. By manipulating both sides of the energy balance at the same time one of the most challenging difficulties during weight loss interventions, e.g. compensation (Hall et al., 2012) could be coped.

The misery of losing weight

In humans, the defense of body weight is a remnant from times when the law of survival of the fittest was still valid. Without the capacity to store energy in form of fat, we would have been unlikely to survive through millions of years including periods of famine. Fat is a very sensible

way to do this due to its energy dense character. In times when many people significantly exceed a healthy amount of body fat, the sophisticated protection of fat stores is more of an obstacle to weight loss than an evolutionary advantage. Reducing energy intake, whether voluntarily by life style changes or pharmacologically assisted, is inevitably counteracted by a reduction in metabolic rate to defend the current body mass through energy homeostatic systems (Mole, 1990). Conversely, unconscious overeating (Blundell et al., 2003; King et al., 2007) will antagonize body mass loss as result of an increased energy expenditure due to regular workouts.

Thus, a safe drug that increases energy expenditure and at the same time counteracts hyperphagia would be the first-line therapy in the field of metabolic diseases. In fact, first steps towards combining different therapeutic effects by the concurrent use of multiple medications called polypharmacy have been already established for the treatment of type 2 diabetes. Providing glycaemic control and weight loss simultaneously by a GLP1 and glucagon receptor dual agonist is groundbreaking as weight loss is often key in the management of obese patients with type 2 diabetes (Ambery et al., 2018). With regard to the impact of both energy intake and energy expenditure in the control of energy balance, the secretin-BAT-brain axis discovered in the present study constitutes a unique regulatory pathway that is being target in the search for such a compound in order to treat obesity.

Targeting secretin-brown fat-brain-axis to achieve weight loss

One of the most important prerequisites for the use of a concept in therapy is the transferability of basic research to humans. This study demonstrated that secretin increases glucose uptake into human brown adipose tissue and the prandial rise of secretin is positively correlated with BAT activity assessed as oxygen and fatty acid uptake.

Porcine secretin is approved for secretin-enhanced magnetic resonance cholangiopancreathography to evaluate pancreatic function and anatomy in radiology. Furthermore, intravenous secretin was tested as treatment for autism in several studies, but failed to effectively improve symptoms of autism (Williams et al., 2012). So far, an influence on body weight or appetite has not been described. The reason for this is probably that in all studies secretin was only administered in a single dose, even though its half-life of about 2.5 min is rather short. The results of the present study imply that a chronic administration is essential for obesity therapy. Safety has been demonstrated for single doses of secretin only, and therefore needs to be investigated for chronic application. The gut hormone controls pancreatic and gastric functions required for digestion and resorption of food. As a prerequisite for chronic systemic treatment, the concentration of a secretin receptor agonist required to activate brown fat and induce satiation must be below the threshold of activating gastric and pancreatic functions. Alternatively, targeted pharmacotherapy, which enables brown fat specific activation of secretin receptor signaling, would be conceivable. Thus, to fully estimate the potential of secretin for obesity therapy, pharmacokinetics and dose-response relationships

for the potency of secretin to activate pancreas functions and brown fat thermogenesis needs to be assessed and compared, respectively.

To get first insights into the therapeutic potential of secretin in obesity therapy its chronic effect on body weight and energy expenditure has been determined in DIO mice. Chronic secretin administration was conducted via a mini pump. In order to stabilize secretin in the pump, a modified secretin analog with the same binding affinity and biological activity but increased stability in solution was included in the analysis (Dong et al., 2011). While native secretin had no effect on both body weight and energy expenditure, the modified analog transiently increased total energy expenditure without affecting body weight at thermoneutrality. At first glance, secretin therefore seems rather unsuitable for long-term weight management. There are several possible reasons why the effect is only temporary and these should be investigated in detail. On the one hand, secretin acts via a member of GPCRs which are subject to homologous desensitization in case of chronic presence of high agonist concentrations. This mechanism can occur within seconds to minutes and is mediated by G-protein coupled receptor kinase (GRK) and β-arrestin. The subsequent phosphorylation of the activated GPCR leads to receptor uncoupling or endocytosis. In that case, modification of secretin analogs in terms of prolonged half-life would not solve the problem and a different approach would be inevitable. The selective regulation of GRKs and arrestins appears promising to overcome the transient character of secretin's effect on energy expenditure involving both conventional small molecule therapeutics and gene therapy (Gurevich and Gurevich, 2019). On the other hand, the administration of biological drugs (e.g. proteins), especially serial exposures to treat chronic conditions, carries a risk of eliciting anti-drug antibodies (WHO, 2013). These antibodies may reduce the efficacy of agents by blocking or neutralizing their biological activity (Schellekens and Casadevall, 2004). Although secretin is a naturally occurring peptide, the induction of anti-drug antibodies cannot be ruled out, as recombinant human insulin for example elicited antibody production in 44% of patients with diabetes (Fineberg et al., 1983). For the stabilized secretin analog carrying a lactam-bridge, however, it is even more conceivable. In this particular case, the therapeutic protein is almost identical to the endogenous secretin and may provoke antibodies that bind to both the endogenous and the therapeutic protein.

From this point of view, a chronic secretin administration seems rather problematic. To circumvent the problems mentioned, endogenous secretin released during food intake could be increased instead of supplying exogenous secretin. The manipulation of secretin and brown fat did not change total daily energy intake, but resulted in a reduced number of meals and increased size and meal duration. Thus, it seems more likely to target eating behavior rather than long-term energy intake. By increasing the yield of prandial secretin by different means like secretagogues or cleavage-inhibitors and a subsequent faster, longer or stronger activation of brown adipose tissue, one could achieve a faster meal termination and thereby a

reduced energy intake (Klingenspor, 2019). The most natural approach to boost the prandial secretin release is the proper choice of food. The primary stimulus for secretin release from S-cells in the epithelium of the duodenum into the circulation is the duodenal acidification due to gastric juice. Thus, meal composition could be crucial for an optimal secretin release and subsequent brown fat activation. Thus, further analysis of macronutrient-specific secretin release and brown fat activation could pave the way to an absolutely natural and non-invasive strategy to manipulate meal-associated thermogenesis and therefore energy expenditure and food intake (**Fig. 5**).

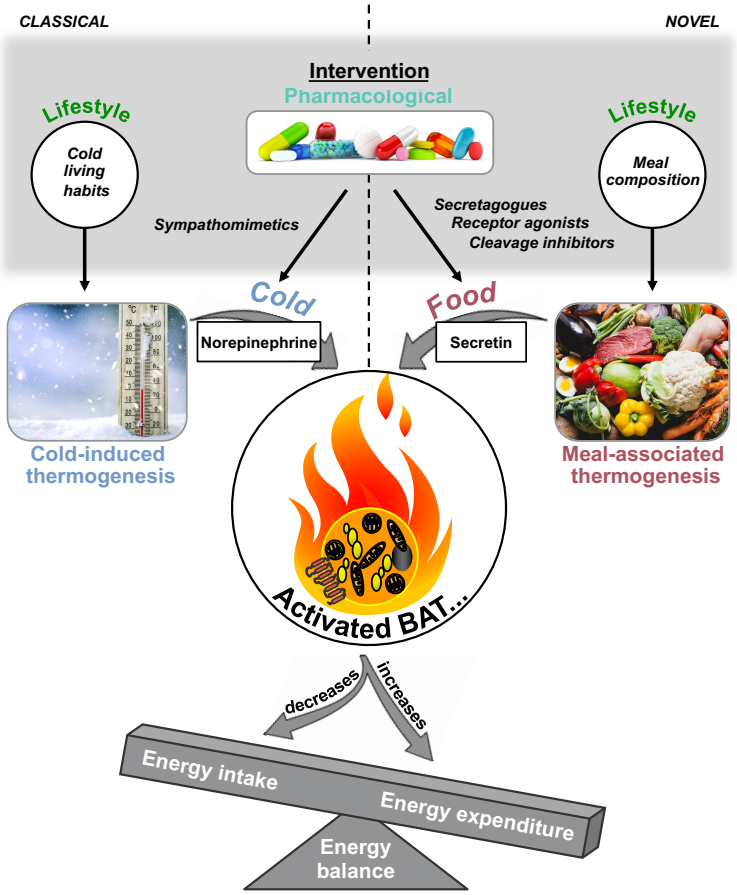

Figure 5: Targeting brown fat in obesity therapy.
Classically, brown adipose tissue (BAT) is activated in response to cold exposure by norepinephrine from the sympathetic nervous system. Additionally, meal-associated BAT thermogenesis is mediated by the gut hormone secretin. Upon activation, BAT increases energy expenditure and decreases energy intake. Thus, it has an overall negative impact on energy balance. To take pharmacological advantage of this, a drug-induced activation of BAT thermogenesis is conceivable. This activation can either be done directly by secretin receptor or β_3-AR agonists, or via an augmentation of prandial released secretin, by means of proper meal composition, secretagogues or cleavage inhibitors.

Nevertheless, the presence and functionality of the secretin-BAT-brain axis in obese individuals is crucial for the success to target it in obesity therapy and thus has to be demonstrated first.

Critical evaluation of brown fat activation in obesity therapy

When considering BAT as target for obesity treatment, it has to be taken into account, that the incidence of active BAT is promoted by age, sex, body mass, plasma glucose, time of season, outdoor temperature and certain drugs taken by patients (Carey et al., 2013; Hanssen et al., 2015; Lee et al., 2010; Nedergaard et al., 2010; Ouellet et al., 2011; Persichetti et al., 2013; Skillen et al., 2012). Although there is some evidence, that the prevalence of brown fat is not affected by body mass index, there seems to be no doubt that active BAT declines with age (Gerngross et al., 2017). Thus, in addition to the usual obstacles of bringing a concept into therapeutic application, the challenge here is even double: Not only must the thermogenic process be activated, but ideally a drug would also increase the total mass and oxidative

capacity of BAT in the human body, since this can be considered to be proportional to the effect size of BAT activity.

To date it is unclear whether sufficient brown fat capacity for energy expenditure can be recruited in people with obesity to reduce weight effectively (Marlatt and Ravussin, 2017). In the positive case, this would require that increased brown fat thermogenesis is not fully compensated by increasing food intake (Cannon and Nedergaard, 2009) as already discussed above. Based on the results of the present study compensation mechanisms seem to be rather negligible due to the dual effect of BAT on energy balance. Of course, the capacity or potential of BAT to burn calories must be carefully examined. Calculations based on total estimated brown fat mass obtained from PET-CT scans and substrate utilization (Ma and Foster, 1986) came to the conclusion that BAT would burn an amount of energy equivalent to approximately 4.1 kg adipose tissue over the course of one year, if it is fully activated (Virtanen et al., 2009). Since BAT mass may have been underestimated in these seminal studies a decade ago (Gerngross et al., 2017), it seems feasible to expect a significant contribution of BAT to the defense of energy balance in humans. For sure, dependent on the degree of obesity, targeting BAT as sole treatment for the disease may not be sufficient. However it can at least support weight loss and definitely counteract the positive weight trend during aging, which is approximately 0.5 – 1 kg/year (Dutton et al., 2016; Norman et al., 2003), especially due to its dual effect on energy balance.

Conclusion and Outlook

BAT has seen a renaissance in obesity research, especially since the discovery of functional brown fat in humans. The capacity of this heater organ to increase resting metabolic rate has attracted great attention. The present study gives an impetus to rethink the role of BAT as a mere catabolic heater organ. The fact, that the activation of a gut-BAT-brain axis not only increases energy expenditure but also induces satiation, qualifies it as an attractive target for the treatment of obesity. Any stimulus of brown adipose tissue may potentially induce satiation, but especially targeting the secretin-BAT-brain axis may allow a natural manipulation of energy balance without causing severe side effects. A further investigation of this mechanism, in particular the transfer of information from BAT to the brain may reveal new indications for a more effective induction of satiation. Based on the findings of this study favoring the hypothesis that heat production is responsible for feedback signals to the brain, one may think of a specific up-heating of brain-near regions by e.g. means of a scarf to achieve satiation without directly interfering with the body. Thus, in this PhD project not only novel non-adrenergic activators of brown fat have been revealed, but even more importantly the perspective of BAT in energy balance has been updated and thereby new possibilities of developing obesity therapies though BAT activation have been established.

5 REFERENCE LIST

Ambery, P., Parker, V.E., Stumvoll, M., Posch, M.G., Heise, T., Plum-Moerschel, L., Tsai, L.F., Robertson, D., Jain, M., Petrone, M.*, et al.* (2018). MEDI0382, a GLP-1 and glucagon receptor dual agonist, in obese or overweight patients with type 2 diabetes: a randomised, controlled, double-blind, ascending dose and phase 2a study. Lancet *391*, 2607-2618.

Arch, J.R. (2008). The discovery of drugs for obesity, the metabolic effects of leptin and variable receptor pharmacology: perspectives from beta3-adrenoceptor agonists. Naunyn Schmiedebergs Arch Pharmacol *378*, 225-240.

Au-Yong, I.T., Thorn, N., Ganatra, R., Perkins, A.C., and Symonds, M.E. (2009). Brown adipose tissue and seasonal variation in humans. Diabetes *58*, 2583-2587.

Bartelt, A., Bruns, O.T., Reimer, R., Hohenberg, H., Ittrich, H., Peldschus, K., Kaul, M.G., Tromsdorf, U.I., Weller, H., Waurisch, C.*, et al.* (2011). Brown adipose tissue activity controls triglyceride clearance. Nature medicine *17*, 200-205.

Bartelt, A., and Heeren, J. (2014). Adipose tissue browning and metabolic health. Nat Rev Endocrinol *10*, 24-36.

Bayliss, W.M., and Starling, E.H. (1902). The mechanism of pancreatic secretion. The Journal of physiology *28*, 325-353.

Beiroa, D., Imbernon, M., Gallego, R., Senra, A., Herranz, D., Villarroya, F., Serrano, M., Ferno, J., Salvador, J., Escalada, J.*, et al.* (2014). GLP-1 agonism stimulates brown adipose tissue thermogenesis and browning through hypothalamic AMPK. Diabetes *63*, 3346-3358.

Bista, B., and Beck, N. (2014). Cushing syndrome. Indian J Pediatr *81*, 158-164.

Blessing, W., Mohammed, M., and Ootsuka, Y. (2013). Brown adipose tissue thermogenesis, the basic rest-activity cycle, meal initiation, and bodily homeostasis in rats. Physiology & behavior *121*, 61-69.

Blouet, C., and Schwartz, G.J. (2012). Duodenal lipid sensing activates vagal afferents to regulate non-shivering brown fat thermogenesis in rats. PloS one *7*, e51898.

Blundell, J.E., Stubbs, R.J., Hughes, D.A., Whybrow, S., and King, N.A. (2003). Cross talk between physical activity and appetite control: does physical activity stimulate appetite? The Proceedings of the Nutrition Society *62*, 651-661.

Bordicchia, M., Liu, D., Amri, E.Z., Ailhaud, G., Dessi-Fulgheri, P., Zhang, C., Takahashi, N., Sarzani, R., and Collins, S. (2012). Cardiac natriuretic peptides act via p38 MAPK to induce the brown fat thermogenic program in mouse and human adipocytes. The Journal of clinical investigation *122*, 1022-1036.

Braun, K., Oeckl, J., Westermeier, J., Li, Y., and Klingenspor, M. (2018). Non-adrenergic control of lipolysis and thermogenesis in adipose tissues. J Exp Biol *221*.

Brobeck, J.R. (1948). Food Intake as a Mechanism of Temperature Regulation. The Yale Journal of Biology and Medicine *20*, 545-552.

Buhl, A.M., Johnson, N.L., Dhanasekaran, N., and Johnson, G.L. (1995). G alpha 12 and G alpha 13 stimulate Rho-dependent stress fiber formation and focal adhesion assembly. The Journal of biological chemistry *270*, 24631-24634.

Butcher, R.W., and Carlson, L.A. (1970). Effects of secretin on fat mobilizing lipolysis and cyclic AMP levels in rat adipose tissue. Acta physiologica Scandinavica *79*, 559-563.

Cannon, B., and Nedergaard, J. (2004). Brown adipose tissue: function and physiological significance. Physiological reviews *84*, 277-359.

Cannon, B., and Nedergaard, J. (2009). Thermogenesis challenges the adipostat hypothesis for body-weight control. The Proceedings of the Nutrition Society *68*, 401-407.

Carey, A.L., Formosa, M.F., Van Every, B., Bertovic, D., Eikelis, N., Lambert, G.W., Kalff, V., Duffy, S.J., Cherk, M.H., and Kingwell, B.A. (2013). Ephedrine activates brown adipose tissue in lean but not obese humans. Diabetologia *56*, 147-155.

Carey, A.L., and Kingwell, B.A. (2013). Brown adipose tissue in humans: therapeutic potential to combat obesity. Pharmacol Ther *140*, 26-33.

Celi, F.S. (2009). Brown adipose tissue--when it pays to be inefficient. The New England journal of medicine *360*, 1553-1556.

Chaudhri, O., Small, C., and Bloom, S. (2006). Gastrointestinal hormones regulating appetite. Philosophical transactions of the Royal Society of London Series B, Biological sciences *361*, 1187-1209.

Chaudhry, A., and Granneman, J.G. (1999). Differential regulation of functional responses by beta-adrenergic receptor subtypes in brown adipocytes. The American journal of physiology *277*, R147-153.

Cheng, C.Y., Chu, J.Y., and Chow, B.K. (2011). Central and peripheral administration of secretin inhibits food intake in mice through the activation of the melanocortin system. Neuropsychopharmacology *36*, 459-471.

Chondronikola, M., Volpi, E., Borsheim, E., Porter, C., Annamalai, P., Enerback, S., Lidell, M.E., Saraf, M.K., Labbe, S.M., Hurren, N.M.*, et al.* (2014). Brown adipose tissue improves whole-body glucose homeostasis and insulin sensitivity in humans. Diabetes *63*, 4089-4099.

Christensen, C.R., Clark, P.B., and Morton, K.A. (2006). Reversal of hypermetabolic brown adipose tissue in F-18 FDG PET imaging. Clin Nucl Med *31*, 193-196.

Chu, J.Y., Cheng, C.Y., Sekar, R., and Chow, B.K. (2013). Vagal afferent mediates the anorectic effect of peripheral secretin. PloS one *8*, e64859.

Cinti, S. (2005). The adipose organ. Prostaglandins Leukot Essent Fatty Acids *73*, 9-15.

Cinti, S. (2006). The role of brown adipose tissue in human obesity. Nutr Metab Cardiovasc Dis *16*, 569-574.

Coate, K.C., Kliewer, S.A., and Mangelsdorf, D.J. (2014). SnapShot: Hormones of the gastrointestinal tract. Cell *159*, 1478 e1471.

Cohade, C., Mourtzikos, K.A., and Wahl, R.L. (2003). "USA-Fat": prevalence is related to ambient outdoor temperature-evaluation with 18F-FDG PET/CT. Journal of nuclear medicine : official publication, Society of Nuclear Medicine *44*, 1267-1270.

Cousin, B., Cinti, S., Morroni, M., Raimbault, S., Ricquier, D., Penicaud, L., and Casteilla, L. (1992). Occurrence of brown adipocytes in rat white adipose tissue: molecular and morphological characterization. J Cell Sci *103 (Pt 4)*, 931-942.

Cummings, D.E., and Overduin, J. (2007). Gastrointestinal regulation of food intake. The Journal of clinical investigation *117*, 13-23.

Cypess, A.M., Chen, Y.C., Sze, C., Wang, K., English, J., Chan, O., Holman, A.R., Tal, I., Palmer, M.R., Kolodny, G.M.*, et al.* (2012). Cold but not sympathomimetics activates human brown adipose tissue in vivo. Proceedings of the National Academy of Sciences of the United States of America *109*, 10001-10005.

Cypess, A.M., Lehman, S., Williams, G., Tal, I., Rodman, D., Goldfine, A.B., Kuo, F.C., Palmer, E.L., Tseng, Y.H., Doria, A.*, et al.* (2009). Identification and importance of brown adipose tissue in adult humans. The New England journal of medicine *360*, 1509-1517.

Cypess, A.M., Weiner, L.S., Roberts-Toler, C., Franquet Elia, E., Kessler, S.H., Kahn, P.A., English, J., Chatman, K., Trauger, S.A., Doria, A.*, et al.* (2015). Activation of human brown adipose tissue by a beta3-adrenergic receptor agonist. Cell metabolism *21*, 33-38.

Cypess, A.M., White, A.P., Vernochet, C., Schulz, T.J., Xue, R., Sass, C.A., Huang, T.L., Roberts-Toler, C., Weiner, L.S., Sze, C.*, et al.* (2013). Anatomical localization, gene expression profiling and functional characterization of adult human neck brown fat. Nature medicine *19*, 635-639.

Del Mar Gonzalez-Barroso, M., Ricquier, D., and Cassard-Doulcier, A.M. (2000). The human uncoupling protein-1 gene (UCP1): present status and perspectives in obesity research. Obes Rev *1*, 61-72.

Dong, M., Te, J.A., Xu, X., Wang, J., Pinon, D.I., Storjohann, L., Bordner, A.J., and Miller, L.J. (2011). Lactam constraints provide insights into the receptor-bound conformation of secretin and stabilize a receptor antagonist. Biochemistry *50*, 8181-8192.

Dutton, G.R., Kim, Y., Jacobs, D.R., Jr., Li, X., Loria, C.M., Reis, J.P., Carnethon, M., Durant, N.H., Gordon-Larsen, P., Shikany, J.M.*, et al.* (2016). 25-year weight gain in a racially balanced sample of U.S. adults: The CARDIA study. Obesity *24*, 1962-1968.

Fineberg, S.E., Galloway, J.A., Fineberg, N.S., Rathbun, M.J., and Hufferd, S. (1983). Immunogenicity of recombinant DNA human insulin. Diabetologia *25*, 465-469.

Galmozzi, A., Sonne, S.B., Altshuler-Keylin, S., Hasegawa, Y., Shinoda, K., Luijten, I.H.N., Chang, J.W., Sharp, L.Z., Cravatt, B.F., Saez, E.*, et al.* (2014). ThermoMouse: an in vivo model to identify modulators of UCP1 expression in brown adipose tissue. Cell Rep *9*, 1584-1593.

Garcia, C.A., Van Nostrand, D., Atkins, F., Acio, E., Butler, C., Esposito, G., Kulkarni, K., and Majd, M. (2006). Reduction of brown fat 2-deoxy-2-[F-18]fluoro-D-glucose uptake by controlling environmental temperature prior to positron emission tomography scan. Mol Imaging Biol *8*, 24-29.

Gerngross, C., Schretter, J., Klingenspor, M., Schwaiger, M., and Fromme, T. (2017). Active Brown Fat During (18)F-FDG PET/CT Imaging Defines a Patient Group with Characteristic Traits and an Increased Probability of Brown Fat Redetection. Journal of nuclear medicine : official publication, Society of Nuclear Medicine *58*, 1104-1110.

Glick, Z. (1982). Inverse relationship between brown fat thermogenesis and meal size: the thermostatic control of food intake revisited. Physiology & behavior *29*, 1137-1140.

Glick, Z., Teague, R.J., and Bray, G.A. (1981). Brown adipose tissue: thermic response increased by a single low protein, high carbohydrate meal. Science (New York, NY) *213*, 1125-1127.

Gnad, T., Scheibler, S., von Kugelgen, I., Scheele, C., Kilic, A., Glode, A., Hoffmann, L.S., Reverte-Salisa, L., Horn, P., Mutlu, S.*, et al.* (2014). Adenosine activates brown adipose tissue and recruits beige adipocytes via A2A receptors. Nature *516*, 395-399.

Grujic, D., Susulic, V.S., Harper, M.E., Himms-Hagen, J., Cunningham, B.A., Corkey, B.E., and Lowell, B.B. (1997). Beta3-adrenergic receptors on white and brown adipocytes mediate beta3-selective agonist-induced effects on energy expenditure, insulin secretion, and food intake. A study using transgenic and gene knockout mice. The Journal of biological chemistry *272*, 17686-17693.

Guerra, C., Koza, R.A., Yamashita, H., Walsh, K., and Kozak, L.P. (1998). Emergence of brown adipocytes in white fat in mice is under genetic control. Effects on body weight and adiposity. The Journal of clinical investigation *102*, 412-420.

Gurevich, V.V., and Gurevich, E.V. (2019). GPCR Signaling Regulation: The Role of GRKs and Arrestins. Front Pharmacol *10*, 125.

Hall, K.D., Heymsfield, S.B., Kemnitz, J.W., Klein, S., Schoeller, D.A., and Speakman, J.R. (2012). Energy balance and its components: implications for body weight regulation. The American journal of clinical nutrition *95*, 989-994.

Hanssen, M.J., Wierts, R., Hoeks, J., Gemmink, A., Brans, B., Mottaghy, F.M., Schrauwen, P., and van Marken Lichtenbelt, W.D. (2015). Glucose uptake in human brown adipose tissue is impaired upon fasting-induced insulin resistance. Diabetologia *58*, 586-595.

Hany, T.F., Gharehpapagh, E., Kamel, E.M., Buck, A., Himms-Hagen, J., and von Schulthess, G.K. (2002). Brown adipose tissue: a factor to consider in symmetrical tracer uptake in the neck and upper chest region. Eur J Nucl Med Mol Imaging *29*, 1393-1398.

Hauser, A.S., Attwood, M.M., Rask-Andersen, M., Schioth, H.B., and Gloriam, D.E. (2017). Trends in GPCR drug discovery: new agents, targets and indications. Nat Rev Drug Discov *16*, 829-842.

Heinzmann, J.M., Thoeringer, C.K., Knapman, A., Palme, R., Holsboer, F., Uhr, M., Landgraf, R., and Touma, C. (2010). Intrahippocampal corticosterone response in mice selectively bred for extremes in stress reactivity: a microdialysis study. J Neuroendocrinol *22*, 1187-1197.

Heldmaier, G., and Neuweiler, G. (2004). Vergleichende Tierphysiologie, Vol Band 2 (Springer).

Himms-Hagen, J. (1995). Role of brown adipose tissue thermogenesis in control of thermoregulatory feeding in rats: a new hypothesis that links thermostatic and glucostatic hypotheses for control of food intake. Proceedings of the Society for Experimental Biology and Medicine Society for Experimental Biology and Medicine (New York, NY) *208*, 159-169.

Himms-Hagen, J. (2001). Does brown adipose tissue (BAT) have a role in the physiology or treatment of human obesity? Rev Endocr Metab Disord *2*, 395-401.

Himms-Hagen, J., Melnyk, A., Zingaretti, M.C., Ceresi, E., Barbatelli, G., and Cinti, S. (2000). Multilocular fat cells in WAT of CL-316243-treated rats derive directly from white adipocytes. American journal of physiology Cell physiology *279*, C670-681.

Hondares, E., Iglesias, R., Giralt, A., Gonzalez, F.J., Giralt, M., Mampel, T., and Villarroya, F. (2011). Thermogenic activation induces FGF21 expression and release in brown adipose tissue. The Journal of biological chemistry *286*, 12983-12990.

Ishibashi, J., and Seale, P. (2010). Medicine. Beige can be slimming. Science (New York, NY) *328*, 1113-1114.

Khera, R., Murad, M.H., Chandar, A.K., Dulai, P.S., Wang, Z., Prokop, L.J., Loomba, R., Camilleri, M., and Singh, S. (2016). Association of Pharmacological Treatments for Obesity With Weight Loss and Adverse Events: A Systematic Review and Meta-analysis. JAMA *315*, 2424-2434.

King, N.A., Caudwell, P., Hopkins, M., Byrne, N.M., Colley, R., Hills, A.P., Stubbs, J.R., and Blundell, J.E. (2007). Metabolic and behavioral compensatory responses to exercise interventions: barriers to weight loss. Obesity *15*, 1373-1383.

Klepac, K., Kilic, A., Gnad, T., Brown, L.M., Herrmann, B., Wilderman, A., Balkow, A., Glode, A., Simon, K., Lidell, M.E.*, et al.* (2016). The Gq signalling pathway inhibits brown and beige adipose tissue. Nat Commun *7*, 10895.

Klingenspor, M. (2019). Secretin Links Brown Fat to Food Intake: New Perspectives for Targeting Energy Balance in Humans. Obesity *27*, 875-877.

Klingenspor, M., Bast, A., Bolze, F., Li, Y., Maurer, S.F., Schweizer, S., Willershäuser, M., and Fromme, T. (2017). Brown Adipose Tissue. In Adipose tissue biology, M.E. Symonds, ed. (Springer, cham), pp. 91-147.

Kobilka, B.K. (2011). Structural insights into adrenergic receptor function and pharmacology. Trends Pharmacol Sci *32*, 213-218.

Lacroix, A., Feelders, R.A., Stratakis, C.A., and Nieman, L.K. (2015). Cushing's syndrome. Lancet *386*, 913-927.

Larsen, T.M., Toubro, S., van Baak, M.A., Gottesdiener, K.M., Larson, P., Saris, W.H., and Astrup, A. (2002). Effect of a 28-d treatment with L-796568, a novel beta(3)-adrenergic receptor agonist, on energy expenditure and body composition in obese men. The American journal of clinical nutrition *76*, 780-788.

Lasar, D., Julius, A., Fromme, T., and Klingenspor, M. (2013). Browning attenuates murine white adipose tissue expansion during postnatal development. Biochimica et biophysica acta *1831*, 960-968.

Latek, D., Modzelewska, A., Trzaskowski, B., Palczewski, K., and Filipek, S. (2012). G protein-coupled receptors--recent advances. Acta Biochim Pol *59*, 515-529.

Lee, P., Greenfield, J.R., Ho, K.K., and Fulham, M.J. (2010). A critical appraisal of the prevalence and metabolic significance of brown adipose tissue in adult humans. American journal of physiology Endocrinology and metabolism *299*, E601-606.

Lefkowitz, R.J. (2007). Seven transmembrane receptors: something old, something new. Acta Physiol (Oxf) *190*, 9-19.

Li, Y., Bolze, F., Fromme, T., and Klingenspor, M. (2014a). Intrinsic differences in BRITE adipogenesis of primary adipocytes from two different mouse strains. Biochimica et biophysica acta *1841*, 1345-1352.

Li, Y., Fromme, T., and Klingenspor, M. (2017). Meaningful respirometric measurements of UCP1-mediated thermogenesis. Biochimie *134*, 56-61.

Li, Y., Fromme, T., Schweizer, S., Schottl, T., and Klingenspor, M. (2014b). Taking control over intracellular fatty acid levels is essential for the analysis of thermogenic function in cultured primary brown and brite/beige adipocytes. EMBO Rep *15*, 1069-1076.

Ma, S.W., and Foster, D.O. (1986). Uptake of glucose and release of fatty acids and glycerol by rat brown adipose tissue in vivo. Can J Physiol Pharmacol *64*, 609-614.

Malik, M., van Gelderen, E.M., Lee, J.H., Kowalski, D.L., Yen, M., Goldwater, R., Mujais, S.K., Schaddelee, M.P., de Koning, P., Kaibara, A.*, et al.* (2012). Proarrhythmic safety of repeat doses of mirabegron in healthy subjects: a randomized, double-blind, placebo-, and active-controlled thorough QT study. Clin Pharmacol Ther *92*, 696-706.

Marette, A., and Bukowiecki, L.J. (1990). Mechanism of norepinephrine stimulation of glucose transport in isolated rat brown adipocytes. Int J Obes *14*, 857-867.

Marlatt, K.L., and Ravussin, E. (2017). Brown Adipose Tissue: an Update on Recent Findings. Curr Obes Rep *6*, 389-396.

Maurer, S.F., Fromme, T., Grossman, L.I., Huttemann, M., and Klingenspor, M. (2015). The brown and brite adipocyte marker Cox7a1 is not required for non-shivering thermogenesis in mice. Sci Rep *5*, 17704.

Meyer, C.W., Willershauser, M., Jastroch, M., Rourke, B.C., Fromme, T., Oelkrug, R., Heldmaier, G., and Klingenspor, M. (2010). Adaptive thermogenesis and thermal conductance in wild-type and UCP1-KO mice. American journal of physiology Regulatory, integrative and comparative physiology *299*, R1396-1406.

Miegueu, P., Cianflone, K., Richard, D., and St-Pierre, D.H. (2013). Effect of secretin on preadipocyte, differentiating and mature adipocyte functions. International journal of obesity *37*, 366-374.

Mole, P.A. (1990). Impact of energy intake and exercise on resting metabolic rate. Sports Med *10*, 72-87.

Nedergaard, J., Bengtsson, T., and Cannon, B. (2007). Unexpected evidence for active brown adipose tissue in adult humans. American journal of physiology Endocrinology and metabolism *293*, E444-452.

Nedergaard, J., Bengtsson, T., and Cannon, B. (2010). Three years with adult human brown adipose tissue. Annals of the New York Academy of Sciences *1212*, E20-36.

Neves, S.R., Ram, P.T., and Iyengar, R. (2002). G protein pathways. Science (New York, NY) *296*, 1636-1639.

Norman, J.E., Bild, D., Lewis, C.E., Liu, K., West, D.S., and Study, C. (2003). The impact of weight change on cardiovascular disease risk factors in young black and white adults: the CARDIA study. International journal of obesity and related metabolic disorders : journal of the International Association for the Study of Obesity *27*, 369-376.

Ouellet, V., Routhier-Labadie, A., Bellemare, W., Lakhal-Chaieb, L., Turcotte, E., Carpentier, A.C., and Richard, D. (2011). Outdoor temperature, age, sex, body mass index, and diabetic status determine the prevalence, mass, and glucose-uptake activity of 18F-FDG-detected BAT in humans. The Journal of clinical endocrinology and metabolism *96*, 192-199.

Parysow, O., Mollerach, A.M., Jager, V., Racioppi, S., San Roman, J., and Gerbaudo, V.H. (2007). Low-dose oral propranolol could reduce brown adipose tissue F-18 FDG uptake in patients undergoing PET scans. Clin Nucl Med *32*, 351-357.

Persichetti, A., Sciuto, R., Rea, S., Basciani, S., Lubrano, C., Mariani, S., Ulisse, S., Nofroni, I., Maini, C.L., and Gnessi, L. (2013). Prevalence, mass, and glucose-uptake activity of (1)(8)F-FDG-detected brown adipose tissue in humans living in a temperate zone of Italy. PloS one *8*, e63391.

Petrovic, N., Walden, T.B., Shabalina, I.G., Timmons, J.A., Cannon, B., and Nedergaard, J. (2010). Chronic peroxisome proliferator-activated receptor gamma (PPARgamma) activation of epididymally derived white adipocyte cultures reveals a population of thermogenically competent, UCP1-containing adipocytes molecularly distinct from classic brown adipocytes. The Journal of biological chemistry *285*, 7153-7164.

Pilitsi, E., Farr, O.M., Polyzos, S.A., Perakakis, N., Nolen-Doerr, E., Papathanasiou, A.E., and Mantzoros, C.S. (2019). Pharmacotherapy of obesity: Available medications and drugs under investigation. Metabolism: clinical and experimental *92*, 170-192.

Rauch, J.C., and Hayward, J.S. (1969). Topography and vascularization of brown fat in a small nonhibernator (deer mouse, Peromyscus maniculatus). Can J Zool *47*, 1301-1314.

Reber, J., Willershauser, M., Karlas, A., Paul-Yuan, K., Diot, G., Franz, D., Fromme, T., Ovsepian, S.V., Beziere, N., Dubikovskaya, E.*, et al.* (2018). Non-invasive Measurement of Brown Fat Metabolism Based on Optoacoustic Imaging of Hemoglobin Gradients. Cell metabolism *27*, 689-701 e684.

Redman, L.M., de Jonge, L., Fang, X., Gamlin, B., Recker, D., Greenway, F.L., Smith, S.R., and Ravussin, E. (2007). Lack of an effect of a novel beta3-adrenoceptor agonist, TAK-677, on energy metabolism in obese individuals: a double-blind, placebo-controlled randomized study. The Journal of clinical endocrinology and metabolism *92*, 527-531.

Robidoux, J., Kumar, N., Daniel, K.W., Moukdar, F., Cyr, M., Medvedev, A.V., and Collins, S. (2006). Maximal beta3-adrenergic regulation of lipolysis involves Src and epidermal growth factor receptor-dependent ERK1/2 activation. The Journal of biological chemistry *281*, 37794-37802.

Rochon, L., and Bukowiecki, L.J. (1990). Alterations in adipocyte response to lipolytic hormones during cold acclimation. The American journal of physiology *258*, C835-840.

Rothwell, N.J., and Stock, M.J. (1979). A role for brown adipose tissue in diet-induced thermogenesis. Nature *281*, 31-35.

Rudman, D., and Del Rio, A.E. (1969). Lipolytic activity of a peptide fragment of porcine secretin. Endocrinology *85*, 610-611.

Saito, M., Okamatsu-Ogura, Y., Matsushita, M., Watanabe, K., Yoneshiro, T., Nio-Kobayashi, J., Iwanaga, T., Miyagawa, M., Kameya, T., Nakada, K*., et al.* (2009). High incidence of metabolically active brown adipose tissue in healthy adult humans: effects of cold exposure and adiposity. Diabetes *58*, 1526-1531.

Saito, M., and Yoneshiro, T. (2013). Capsinoids and related food ingredients activating brown fat thermogenesis and reducing body fat in humans. Curr Opin Lipidol *24*, 71-77.

Santos, R., Ursu, O., Gaulton, A., Bento, A.P., Donadi, R.S., Bologa, C.G., Karlsson, A., Al-Lazikani, B., Hersey, A., Oprea, T.I*., et al.* (2017). A comprehensive map of molecular drug targets. Nat Rev Drug Discov *16*, 19-34.

Schellekens, H., and Casadevall, N. (2004). Immunogenicity of recombinant human proteins: causes and consequences. J Neurol *251 Suppl 2*, II4-9.

Sekar, R., and Chow, B.K. (2014). Lipolytic actions of secretin in mouse adipocytes. Journal of lipid research *55*, 190-200.

Sengenes, C., Berlan, M., De Glisezinski, I., Lafontan, M., and Galitzky, J. (2000). Natriuretic peptides: a new lipolytic pathway in human adipocytes. FASEB journal : official publication of the Federation of American Societies for Experimental Biology *14*, 1345-1351.

Sengenes, C., Zakaroff-Girard, A., Moulin, A., Berlan, M., Bouloumie, A., Lafontan, M., and Galitzky, J. (2002). Natriuretic peptide-dependent lipolysis in fat cells is a primate specificity. American journal of physiology Regulatory, integrative and comparative physiology *283*, R257-265.

Shih, M.F., and Taberner, P.V. (1995). Selective activation of brown adipocyte hormone-sensitive lipase and cAMP production in the mouse by beta 3-adrenoceptor agonists. Biochem Pharmacol *50*, 601-608.

Skillen, A., Currie, G.M., and Wheat, J.M. (2012). Thermal control of brown adipose tissue in 18F-FDG PET. J Nucl Med Technol *40*, 99-103.

Soderlund, V., Larsson, S.A., and Jacobsson, H. (2007). Reduction of FDG uptake in brown adipose tissue in clinical patients by a single dose of propranolol. Eur J Nucl Med Mol Imaging *34*, 1018-1022.

Susulic, V.S., Frederich, R.C., Lawitts, J., Tozzo, E., Kahn, B.B., Harper, M.E., Himms-Hagen, J., Flier, J.S., and Lowell, B.B. (1995). Targeted disruption of the beta 3-adrenergic receptor gene. The Journal of biological chemistry *270*, 29483-29492.

Takasu, T., Ukai, M., Sato, S., Matsui, T., Nagase, I., Maruyama, T., Sasamata, M., Miyata, K., Uchida, H., and Yamaguchi, O. (2007). Effect of (R)-2-(2-aminothiazol-4-yl)-4'-{2-[(2-hydroxy-2-phenylethyl)amino]ethyl} acetanilide (YM178), a novel selective beta3-adrenoceptor agonist, on bladder function. The Journal of pharmacology and experimental therapeutics *321*, 642-647.

Tseng, Y.H., Cypess, A.M., and Kahn, C.R. (2010). Cellular bioenergetics as a target for obesity therapy. Nat Rev Drug Discov *9*, 465-482.

U Din, M., Saari, T., Raiko, J., Kudomi, N., Maurer, S.F., Lahesmaa, M., Fromme, T., Amri, E.Z., Klingenspor, M., Solin, O*., et al.* (2018). Postprandial Oxidative Metabolism of Human Brown Fat Indicates Thermogenesis. Cell metabolism *28*, 207-216 e203.

Ursino, M.G., Vasina, V., Raschi, E., Crema, F., and De Ponti, F. (2009). The beta3-adrenoceptor as a therapeutic target: current perspectives. Pharmacol Res *59*, 221-234.

Valet, P., Berlan, M., Beauville, M., Crampes, F., Montastruc, J.L., and Lafontan, M. (1990). Neuropeptide Y and peptide YY inhibit lipolysis in human and dog fat cells through a pertussis toxin-sensitive G protein. The Journal of clinical investigation *85*, 291-295.

van den Beukel, J.C., Grefhorst, A., Quarta, C., Steenbergen, J., *et al.* (2014). Direct activating effects of adrenocorticotropic hormone (ACTH) on brown adipose tissue are attenuated by corticosterone. FASEB journal : official publication of the Federation of American Societies for Experimental Biology *28*, 4857-4867.

van der Lans, A.A., Hoeks, J., Brans, B., Vijgen, G.H., Visser, M.G., Vosselman, M.J., Hansen, J., Jorgensen, J.A., Wu, J., Mottaghy, F.M.*, et al.* (2013). Cold acclimation recruits human brown fat and increases nonshivering thermogenesis. The Journal of clinical investigation *123*, 3395-3403.

van Marken Lichtenbelt, W.D., Vanhommerig, J.W., Smulders, N.M., Drossaerts, J.M., Kemerink, G.J., Bouvy, N.D., Schrauwen, P., and Teule, G.J. (2009). Cold-activated brown adipose tissue in healthy men. The New England journal of medicine *360*, 1500-1508.

Velazquez-Villegas, L.A., Perino, A., Lemos, V., Zietak, M., Nomura, M., Pols, T.W.H., and Schoonjans, K. (2018). TGR5 signalling promotes mitochondrial fission and beige remodelling of white adipose tissue. Nat Commun *9*, 245.

Virtanen, K.A., Lidell, M.E., Orava, J., Heglind, M., Westergren, R., Niemi, T., Taittonen, M., Laine, J., Savisto, N.J., Enerback, S.*, et al.* (2009). Functional brown adipose tissue in healthy adults. The New England journal of medicine *360*, 1518-1525.

Virtue, S., and Vidal-Puig, A. (2013). Assessment of brown adipose tissue function. Front Physiol *4*, 128.

Vosselman, M.J., Brans, B., van der Lans, A.A., Wierts, R., van Baak, M.A., Mottaghy, F.M., Schrauwen, P., and van Marken Lichtenbelt, W.D. (2013). Brown adipose tissue activity after a high-calorie meal in humans. The American journal of clinical nutrition *98*, 57-64.

Vosselman, M.J., van der Lans, A.A., Brans, B., Wierts, R., van Baak, M.A., Schrauwen, P., and van Marken Lichtenbelt, W.D. (2012). Systemic beta-adrenergic stimulation of thermogenesis is not accompanied by brown adipose tissue activity in humans. Diabetes *61*, 3106-3113.

Wang, H., Willershauser, M., Karlas, A., Gorpas, D., Reber, J., Ntziachristos, V., Maurer, S., Fromme, T., Li, Y., and Klingenspor, M. (2019). A dual Ucp1 reporter mouse model for imaging and quantitation of brown and brite fat recruitment. Mol Metab *20*, 14-27.

Wang, Y., Falting, J.M., Mattsson, C.L., Holmstrom, T.E., and Nedergaard, J. (2013). In brown adipocytes, adrenergically induced beta(1)-/beta(3)-(Gs)-, alpha(2)-(Gi)- and alpha(1)-(Gq)-signalling to Erk1/2 activation is not mediated via EGF receptor transactivation. Exp Cell Res *319*, 2718-2727.

Watanabe, M., Houten, S.M., Mataki, C., Christoffolete, M.A., Kim, B.W., Sato, H., Messaddeq, N., Harney, J.W., Ezaki, O., Kodama, T.*, et al.* (2006). Bile acids induce energy expenditure by promoting intracellular thyroid hormone activation. Nature *439*, 484-489.

Welle, S., Lilavivat, U., and Campbell, R.G. (1981). Thermic effect of feeding in man: increased plasma norepinephrine levels following glucose but not protein or fat consumption. Metabolism: clinical and experimental *30*, 953-958.

Wettschureck, N., and Offermanns, S. (2005). Mammalian G proteins and their cell type specific functions. Physiological reviews *85*, 1159-1204.

Weyer, C., Tataranni, P.A., Snitker, S., Danforth, E., Jr., and Ravussin, E. (1998). Increase in insulin action and fat oxidation after treatment with CL 316,243, a highly selective beta3-adrenoceptor agonist in humans. Diabetes *47*, 1555-1561.

White, J.E., and Engel, F.L. (1958). Lipolytic action of corticotropin on rat adipose tissue in vitro. The Journal of clinical investigation *37*, 1556-1563.

Williams, K., Wray, J.A., and Wheeler, D.M. (2012). Intravenous secretin for autism spectrum disorders (ASD). Cochrane Database Syst Rev, CD003495.

Yoneshiro, T., Aita, S., Matsushita, M., Kayahara, T., Kameya, T., Kawai, Y., Iwanaga, T., and Saito, M. (2013). Recruited brown adipose tissue as an antiobesity agent in humans. The Journal of clinical investigation *123*, 3404-3408.

York, D.A., and Al-Baker, I. (1984). Effect of corticotropin on brown adipose tissue mitochondrial GDP binding in obese rats. The Biochemical journal *223*, 263-266.

Young, P., Arch, J.R., and Ashwell, M. (1984). Brown adipose tissue in the parametrial fat pad of the mouse. FEBS letters *167*, 10-14.

WHO 2013. World Health Organization. Guidelines on the Quality, Safety and Efficacy of Biotherapeutic Protein Products Prepared by Recombinant DNA Technology; World Health Organization: Geneva, Switzerland, 2013.

WHO 2016. Obesity fact sheet N°375.

Zimmermann, R., Strauss, J.G., Haemmerle, G., Schoiswohl, G., Birner-Gruenberger, R., Riederer, M., Lass, A., Neuberger, G., Eisenhaber, F., Hermetter, A.*, et al.* (2004). Fat mobilization in adipose tissue is promoted by adipose triglyceride lipase. Science (New York, NY) *306*, 1383-1386.

6 APPENDIX

6.1 ORIGINAL PUBLICATIONS

© 2018. Published by The Company of Biologists Ltd | Journal of Experimental Biology (2018) 221, jeb165381. doi:10.1242/jeb.165381

REVIEW

Non-adrenergic control of lipolysis and thermogenesis in adipose tissues

Katharina Braun[1,2,3], Josef Oeckl[1,2,3], Julia Westermeier[1,2], Yongguo Li[1,2] and Martin Klingenspor[1,2,3,*]

ABSTRACT

The enormous plasticity of adipose tissues, to rapidly adapt to altered physiological states of energy demand, is under neuronal and endocrine control. In energy balance, lipolysis of triacylglycerols and re-esterification of free fatty acids are opposing processes operating in parallel at identical rates, thus allowing a more dynamic transition from anabolism to catabolism, and vice versa. In response to alterations in the state of energy balance, one of the two processes predominates, enabling the efficient mobilization or storage of energy in a negative or positive energy balance, respectively. The release of noradrenaline from the sympathetic nervous system activates lipolysis in a depot-specific manner by initiating the canonical adrenergic receptor–G_s-protein–adenylyl cyclase–cyclic adenosine monophosphate–protein kinase A pathway, targeting proteins of the lipolytic machinery associated with the interface of the lipid droplets. In brown and brite adipocytes, lipolysis stimulated by this signaling pathway is a prerequisite for the activation of non-shivering thermogenesis. Free fatty acids released by lipolysis are direct activators of uncoupling protein 1-mediated leak respiration. Thus, pro- and anti-lipolytic mediators are bona fide modulators of thermogenesis in brown and brite adipocytes. In this Review, we discuss adrenergic and non-adrenergic mechanisms controlling lipolysis and thermogenesis and provide a comprehensive overview of pro- and anti-lipolytic mediators.

KEY WORDS: Brown adipocytes, Hormones, Receptors, Signalling pathways, Uncoupling protein 1, Energy balance

Introduction

Lipids encompass a large variety of molecules with diverse functions, including simple lipids (triacylglycerols and waxes), compound lipids (e.g. phospholipids and sphingolipids), steroids, fatty acids and terpenes. The triacylglycerols, also known as fat, consist of three fatty acids esterified to a glycerol backbone molecule. On a quantity basis, fat makes up 90% of all lipids in the human body and constitutes the major storage form of chemical energy. In the so called 'reference man' with a body mass of 70 kg, the body fat compartment makes up >70% of the total body energy content (12 kg=470 MJ). These fats are stored in lipid droplets (fat droplets), which can be found in every cell type but are most abundant in adipocytes. In humans, more than 80% of total body fat is stored in adipocytes located in subcutaneous adipose tissue depots and less than 20% is stored in adipocytes in intra-abdominal depots.

Stored fat mainly originates from dietary fat absorbed in the intestine and from *de novo* lipogenesis in the liver. As transport vehicles for triacylglycerol, lipid-rich lipoproteins are secreted from the gut into the lymphatic system (chylomicrons) or from the liver into the sinusoidal hepatic capillaries (very-low-density lipoprotein, VLDL). Once in circulation, the fat-laden chylomicrons and VLDLs are hydrolyzed by lipoprotein lipase in the capillary endothelium of adipose tissues. Fatty acid transporters, such as platelet glycoprotein 4 (CD36) and fatty acid transport proteins (FATPs), deliver free fatty acids (FFAs) into adipocytes. Once in the cell, fatty acids are re-esterified with glycerol and deposited as triacylglycerol in lipid droplets. *De novo* lipogenesis in adipocytes is normally low but may rise significantly in nutritional states of limited fatty acid import and excess glucose supply to adipocytes. Insulin is the only endocrine signal that orchestrates these anabolic processes in fat metabolism and promotes fat storage in adipocytes. The enormous capacity for hypertrophy, i.e. cell expansion owing to fat storage, is a unique hallmark of adipocytes, as illustrated by maximal cell diameters in the range of 10–180 µm (Lafontan, 2012). The ability of adipose tissue to expand is further augmented by hyperplastic growth, which recruits adipocytes from a progenitor cell pool residing in stem cell niches of the tissue.

Adipocytes not only accumulate but also mobilize large amounts of fatty acids from triacylglycerol stored in lipid droplets. Therefore, the size and number of lipid droplets change dynamically, mostly in response to variations in dietary caloric intake and energy expenditure. Thus, the key function of adipocytes is energy storage and mobilization of stored energy according to the energy requirements of the major high-metabolic rate organs, such as the heart, skeletal muscle and liver. Like many other metabolic pathways, these opposing processes are finely tuned by futile cycling. The breakdown of triacylglycerols and re-esterification of fatty acids occur in parallel with only a fraction of the fatty acids released from triacylglycerols being exported into circulation. It is generally assumed that futile cycling will allow a more dynamic transition from anabolism to catabolism, or vice versa, enabling larger changes in net flux through the pathway. Moreover, futile cycling fine tunes the cellular control of FFA levels and, thereby, prevents lipotoxicity. In addition, futile cycles also represent adenosine triphosphate (ATP) sinks, driving additional need for the regeneration of adenosine diphosphate by mitochondrial oxidative phosphorylation, and result in higher metabolic flux rates associated with increased heat dissipation. Futile ATP sinks may contribute to thermoregulatory heat production in endotherms and the discussion about their contribution to whole-body heat production has been revitalized recently (Flachs et al., 2017; Kazak et al., 2015; Rohm et al., 2016).

In catabolic states, such as fasting, exercise or cold exposure, endogenous stores of energy are mobilized. In respect to

[1]Chair of Molecular Nutritional Medicine, Technical University of Munich, TUM School of Life Sciences Weihenstephan, Gregor-Mendel-Str. 2, D-85354 Freising, Germany. [2]EKFZ – Else Kröner-Fresenius Center for Nutritional Medicine, Technical University of Munich, Gregor-Mendel-Str. 2, D-85354 Freising, Germany. [3]ZIEL – Institute for Food & Health, Technical University of Munich, Gregor-Mendel-Str. 2, D-85354 Freising, Germany.

*Author for correspondence (mk@tum.de)

M.K., 0000-0002-4502-6664

Journal of Experimental Biology

REVIEW Journal of Experimental Biology (2018) 221, jeb165381. doi:10.1242/jeb.165381

carbohydrates, the storage capacity of the body is low. Approximately 75 g of glycogen can be mobilized from storage granules in hepatocytes worth ∼1275 kJ, which can only fuel the resting metabolic rate for a couple of hours (Van Itallie et al., 1953), and is depleted even faster during exercise. To meet energetic demand, lipolysis is activated; the rate of lipolysis largely exceeds the rate of re-esterification, thereby promoting a net increase in the export of fatty acids and glycerol out of the adipocyte. Once exported into the extracellular matrix, fatty acids can either reenter the adipocyte or they cross the endothelial barrier into the capillary lumen and are transported, bound to serum albumin, to the peripheral tissues with highest metabolic demands. At the same time, the turnover of proteins is reduced and amino acids are spared for gluconeogenesis.

Activation of lipolysis is conveyed by the sympathetic nervous system (SNS). Post-ganglionic sympathetic nerve fibers innervate adipose tissue depots that are mainly located at subcutaneous, intra-abdominal and intra-thoracic sites, whereas parasympathetic innervation is mostly negligible (Vaughan et al., 2014). The tone of the sympathetic innervation exerts master control on lipolysis by the release of noradrenaline (also known as norepinephrine) and from varicosities and synapses in the parenchyma of adipose tissues, as demonstrated by surgical and chemical denervation experiments and retrograde tracing of sympathetic nerve fibers innervating adipose tissues (Vaughan et al., 2014). Experiments with adrenodemedullated rats underline that the contribution of circulating noradrenaline and adrenaline (also known as epinephrine) is negligible (Paschoalini and Migliorini, 1990). The functionality of the sympathetic nerves to activate lipolysis was verified recently *in vivo* using optogenetic depolarization of the sympathetic nerves projecting into the inguinal subcutaneous white fat depot. Unilateral nerve depolarization stimulated phosphorylation of HSL and reduced fat depot mass when applied chronically (Zeng et al., 2015). Melanocortins signaling via the melanocortin 4 receptor (MC4R) in the central nervous system (CNS) play a key role in regulating SNS activity (Berglund et al., 2014). Central stimulation of melanocortin receptor signaling in the brain, which mimics the physiological neuroendocrine sensation of a positive energy balance, increases the activity of postganglionic sympathetic nerves in a differential depot-specific manner. Sympathetic drive is increased selectively in inguinal, retroperitoneal and dorsosubcutaneous white adipose tissue (WAT) depots, but not in the epididymal WAT depot (Brito et al., 2007). Thus, in general, there is convincing evidence that the CNS–SNS axis plays a role in modulating lipolysis in adipose tissue. Various hormones secreted by peripheral tissues, such as glucagon-like peptide-1 (GLP-1) and leptin, regulate fat metabolism via the CNS–SNS axis (Lockie et al., 2012; Zeng et al., 2015). Efforts to devise pharmacological treatments for metabolic disease by selectively targeting the CNS–SNS–adipose axis have turned out to be complex. Nonselective activators of the SNS successfully promoted negative energy balance and weight loss; however, the cardiovascular side-effects prevented their use in clinical settings (Yen and Ewald, 2012). The search for other activators of adipose tissue operating in an SNS-independent fashion may be a promising alternative.

In isolated adipocytes, adrenaline and noradrenaline have dual effects on lipolysis owing to the cell surface expression of different adrenergic receptor (AR) paralogs with either anti- or pro-lipolytic action. At low ligand concentrations, their high affinity to α2-ARs triggers anti-lipolytic action, whereas at higher concentrations, the pro-lipolytic action mediated by highly abundant β-ARs prevails (Bousquet-Melou et al., 1995). These G-protein coupled β-receptors activate adipose triglyceride lipase (ATGL) through a signaling pathway targeting 5′-adenosine monophosphate-activated protein kinase and hormone-sensitive lipase (HSL) through the canonical AR–G_s–adenylyl cyclase–cyclic adenosine monophosphate (cAMP)–protein kinase A (PKA) pathway by phosphorylation.

Beyond their enormous capacity for hypertrophy and hyperplasia, adipose tissues are characterized by morphological and functional plasticity (Cannon and Nedergaard, 2012). Adipocytes comprise three subtypes: white adipocytes, brown adipocytes and inducible brown-like adipocytes found interspersed in WAT depots (Kajimura et al., 2015; Wang and Seale, 2016). The latter are most commonly referred to as brite (brown-in-white adipocytes) or beige adipocytes (Klingenspor et al., 2012). White adipocytes contain few mitochondria and their intrinsic metabolic rate contributes little to whole-body energy expenditure. In contrast, brown adipocytes are packed with mitochondria and show the highest respiration capacity among mammalian cells (Klingenspor et al., 2017). This extraordinary respiration capacity is employed to dissipate heat. In a cold-acclimated rodent, thermogenesis in brown adipose tissue (BAT) can contribute up to 50% of the total body heat production at rest, despite the tissue wet weight only representing 5% of total body mass (Foster and Frydman, 1979; Klingenspor et al., 2017). Brite adipocytes are brown-like adipocytes in respect to their cytoarchitecture, high respiration capacity and molecular signature; however, their contribution to whole-body thermogenesis may have been overestimated.

Like white adipocytes, lipolysis in brown and brite adipocytes is controlled by the neuronal release of noradrenaline from the sympathetic innervation of the tissue (Klingenspor et al., 2017). However, the physiological range of circulating catecholamine levels are insufficient to activate brown fat metabolism (Girardier and Seydoux, 1986). In response to cold exposure, a well-characterized somatosensory reflex relayed in the hypothalamic preoptical area translates cold sensation in the periphery to increased efferent sympathetic drive in BAT and WAT depots (Nakamura and Morrison, 2011). In contrast, fasting decreases sympathetic drive in BAT while increasing sympathetic drive in WAT (Brito et al., 2008).

Upon cold exposure, the neurotransmitter noradrenaline stimulates the same canonical AR–G_s–adenylyl cyclase–cAMP–PKA pathway, resulting in the lipolytic mobilization of fatty acids. In brown and brite adipocytes, these fatty acids activate uncoupling protein 1 (UCP1), which enables maximal mitochondrial oxidation rates without ATP synthesis, and serve as fuel to maintain high rates of thermogenesis. In brown and brite adipocytes, the mobilization of FFAs by lipolysis is essentially required for thermogenesis. Indeed, pharmacological inhibition of ATGL and HSL, which catalyze the first two steps in the hydrolysis of triglycerides, completely diminishes adrenergic stimulation of thermogenesis (Li et al., 2014). Moreover, the addition of FFAs stimulates thermogenesis in brown adipocytes in the absence of adrenergic stimulation.

After a brief summary of the present knowledge on adrenergic control, we will address non-adrenergic mechanisms in the control of lipolysis and thermogenesis in adipocytes. Without putting the dominant role of adrenergic signaling aside, a closer inspection and functional evaluation of other ligands, receptors and intracellular signaling pathways in the control of lipolysis in adipocytes seems to be a rewarding exercise, promising new insights into lipid metabolism and energy balance physiology. Our reviews of the published literature revealed several non-adrenergic biomolecules that have been identified to effect lipolysis in white adipocytes, only

Journal of Experimental Biology

REVIEW Journal of Experimental Biology (2018) 221, jeb165381. doi:10.1242/jeb.165381

a few of which have been examined for their lipolytic action in brown and brite adipocytes (Duncan et al., 2007; Lafontan, 2012). As a working hypothesis, any stimulus affecting the balance of lipolysis and re-esterification potentially attenuates or activates thermogenesis in brown and brite adipocytes (Li et al., 2017) (Fig. 1). In this Review, we aim to provide a comprehensive coverage and discussion of biomolecules that modulate lipolysis in adipocytes by either receptor-dependent or independent mechanisms. Information on comparative aspects, species differences and effects on brown and brite adipocyte lipolysis and thermogenesis is provided where available.

Dual role of catecholamines in the adrenergic control of lipolysis

Adrenaline and noradrenaline

Adrenaline and noradrenaline both elicit distinct adrenergic signaling pathways in adipocytes by activating α- and β-ARs, which belong to the family of G-protein coupled receptors (GPCRs). The fat-laden cells express several paralogs of adrenergic GPCRs, mainly ADRA1, ADRA2 and ADRB1/2/3, which couple to G_s-, G_i - or G_q-dependent intracellular signaling modules. Although adrenaline and noradrenaline have greater affinity to α- than to β-receptors, the receptor abundance largely determines which signaling modules are activated. The β-3-AR ADRB3 is the predominant AR paralog expressed in rodent adipocytes. Noradrenaline released as a neurotransmitter from sympathetic nerves is the prime driver of lipolysis in adipose tissues by activating ADRB3, which signals through the canonical G_s–adenylyl cyclase–cAMP–PKA pathway (Fig. 2). Previous pharmacological studies of lipolysis comparing white adipocytes from different mammalian species concluded that guinea pigs and primates (humans and macacus monkeys) are hyporesponsive to ADRB3 agonists, whereas rodents (rats, golden hamsters and dormice) are hyperresponsive (Lafontan and Berlan, 1993). However, the lack of lipolytic action in guinea pigs and primates is likely owing to lower ADRB3 expression and the poor cross-species pharmacology of ligands available at that time.

Other α- and β-ARs differ regionally in their abundance between depots and between mammalian species. In white adipocytes, α2-AR (ADRA2) signaling opposes the stimulation of lipolysis by ADRB3. ADRA2 couples to G_i signaling, which reduces cAMP levels by inhibiting adenylyl cyclase (Lafontan and Berlan, 1993). Upon stimulation of adipocytes with adrenaline or noradrenaline, the effect on lipolysis largely depends on the balance of ADRA2 and ADRB1/2/3 expression. For example, adrenaline has anti-lipolytic effects in human subcutaneous fat where ADRA2 is more abundant than ADRB1/2/3. In contrast, lipolysis in omental fat with low ADRA2 expression is stimulated by adrenaline. A comparison of mammalian species revealed a large variation in the anti-lipolytic response to ADRA2 stimulation. Strong inhibition of lipolysis was observed in white adipocytes isolated from hamsters, humans, rabbits and dogs, whereas inhibition was low in jerboas, dormice, guinea pigs and rats. The different anti-lipolytic action observed in these species is associated with high and low ADRA2 expression in adipocytes of these species (Castan et al., 1994). Thus, species differences exist in the relative expression of ADRA2 and ADRB1/2/3. This α2-AR–β-AR balance is the cause of the anti-lipolytic effects of adrenaline in human but not in rat adipocytes.

ADRA2 is also expressed in brown adipocytes. Activation results in G_i-mediated inhibition of adenylyl cyclase and a reduction of cAMP levels and, hence, binding of noradrenaline to ADRA2 exerts an anti-lipolytic action. Indeed, pharmacological inhibition of ADRA2 increases the lipolytic and the thermogenic action of noradrenaline. Like white adipocytes, noradrenaline has a dual role in brown adipocytes, both inhibiting as well as stimulating lipolysis and thermogenesis. However, owing to the much higher expression levels of ADRB3 compared with ADRA2, the stimulatory action prevails.

Although ADRB3 is quantitatively the most abundant AR in the BAT of rodents, this is not the case in humans. In human brown adipocytes, ADRB3 is far less abundant than ADRB1 and ADRB2

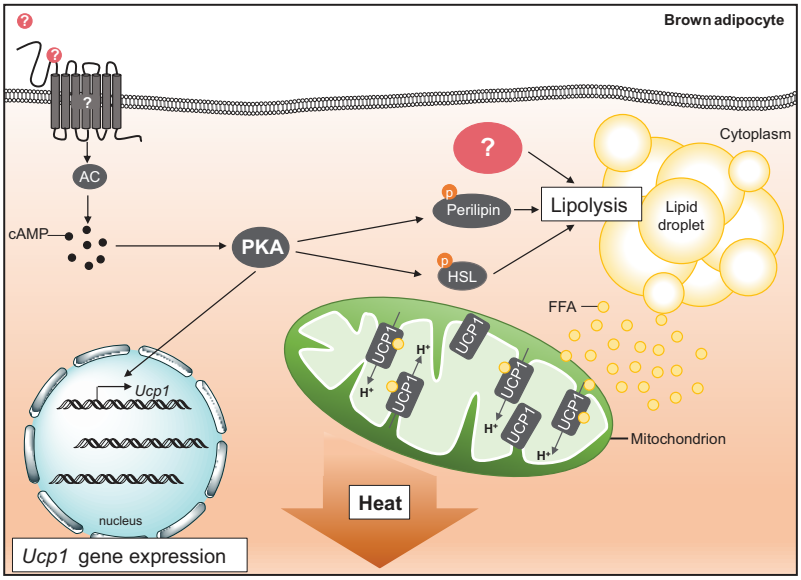

Fig. 1. Working hypothesis: lipolytic agents are potential activators of thermogenesis in brown adipocytes. Lipolysis is an essential prerequisite for thermogenesis in brown and brite adipocytes. We therefore hypothesize that any pro-lipolytic stimulus potentially activates thermogenesis in these cells. Free fatty acids (FFAs) released from lipid droplets as a result of lipolysis act as both fuel for mitochondrial β-oxidation and activators of the uncoupling protein 1 (UCP1). UCP1 is a unique feature of brown and brite adipocytes located in the inner mitochondrial membrane. Upon activation by FFAs, UCP1 uncouples oxygen consumption from adenosine triphosphate (ATP) synthesis by allowing protons (H^+) to reenter the mitochondrial matrix without generating ATP. Thus, the chemical energy of nutrients is dissipated as heat. Extracellular stimulation of lipolysis via the canonical adenylyl cyclase–cyclic adenosine monophosphate–protein kinase A (AC–cAMP–PKA) pathway not only leads to the phosphorylation of perilipin and hormone-sensitive lipase (HSL) but also induces *Ucp1* gene expression.

Journal of Experimental Biology

REVIEW Journal of Experimental Biology (2018) 221, jeb165381. doi:10.1242/jeb.165381

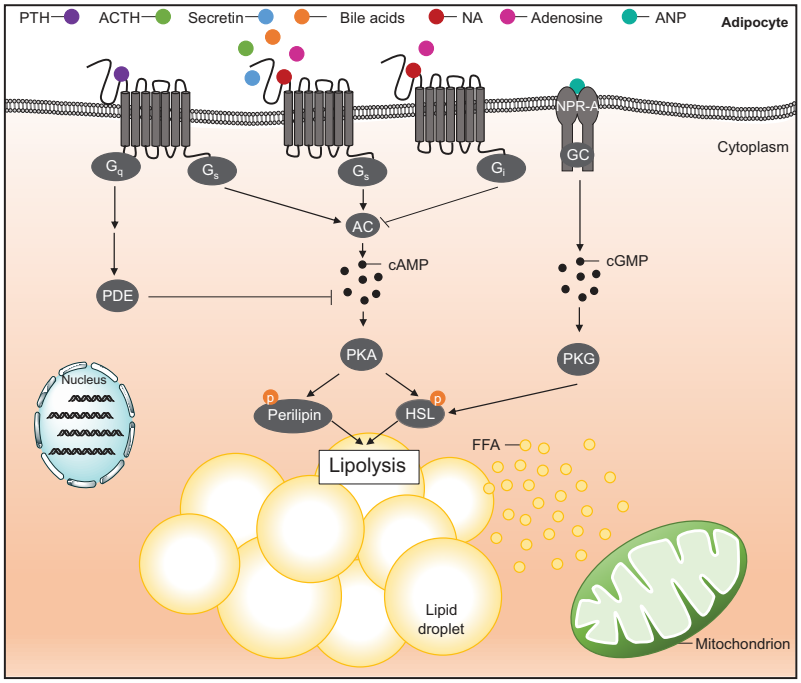

Fig. 2. Receptor-dependent pathways regulating lipolysis in adipocytes. Ligand binding of a G_s protein-coupled receptor leads to the activation of adenylyl cyclase (AC) and a rise in cyclic adenosine monophosphate (cAMP) levels, which in turn activates protein kinase A (PKA). Activated PKA phosphorylates perilipin and hormone-sensitive lipase (HSL) leading to lipolysis. Examples of such G_s protein-coupled receptors and their respective ligands are: membrane-bound bile acid receptor (TGR5) and bile acids; melanocortin receptor 2 (MC2R) and adrenocorticotropic hormone (ACTH); adenosine receptor 2a (ADORA2A) and adenosine; β-adrenergic receptor (β-AR) and noradrenaline (NA). Gi protein-coupled signaling inhibits AC and, thereby, exerts anti-lipolytic effects. Thus, activation of α-AR by NA or activation of adenosine receptor 1 (ADORA1) by adenosine attenuates lipolysis. Binding of parathyroid hormone (PTH) to parathyroid hormone receptor 1 (PTHR1) activates Gs- and Gq-coupled signaling. Whereas Gs activates the AC–cAMP–PKA pathway, Gq signaling events lead to increased sequestration of cAMP by phosphodiesterase (PDE) activation, which counteracts the lipolytic effects of Gs-coupled signaling elicited by PTHR1. Atrial natriuretic peptide (ANP) binds to natriuretic peptide receptor A (NPR-A), leading to the activation of the guanylyl cyclase (GC) domain of NPR-A and the rise of cyclic guanine monophosphate (cGMP) levels, with the subsequent activation of protein kinase G (PKG). PKG phosphorylates and thereby activates HSL.

(see RNA-Seq data SAMEA2563965 at https://www.ebi.ac.uk/ena/data/view/SAMEA2563965 by Shinoda et al., 2015; Revelli et al., 1993). The species-related differences may partly explain the poor responsiveness of human fat cells to β−3 agonists compared with murine adipocytes. The low β3-AR abundance does not inspire confidence that ADRB3 would be a suitable molecular target in humans and, hence, it is remarkable that a recently developed human ADRB3 agonist acutely increased serum FFA levels and activated brown fat thermogenesis in human subjects (Cypess et al., 2015).

Anti-lipolytic effectors

Adenosine

Adenosine is a purine nucleoside generated in cellular adenine nucleotide metabolism that activates purine receptors in the plasma membrane. Extracellular adenosine in the tissue can arise from different sources. Adipocytes liberate adenosine into the extracellular space where it acts in an autocrine/paracrine fashion. Moreover, extracellular ecto-5′-nucleotidase (CD37) generates adenosine from ATP released by either parenchymal cells or sympathetic neurons as a purinergic co-transmitter of noradrenaline. Four adenosine receptors of the GPCR1 family are known, of which the two paralogs ADORA1 and ADORA2A are of functional relevance in adipose tissues. These two adenosine receptors have opposing roles in the regulation of cAMP levels. ADORA1 inhibits adenylyl cyclase through G_i, whereas ADORA2A activates adenylyl cyclase through G_s (Fig. 2). Adenosine has anti-lipolytic action because ADORA1 expression predominates in adipocytes.

The addition of adenosine deaminase (ADA) in cell-based assays of lipolysis sequesters extracellular adenosine in the medium and, thereby, attenuates the anti-lipolytic action. For example, in white adipocytes isolated from murine epididymal WAT, basal lipolysis was increased more than sevenfold in the presence of ADA (0.1 U ml^{-1}), and >18-fold in a combined treatment with ADA and noradrenaline (10 nmol l^{-1}). In the absence of ADA, a more than ninefold increase was observed in response to noradrenaline (Johansson et al., 2008). These pro-lipolytic effects of ADA are owing to the clearance of adenosine, which inhibits adenylyl cyclase activity via ADORA1. Experimental variation (technical and biological) in the extracellular adenosine concentrations challenges the robustness of lipolysis assays in cell culture systems. Therefore, the addition of both ADA and the ADORA1-specific agonist phenylisopropyladenosine (PIA) was introduced to clamp a defined state of anti-lipolysis in the experimental set-up (Honnor et al., 1985), and was recommended as state-of-the-art (Lee and Fried, 2014). Pharmacological activation and genetic ablation

Journal of Experimental Biology

REVIEW Journal of Experimental Biology (2018) 221, jeb165381. doi:10.1242/jeb.165381

demonstrated that ADORA1 inhibits lipolysis in adipocytes isolated from diverse mammalian species, including hamsters (Rosak and Hittelman, 1977; Schimmel and McMahon, 1980), rats (Honnor et al., 1985), mice (Johansson et al., 2008) and humans (Heseltine et al., 1995). The anti-lipolytic action of adenosine was therefore assigned as an obligatory paracrine mechanism in mammals (Castan et al., 1994). Although the anti-lipolytic action of adenosine potentially extends the dynamic range of lipolysis rates in adipocytes, the physiological relevance was repeatedly questioned. In human subcutaneous adipose tissue, interstitial adenosine concentrations, as assessed by microdialysis in the unstimulated state, ranged from 25 to 300 nmol l^{-1} (Lonnroth et al., 1989). In isolated human white adipocytes, noradrenaline-stimulated lipolysis was inhibited by stable analog 2-chloroadenosine concentrations equipotent to 150–300 nmol l^{-1} adenosine. Thus, adenosine concentrations in the intercellular space of human adipose tissue are sufficiently high to counteract sympathetic stimulation of lipolysis (Lonnroth et al., 1989). In germline knockout mice, although loss of ADORA1 function ablated the anti-lipolytic effects of adenosine, phenotypically the ADORA1 knockout mice did not show increased lipolysis and decreased triglyceride storage in WAT. Thus, a putative physiological function of adenosine as a negative modulator of lipolysis could not be established in this model, possibly owing to pleiotropic functions of ADORA1 expressed in other tissues (Johansson et al., 2008).

In 1981, Bukowiecki and colleagues proposed that '*mitochondrial respiration would principally be regulated by the activity of the hormone sensitive lipases that would represent the flux generating step controlling brown adipose tissue oxidative metabolism*' (Bukowiecki et al., 1981). In line with this proposal, an anti-lipolytic effector should put a break on thermogenesis in brown adipocytes. Adenosine was therefore studied early on as a putative inhibitor of brown fat thermogenesis. In brown adipocytes isolated from golden hamsters, the anti-lipolytic action of adenosine is associated with a pronounced attenuation of noradrenaline-stimulated thermogenesis, an effect that can be reversed by adding ADA (Szillat and Bukowiecki, 1983). These observations were later confirmed in brown adipocytes isolated from rat interscapular BAT (Woodward and Saggerson, 1986).

Unexpectedly, a recent study revealed pro-lipolytic action of adenosine at low concentrations ranging from 10 to 100 nmol l^{-1} in human and mouse brown adipocytes (Gnad et al., 2014). Analysis of gene expression revealed ADORA2A as the most abundantly expressed adenosine receptor in BAT of humans and mice. Based on subsequent pharmacological analysis and genetic ablation, the pro-lipolytic action of adenosine was conveyed by stimulating adenylyl cyclase activity through G_s-coupled ADORA2A signaling. In brown adipocytes from ADORA2A-ablated mice, the pro-lipolytic action required higher concentrations of adenosine. Treatment of murine brown adipocytes, either with adenosine or with a specific ADORA2A agonist, increased cAMP levels, lipolysis and the oxygen consumption rate (Gnad et al., 2014). The anti-lipolytic effect of adenosine in hamster brown adipocytes is most likely owing to higher levels of expression of ADORA1 relative to ADORA2A (Gnad et al., 2014). Nevertheless, the physiological relevance of potentially opposing adenosine effects on brown adipocytes in different mammalian species remains elusive and merits further investigation.

It is conceivable that other ligands binding to Gi-coupled GPCRs will inhibit adenylyl cyclase and decrease cAMP production, therefore harboring anti-lipolytic effects. Organic acids, such as lactate, succinate and short-chain fatty acids (acetate and propionate), and the ketone body β-hydroxybutyrate (β-OHB), through binding to their respective Gi-coupled receptors GPR81 (Liu et al., 2009), GPR91 (Regard et al., 2008), GPR43 (Ge et al., 2008) and HM74a (Taggart et al., 2005), fall into this category. A comprehensive review of these anti-lipolytic effectors has been published (Nielsen et al., 2014).

Pro-lipolytic effectors and signaling pathways

Melanocortins

The POMC gene encodes for prepro-opiomelanocortin. Posttranslational cleavage of POMC by prohormone convertases generates several biologically active peptides classified as melanocortins. Beyond their central action via melanocortin receptors in the CNS, some melanocortins mediate their effects via melanocortin receptors in the periphery, of which α-melanocyte-stimulating hormone (αMSH) and corticotropin (adrenocorticotropic hormone, ACTH) are known for their significant pro-lipolytic action in adipocytes of rodents, as first reported in 1958 (Lafontan, 2012). In rodent adipocytes, ACTH binds to the melanocortin 2 receptor, which stimulates lipolysis via Gs-coupled cAMP–PKA-mediated phosphorylation of HSL (Cho et al., 2005) (Fig. 2). However, in human adipocytes, ACTH and αMSH lack lipolytic activity, which is likely owing to differential expression of melanocortin receptors in primates and rodents (Kiwaki and Levine, 2003; Lafontan and Langin, 2009).

Shortly after the initial demonstration of BAT function as a heater organ (Smith, 1961), the potential role of ACTH, glucocorticoids and steroids for non-shivering thermogenesis was explored (Jansky et al., 1969). In the European hedgehog, pharmacological inhibition of adrenal glucocorticoid synthesis stimulated resting energy expenditure, possibly owing to an accumulation of the corticosterone precursor 11-deoxycorticosterone or an increase of pituitary ACTH secretion (Werner and Wunnenberg, 1980). However, the crucial role of pituitary hormones and their effector hormones for brown fat recruitment during cold acclimation was questioned (Fellenz et al., 1982), and inhibitory actions of corticosterone as the effector hormone of the hypothalamus–pituitary–adrenal (HPA) axis on brown fat were reported (Galpin et al., 1983). In dietary or genetically obese rats, BAT function was enhanced by ACTH, an effect opposed by corticosterone and dietary status (Rothwell and Stock, 1985; York and Al-Baker, 1984).

The role of the HPA axis for brown fat function in mice was recently revisited and further specified. Cold exposure for one day activates the HPA axis resulting in increased levels of circulating ACTH and increased fecal corticosterone excretion (van den Beukel et al., 2014). Like white adipocytes, in murine immortalized brown adipocytes, ACTH stimulates intracellular cAMP concentrations in a dose-dependent manner, even exceeding the effect of noradrenaline. ACTH at a dose of 50 nmol l^{-1} increases glycerol release by ∼50% of noradrenaline-stimulated lipolysis at 1 µmol l^{-1} (van den Beukel et al., 2014). Further analysis revealed that ACTH also increased UCP1 messenger ribonucleic acid and protein levels, which is mediated by p38 mitogen-activated protein kinase (MAPK) signaling (Iwen et al., 2008). Notably, ACTH stimulated oligomycin-insensitive oxygen consumption in brown adipocytes by 40%, suggesting activation of a UCP1-dependent proton leak. This observation needs further validation because the experimental design did not control for a possible uncoupling effect of fatty acids (Li et al., 2014). *In vivo*, positron-emission tomography (PET) demonstrated that ^{18}fluorodeoxyglucose (^{18}FDG) uptake was stimulated by ACTH. Interestingly, increased basal glucose

REVIEW Journal of Experimental Biology (2018) 221, jeb165381. doi:10.1242/jeb.165381

uptake and an enhanced level of stimulation by ACTH were observed in mice treated with a glucocorticoid receptor antagonist. These results further manifest the conclusion from previous studies that the enhancing effect of ACTH on BAT function is attenuated by corticosterone in rodents. Acute stress may lead to a transient activation of BAT thermogenesis that is downregulated by the subsequent rise of corticosterone. However, it remains to be clarified whether the physiological peak concentrations of ACTH in plasma in response to stress are sufficiently high to activate BAT thermogenesis *in vivo* (van den Beukel et al., 2014).

Glucocorticoids

In contrast to the findings in rodents, glucocorticoids can activate BAT in humans. Administering healthy male subjects with three doses of prednisolone (the first dose was administered 24 h before visiting the research facility) had no effect on basal BAT activity; however, PET and infrared thermography of skin temperature in the supraclavicular region revealed that cold-induced glucose uptake in BAT and skin temperature were enhanced by prednisolone (Ramage et al., 2016). An independent study using infrared thermography demonstrated that infusing healthy male subjects with hydrocortisone for 24 h had no effect at room temperature; however, a cold-induced increase in skin temperature of the supraclavicular region was enhanced (Scotney et al., 2017). Results obtained in cell culture are in line with these observations. In respiration experiments directly comparing human and mouse brown adipocytes, cortisol stimulated the metabolic rate in human brown adipocytes but inhibited isoproterenol-induced respiration in murine brown adipocytes. For this species comparison, brown adipocytes were pretreated with cortisol for 24 h. Importantly, these thermogenic effects are likely owing to genomic effects of glucocorticoids as indicated by corresponding changes in *Ucp1* gene expression. To date, acute non-genomic effects of glucocorticoids on brown fat thermogenesis have not been reported.

The biological significance for the differential effects of ACTH and glucocorticoids in the control of lipolysis and thermogenesis in WAT and BAT of human and mouse is not understood. In humans, higher doses of cortisol, and more chronic elevations of glucocorticoids inhibit BAT activity, as concluded from cell culture data and clinical observations reporting a lower prevalence of BAT negative patients during chronic glucocorticoid therapy (Ramage et al., 2016).

Natriuretic peptides

Natriuretic peptides comprise a family of three structurally related peptides mediating a wide range of physiological functions centered around blood pressure control and volume homeostasis. Atrial natriuretic peptide (ANP), the first member of this family, was discovered in 1981 by de Bold (de Bold et al., 1981). B-type natriuretic peptide (BNP) and C-type natriuretic peptide (CNP) were subsequently characterized in 1989 and 1991, respectively (Sudoh et al., 1988, 1990).

All natriuretic peptides are synthesized as preprohormones and further processed to prohormones. ProANP is the major form of ANP stored in atrial granules (Oikawa et al., 1984). Upon its release, proANP is readily cleaved into the biologically active form of ANP (Yan et al., 2000). The sequence of mature ANP is highly conserved across different species; it is identical in humans, chimps, dogs, pigs, horses and sheep (Potter et al., 2009). ANP release is triggered by atrial distension and by neurohumoral stimulation (Dietz, 1984; Mukoyama et al., 1991). In general, natriuretic peptides are either enzymatically degraded or removed from circulation by binding to their clearance receptor (Nussenzveig et al., 1990; Stephenson and Kenny, 1987).

BNP was initially purified from porcine brain, thus, it was originally termed ‘brain natriuretic peptide’ (Sudoh et al., 1988). However, after much higher BNP concentrations were detected in atrial ventricles, the neutral terminology ‘B-type’ was adopted (Mukoyama et al., 1991). BNP is produced in response to states of high pre- and afterload pressures (Thuerauf et al., 1994). In addition to the effects of BNP on blood pressure, studies suggest that BNP might act as a paracrine regulator of cardiac remodeling (Tamura et al., 2000).

CNP is mainly expressed in vascular endothelial cells, neurons and in testicles; however, there are no convincing data to support the expression of CNP in cardiomyocytes (Herman et al., 1993; Middendorff et al., 1996; Suga et al., 1992b; Takahashi et al., 1992). CNP is not stored in granules and its release is triggered by growth factors, sheer stress and in response to vascular injuries (Brown et al., 1997; Chun et al., 1997; Suga et al., 1992b). CNP is primarily known to stimulate long bone growth (Mericq et al., 2000). The half-life times of natriuretic peptides in the human circulation are ∼2–3 min for ANP and CNP (Hunt et al., 1994; Yandle et al., 1986) and 20 min for BNP (Mukoyama et al., 1990).

The various effects of natriuretic peptides are mediated by the natriuretic peptide receptors A, B and C (NPR-A/-B/-C). NPRs are expressed in a broad range of tissues, including kidney (Goy et al., 2001), lung (Lowe et al., 1989), adipose (Jeandel et al., 1989), brain (Herman et al., 1996), heart (Lin et al., 1995), testis, adrenal, bone, liver (Sarzani et al., 1996) and vascular smooth muscle tissues (Schiffrin et al., 1986). The intracellular domain of NPR-A as well as NPR-B has guanylyl cyclase activity, thereby catalyzing the synthesis of the second messenger cyclic guanine monophosphate (cGMP; Miyagi and Misono, 2000). NPR-C does not exhibit cyclase activity; thus, it was initially considered to be a clearance receptor only. However, studies have revealed that NPR-C mediates intracellular effects through G_i-signaling and the consequent inhibition of adenylyl cyclase and phospholipase C activation (Rose and Giles, 2008). NPR-A is the principal receptor for ANP and BNP, whereas NPR-B preferentially binds CNP (Bennett et al., 1991; Suga et al., 1992a). Among NPRs, NPR-C is the most widely and abundantly expressed receptor (Anand-Srivastava, 2005). Beyond the regulation of blood pressure and fluid homeostasis, an important role for ANP, BNP and CNP in the control of adipose tissue metabolism has emerged over the past decades (Sengenès et al., 2000).

Almost 30 years ago, the first studies demonstrated that ANP stimulated cGMP levels in rat adipocytes, although ANP failed to increase lipolysis (Jeandel et al., 1989; Okamura et al., 1988). In 2000, the first report demonstrated that ANP as well as BNP, and to a lesser degree CNP, can induce lipolysis in human subcutaneous fat in a cGMP-dependent fashion (Sengenès et al., 2000). ANP has a lipolytic potency comparable to that of catecholamines. The order of potency is: ANP>BNP>>CNP. ANP and isoproterenol have additive effects at low concentrations; however, the maximal lipolytic effect of isoproterenol is not significantly amplified by ANP (Moro et al., 2004b; Sengenès et al., 2000). The precise lipolytic pathway was discovered only a few years later. ANP binds to NPR-A, guanylyl cyclase is activated, cGMP levels are increased and protein kinase G is activated, leading to the subsequent phosphorylation of HSL (Sengenès et al., 2003) (Fig. 2). Nevertheless, lipolytic pathways mediated by β- and α2-ARs and the ANP-dependent pathway do not interact. In contrast to the adrenergic pathway, insulin does not modulate the lipolytic effect of

REVIEW Journal of Experimental Biology (2018) 221, jeb165381. doi:10.1242/jeb.165381

ANP. Similar to isoproterenol-stimulated lipolysis, the ANP-dependent lipolytic pathway exhibits homologous desensitization; however, there is no cross-interaction between isoproterenol and ANP (Moro et al., 2004b; Sengenès et al., 2000, 2002). Moreover, the effect of natriuretic peptides on lipid metabolism was confirmed in healthy humans. Infusion of ANP triggered peripheral lipid mobilization and increased circulating FFA levels (Birkenfeld et al., 2005). Although the physiological relevance of the ANP-mediated lipolytic pathway in humans is still not clear, further studies have shown that increased circulating ANP concentrations may trigger exercise-induced lipolysis (Moro et al., 2004a). However, natriuretic peptides can only elicit a lipolytic response in primates: for instance, the amount of NPR-C is much higher in the adipose tissue of rodents than in humans, thereby diminishing the pro-lipolytic stimulus (Sengenès et al., 2002). Notably, it was demonstrated that this effect can be completely reversed by the ablation of NPR-C in mice (Bordicchia et al., 2012). Consequently, ANP as well as BNP can induce a brown thermogenic signature in the white adipocytes of NPR-C$^{-/-}$ mice and humans by activating p38-MAPK, triggering mitochondrial biogenesis, and increasing the expression of UCP1 and PGC1-α. Likewise, treatment of NPR-C$^{-/-}$ mice with BNP caused browning of white fat and the activation of already existing brown fat (Bordicchia et al., 2012). In wild-type mice, an increase in ANP and BNP expression and a shift in the adipose tissue NPR-A/NPR-C ratio, favoring adipose tissue activation, was observed during cold exposure (Bordicchia et al., 2012). A similar change in adipose tissue NPR patterns was reported in rats upon food deprivation (Sarzani et al., 1996).

Taken together, the ability of natriuretic peptides to initiate lipolysis, induce browning of WAT, and to activate UCP1 might bring further clinical benefits. However, the basic role of natriuretic peptides in metabolism and their full range of effects has yet to be discovered.

Bile acids

Bile acids are essential factors in dietary lipid absorption and end products of cholesterol catabolism (Lefebvre et al., 2009; Watanabe et al., 2006). They are synthesized from cholesterol in the liver, stored in the gallbladder, and secreted after meals to promote absorption of fat from the intestine. Bile acids are then either excreted or reabsorbed into the enterohepatic circulation. Beyond this well-established role, functions for bile acids as signaling molecules have emerged in recent years. Bile acids are natural ligands for the nuclear hormone receptor farnesoid X receptor (FXR) (Kawamata et al., 2003; Maruyama et al., 2002), which controls the synthesis and enterohepatic circulation of bile acids by adjusting the expression of essential gene products involved in bile acid synthesis, transport, conjugation and detoxification (Houten and Auwerx, 2004; Russell, 2003). In addition to FXR, bile acids signal through another pathway involving the G_s-coupled receptor TGR5 (also GBAR1, M-Bar, BG37) (Fig. 2). In both rodents and humans, BAT is targeted by bile acids. In C57BL/6 mice, dietary supplementation with cholic acid increased the thermogenetic capacity of BAT even in a thermoneutral environment and prevented diet-induced obesity (Teodoro et al., 2014; Watanabe et al., 2006; Zietak and Kozak, 2016). Mechanistically, the binding of bile acids to the TGR5 receptor increased the intracellular concentrations of the second messenger cAMP, which activates expression of the gene encoding for type 2 deiodinase (DIO2). This enzyme converts the inactive thyroid hormone thyroxine (T4) to active 3-5-3′-triiodothyronine (T3). Increased saturation of thyroid hormone receptors with T3 enforces the expression of Pgc1-α, a transcriptional coactivator of mitochondrial biogenesis and Ucp1. As a result, bile acids boost the thermogenic capacity of BAT. In humans, two oral ingestions of the primary bile acid chenodeoxycholic acid (CDCA) within 24 h enhanced cold-induced glucose uptake into BAT. In support of this thermogenic action, CDCA also triggered increased uncoupled leak respiration in primary brown adipocytes upon acute treatment (Broeders et al., 2015). The latter observation was also reported for human skeletal muscle cells (Watanabe et al., 2006); however, to date, such acute activation has not been demonstrated in mice. Moreover, all these findings have not been substantiated in TGR5 knockout mice, which are readily available (Maruyama et al., 2002). It is reasonable to postulate that bile acids are pro-lipolytic given that TGR5 is a G_s-coupled receptor. However, direct evidence is lacking. Bile acid deoxycholate has no pro-lipolytic activity in 3T3L-1 adipocytes (Klein et al., 2009). Therefore, further studies are needed to decipher the pro-lipolytic effects of bile acids.

Parathyroid hormone

The parathyroid hormone (PTH) is a peptide hormone controlling minute-to-minute levels of ionized calcium in the blood and in the extracellular fluid. It is released by the parathyroid gland in response to low calcium plasma levels detected by calcium-sensing receptors and counteracts calcitonin. PTH binds to cell surface receptors in bone and kidney tissue, triggering responses that increase blood calcium. PTH also increases renal synthesis of calcitriol, the hormonally active form of vitamin D, which then acts on the intestine to augment absorption of dietary calcium, in addition to promoting calcium fluxes into blood from bone and kidney tissue. The resulting increase in blood calcium and in calcitriol feeds back on the parathyroid glands to decrease the secretion of PTH. The parathyroid glands, bones, kidney and gut are, thus, the crucial organs that participate in PTH-mediated calcium homeostasis.

The pro-lipolytic nature of PTH was first demonstrated by Werner and Löw in 1973 (Werner and Löw, 1973). The authors showed that PTH stimulated lipolysis three- to fivefold in rat epididymal adipose tissue measured *in vitro* as glycerol release. PTH was then shown to also stimulate lipolysis in human adipocytes. The N-terminal 1–34 fragment of the peptide hormone was shown to be sufficient to elevate the intracellular cAMP level and thereby mediate the lipolytic action of PTH (Sinha et al., 1976).

In murine primary brown adipocytes, PTH also induces the activation of the cAMP–PKA pathway; however, the lipolytic action of PTH is quite low compared with the non-selective β-adrenergic agonist isoproterenol. The enzyme that degrades cAMP is phosphodiesterase 4 (PDE4). PDE4 inhibitors block the degradative action of the enzyme and thereby increase cAMP levels. Whereas the lipolytic action of isoproterenol is not affected by PDE4 inhibition, the lipolytic action of PTH is strongly potentiated (Larsson et al., 2016). Thus, isoproterenol predominantly induces lipolysis by increasing cAMP, whereas PTH stimulation to a much larger extent leads to anti-lipolysis by sequestering cAMP. This suggests that the balance between lipolytic and anti-lipolytic actions is quite distinct for isoproterenol and PTH. The PTH receptor type 1 (PTHR1) is a family B GPCR that binds and is activated by the endocrine ligand PTH, as well as the paracrine ligand PTH-related protein (PTHrP) to mediate divergent functions in different tissues. Other than isoproterenol binding to the ADRB receptors, PTH binding to PTHR1 activates multiple intracellular signaling pathways, including coupling to Gs and Gq signaling. Whereas Gs activates the adenylyl cyclase–cAMP–PKA pathway, Gq activates the

Journal of Experimental Biology

REVIEW Journal of Experimental Biology (2018) 221, jeb165381. doi:10.1242/jeb.165381

phospholipase C (PLC)-dependent formation of diacylglycerol and β-inositol triphosphate, resulting in a rise of cytosolic Ca^{2+} and protein kinase C activity. These Gq signaling events may lead to increased sequestration of cAMP by PDE4 activation and thereby counteract Gs signaling elicited by PTHR1 (Fig. 2). Therefore, the application of a PDE4 inhibitor is recommended to attain the full lipolytic potential of PTH. Compared with physiological PTH concentrations of 1–10 pmol l^{-1} (10–65 pg ml^{-1}) in healthy adults, effective doses of 10 nmol l^{-1}–1 µmol l^{-1} are considered as supraphysiological.

The molecular basis in terms of specific interactions of ligands with PTHR1 and the post-binding events triggering downstream signals controlling entirely different functions needs further exploration (Cheloha et al., 2015; Gardella and Vilardaga, 2015). In comparison to synthetic $hPTH_{3–34}$ (human PTH), $hPTH_{1–34}$ was reported to significantly stimulate lipolysis in human adipose tissue, indicating that amino acids at positions 1 (serine) and 2 (valine) are crucial for the lipolytic action of PTH. Costimulation with $hPTH_{3–34}$ and $hPTH_{1–34}$, or with isoproterenol or forskolin revealed a dose-dependent inhibition of $hPTH_{1–34}$-stimulated lipolysis but had no effect on forskolin- and isoproterenol-stimulated lipolysis (Taniguchi et al., 1985). This indicates that the truncated peptide does competitively bind to the receptor but does not activate cAMP signaling, which normally results in lipolysis. Thus, PTH_{3-34} could be considered as an antagonist for the PTH receptor. Given that the β-blocker propranolol dose-dependently inhibited isoproterenol-induced lipolysis, but had no effect on PTH-stimulated lipolysis, it has been suggested that PTH causes lipolysis after binding to receptors distinct from β-ARs (Taniguchi et al., 1985).

PTH and the PTHrP share one common function. Kir et al. (2014) demonstrated that tumor-derived PTHrP plays an important role in tumor cachexia and adipose tissue browning. Treatment with both PTH and PTHrP results in increased basal respiration and maximal respiration in primary white adipocytes, and is accompanied by increased thermogenic gene expression (Kir et al., 2014). Consistent with these results and given that PTHrP binds the same receptor as PTH, PTHrP might exert similar lipolytic action in adipose tissue as PTH.

Secretin

Secretin is synthesized predominantly by enteroendocrine S cells in the duodenum and proximal jejunum. Gastric acid, bile salts and luminal nutrients stimulate secretin, and somatostatin inhibits its release. Secretin stimulates pancreatic and biliary hydrogen carbonate and water secretion, and it may regulate pancreatic enzyme secretion. Secretin also stimulates the gastric secretion of pepsinogen and inhibits lower esophageal sphincter tone, postprandial gastric emptying, gastrin release and gastric acid secretion.

The 27-amino acid peptide is initially synthesized as a larger precursor, composed of a signal peptide, an N-terminal peptide, secretin, a Gly-Lys-Arg amidation-cleavage sequence and a 72-amino acid C-terminal peptide, before it is cleaved proteolytically into the active hormone (Kopin et al., 1990). In solution, the secretin protein has a partial helical conformation (Bodanszky et al., 1969).

Approximately 80 years after the discovery of secretin, the presence of a high-affinity receptor in pancreatic acinar cells was reported (Jensen et al., 1983). The secretin receptor belongs to the superfamily of class B1 GPCRs. Depending on the cell type, this class of receptors can activate G_s- and G_q-protein-coupled signaling pathways (Siu et al., 2006).

Research investigating the metabolic role of secretin began shortly after its discovery. The involvement of the hormone in fatty acid metabolism, glucose homeostasis and food intake regulation were examined by different groups in various organisms (Bainbridge and Beddard, 1906; Butcher and Carlson, 1970; Dehaye et al., 1977; Frandsen and Moody, 1973; Glick et al., 1971; Grovum, 1981; Rodbell et al., 1970). However, drawing clear conclusions from these data was challenging owing to contradictory results. In rat white adipocytes, the lipolytic actions of secretin were associated with elevated intracellular cAMP levels (Butcher and Carlson, 1970; Rodbell et al., 1970); however, this lipolytic action of secretin was not observed in white adipocytes isolated from chicken and mice (Dehaye et al., 1977; Frandsen and Moody, 1973). More recent studies appear to confirm that secretin can directly impact adipocyte development and metabolism. In the murine 3T3-L1 preadipocyte cell line, secretin promotes the early phase of adipogenesis by stimulating preadipocyte proliferation, mitochondrial activity and cellular triglyceride content (Miegueu et al., 2013). In mature adipocytes, secretin further enhanced substrate cycling by stimulating the uptake of fatty acids and glucose into white adipocytes in parallel with the lipolytic release of fatty acids and glycerol (Miegueu et al., 2013). The acute lipolytic effect of secretin was confirmed recently in primary epididymal white adipocytes of mice (Sekar and Chow, 2014) (Fig. 2). The effect of secretin on lipolysis and thermogenesis in brown adipocytes is unknown.

Receptor-independent pro-lipolytic effectors

Besides the above-mentioned receptor-dependent lipolysis modulators, biomolecules that bypass receptor-mediated activation and directly stimulate lipolysis in adipocytes have also been identified. For example, α-β hydrolase domain-containing protein 5 (ABHD5), also known as CGI-58 (comparative gene identification 58), is a protein binding to perilipin on lipid droplets under basal conditions, preventing interaction with ATGL. Upon activation, perilipin is phosphorylated by PKA, and ABHD5 rapidly disperses into the cytoplasm, enabling lipase coactivation. Its synthetic ligands SR-4995 and SR-4559, which disrupt the interaction of ABHD5 with perilipin-1 (PLIN1) or perilipin-5 (PLIN5), rapidly stimulate lipolysis in cultured brown adipocytes (Sanders et al., 2015). Similarly, blocking protein serine/threonine phosphatase activity with potent inhibitors such as okadaic acid and calyculins promotes perilipin phosphorylation and increases lipolysis in primary rat adipocytes (He et al., 2006) (Fig. 3). These lipolytic effects occur independently of cAMP and PKA. Therefore, these studies showcase alternative strategies to modulate lipolysis while bypassing the canonical G_s-coupled signaling cascade. This may provide means of activating these processes under conditions where receptor signaling is compromised given that prolonged agonist stimulation results in down-regulation of most G protein-coupled receptors.

Additional pro-lipolytic effectors

As well as the aforementioned examples of pro-lipolytic effectors, additional regulators of lipolysis have been identified (listed in Table 1). Given that lipolysis activation represents the canonical pathway to stimulate thermogenesis, these pro-lipolytic molecules qualify as putative thermogenic mediators in brown and brite adipocytes. A stringent validation of their thermogenic potential using the recently developed microplate-based respirometry assay should shed new light on this aspect (Li et al., 2014). However, the lipolytic actions of some effectors may have a lag period of up to

REVIEW Journal of Experimental Biology (2018) 221, jeb165381. doi:10.1242/jeb.165381

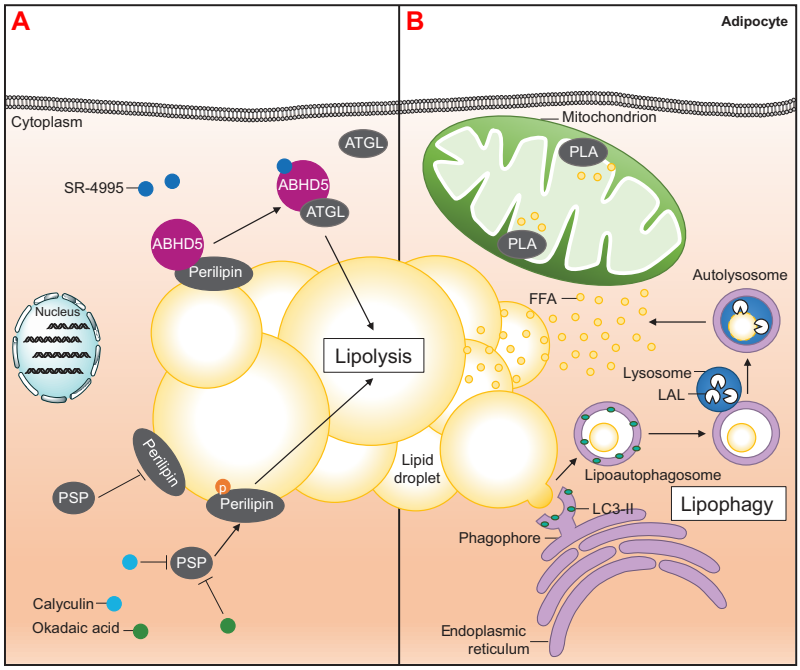

Fig. 3. Receptor-independent modulators of lipolysis and alternative sources of free fatty acids (FFAs). (A) α-β Hydrolase domain-containing protein 5 (ABHD5) binds to perilipin under basal conditions, preventing interaction with adipose triacylglyceride lipase (ATGL). Binding of synthetic ligands of ABDH5, such as SR-4995, leads to the dissociation of perilipin and ABDH5, enabling the binding of ABDH5 to ATGL, which translocates ATGL to the lipid droplet and to subsequent lipolysis. Protein serine/threonine phosphatase (PSP) dephosphorylates perilipin, leading to reduced lipolysis. Potent inhibitors blocking PSP activity such as calyculin or okadaic acid promote perilipin phosphorylation and, thereby, increase lipolysis. (B) Ca^{2+}-independent mitochondrial phospholipase (PLA) liberates FFAs from phospholipids of the inner mitochondrial membrane. In a process termed lipophagy, enabling the selective degradation of lipid droplets via autophagy, a portion of larger lipid droplets is sequestered or smaller lipid droplets are engulfed by LC3-phosphatidylethanolamine-bound phagophore membranes leading to the formation of a lipoautophagosome. Fusion of the latter with lysosomal acid lipase (LAL)-containing lysosomes results in the generation of an autolysosome, wherein LAL degrades the lipid droplet portion and FFAs are released into the cytoplasm.

hours, which is in contrast to virtually no lag period for catecholamines. For example, the lipolytic effect of growth hormone was seen only after a lag period of 1–2 h (Fain et al., 1971). A potential lag period for lipolysis activation by these regulators should be taken into account when testing their thermogenic activity.

Conclusions and perspectives

Given that adipose tissue not only functions as the major organ for fat storage and mobilization but also as an endocrine and thermogenic organ, research on lipolytic modulators has intensified. Other than being a catabolic substrate in mitochondrial β-oxidation, fatty acids liberated by lipolysis are transformed into paracrine/autocrine and endocrine signaling molecules. Moreover, lipolysis is an essential prerequisite for thermogenesis in brown and brite adipocytes. Endogenous and xenobiotic biomolecules affecting the balance between lipolysis and re-esterification of fatty acids are therefore of pertinent interest. In this Review, we discuss an extensive assembly of pro- and anti-lipolytic biomolecules of various origins and physiological functions. For most of these molecules, our knowledge about their impact on the lipid metabolism of adipocytes is mostly limited to white adipocytes cultured *in vivo*, with little or no insights available on their physiological function *in vivo*. Moreover, to date, few of these modulators have been studied for their effects on lipolysis in brown or brite adipocytes. Given that lipolysis is an essential requirement for the activation of UCP1-mediated thermogenesis in these cells, the collection of modulators discussed in this Review can be regarded as a list of potentially pro- or anti-thermogenic modulators of metabolism. Importantly, pro-lipolytic effectors working through the cAMP–PKA pathway are very likely to also induce *Ucp1* gene expression in brown and brite adipocytes. In this respect, their biological activity remains to be determined. Beyond the single effects of individual molecules, it would be interesting to analyze their putative additive or synergistic effects on lipid metabolism in adipocytes and adipose tissues, respectively.

In attempting to investigate pro-lipolytic effectors for their potential to activate UCP1-mediated thermogenesis in brown adipocytes, one has to take into account additional sources of FFAs other than the hydrolysis of triacylglycerol in lipid droplets via the classical lipolytic pathway. For example, mitochondrial phospholipase 2 (PLA2) provides long-chain fatty acids within the inner mitochondrial membrane, which may serve as a physiological mechanism of UCP1 regulation, along with the generation of FFAs by lipolysis of cytoplasmic lipid droplets (Fedorenko et al., 2012).

Journal of Experimental Biology

REVIEW Journal of Experimental Biology (2018) 221, jeb165381. doi:10.1242/jeb.165381

Table 1. Biomolecules with pro-lipolytic effects on adipocytes categorized as protein, small molecules and plant extracts

Regulators	Mechanism	Model	References
Protein			
ANGPTL3	Unknown	Mice and 3T3-L1 adipocyte	Shimamura et al., 2003
ANGPTL4	cAMP–PKA	Mice and adipocytes	McQueen et al., 2017
ApoA-I Milano	Unknown but independent of cAMP–PKA	In mice and primary epididymal cells	Lindahl et al., 2015
β-Lipotropin	Possibly a melanocortin receptor	Rabbit adipocyte	Richter and Schwandt, 1985
Cardiotrophin-1	cAMP–PKA	3T3-L1 adipocyte	Lopez-Yoldi et al., 2014
Endorphins, enkephalins and naloxone	cAMP–PKA	Rabbit adipocyte	Baptiste and Rizack, 1980
Growth differentiation factor 15	TGF-β signaling	3T3-L1 adipocyte	Chung et al., 2017
Heptapeptide Met-Arg-His-Phe-Arg-Trp-Gly	Melanocortin receptor	Rabbit adipocytes	Draper et al., 1973
Growth hormone	cAMP–PKA	Human and 3T3-F442A adipocyte	Dietz and Schwartz, 1991; Ottosson et al., 2000
Lactoferrin	cAMP–PKA	Rat adipocyte	Ono et al., 2013
MSH (α, β, VA-β-MSH)	Melanocortin receptor	3T3-L1 adipocyte	Fricke et al., 2005
Thyroid-stimulating hormone	cAMP–PKA	Human and 3T3-L1 adipocyte	Gagnon et al., 2010
Zinc α2-glycoprotein	β3-adrenoceptor	Mice and epididymal adipocytes	Russell et al., 2004
Small molecules			
α-Lipoic acid	cAMP–PKA	3T3-L1 adipocyte	Fernández-Galilea et al., 2012
Flavonoids – quercetin	Phosphodiesterase inhibition	Rat adipocyte	Kuppusamy and Das, 1992
Hydroxytyrosol	PKA and ERK1/2 pathway	3T3-L1 adipocyte	Drira and Sakamoto, 2014
Pycnogenol	β-receptor-mediated activity	3T3-L1 adipocyte	Mochizuki and Hasegawa, 2004
Medium-chain enriched diacylglycerol oil	Unknown	Mice	Kim et al., 2017
Procyanidin	cAMP–PKA	3T3-L1 adipocyte	Pinent et al., 2005
Sphingosine-1-phosphate	cAMP–PKA	Rat adipocytes	Jun et al., 2006
Sulforaphane	HSL activation	3T3-L1 adipocyte	Lee et al., 2012
Ursolic acid	cAMP–PKA	3T3-L1 adipocyte	Li et al., 2010
YC-1	cGMP–PKG pathway	Rat adipocytes	Chin et al., 2012
Plant extracts			
Biflavones of *Ginkgo biloba*	Inhibition of cAMP-phosphodiesterase	3T3-L1 adipocyte	Dell'Agli and Bosisio, 2002
Constituents from the leaves of *Nelumbo nucifera*	β-AR pathway	Mice	Ohkoshi et al., 2007
Ethanolic extracts of *Brassica campestris* spp. *rapa* roots	β3-adrenoceptor	Mice and 3T3-L1 adipocyte	An et al., 2010

Potential mechanisms of action, experimental models and references are provided.
Abbreviations: β-AR, β-adrenergic receptor; cAMP, cyclic adenosine monophosphate; cGMP, cyclic guanine monophosphate; ERK1/2; extracellular signal-regulated kinase 1/2; HSL, hormone-sensitive lipase; PKA, protein kinase A; PKG, protein kinase G; TGF-β, transforming growth factor β; VA-β-MSH, VA-β-melanocyte-stimulating hormone (where V is valine and A is alanine).

Furthermore, lipophagy, which is one form of macroautophagy, contributes to the hydrolysis of triacylglycerols stored in lipid droplets (Singh et al., 2009). The large size of lipid droplets impedes their recruitment into lipoautophagosomes, therefore lipophagy only recruits small portions of lipid droplets. Although the potential mechanisms of lipid droplet fragmentation remain unidentified, lipoautophagosomes fuse with lysosomes and within the resultant autolysosomes, lysosomal acid lipase (LAL) presumably hydrolyses triacylglycerols and FFAs are subsequently released into the cytoplasm (Fig. 3). A substantial contribution of lipophagy to the catabolism of triacylglycerols has been demonstrated in various cell types, including brown adipocytes (Saftig et al., 2008).

Storage, mobilization and dissipation of energy are essential for survival so we should not be too surprised that these key functions in energy balance are controlled by multiple redundant pathways. As outlined in this Review, these encompass neuronal control by the SNS, endocrine regulation and metabolic modulators. However, with regard to the number and diversity of endogenous non-adrenergic endocrine and metabolic modulators of lipolysis and thermogenesis in mammals, the physiological relevance of their impact on lipid storage and mobilization in relation to the dominant adrenergic control by the SNS remains to be addressed in more detail. The available studies mostly investigated single effects of molecules; however, to date, only a few of these studies have provided insights regarding additive or synergistic effects. Beyond this complexity within the organism, species-specific differences reported in the literature for some modulators, such as adrenergic agonists, natriuretic peptides, glucocorticoids and corticotropin, remain at the descriptive and mechanistic level without addressing the biological significance of such differences. A general question in this context, is whether differences between species are the result of divergent evolutionary histories and resulting physiological constraints. Traits such as body size and composition, metabolic rate, feeding habits and nutrient selection, energy partitioning in the body, tolerance to fasting, life style and activity behavior, as well as

Table 2. Pro-lipolytic effectors with species-specific differences in the regulation of lipolysis (see text for details and references)

Effectors	Rodents	Humans
β3 agonists	++++	+
Corticotropin (adrenocorticotropic hormone)	+++	–
Glucocorticoids	–	++
Natriuretic peptides	–	+++

torpor/hibernation are likely to have strongly influenced the mechanisms that evolved for the management of body fat stores. Indeed, in small rodents, rapid responses triggered by the SNS and the HPA axis seem to dominate; whereas in humans, endocrine regulation with a slower response time prevails, as exemplified by natriuretic peptides and glucocorticoids (Table 2). However, one may also conclude that more dedicated comparative studies are required to consolidate apparent species-specific differences.

Competing interests
The authors declare no competing or financial interests.

Funding
The Chair of Molecular Nutritional Medicine at TUM is supported by grants to M.K. by the German Research Foundation (Deutsche Forschungsgemeinschaft: KL973/11-1 and KL973/12-1, RTG1482), the Else Kröner-Fresenius Stiftung (EKFS) and the ZIEL – Institute for Food & Health. K.B. is a fellow of the Deutsche Forschungsgemeinschaft - Research Training Group 1482.

References

An, S., Han, J. I., Kim, M. J., Park, J. S., Han, J. M., Baek, N. I., Chung, H. G., Choi, M. S., Lee, K. T. and Jeong, T. S. (2010). Ethanolic extracts of Brassica campestris spp. rapa roots prevent high-fat diet-induced obesity via beta(3)-adrenergic regulation of white adipocyte lipolytic activity. *J. Med. Food* **13**, 406-414.

Anand-Srivastava, M. B. (2005). Natriuretic peptide receptor-C signaling and regulation. *Peptides* **26**, 1044-1059.

Bainbridge, F. A. and Beddard, A. P. (1906). Secretin in relation to diabetes mellitus. *Biochem. J.* **1**, 429-445.

Baptiste, E. J. and Rizack, M. A. (1980). In vitro cyclic AMP-mediated lipolytic activity of endorphins, enkephalins and naloxone. *Life Sci.* **27**, 135-141.

Bennett, B. D., Bennett, G. L., Vitangcol, R. V., Jewett, J. R., Burnier, J., Henzel, W. and Lowe, D. G. (1991). Extracellular domain-IgG fusion proteins for three human natriuretic peptide receptors. Hormone pharmacology and application to solid phase screening of synthetic peptide antisera. *J. Biol. Chem.* **266**, 23060-23067.

Berglund, E. D., Liu, T., Kong, X., Sohn, J.-W., Vong, L., Deng, Z., Lee, C. E., Lee, S., Williams, K. W., Olson, D. P. et al. (2014). Melanocortin 4 receptors in autonomic neurons regulate thermogenesis and glycemia. *Nat. Neurosci.* **17**, 911-913.

Birkenfeld, A. L., Boschmann, M., Moro, C., Adams, F., Heusser, K., Franke, G., Berlan, M., Luft, F. C., Lafontan, M. Jordan, J. (2005). Lipid mobilization with physiological atrial natriuretic peptide concentrations in humans. *J. Clin. Endocrinol. Metab.* **90**, 3622-3628.

Bodanszky, A., Ondetti, M. A., Mutt, V. and Bodanszky, M. (1969). Synthesis of secretin. IV. Secondary structure in a miniature protein. *J. Am. Chem. Soc.* **91**, 944-949.

Bordicchia, M., Liu, D., Amri, E.-Z., Ailhaud, G., Dessi-Fulgheri, P., Zhang, C., Takahashi, N., Sarzani, R. and Collins, S. (2012). Cardiac natriuretic peptides act via p38 MAPK to induce the brown fat thermogenic program in mouse and human adipocytes. *J. Clin. Invest.* **122**, 1022-1036.

Bousquet-Melou, A., Galitzky, J., Lafontan, M. and Berlan, M. (1995). Control of lipolysis in intra-abdominal fat cells of nonhuman primates: comparison with humans. *J. Lipid Res.* **36**, 451-461.

Brito, M. N., Brito, N. A., Baro, D. J., Song, C. K. and Bartness, T. J. (2007). Differential activation of the sympathetic innervation of adipose tissues by melanocortin receptor stimulation. *Endocrinology* **148**, 5339-5347.

Brito, N. A., Brito, M. N. and Bartness, T. J. (2008). Differential sympathetic drive to adipose tissues after food deprivation, cold exposure or glucoprivation. *Am. J. Physiol. Regul. Integr. Comp. Physiol.* **294**, R1445-R1452.

Broeders, E. P. M., Nascimento, E. B. M., Havekes, B., Brans, B., Roumans, K. H. M., Tailleux, A., Schaart, G., Kouach, M., Charton, J., Deprez, B. et al. (2015). The bile acid chenodeoxycholic acid increases human brown adipose tissue activity. *Cell Metab.* **22**, 418-426.

Brown, J., Chen, Q. and Hong, G. (1997). An autocrine system for C-type natriuretic peptide within rat carotid neointima during arterial repair. *Am. J. Physiol.* **272**, H2919-H2931.

Bukowiecki, L. J., Follea, N., Lupien, J. and Paradis, A. (1981). Metabolic relationships between lipolysis and respiration in rat brown adipocytes. The role of long chain fatty acids as regulators of mitochondrial respiration and feedback inhibitors of lipolysis. *J. Biol. Chem.* **256**, 12840-12848.

Butcher, R. W. and Carlson, L. A. (1970). Effects of secretin on fat mobilizing lipolysis and cyclic AMP levels in rat adipose tissue. *Acta Physiol. Scand.* **79**, 559-563.

Cannon, B. and Nedergaard, J. (2012). Cell biology: neither brown nor white. *Nature* **488**, 286-287.

Castan, I., Valet, P., Quideau, N., Voisin, T., Ambid, L., Laburthe, M., Lafontan, M. and Carpene, C. (1994). Antilipolytic effects of alpha 2-adrenergic agonists, neuropeptide Y, adenosine, and PGE1 in mammal adipocytes. *Am. J. Physiol.* **266**, R1141-R1147.

Cheloha, R. W., Gellman, S. H., Vilardaga, J.-P. and Gardella, T. J. (2015). PTH receptor-1 signalling-mechanistic insights and therapeutic prospects. *Nat. Rev. Endocrinol.* **11**, 712-724.

Chin, C.-H., Tsai, F.-C., Chen, S.-P., Wang, K.-C., Chang, C.-C., Pai, M.-H. and Fong, T.-H. (2012). YC-1, a potent antithrombotic agent, induces lipolysis through the PKA pathway in rat visceral fat cells. *Eur. J. Pharmacol.* **689**, 1-7.

Cho, K.-J., Shim, J.-H., Cho, M.-C., Choe, Y.-K., Hong, J.-T., Moon, D.-C., Kim, J.-W. and Yoon, D.-Y. (2005). Signaling pathways implicated in alpha-melanocyte stimulating hormone-induced lipolysis in 3T3-L1 adipocytes. *J. Cell. Biochem.* **96**, 869-878.

Chun, T.-H., Itoh, H., Ogawa, Y., Tamura, N., Takaya, K., Igaki, T., Yamashita, J., Doi, K., Inoue, M., Masatsugu, K. et al. (1997). Shear stress augments expression of C-type natriuretic peptide and adrenomedullin. *Hypertension* **29**, 1296-1302.

Chung, H. K., Ryu, D., Kim, K. S., Chang, J. Y., Kim, Y. K., Yi, H.-S., Kang, S. G., Choi, M. J., Lee, S. E., Jung, S.-B. et al. (2017). Growth differentiation factor 15 is a myomitokine governing systemic energy homeostasis. *J. Cell Biol.* **216**, 149-165.

Cypess, A. M., Weiner, L. S., Roberts-Toler, C., Franquet Elia, E., Kessler, S. H., Kahn, P. A., English, J., Chatman, K., Trauger, S. A., Doria, A. et al. (2015). Activation of human brown adipose tissue by a beta3-adrenergic receptor agonist. *Cell Metab.* **21**, 33-38.

de Bold, A. J., Borenstein, H. B., Veress, A. T. and Sonnenberg, H. (1981). A rapid and potent natriuretic response to intravenous injection of atrial myocardial extract in rats. *Life Sci.* **28**, 89-94.

Dehaye, J. P., Winand, J. and Christophe, J. (1977). Lipolysis and cyclic AMP levels in epididymal adipose tissue of obese-hyperglycaemic mice. *Diabetologia* **13**, 553-561.

Dell'Agli, M. and Bosisio, E. (2002). Biflavones of Ginkgo biloba stimulate lipolysis in 3T3-L1 adipocytes. *Planta Med.* **68**, 76-79.

Dietz, J. R. (1984). Release of natriuretic factor from rat heart-lung preparation by atrial distension. *Am. J. Physiol.* **247**, R1093-R1096.

Dietz, J. and Schwartz, J. (1991). Growth hormone alters lipolysis and hormone-sensitive lipase activity in 3T3-F442A adipocytes. *Metabolism* **40**, 800-806.

Draper, M. W., Merrifield, R. B. and Rizack, M. A. (1973). Lipolytic activity of Met-Arg-His-Phe-Arg-Trp-Gly, a synthetic analog of the ACTH (4-10) core sequence. *J. Med. Chem.* **16**, 1326-1330.

Drira, R. and Sakamoto, K. (2014). Hydroxytyrosol stimulates lipolysis via A-kinase and extracellular signal-regulated kinase activation in 3T3-L1 adipocytes. *Eur. J. Nutr.* **53**, 743-750.

Duncan, R. E., Ahmadian, M., Jaworski, K., Sarkadi-Nagy, E. and Sul, H. S. (2007). Regulation of lipolysis in adipocytes. *Annu. Rev. Nutr.* **27**, 79-101.

Fain, J. N., Dodd, A. and Novak, L. (1971). Enzyme regulation in gluconeogenesis and lipogenesis. Relationship of protein synthesis and cyclic AMP to lipolytic action of growth hormone and glucocorticoids. *Metabolism* **20**, 109-118.

Fedorenko, A., Lishko, P. V. and Kirichok, Y. (2012). Mechanism of fatty-acid-dependent UCP1 uncoupling in brown fat mitochondria. *Cell* **151**, 400-413.

Fellenz, M., Triandafillou, J., Gwilliam, C. and Himms-Hagen, J. (1982). Growth of interscapular brown adipose tissue in cold-acclimated hypophysectomized rats maintained on thyroxine and corticosterone. *Can. J. Biochem.* **60**, 838-842.

Fernández-Galilea, M., Perez-Matute, P., Prieto-Hontoria, P. L., Martinez, J. A. and Moreno-Aliaga, M. J. (2012). Effects of lipoic acid on lipolysis in 3T3-L1 adipocytes. *J. Lipid Res.* **53**, 2296-2306.

Flachs, P., Adamcova, K., Zouhar, P., Marques, C., Janovska, P., Viegas, I., Jones, J. G., Bardova, K., Svobodova, M., Hansikova, J. et al. (2017). Induction of lipogenesis in white fat during cold exposure in mice: link to lean phenotype. *Int. J. Obes. (Lond)* **41**, 372-380.

Foster, D. O. and Frydman, M. L. (1979). Tissue distribution of cold-induced thermogenesis in conscious warm- or cold-acclimated rats reevaluated from changes in tissue blood flow: the dominant role of brown adipose tissue in the replacement of shivering by nonshivering thermogenesis. *Can. J. Physiol. Pharmacol.* **57**, 257-270.

Frandsen, E. K. and Moody, A. J. (1973). Lipolytic action of a newly isolated vasoactive intestinal polypeptide. *Horm. Metab. Res.* **5**, 196-199.

Fricke, K., Schulz, A., John, H., Forssmann, W.-G. and Maronde, E. (2005). Isolation and characterization of a novel proopiomelanocortin-derived peptide from hemofiltrate of chronic renal failure patients. *Endocrinology* **146**, 2060-2068.

Gagnon, A., Antunes, T. T., Ly, T., Pongsuwan, P., Gavin, C., Lochnan, H. A. and Sorisky, A. (2010). Thyroid-stimulating hormone stimulates lipolysis in adipocytes in culture and raises serum free fatty acid levels in vivo. *Metabolism* **59**, 547-553.

Galpin, K. S., Henderson, R. G., James, W. P. T. and Trayhurn, P. (1983). GDP binding to brown-adipose-tissue mitochondria of mice treated chronically with corticosterone. *Biochem. J.* **214**, 265-268.

Journal of Experimental Biology

Gardella, T. J. and Vilardaga, J. P. (2015). International Union of Basic and Clinical Pharmacology. XCIII. The parathyroid hormone receptors–family B G protein-coupled receptors. *Pharmacol. Rev.* **67**, 310-337.
Ge, H., Li, X., Weiszmann, J., Wang, P., Baribault, H., Chen, J.-L., Tian, H. and Li, Y. (2008). Activation of G protein-coupled receptor 43 in adipocytes leads to inhibition of lipolysis and suppression of plasma free fatty acids. *Endocrinology* **149**, 4519-4526.
Girardier, L. and Seydoux, J. (1986). Neural control of brown adipose tissue. In *Brown Adipose Tissue* (ed. P. Trayhurn and D. G. Nicholls), pp. 122-151. London Eng.; Baltimore, MD, USA: E. Arnold.
Glick, Z., Thomas, D. W. and Mayer, J. (1971). Absence of effect of injections of the intestinal hormones secretin and choecystokinin-pancreozymin upon feeding behavior. *Physiol. Behav.* **6**, 5-8.
Gnad, T., Scheibler, S., von Kugelgen, I., Scheele, C., Kilić, A., Glöde, A., Hoffmann, L. S., Reverte-Salisa, L., Horn, P., Mutlu, S. et al. (2014). Adenosine activates brown adipose tissue and recruits beige adipocytes via A2A receptors. *Nature* **516**, 395-399.
Goy, M. F., Oliver, P. M., Purdy, K. E., Knowles, J. W., Fox, J. E., Mohler, P. J., Qian, X., Smithies, O. and Maeda, N. (2001). Evidence for a novel natriuretic peptide receptor that prefers brain natriuretic peptide over atrial natriuretic peptide. *Biochem. J.* **358**, 379-387.
Grovum, W. L. (1981). Factors affecting the voluntary intake of food by sheep. 3. The effect of intravenous infusions of gastrin, cholecystokinin and secretin on motility of the reticulo-rumen and intake. *Br. J. Nutr.* **45**, 183-201.
He, J., Jiang, H., Tansey, J. T., Tang, C., Pu, S. and Xu, G. (2006). Calyculin and okadaic acid promote perilipin phosphorylation and increase lipolysis in primary rat adipocytes. *Biochim. Biophys. Acta* **1761**, 247-255.
Herman, J. P., Langub, M. C., Jr. and Watson, R. E. Jr. (1993). Localization of C-type natriuretic peptide mRNA in rat hypothalamus. *Endocrinology* **133**, 1903-1906.
Herman, J. P., Dolgas, C. M., Marcinek, R. and Langub, M. C. Jr. (1996). Expression and glucocorticoid regulation of natriuretic peptide clearance receptor (NPR-C) mRNA in rat brain and choroid plexus. *J. Chem. Neuroanat.* **11**, 257-265.
Heseltine, L., Webster, J. M. and Taylor, R. (1995). Adenosine effects upon insulin action on lipolysis and glucose transport in human adipocytes. *Mol. Cell. Biochem.* **144**, 147-151.
Honnor, R. C., Dhillon, G. S. and Londos, C. (1985). cAMP-dependent protein kinase and lipolysis in rat adipocytes. II. Definition of steady-state relationship with lipolytic and antilipolytic modulators. *J. Biol. Chem.* **260**, 15130-15138.
Houten, S. M. and Auwerx, J. (2004). The enterohepatic nuclear receptors are major regulators of the enterohepatic circulation of bile salts. *Ann. Med.* **36**, 482-491.
Hunt, P. J., Richards, A. M., Espiner, E. A., Nicholls, M. G. and Yandle, T. G. (1994). Bioactivity and metabolism of C-type natriuretic peptide in normal man. *J. Clin. Endocrinol. Metab.* **78**, 1428-1435.
Iwen, K. A. H., Senyaman, O., Schwartz, A., Drenckhan, M., Meier, B., Hadaschik, D. and Klein, J. (2008). Melanocortin crosstalk with adipose functions: ACTH directly induces insulin resistance, promotes a pro-inflammatory adipokine profile and stimulates UCP-1 in adipocytes. *J. Endocrinol.* **196**, 465-472.
Jansky, L., Bartunkova, R., Kockova, J., Mejsnar, J. and Zeisberger, E. (1969). Interspecies differences in cold adaptation and nonshivering thermogenesis. *Fed. Proc.* **28**, 1053-1058.
Jeandel, L., Okamura, H., Belles-Isles, M., Chabot, J.-G., Dihl, F., Morel, G., Kelly, P. A. and Heisler, S. (1989). Immunocytochemical localization, binding, and effects of atrial natriuretic peptide in rat adipocytes. *Mol. Cell. Endocrinol.* **62**, 69-78.
Jensen, R. T., Charlton, C. G., Adachi, H., Jones, S. W., O'Donohue, T. L. and Gardner, J. D. (1983). Use of 125I-secretin to identify and characterize high-affinity secretin receptors on pancreatic acini. *Am. J. Physiol.* **245**, G186-G195.
Johansson, S. M., Lindgren, E., Yang, J.-N., Herling, A. W. and Fredholm, B. B. (2008). Adenosine A1 receptors regulate lipolysis and lipogenesis in mouse adipose tissue-interactions with insulin. *Eur. J. Pharmacol.* **597**, 92-101.
Jun, D.-J., Lee, J.-H., Choi, B.-H., Koh, T.-K., Ha, D.-C., Jeong, M.-W. and Kim, K.-T. (2006). Sphingosine-1-phosphate modulates both lipolysis and leptin production in differentiated rat white adipocytes. *Endocrinology* **147**, 5835-5844.
Kajimura, S., Spiegelman, B. M. and Seale, P. (2015). Brown and beige fat: physiological roles beyond heat generation. *Cell Metab.* **22**, 546-559.
Kawamata, Y., Fujii, R., Hosoya, M., Harada, M., Yoshida, H., Miwa, M., Fukusumi, S., Habata, Y., Itoh, T., Shintani, Y. et al. (2003). A G protein-coupled receptor responsive to bile acids. *J. Biol. Chem.* **278**, 9435-9440.
Kazak, L., Chouchani, E. T., Jedrychowski, M. P., Erickson, B. K., Shinoda, K., Cohen, P., Vetrivelan, R., Lu, G. Z., Laznik-Bogoslavski, D., Hasenfuss, S. C. et al. (2015). A creatine-driven substrate cycle enhances energy expenditure and thermogenesis in beige fat. *Cell* **163**, 643-655.
Kim, H., Choe, J. H., Choi, J. H., Kim, H. J., Park, S. H., Lee, M. W., Kim, W. and Go, G. W. (2017). Medium-Chain Enriched Diacyglycerol (MCE-DAG) oil decreased body fat mass in mice by increasing lipolysis and thermogenesis in adipose tissue. *Lipids* **52**, 665-673.
Kir, S., White, J. P., Kleiner, S., Kazak, L., Cohen, P., Baracos, V. E. and Spiegelman, B. M. (2014). Tumor-derived PTH-related protein triggers adipose tissue browning and cancer cachexia. *Nature* **513**, 100-104.
Kiwaki, K. and Levine, J. A. (2003). Differential effects of adrenocorticotropic hormone on human and mouse adipose tissue. *J. Comp. Physiol. B* **173**, 675-678.
Klein, S. M., Schreml, S., Nerlich, M. and Prantl, L. (2009). In vitro studies investigating the effect of subcutaneous phosphatidylcholine injections in the 3T3-L1 adipocyte model: lipolysis or lipid dissolution? *Plast. Reconstr. Surg.* **124**, 419-427.
Klingenspor, M., Herzig, S. and Pfeifer, A. (2012). Brown fat develops a brite future. *Obes. Facts* **5**, 890-896.
Klingenspor, M., Bast, A., Bolze, F., Li, Y., Maurer, S., Schweizer, S., Willershäuser, M. and Fromme, T. (2017). Brown adipose tissue. In *Adipose Tissue Biology* (ed. M. E. Symonds), pp. 91-147. Cham: Springer International Publishing.
Kopin, A. S., Wheeler, M. B. and Leiter, A. B. (1990). Secretin: structure of the precursor and tissue distribution of the mRNA. *Proc. Natl. Acad. Sci. USA* **87**, 2299-2303.
Kuppusamy, U. R. and Das, N. P. (1992). Effects of flavonoids on cyclic AMP phosphodiesterase and lipid mobilization in rat adipocytes. *Biochem. Pharmacol.* **44**, 1307-1315.
Lafontan, M. (2012). Historical perspectives in fat cell biology: the fat cell as a model for the investigation of hormonal and metabolic pathways. *Am. J. Physiol. Cell Physiol.* **302**, C327-C359.
Lafontan, M. and Berlan, M. (1993). Fat cell adrenergic receptors and the control of white and brown fat cell function. *J. Lipid. Res.* **34**, 1057-1091.
Lafontan, M. and Langin, D. (2009). Lipolysis and lipid mobilization in human adipose tissue. *Prog. Lipid Res.* **48**, 275-297.
Larsson, S., Jones, H. A., Göransson, O., Degerman, E. and Holm, C. (2016). Parathyroid hormone induces adipocyte lipolysis via PKA-mediated phosphorylation of hormone-sensitive lipase. *Cell Signal.* **28**, 204-213.
Lee, M.-J. and Fried, S. K. (2014). Optimal protocol for the differentiation and metabolic analysis of human adipose stromal cells. *Methods Enzymol.* **538**, 49-65.
Lee, J.-H., Moon, M.-H., Jeong, J.-K., Park, Y.-G., Lee, Y.-J., Seol, J.-W. and Park, S.-Y. (2012). Sulforaphane induced adipolysis via hormone sensitive lipase activation, regulated by AMPK signaling pathway. *Biochem. Biophys. Res. Commun.* **426**, 492-497.
Lefebvre, P., Cariou, B., Lien, F., Kuipers, F. and Staels, B. (2009). Role of bile acids and bile acid receptors in metabolic regulation. *Physiol. Rev.* **89**, 147-191.
Li, Y., Kang, Z., Li, S., Kong, T., Liu, X. and Sun, C. (2010). Ursolic acid stimulates lipolysis in primary-cultured rat adipocytes. *Mol. Nutr. Food Res.* **54**, 1609-1617.
Li, Y., Fromme, T., Schweizer, S., Schottl, T. and Klingenspor, M. (2014). Taking control over intracellular fatty acid levels is essential for the analysis of thermogenic function in cultured primary brown and brite/beige adipocytes. *EMBO Rep.* **15**, 1069-1076.
Li, Y., Fromme, T. and Klingenspor, M. (2017). Meaningful respirometric measurements of UCP1-mediated thermogenesis. *Biochimie* **134**, 56-61.
Lin, X., Hanze, J., Heese, F., Sodmann, R. and Lang, R. E. (1995). Gene expression of natriuretic peptide receptors in myocardial cells. *Circ. Res.* **77**, 750-758.
Lindahl, M., Petrlova, J., Dalla-Riva, J., Wasserstrom, S., Rippe, C., Domingo-Espin, J., Kotowska, D., Krupinska, E., Berggreen, C., Jones, H. A. et al. (2015). ApoA-I Milano stimulates lipolysis in adipose cells independently of cAMP/PKA activation. *J. Lipid Res.* **56**, 2248-2259.
Liu, C., Wu, J., Zhu, J., Kuei, C., Yu, J., Shelton, J., Sutton, S. W., Li, X., Yun, S. J., Mirzadegan, T. et al. (2009). Lactate inhibits lipolysis in fat cells through activation of an orphan G-protein-coupled receptor, GPR81. *J. Biol. Chem.* **284**, 2811-2822.
Lockie, S. H., Heppner, K. M., Chaudhary, N., Chabenne, J. R., Morgan, D. A., Veyrat-Durebex, C., Ananthakrishnan, G., Rohner-Jeanrenaud, F., Drucker, D. J., DiMarchi, R. et al. (2012). Direct control of brown adipose tissue thermogenesis by central nervous system glucagon-like peptide-1 receptor signaling. *Diabetes* **61**, 2753-2762.
Lonnroth, P., Jansson, P. A., Fredholm, B. B. and Smith, U. (1989). Microdialysis of intercellular adenosine concentration in subcutaneous tissue in humans. *Am. J. Physiol.* **256**, E250-E255.
López-Yoldi, M., Fernández-Galilea, M., Laiglesia, L. M., Larequi, E., Prieto, J., Martínez, J. A., Bustos, M. and Moreno-Aliaga, M. J. (2014). Cardiotrophin-1 stimulates lipolysis through the regulation of main adipose tissue lipases. *J. Lipid Res.* **55**, 2634-2643.
Lowe, D. G., Chang, M. S., Hellmiss, R., Chen, E., Singh, S., Garbers, D. L. and Goeddel, D. V. (1989). Human atrial natriuretic peptide receptor defines a new paradigm for second messenger signal transduction. *EMBO J.* **8**, 1377-1384.
Maruyama, T., Miyamoto, Y., Nakamura, T., Tamai, Y., Okada, H., Sugiyama, E., Nakamura, T., Itadani, H. and Tanaka, K. (2002). Identification of membrane-type receptor for bile acids (M-BAR). *Biochem. Biophys. Res. Commun.* **298**, 714-719.
McQueen, A. E., Kanamaluru, D., Yan, K., Gray, N. E., Wu, L., Li, M. L., Chang, A., Hasan, A., Stifler, D., Koliwad, S. K. and Wang, J. C. (2017). The C-terminal

fibrinogen-like domain of angiopoietin-like 4 stimulates adipose tissue lipolysis and promotes energy expenditure. *J. Biol. Chem.* **292**, 16122-16134.
Mericq, V., Uyeda, J. A., Barnes, K. M., de Luca, F. and Baron, J. (2000). Regulation of fetal rat bone growth by C-type natriuretic peptide and cGMP. *Pediatr. Res.* **47**, 189-193.
Middendorff, R., Muller, D., Paust, H. J., Davidoff, M. S. and Mukhopadhyay, A. K. (1996). Natriuretic peptides in the human testis: evidence for a potential role of C-type natriuretic peptide in Leydig cells. *J. Clin. Endocrinol. Metab.* **81**, 4324-4328.
Miegueu, P., Cianflone, K., Richard, D. and St-Pierre, D. H. (2013). Effect of secretin on preadipocyte, differentiating and mature adipocyte functions. *Int. J. Obes. (Lond)* **37**, 366-374.
Miyagi, M. and Misono, K. S. (2000). Disulfide bond structure of the atrial natriuretic peptide receptor extracellular domain: conserved disulfide bonds among guanylate cyclase-coupled receptors. *Biochim. Biophys. Acta* **1478**, 30-38.
Mochizuki, M. and Hasegawa, N. (2004). Pycnogenol stimulates lipolysis in 3t3-L1 cells via stimulation of beta-receptor mediated activity. *Phytother. Res.* **18**, 1029-1030.
Moro, C., Crampes, F., Sengenès, C., De Glisezinski, I., Galitzky, J., Thalamas, C., Lafontan, M. and Berlan, M. (2004a). Atrial natriuretic peptide contributes to physiological control of lipid mobilization in humans. *FASEB J.* **18**, 908-910.
Moro, C., Galitzky, J., Sengenès, C., Crampes, F., Lafontan, M. and Berlan, M. (2004b). Functional and pharmacological characterization of the natriuretic peptide-dependent lipolytic pathway in human fat cells. *J. Pharmacol. Exp. Ther.* **308**, 984-992.
Mukoyama, M., Nakao, K., Saito, Y., Ogawa, Y., Hosoda, K., Suga, S., Shirakami, G., Jougasaki, M. and Imura, H. (1990). Increased human brain natriuretic peptide in congestive heart failure. *N. Engl. J. Med.* **323**, 757-758.
Mukoyama, M., Nakao, K., Hosoda, K., Suga, S., Saito, Y., Ogawa, Y., Shirakami, G., Jougasaki, M., Obata, K., Yasue, H. et al. (1991). Brain natriuretic peptide as a novel cardiac hormone in humans. Evidence for an exquisite dual natriuretic peptide system, atrial natriuretic peptide and brain natriuretic peptide. *J. Clin. Invest.* **87**, 1402-1412.
Nakamura, K. and Morrison, S. F. (2011). Central efferent pathways for cold-defensive and febrile shivering. *J. Physiol.* **589**, 3641-3658.
Nielsen, T. S., Jessen, N., Jorgensen, J. O. L., Moller, N. and Lund, S. (2014). Dissecting adipose tissue lipolysis: molecular regulation and implications for metabolic disease. *J. Mol. Endocrinol.* **52**, R199-R222.
Nussenzveig, D. R., Lewicki, J. A. and Maack, T. (1990). Cellular mechanisms of the clearance function of type C receptors of atrial natriuretic factor. *J. Biol. Chem.* **265**, 20952-20958.
Ohkoshi, E., Miyazaki, H., Shindo, K., Watanabe, H., Yoshida, A. and Yajima, H. (2007). Constituents from the leaves of Nelumbo nucifera stimulate lipolysis in the white adipose tissue of mice. *Planta Med.* **73**, 1255-1259.
Oikawa, S., Imai, M., Ueno, A., Tanaka, S., Noguchi, T., Nakazato, H., Kangawa, K., Fukuda, A. and Matsuo, H. (1984). Cloning and sequence analysis of cDNA encoding a precursor for human atrial natriuretic polypeptide. *Nature* **309**, 724-726.
Okamura, H., Kelly, P. A., Chabot, J. G., Morel, G., Belles-Isles, M. and Heisler, S. (1988). Atrial natriuretic peptide receptors are present in brown adipose tissue. *Biochem. Biophys. Res. Commun.* **156**, 1000-1006.
Ono, T., Fujisaki, C., Ishihara, Y., Ikoma, K., Morishita, S., Murakoshi, M., Sugiyama, K., Kato, H., Miyashita, K., Yoshida, T. et al. (2013). Potent lipolytic activity of lactoferrin in mature adipocytes. *Biosci. Biotechnol. Biochem.* **77**, 566-571.
Ottosson, M., Lonnroth, P., Bjorntorp, P. and Eden, S. (2000). Effects of cortisol and growth hormone on lipolysis in human adipose tissue. *J. Clin. Endocrinol. Metab.* **85**, 799-803.
Paschoalini, M. A. and Migliorini, R. H. (1990). Participation of the CNS in the control of FFA mobilization during fasting in rabbits. *Physiol. Behav.* **47**, 461-465.
Pinent, M., Bladé, M. C., Salvadó, M. J., Arola, L. and Ardévol, A. (2005). Intracellular mediators of procyanidin-induced lipolysis in 3T3-L1 adipocytes. *J. Agric. Food Chem.* **53**, 262-266.
Potter, L. R., Yoder, A. R., Flora, D. R., Antos, L. K. and Dickey, D. M. (2009). Natriuretic peptides: their structures, receptors, physiologic functions and therapeutic applications. *Handb. Exp. Pharmacol.***191**, 341-366.
Ramage, L. E., Akyol, M., Fletcher, A. M., Forsythe, J., Nixon, M., Carter, R. N., van Beek, E. J. R., Morton, N. M., Walker, B. R. and Stimson, R. H. (2016). Glucocorticoids acutely increase brown adipose tissue activity in humans, revealing species-specific differences in UCP-1 regulation. *Cell Metab.* **24**, 130-141.
Regard, J. B., Sato, I. T. and Coughlin, S. R. (2008). Anatomical profiling of G protein-coupled receptor expression. *Cell* **135**, 561-571.
Revelli, J.-P., Muzzin, P., Paoloni, A., Moinat, M. and Giacobino, J.-P. (1993). Expression of the beta 3-adrenergic receptor in human white adipose tissue. *J. Mol. Endocrinol.* **10**, 193-197.
Richter, W. O. and Schwandt, P. (1985). Physiologic concentrations of beta-lipotropin stimulate lipolysis in rabbit adipocytes. *Metabolism* **34**, 539-543.
Rodbell, M., Birnbaumer, L. and Pohl, S. L. (1970). Adenyl cyclase in fat cells. 3. Stimulation by secretin and the effects of trypsin on the receptors for lipolytic hormones. *J. Biol. Chem.* **245**, 718-722.
Rohm, M., Schäfer, M., Laurent, V., Üstünel, B. E., Niopek, K., Algire, C., Hautzinger, O., Sijmonsma, T. P., Zota, A., Medrikova, D. et al. (2016). An AMP-activated protein kinase-stabilizing peptide ameliorates adipose tissue wasting in cancer cachexia in mice. *Nat. Med.* **22**, 1120-1130.
Rosak, C. and Hittelman, K. J. (1977). Characterization of lipolytic responses of isolated white adipocytes from hamsters. *Biochim. Biophys. Acta* **496**, 458-474.
Rose, R. A. and Giles, W. R. (2008). Natriuretic peptide C receptor signalling in the heart and vasculature. *J. Physiol.* **586**, 353-366.
Rothwell, N. J. and Stock, M. J. (1985). Acute and chronic effects of ACTH on thermogenesis and brown adipose tissue in the rat. *Comp. Biochem. Physiol. A Comp. Physiol.* **81**, 99-102.
Russell, D. W. (2003). The enzymes, regulation, and genetics of bile acid synthesis. *Annu. Rev. Biochem.* **72**, 137-174.
Russell, S. T., Zimmerman, T. P., Domin, B. A. and Tisdale, M. J. (2004). Induction of lipolysis in vitro and loss of body fat in vivo by zinc-alpha2-glycoprotein. *Biochim. Biophys. Acta* **1636**, 59-68.
Saftig, P., Beertsen, W. and Eskelinen, E. L. (2008). LAMP-2: a control step for phagosome and autophagosome maturation. *Autophagy* **4**, 510-512.
Sanders, M. A., Madoux, F., Mladenovic, L., Zhang, H., Ye, X., Angrish, M., Mottillo, E. P., Caruso, J. A., Halvorsen, G., Roush, W. R. et al. (2015). Endogenous and synthetic ABHD5 ligands regulate ABHD5-perilipin interactions and lipolysis in fat and muscle. *Cell Metab.* **22**, 851-860.
Sarzani, R., Dessi-Fulgheri, P., Paci, V. M., Espinosa, E. and Rappelli, A. (1996). Expression of natriuretic peptide receptors in human adipose and other tissues. *J. Endocrinol. Invest.* **19**, 581-585.
Schiffrin, E. L., Poissant, L., Cantin, M. and Thibault, G. (1986). Receptors for atrial natriuretic factor in cultured vascular smooth muscle cells. *Life Sci.* **38**, 817-826.
Schimmel, R. J. and McMahon, K. K. (1980). Inhibition of lipolysis and cyclic AMP accumulation by adenosine analogues in hamster epididymal adipocytes exposed to cholera toxin. *Biochim. Biophys. Acta* **633**, 237-244.
Scotney, H., Symonds, M. E., Law, J., Budge, H., Sharkey, D. and Manolopoulos, K. N. (2017). Glucocorticoids modulate human brown adipose tissue thermogenesis in vivo. *Metabolism* **70**, 125-132.
Sekar, R. and Chow, B. K. C. (2014). Lipolytic actions of secretin in mouse adipocytes. *J. Lipid Res.* **55**, 190-200.
Sengenès, C., Berlan, M., De Glisezinski, I., Lafontan, M. and Galitzky, J. (2000). Natriuretic peptides: a new lipolytic pathway in human adipocytes. *FASEB J.* **14**, 1345-1351.
Sengenès, C., Zakaroff-Girard, A., Moulin, A., Berlan, M., Bouloumié, A., Lafontan, M. and Galitzky, J. (2002). Natriuretic peptide-dependent lipolysis in fat cells is a primate specificity. *Am. J. Physiol. Regul. Integr. Comp. Physiol.* **283**, R257-R265.
Sengenès, C., Bouloumie, A., Hauner, H., Berlan, M., Busse, R., Lafontan, M. and Galitzky, J. (2003). Involvement of a cGMP-dependent pathway in the natriuretic peptide-mediated hormone-sensitive lipase phosphorylation in human adipocytes. *J. Biol. Chem.* **278**, 48617-48626.
Shimamura, M., Matsuda, M., Kobayashi, S., Ando, Y., Ono, M., Koishi, R., Furukawa, H., Makishima, M. and Shimomura, I. (2003). Angiopoietin-like protein 3, a hepatic secretory factor, activates lipolysis in adipocytes. *Biochem. Biophys. Res. Commun.* **301**, 604-609.
Shinoda, K., Luijten, I. H., Hasegawa, Y., Hong, H., Sonne, S. B., Kim, M., Xue, R., Chondronikola, M., Cypess, A. M., Tseng, Y. H. et al. (2015). Genetic and functional characterization of clonally derived adult human brown adipocytes. *Nat. Med.* **21**, 389-394.
Singh, R., Kaushik, S., Wang, Y., Xiang, Y., Novak, I., Komatsu, M., Tanaka, K., Cuervo, A. M. and Czaja, M. J. (2009). Autophagy regulates lipid metabolism. *Nature* **458**, 1131-1135.
Sinha, T. K., Thajchayapong, P., Queener, S. F., Allen, D. O. and Bell, N. H. (1976). On the lipolytic action of parathyroid hormone in man. *Metabolism* **25**, 251-260.
Siu, F. K. Y., Lam, I. P. Y., Chu, J. Y. S. and Chow, B. K. C. (2006). Signaling mechanisms of secretin receptor. *Regul. Pept.* **137**, 95-104.
Smith, R. (1961). Thermogenic activity of the hibernating gland in the cold-acclimated rat. *Physiologist* **4**, 113.
Stephenson, S. L. and Kenny, A. J. (1987). The hydrolysis of alpha-human atrial natriuretic peptide by pig kidney microvillar membranes is initiated by endopeptidase-24.11. *Biochem. J.* **243**, 183-187.
Sudoh, T., Kangawa, K., Minamino, N. and Matsuo, H. (1988). A new natriuretic peptide in porcine brain. *Nature* **332**, 78-81.
Sudoh, T., Minamino, N., Kangawa, K. and Matsuo, H. (1990). C-type natriuretic peptide (CNP): a new member of natriuretic peptide family identified in porcine brain. *Biochem. Biophys. Res. Commun.* **168**, 863-870.
Suga, S., Nakao, K., Hosoda, K., Mukoyama, M., Ogawa, Y., Shirakami, G., Arai, H., Saito, Y., Kambayashi, Y., Inouye, K. et al. (1992a). Receptor selectivity of natriuretic peptide family, atrial natriuretic peptide, brain natriuretic peptide, and C-type natriuretic peptide. *Endocrinology* **130**, 229-239.

Suga, S., Nakao, K., Itoh, H., Komatsu, Y., Ogawa, Y., Hama, N. and Imura, H. (1992b). Endothelial production of C-type natriuretic peptide and its marked augmentation by transforming growth factor-beta. Possible existence of "vascular natriuretic peptide system". *J. Clin. Invest.* **90**, 1145-1149.

Szillat, D. and Bukowiecki, L. J. (1983). Control of brown adipose tissue lipolysis and respiration by adenosine. *Am. J. Physiol.* **245**, E555-E559.

Taggart, A. K. P., Kero, J., Gan, X., Cai, T.-Q., Cheng, K., Ippolito, M., Ren, N., Kaplan, R., Wu, K., Wu, T.-J. et al. (2005). (D)-beta-Hydroxybutyrate inhibits adipocyte lipolysis via the nicotinic acid receptor PUMA-G. *J. Biol. Chem.* **280**, 26649-26652.

Takahashi, T., Allen, P. D. and Izumo, S. (1992). Expression of A-, B-, and C-type natriuretic peptide genes in failing and developing human ventricles. Correlation with expression of the Ca(2+)-ATPase gene. *Circ. Res.* **71**, 9-17.

Tamura, N., Ogawa, Y., Chusho, H., Nakamura, K., Nakao, K., Suda, M., Kasahara, M., Hashimoto, R., Katsuura, G., Mukoyama, M. et al. (2000). Cardiac fibrosis in mice lacking brain natriuretic peptide. *Proc. Natl. Acad. Sci. USA* **97**, 4239-4244.

Taniguchi, A., Kataoka, K., Kono, T., Oseko, F., Okuda, H., Nagata, I. and Imura, H. (1987). Parathyroid hormone-induced lipolysis in human adipose tissue. *J. Lipid Res.* **28**, 490-494.

Teodoro, J. S., Zouhar, P., Flachs, P., Bardova, K., Janovska, P., Gomes, A. P., Duarte, F. V., Varela, A. T., Rolo, A. P., Palmeira, C. M. et al. (2014). Enhancement of brown fat thermogenesis using chenodeoxycholic acid in mice. *Int. J. Obes. (Lond)* **38**, 1027-1034.

Thuerauf, D. J., Hanford, D. S. and Glembotski, C. C. (1994). Regulation of rat brain natriuretic peptide transcription. A potential role for GATA-related transcription factors in myocardial cell gene expression. *J. Biol. Chem.* **269**, 17772-17775.

van den Beukel, J. C., Grefhorst, A., Quarta, C., Steenbergen, J., Mastroberardino, P. G., Lombes, M., Delhanty, P. J., Mazza, R., Pagotto, U., van der Lely, A. J. et al. (2014). Direct activating effects of adrenocorticotropic hormone (ACTH) on brown adipose tissue are attenuated by corticosterone. *FASEB J.* **28**, 4857-4867.

Van Itallie, T. B., Beaudoin, R. and Mayer, J. (1953). Arteriovenous glucose differences, metabolic hypoglycemia and food intake in man. *J. Clin. Nutr.* **1**, 208-217.

Vaughan, C. H., Zarebidaki, E., Ehlen, J. C. and Bartness, T. J. (2014). Analysis and measurement of the sympathetic and sensory innervation of white and brown adipose tissue. *Methods Enzymol.* **537**, 199-225.

Wang, W. and Seale, P. (2016). Control of brown and beige fat development. *Nat. Rev. Mol. Cell Biol.* **17**, 691-702.

Watanabe, M., Houten, S. M., Mataki, C., Christoffolete, M. A., Kim, B. W., Sato, H., Messaddeq, N., Harney, J. W., Ezaki, O., Kodama, T. et al. (2006). Bile acids induce energy expenditure by promoting intracellular thyroid hormone activation. *Nature* **439**, 484-489.

Werner, S. and Löw, H. (1973). Stimulation of lipolysis and calcium accumulation by parathyroid hormone in rat adipose tissue in vitro after adrenalectomy and administration of high doses of cortisone acetate. *Horm. Metab. Res.* **4**, 292-296.

Werner, R. and Wunnenberg, W. (1980). Effect of the adrenocorticostatic agent, metopirone, on thermoregulatory heat production in the European hedgehog*. *Pflugers Arch.* **385**, 25-28.

Woodward, J. A. and Saggerson, E. D. (1986). Effect of adenosine deaminase, N6-phenylisopropyladenosine and hypothyroidism on the responsiveness of rat brown adipocytes to noradrenaline. *Biochem. J.* **238**, 395-403.

Yan, W., Wu, F., Morser, J. and Wu, Q. (2000). Corin, a transmembrane cardiac serine protease, acts as a pro-atrial natriuretic peptide-converting enzyme. *Proc. Natl. Acad. Sci. USA* **97**, 8525-8529.

Yandle, T. G., Richards, A. M., Nicholls, M. G., Cuneo, R., Espiner, E. A. and Livesey, J. H. (1986). Metabolic clearance rate and plasma half life of alpha-human atrial natriuretic peptide in man. *Life Sci.* **38**, 1827-1833.

Yen, M. and Ewald, M. B. (2012). Toxicity of weight loss agents. *J. Med. Toxicol.* **8**, 145-152.

York, D. A. and Al-Baker, I. (1984). Effect of corticotropin on brown adipose tissue mitochondrial GDP binding in obese rats. *Biochem. J.* **223**, 263-266.

Zeng, W., Pirzgalska, R. M., Pereira, M. M. A., Kubasova, N., Barateiro, A., Seixas, E., Lu, Y.-H., Kozlova, A., Voss, H., Martins, G. G. et al. (2015). Sympathetic neuro-adipose connections mediate leptin-driven lipolysis. *Cell* **163**, 84-94.

Zietak, M. and Kozak, L. P. (2016). Bile acids induce uncoupling protein 1-dependent thermogenesis and stimulate energy expenditure at thermoneutrality in mice. *Am. J. Physiol. Endocrinol. Metab.* **310**, E346-E354.

Journal of Experimental Biology

frontiers in Physiology

ORIGINAL RESEARCH
published: 17 January 2019
doi: 10.3389/fphys.2018.01931

Opposing Actions of Adrenocorticotropic Hormone and Glucocorticoids on UCP1-Mediated Respiration in Brown Adipocytes

*Katharina Schnabl[1,2,3], Julia Westermeier[1,2], Yongguo Li[1,2] and Martin Klingenspor[1,2,3]**

[1] Chair for Molecular Nutritional Medicine, TUM School of Life Sciences Weihenstephan, Technical University of Munich, Freising, Germany, [2] EKFZ – Else Kröner-Fresenius Zentrum for Nutritional Medicine, Technical University of Munich, Freising, Germany, [3] ZIEL – Institute for Food & Health, Technical University of Munich, Freising, Germany

OPEN ACCESS

Edited by:
Rita De Matteis, Università degli Studi di Urbino Carlo Bo, Italy

Reviewed by:
Alessandro Bartolomucci, University of Minnesota Twin Cities, United States
Vicente Lahera, Complutense University of Madrid, Spain

***Correspondence:**
Martin Klingenspor
mk@tum.de

Specialty section:
This article was submitted to Integrative Physiology, a section of the journal Frontiers in Physiology

Received: *08 October 2018*
Accepted: *21 December 2018*
Published: *17 January 2019*

Citation:
Schnabl K, Westermeier J, Li Y and Klingenspor M (2019) Opposing Actions of Adrenocorticotropic Hormone and Glucocorticoids on UCP1-Mediated Respiration in Brown Adipocytes. Front. Physiol. 9:1931. doi: 10.3389/fphys.2018.01931

Brown fat is a potential target in the treatment of metabolic disorders as recruitment and activation of this thermogenic organ increases energy expenditure and promotes satiation. A large variety of G-protein coupled receptors, known as classical drug targets in pharmacotherapy, is expressed in brown adipocytes. In the present study, we analyzed transcriptome data for the expression of these receptors to identify potential pathways for the recruitment and activation of thermogenic capacity in brown fat. Our analysis revealed 12 G_s-coupled receptors abundantly expressed in murine brown fat. We screened ligands for these receptors in brown adipocytes for their ability to stimulate UCP1-mediated respiration and *Ucp1* gene expression. Adrenocorticotropic hormone (ACTH), a ligand for the melanocortin 2 receptor (MC2R), turned out to be the most potent activator of UCP1 whereas its capability to stimulate *Ucp1* gene expression was comparably low. Adrenocorticotropic hormone is the glandotropic hormone of the endocrine hypothalamus–pituitary–adrenal-axis stimulating the release of glucocorticoids in response to stress. In primary brown adipocytes ACTH acutely increased the cellular respiration rate similar to isoproterenol, a β-adrenergic receptor agonist. The effect of ACTH on brown adipocyte respiration was mediated via the MC2R as confirmed by using an antagonist. Inhibitor-based studies revealed that ACTH-induced respiration was dependent on protein kinase A and lipolysis, compatible with a rise of intracellular cAMP in response to ACTH. Furthermore, it is dependent on UCP1, as cells from UCP1-knockout mice did not respond. Taken together, ACTH is a non-adrenergic activator of murine brown adipocytes, initiating the canonical adenylyl cyclase–cAMP–protein kinase A-lipolysis-UCP1 pathway, and thus a potential target for the recruitment and activation of thermogenic capacity. Based on these findings in primary cell culture, the physiological significance might be that cold-induced ACTH in concert with norepinephrine released from sympathetic

nerves contributes to BAT thermogenesis. Notably, dexamethasone attenuated isoproterenol-induced respiration. This effect increased gradually with the duration of pretreatment. *In vivo*, glucocorticoid release triggered by ACTH might oppose beta-adrenergic stimulation of metabolic fuel combustion in BAT and limit stress-induced hyperthermia.

Keywords: glucocorticoids (GC), brown adipose tissue, non-adrenergic activation, non-shivering thermogenesis, uncoupling protein 1, adrenocorticotropic hormone, obesity

INTRODUCTION

We are facing a worldwide epidemic of obesity, a major risk factor in the development of non-communicable diseases such as diabetes mellitus and arteriosclerosis. In 2016, 1.9 billion adults aged 18 and over were overweight, of which 650 million were obese, representing an almost threefold increase in obesity prevalence since 1975 (WHO, 2018). Obesity is the state of excessive white adipose tissue (WAT) accumulation caused by prolonged positive energy balance. In mammals there is a second type of adipose tissue, brown adipose tissue (BAT), which in contrast to WAT generates heat in response to cold exposure and food consumption (Rosen and Spiegelman, 2006; Vosselman et al., 2013; U Din et al., 2018). It dissipates the chemical energy of macro-nutrients by uncoupling oxygen consumption from ATP synthesis in mitochondria (Klingenspor, 2003). This mechanism, known as non-shivering thermogenesis, is dependent on the presence of mitochondrial uncoupling protein 1 (UCP1), which is a unique feature of brown adipocytes. The activation of BAT increases energy expenditure and opposes positive energy balance. In addition to the activation of UCP1, it is worth noting that cold exposure also induces the thermogenic gene expression program and thereby recruits thermogenic capacity in brown fat (Cannon and Nedergaard, 2004). Furthermore, brown-like adipocytes, also known as inducible brown fat cells, beige (Ishibashi and Seale, 2010) or "brite" (brown-in-white) (Petrovic et al., 2010) adipocytes, can be found interspersed in WAT (Li et al., 2014a). Similar to brown adipocytes in classical brown fat depots brite adipocyte abundance can be increased by adrenergic stimulation (Galmozzi et al., 2014) and cold exposure (Maurer et al., 2015) in a process coined browning of WAT. Besides activation and recruitment of BAT, the browning of WAT displays therapeutic potential with regard to the development of new obesity treatment strategies.

For a long time, the occurrence of metabolically active BAT was believed to be restricted to hibernators, small mammals and human newborns. Adult humans, however, also have metabolically active BAT, as demonstrated by the detection of cold-induced uptake of tracers for glucose, fatty acids and acetate with positron emission tomography (Cypess et al., 2009, 2015; van Marken Lichtenbelt et al., 2009; Virtanen et al., 2009; Ouellet et al., 2011). Furthermore, cold-induced BAT activity is strongly reduced in obese (Saito et al., 2009) and diabetic patients and can be recovered by cold acclimation (van Marken Lichtenbelt et al., 2009).

On this background BAT displays a focal point of current research as it harbors a remarkable capacity to evoke energy expenditure through UCP1 dependent energy dissipation. The recruitment and activation of BAT and appears as an attractive and potentially effective strategy for the prevention and treatment of obesity (Tseng et al., 2010). Importantly, in the attempt to increase energy expenditure, the recruitment of more brown adipocytes with higher UCP1 expression and higher respiration capacity is required, but not sufficient. UCP1 is not constitutively active, but rather must be activated to dissipate mitochondrial proton-motive force as heat. This activation of UCP1 is inevitable to increase carbohydrate and lipid oxidation. Beyond boosting energy expenditure, we recently demonstrated that meal-induced activation of BAT thermogenesis also induces satiation which might also be applicable to promote negative energy balance (Li et al., 2018).

As sympathomimetic drugs exhibit unwanted detrimental cardiovascular effects, their application as BAT-stimulating agents is considered problematic (Cypess et al., 2015). Thus, the identification of druggable non-adrenergic regulators of BAT is one step toward the modulation of the heating organ as a regulator of energy expenditure and body fat in humans.

Besides the β-adrenergic receptors mature brown adipocytes express a variety of around 230 other G protein-coupled receptors (GPCRs) (Klepac et al., 2016) which are responsible for transferring extracellular signals to the cytosol. GPCRs group in a large family of seven transmembrane proteins (Lefkowitz, 2007; Kobilka, 2011) that regulate important biological processes in diverse tissues including adipose tissues (Wettschureck and Offermanns, 2005; Latek et al., 2012). Approximately 30% of all approved drugs target GPCRs, illustrating their importance in disease and therapeutics (Hauser et al., 2017; Santos et al., 2017). These receptors are coupled to heterotrimeric G proteins which are composed of α, β, and γ subunits. Ligand binding and thus activation of GPCRs leads to the dissociation of Gα from the Gβγ dimer, allowing the binding and regulation of signaling effectors. The downstream signaling of GPCRs is in part determined by their G protein coupling (Neves et al., 2002). There are four main sub-classes of Gα proteins: G_s, G_i, G_q and G12/13. Activation of G_s and G_i leads to the stimulation or inhibition the second messenger cyclic adenosine monophosphate (cAMP), respectively, while G_q activates phospholipase C und thus, to an increase of inositol triphosphate. $G_{12/13}$ activates the small GTPase Rho, a pathway also known to be modulated by G_q family proteins (Buhl et al., 1995; Wang et al., 2013). Due to cAMP-PKA activating properties the analysis of BAT GPCRs has mainly focused on G_s-coupled receptors [for example, β-adrenergic (Cannon and Nedergaard, 2004) and adenosine receptors (Gnad et al., 2014)] as they have the potency to activate

UCP1-dependent thermogenesis. Cold-exposure induced release of norepinephrine from sympathetic nerves in BAT activates canonical adenylyl cyclase – cAMP – protein kinase A (PKA) signaling via β-adrenergic receptors. This pathway stimulates lipolysis and activation of UCP1 and therefore induces non-shivering thermogenesis (Klingenspor et al., 2017). Lipolysis plays a crucial role and is an essential requirement for UCP1 activation. Indeed, pharmacological inhibition of ATGL and HSL, the two lipases which catalyze the first two steps in the hydrolysis of triglycerides, completely diminishes adrenergic stimulation of thermogenesis (Li et al., 2014b).

The aim of the present study was to investigate a selection of non-adrenergic G_s-coupled GPCRs in the light of their ability to activate and recruit UCP1-mediated thermogenesis in brown adipocytes.

MATERIALS AND METHODS

Materials

Murine $ACTH_{(1-39)}$ trifluoroacetate salt was purchased from Bachem (H-4998), $ACTH_{(4-10)}$ was ordered from Abcam (ab142255), and the synthetic $ACTH_{(4-10)}$ analog was synthesized and obtained from JPT Peptide Technologies GmbH. H89 was purchased from Tocris. Atglistatin and Hi 76-0079 were a kind gift from Prof. Robert Zimmermann. All other chemicals were ordered from Sigma unless otherwise specified. MC2R antagonist GPS1573 was purchased from Abbiotech (Bouw et al., 2014).

Animals and Primary Cell Culture

All mice were bred at the specific-pathogen free animal facility of the Technical University of Munich registered at the local authorities according to §11 of the German Animal Welfare Act (Az32-568, 01/22/2015). In the present study, mice were killed for the dissection of tissues in deep CO_2 anesthesia as approved by the ethics committee of the state supervisory authority (Government of Upper Bavaria). They had *ad libitum* access to food and water and were maintained at 22 ± 1°C and 50–60% relative humidity in a 12 h:12 h light:dark cycle. Male 129S6/SvEvTac, 129S1/SvEvTac mice ($UCP1^{-/-}$ mice and wild-type littermates $UCP1^{+/+}$) and heterozygous C57BL/6N Ucp1 dual-reporter gene mice (C57BL/6NTac-Ucp1tm3588 $^{(Luciferase-T2A-iRFP-T2A-Ucp1)Arte}$ named here as $Ucp1^{+/ki}$) aged 5–6 weeks, were used to prepare primary cultures of brown and white adipocytes. Latter simultaneously express firefly luciferase and near-infrared fluorescent protein 713 (iRFP713). The *Luciferase-T2A-iRFP713-T2A* sequence was introduced into the 5′-untranslated region of the endogenous *Ucp1* gene (Wang et al., 2018). Interscapular brown and inguinal WATs were dissected and digested with collagenase as described previously (Li et al., 2014a). Stromal vascular fraction cells were seeded, grown to confluency and differentiated into mature adipocytes following a standard protocol. Adipocyte differentiation was induced for 48 h with 5 μg/ml insulin, 1 nM 3,3′,5-triiodo-l-thyronine (T3), 125 μM indomethacin, 500 μM isobutylmethylxanthine (IBMX) and 1 μM dexamethasone in adipocyte culture media (DMEM supplemented with 10% heat-inactivated FBS, penicillin/streptomycin). Cells were then maintained in adipocyte culture media supplemented with 5 μg/ml insulin and 1 nM T3 for 6 days with media changes every 2 days. Assays were performed on day 7 of differentiation.

Luciferase Assay

After overnight stimulation of primary brown adipocytes of $Ucp1^{ki/ki}$ mice luciferase activity was assayed using a commercial kit system (Luciferase Assay System Freezer Pack E4030, Promega GmbH). Primary cells were lysed in 1x reporter lysis buffer by shaking for 20 min at room temperature. 10 μl lysate was mixed with 50 μl luciferase assay substrate solution, and the mixture was measured by FB12 in a luminometer (Single Tube Luminometer, Titertek-Berthold GmbH). Bioluminescence readouts were normalized to total protein content.

Respiration Assays

Oxygen consumption of primary brown adipocytes was measured at 37°C using microplate-based respirometry (XF96 extracellular flux analyzer, Seahorse Bioscience) as described previously (Li et al., 2014b) following the subsequent protocol at day 7 of differentiation. Prior to the respiration measurement, primary cells were washed with warmed, unbuffered assay medium (DMEM basal medium supplemented with 25 mM glucose, 31 mM NaCl, 2 mM GlutaMax and 15 mg/l phenol red, pH 7.4) (basal assay medium). Subsequent to the medium replacement with basal assay medium containing 1–2% essentially fatty acid free bovine serum albumin (BSA), cells were incubated at 37°C in a CO_2-free incubator for 1 h. Assay reagents were loaded into the drug injections ports of the sensor cartridges at 10X in basal assay medium (no BSA). After assessment of basal oxygen consumption in untreated cells oligomycin (5 μM) was injected to inhibit coupled respiration and to determine basal leak respiration. Next, effector was added to investigate UCP1-dependant uncoupled respiration. By the addition of FCCP (1 μM) maximal respiratory capacity was determined. Lastly, non-mitochondrial oxygen consumption was assessed by blocking mitochondrial respiration with antimycin A (5 μM). For some experiments, cells were pretreated for 1 h with 50 μM H89 (PKA inhibitor), 1–100 μM propranolol (β-adrenergic receptor antagonist), 40 μM Atglistatin (ATGL inhibitor) and 40 μM Hi76-0079 (HSL inhibitor) 1 h prior to the measurement. Oxygen consumption rates were automatically calculated by the Seahorse XF-96 software. Each experiment was repeated at least three times with similar results and five to eight replicate wells for every condition in each independent experiment. Results are predominately expressed as stimulated respiration which is calculated as fold increase of basal leak.

Gene Expression Analysis (qRT-PCR)

Total RNA was isolated using Trisure (Bioline) and purified with SV total RNA Isolation System (Promega). Reverse transcriptase reactions were performed using SensiFAST cDNA Synthesis Kit (Bioline). Quantitative real-time PCR (qRT-PCR) was performed with SYBR green fluorescent dye in 384-well format using LightCycler 480 (Roche). General Transcription Factor IIB

(Gtf2b) served as an internal control. To be able to calculate relative gene expression levels of samples, standard reactions containing serial diluted pooled cDNA of all samples (Pure, 1:2, 1:4, 1:8, 1:16, 1:32 and 1:64) as a template were used to establish a standard curve. The RNA abundance of *Ucp1* gene was normalized to the housekeeping gene Gtf2b. The following primers were used:

Ucp1	F:	5′-GTACACCAAGGAAGGACCGA-3′,
	R:	5′-TTTATTCGTGGTCTCCCAGC-3′;
Gtf2b	F:	5′-TGGAGATTTGTCCACCATGA-3′,
	R:	5′-GAATTGCCAAACTCATCAAAACT-3′.

Western Blot Analysis

Primary brown adipocytes were lysed in RIPA buffer for western blot analysis. 30 μg of total lysates were separated by SDS-PAGE (12.5% gels), transferred to Odyssey® nitrocellulose membrane (Millipore), and probed with anti-UCP1 (1:10,000; ab10983, Abcam), and anti-Actin (1:10,000; MAB1501, Millipore). Secondary antibodies conjugated to IRDye^{TM} 680 or IRDye^{TM} 800 (Licor Biosciences) were incubated at a dilution of 1:20,000. Fluorescent images were captured by Odyssey infrared imaging system (Licor Biosciences).

Quantification of Cellular cAMP

Changes in cytosolic cAMP concentrations were determined in primary brown adipocytes in response to ACTH- or isoproterenol stimulation using cAMP-Glo Assay (Promega) following the manufacturer's instructions.

Statistical Analysis

Significant differences for single comparisons were assessed by two-tailed Student's *t*-test. Analysis of variance (ANOVA) with Tukey's *post hoc* tests were used for multiple comparisons (GraphPad Prism 6.0 software). *P*-values < 0.05 were considered a statistically significant difference. All data are presented as mean ± SD.

RESULTS

G_s-Coupled GPCRs Abundantly Expressed in Brown Adipose Tissue

In our search for non-adrenergic targets to activate and recruit UCP1 in BAT, we identified 12 G_s-protein coupled receptors (G_sPCRs) expressed in the interscapular BAT of mice (C57BL/6J, 12 weeks old, room temperature, chow diet) at different abundances (threshold was set at RPKM > 1) based on our recently published RNA-seq data (GEO: GSE119452). Among these G_sPCRs, parathyroid hormone receptor (*Pthr*) showed the highest abundance, whereas adenylate cyclase activating polypeptide 1 receptor concluded with the lowest expression (**Figure 1A**). GPCR64 and GPCR133 turned out to be adhesion receptors and GPCR4 is reported to carry out ligand independent signaling mediated through proton-sensing mechanisms (Ludwig et al., 2003; Bohnekamp and Schoneberg, 2011). We therefore excluded these three receptors for further investigations. In comparison to non-adrenergic receptors, the genes encoding for the β-adrenergic receptors ADRB1/2/3 showed most abundant expression in murine BAT, with *Adrb3* standing out with the highest expression. We used Isoproterenol, a non-selective β-adrenoreceptor agonist, to activate β-adrenergic signaling in brown adipocytes. For all other non-adrenergic receptors, the corresponding ligands were selected to test their capability to activate and recruit UCP1. In case of PTHR and calcitonin gene-related peptide receptor (CALCRL), two established ligands were chosen (Chang et al., 2004; Dean et al., 2006).

Reporter-Assays and Cellular Respirometry Screening of G_s-Coupled GPCR Ligands for UCP1 Activity and Regulation

In our first screen, we tested whether these G_sPCR ligands can activate oxygen consumption acutely in brown adipocytes. UCP1-mediated uncoupled respiration was quantified in cultured adherent intact primary brown adipocytes, according to a protocol established in our lab (Li et al., 2014b). After recording basal respiration and the fraction of coupled and uncoupled respiration, UCP1-dependent respiration was measured. Finally, maximal respiratory capacity and non-mitochondrial oxygen consumption were assessed by adding the uncoupling agent carbonyl cyanide 4-(trifluoromethoxy) phenylhydrazone (FCCP) and antimycin A was added to block the electron transport chain, respectively. All respiration assays were performed in the presence of BSA to buffer free fatty acid (FFA) levels in the respiration medium. For ACTH and secretin, we observed the most prominent induction of UCP1-dependant uncoupled respiration. The potency of these two peptides was comparable to ISO, the β-adrenergic receptor agonist. Both PTH and its related peptide both stimulated UCP1-dependant respiration, although the effect was modest compared to ISO. The weakest effects on cellular respiration were observed for PACAP and α-MSH. All other ligands failed to increase basal leak respiration (**Figures 1B,C**).

We then measured FLUC activity in primary brown adipocytes from Ucp1$^{ki/ki}$ reporter gene mice to determine the effect of the G_sPCR ligands on *Ucp1* gene expression in response to overnight stimulation. As the expression of *Fluc* in these cells is driven by *Ucp1*promoter, FLUC activity served as a surrogate for *Ucp1* expression. We found highest FLUC activities in response to secretin, parathyroid hormone (PTH), parathyroid hormone related peptide (PTHrP), and pituitary adenylate cyclase-activating peptide (PACAP) (**Figure 1D**). Prostaglandin E2 (PGE2), adrenocorticotropic hormone (ACTH) and α-melanocyte-stimulating hormone (α-MSH) showed a moderate rise in FLUC activity. The two ligands for calcitonin receptor-like receptor (CALCRL), calcitonin gene-related peptide (CGRP), and adrenomedullin only had minor effects, whereas thyroid hormone and the adenosine 2A receptor agonist CGS21680 had no effect on FLUC (**Figure 1D**). Comparing the effect sizes for all ligands on the ability to activate respiration and to recruit *Ucp1* expression, ACTH and secretin were most potent to acutely activate respiration. Notably, although secretin,

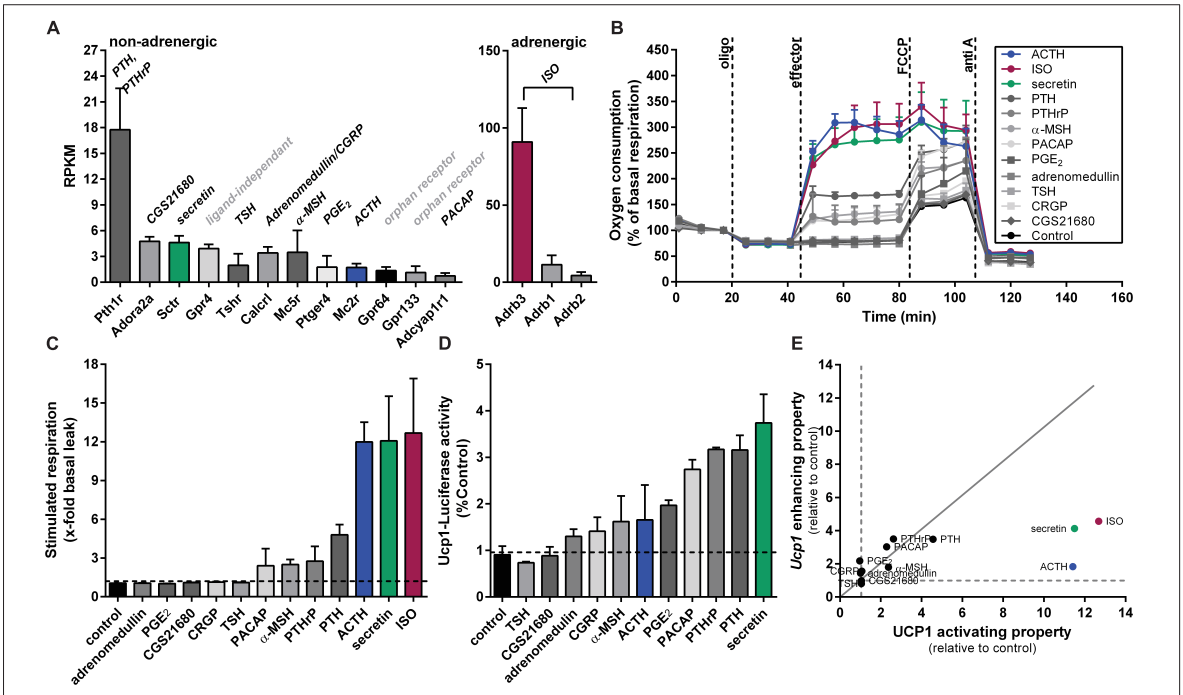

FIGURE 1 | Screening approach of G_sPCR ligands expressed in brown adipose tissue concerning their ability to activate and recruit Ucp1. **(A)** Gene expression of G_s-protein coupled receptors (G_sPCRs) obtained from RNA sequencing of murine brown adipose tissue. Data are shown as RPKM (reads per kilobase per million mapped reads). The respective ligands of the receptors are shown in italics above the bars. G_sPCRs with a lower expression have been neglected for the analysis (n = 4). **(B)** Microplate-based respirometry of primary brown adipocytes following the subsequent protocol. After assessment of basal oxygen consumption oligo (oligomycin) was injected to determine basal leak respiration. Next, compound to be tested was added to investigate uncoupling protein 1-dependant respiration. By the addition of FCCP maximal leak respiration was determined. Lastly, non-mitochondrial oxygen consumption was assessed by injecting anti A. Shown is a time course of oxygen consumption in percentage of basal respiration of primary brown adipocytes (129S6 mice) in response to different stimuli (effectors). **(C)** Stimulated respiration of primary brown adipocytes as fold increase of basal leak respiration (n = 5). **(D)** Overnight stimulation of primary brown adipocytes from $Ucp1^{ki/ki}$ mice expressing the firefly luciferase driven by the gene regulatory elements of endogenous *Ucp1* gene. Measurement of luciferase activity as surrogate for Ucp1 expression (n = 3). **(E)** Plot of Ucp1 enhancing properties against UCP1 activating properties of screened ligands relative to control. Dashed lines indicate control levels (=1), continuous gray line indicates line of equality. Data are presented as means ± SD. ***Pth1r***, parathyroid hormone 1 receptor; ***Adora2a***, adenosine receptor; ***Sctr***, secretin receptor; ***Gpr4***, GPCR4; ***Tshr***, thyroid stimulating hormone receptor; ***Calcrl***, calcitonin receptor-like receptor; ***Mc5r***, melanocortin receptor 5, ***Ptger4***, prostaglandin E receptor 4; ***Mc2r***, melanocortin receptor 2; ***Gpr64***, GPCR 64; ***Gpr133***, GPCR 133; ***Adcyap1r1***, adenylate cyclase activating polypeptide 1 receptor; **TSH**, thyroid stimulating hormone; **CGS21680**, adenosine A2A receptor agonist; **CGRP**, calcitonin gene-related peptide; **α-MSH**, melanocyte-stimulating hormone; **ACTH**, adrenocorticotropic hormone; **PGE_2**, prostaglandin E2; **PTHrP**, parathyroid hormone related peptide; **PTH**, parathyroid hormone; **ISO**, isoproterenol; **oligo**, oligomycin; **FCCP**, carbonyl cyanide 4-(trifluoromethoxy) phenylhydrazone; **anti A**, antimycin A.

PTH and PTHrP showed comparable strong induction of FLUC activity, PTH and PTHrP were much less potent as secretin in the acute activation assay. Moreover, ACTH matched secretin in the acute activation assay, but was much less potent to induce FLUC (**Figure 1E**). Based on the pronounced and relatively preferential stimulatory effect of ACTH on UCP1-mediated respiration we chose the ACTH to further investigate its thermogenic properties.

ACTH Activates Respiration via the Canonical cAMP-PKA-Lipolysis Pathway

The hypothalamic–pituitary–adrenal (HPA) axis plays a critical role in maintaining homeostasis and in mounting appropriate responses to stress. Key components of the stress response are aimed at providing adequate amounts of glucocorticoids which exert pleiotropic effects on energy supply, fuel metabolism, immunity and cardiovascular function. The melanocortin ACTH is the glandotropic hormone of the HPA which stimulates synthesis and release of glucocorticoids by the cortex of the adrenal gland. The 39 amino acid peptide hormone is synthesized within the anterior pituitary by corticotropic cells as a much larger, 241-amino-acid precursor known as pro-opiomelanocortin (POMC) in response to tonic control from the hypothalamus by corticotrophin-releasing hormone (CRH). ACTH is able to activate all five G_s-protein coupled melanocortin receptors, but at physiological circulating plasma levels, the sensitivity of all receptors, except MC2R, is so low that they are not activated. In rodent adipocytes, ACTH binds to the MC2R, which stimulates lipolysis via G_s-coupled cAMP-PKA mediated phosphorylation of HSL (Cho et al., 2005).

Since ACTH was previously reported to stimulate uncoupled respiration in the immortalized murine white fat cell line T37i (van den Beukel et al., 2014), we next investigated UCP1-mediated respiration and its respective signaling pathway in primary brown adipocytes. In a dose–response experiment we found that 200 nM ACTH stimulated respiration, defined as fold increase of respiration over basal leak respiration, with the most robust effect at 1 μM ACTH (**Figure 2A**). This effect of ACTH on brown adipocyte respiration was independent of adrenergic receptors, since pre-treatment of the cells with propranolol, a non-selective β-adrenergic receptor antagonist, did not attenuate ACTH stimulated respiration while blocking the effect of ISO in a dose-dependent manner (**Figure 2B**). The effect of ACTH, however, depends on MC2R, as pretreatment with the MC2R antagonist GPS1573 (100 nM and 750 nM) blunted the effects of ACTH on oxygen consumption (**Figure 2C**). ACTH stimulation of primary brown adipocytes resulted in a dose-dependent increase of cytosolic cAMP levels. Compared to ISO, however, EC_{50} of ACTH was approximately 165-fold higher (9.415 nM vs. 1.493 μM) (**Figure 2D**). Pre-treatment of cells with H89, a selective inhibitor of PKA (**Figure 2E**), or inhibitors targeting the two essential lipases involved in lipolysis (ATGL, adipose triglyceride lipase; HSL, hormone-sensitive lipase), completely blocked the effect on respiration of ACTH (**Figure 2F**). The stimulating effect of ACTH depended on UCP1 as it was attenuated in primary brown adipocytes of $UCP1^{-/-}$ compared to $UCP1^{+/+}$ (**Figure 2G**). As the ACTH-induced stimulated respiration was dependent on UCP1, we consider the effect of the ACTH on brown adipocytes as thermogenic.

Taken together, ACTH activates UCP1-dependent respiration in primary brown adipocytes via the canonical cAMP-PKA-lipolysis pathway.

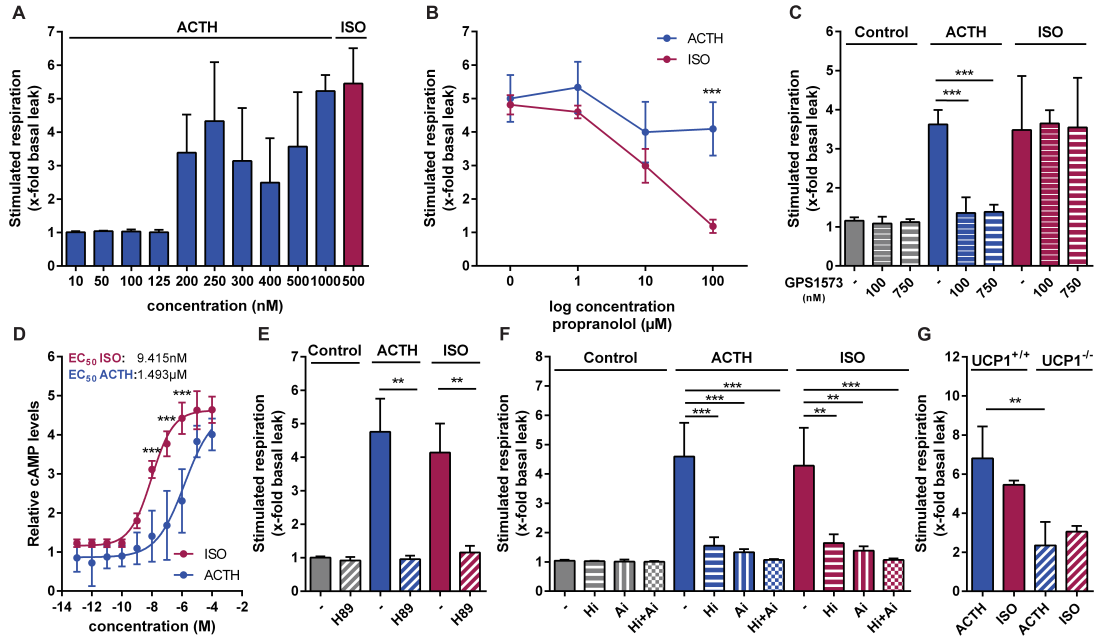

FIGURE 2 | ACTH activates UCP1 via the canonical cAMP-PKA-lipolysis pathway. Oxygen consumption of primary brown adipocytes was assessed using microplate-based respirometry. First, basal respiration was determined and then, oligomycin (oligo) was added, which inhibits adenosine triphosphate (ATP) synthase resulting in basal leak respiration. UCP1 mediated uncoupled respiration was determined after injection of isoproterenol (ISO, 0.5 μM) as a positive control or adrenocorticotropic hormone (ACTH, 1 μM). Next, carbonyl cyanide 4-(trifluoromethoxy) phenylhydrazone (FCCP), an uncoupler that allows assessment of maximal respiratory capacity, was added. Finally, antimycin A (anti A) was added in order to determine non-mitochondrial respiration. **(A)** Dose–response experiment revealing most robust effects at a ACTH concentration of 1 μM assessed as stimulated respiration as fold increase of basal leak respiration. **(B)** ACTH- and ISO-stimulated respiration after 1 h pretreatment with different concentrations of propranolol, a non-selective blocker of adrenergic β-receptors ($n = 4$). **(C)** Effects of different concentrations of GPS1573 (100 nM and 750 nM), a MC2R antagonist, on ACTH- and ISO-stimulated UCP1-mediated uncoupled respiration. **(D)** Cytosolic cAMP abundance after stimulation with increasing ACTH and ISO concentrations for 30 min ($n = 3$). **(E)** Fold increase of basal leak respiration after stimulation with ISO, ACTH and vehicle (control, assay medium) with or without protein kinase A inhibitor H89 (50 μM). Inhibitor was injected together with oligo prior to addition of stimulators ($n = 4$). **(F)** Respiration stimulated by ISO, ACTH or vehicle as fold increase of basal leak after 1 h pre-treatment with lipolysis inhibitors Ai (Atglistatin, ATGL-inhibitor, 40 μM) and Hi (Hi76-0079, HSL-inhibitor, 40 μM) ($n = 4$). **(G)** Stimulated respiration of primary brown adipocytes from $UCP1^{+/+}$ and $UCP1^{-/-}$ mice ($n = 3$). Data are presented as means ± SD. **(B,D,G)** were analyzed by two-way ANOVA (Tukey's test). **(C,E,F)** were analyzed by unpaired *t*-test. **(D)** EC_{50} was determined by non-linear regression analysis. $^{*}p < 0.05$, $^{**}p < 0.01$, $^{***}p < 0.001$.

ACTH Increases *Ucp1* Expression in Primary Brown and White Adipocytes

Next, we aimed to investigate the effect of ACTH on *Ucp1* gene expression in primary brown and white adipocytes. Indeed, treatment of differentiated brown and white adipocytes with two different doses of ACTH caused a dose-dependent increase in *Ucp1* mRNA levels (**Figures 3A,B**). The maximal induction of *Ucp1* mRNA achieved by 1 μM ACTH was comparable to the effect of ISO treatment (500 nM). Concomitant, UCP1 protein was also induced either by ACTH or ISO in primary brown adipocytes. This effect on gene expression was more pronounced after 12 h of stimulation compared to 8 h, and was dose-dependent. At a concentration of 1 μM, ACTH and ISO were equipotent in recruiting UCP1 protein in primary brown adipocytes (**Figures 3C–E**).

A Synthetic ACTH Fragment Slightly Stimulates Respiration and Increases *Ucp1* mRNA Level in Primary Brown Adipocytes

We showed that both ACTH and α-MSH are capable in stimulating uncoupled respiration (**Figures 1B,C**). The heptapeptide sequence, Met-Glu-His-Phe-Arg-Trp-Gly, is common to all the adrenocorticotropic (ACTH), melanotropic (MSH), and lipotropic (LPH) hormones. Structure function studies on melanocortin peptides from the early 1970s using stimulation of lipolysis as a criterion for biological potency revealed that the heptapeptide core sequence exerts biological activity. An amino acid exchange from Glu to Arg in the ACTH core sequence resulted in a fourfold increased activity on the release of FFAs compared to the natural ACTH core sequence (Draper et al., 1973). As lipolysis is an essential prerequisite for the activation of UCP1, we included both the natural and the synthetic version of the ACTH fragment in our study. In primary brown adipocytes, the natural core sequence of ACTH [$ACTH_{(4-10)}$] had no impact on respiration (**Figures 4A,B**), but significantly increased *Ucp1* mRNA expression, although not to the extent as seen for ISO (**Figure 4C**). The mutant ACTH fragment [$synACTH_{(4-10)}$] showed limited potential to activate UCP1 as it mildly increased respiration (**Figures 4D,E**). The induction of *Ucp1* mRNA expression was comparable to that of the natural heptapeptide (**Figure 4F**). As it turned out, the synthetic ACTH fragment has potential to stimulate both thermogenic capacity and activity, and therefore is a potential non-adrenergic activator of BAT thermogenesis.

Acute Glucocorticoid Treatment Attenuates β3-Adrenergic Signaling but Does Not Affect Thermogenic Effects of ACTH

To address the physiological role of ACTH in brown fat thermogenesis we analyzed the expression of its receptor in BAT of mice in response to cold exposure. Indeed, *Mc2r* is down-regulated in response to cold (**Figure 5A**) indicating that its contribution to cold-induced BAT thermogenesis might be rather minor. Nevertheless, subsequent to cold exposure plasma ACTH levels are significantly increased (van den Beukel et al., 2014). Basically, ACTH triggers the release of glucocorticoids from the cortex of the adrenal gland. Circulating glucocorticoids exert negative feedback control on the secretion of CRH and ACTH from the hypothalamus and the anterior pituitary. In addition, it is known that corticosterone reduces *Ucp1* mRNA and UCP1 protein in response to both adrenergic stimulation and ACTH treatment (Soumano et al., 2000; van den Beukel et al., 2014). Furthermore, glucocorticoids may exert rapid non-genomic effects mediated by a putative membrane-bound receptor as reported for the murine brain (Nahar et al., 2016; Shaqura et al., 2016). Therefore, we finally investigated the acute effect of treatment with the glucocorticoid dexamethasone (Dexa) on β-adrenergic and ACTH signaling. Therefore we pretreated primary brown adipocytes with 5 μM Dexa for 0–4 h and analyzed UCP1-dependent uncoupled respiration. One-hour pre-treatment as well as acute stimulation with Dexa had no effect on respiration (**Figure 5B**). With increasing exposure time Dexa attenuated ISO-stimulated respiration whereas ACTH-induced respiration was unaffected (**Figure 5C**). This was not a consequence of reduced or increased expression of the β3-adrenergic or the melanocortin 2 receptor (**Figures 5D,E**). Of note, although there was trend toward a decrease in *Ucp1* mRNA, a 4-h treatment with Dexa had no significant effect on *Ucp1* expression (**Figure 5F**). Our further analysis revealed that Dexa attenuated the ISO induced rise in cellular cAMP levels, whereas no such effect was observed for ACTH (**Figure 5G**). This implies that the inhibitory action of DEXA must occur upstream of cAMP.

DISCUSSION

Targeting brown fat to increase energy expenditure and promote negative energy balance has been a long sought strategy to prevent overweight and treat obesity (Tseng et al., 2010). In line with the hypothesis of thermoregulatory feeding (Himms-Hagen, 1995), our recent identification of an endocrine gut – secretin – brown fat – brain axis inhibiting food intake demonstrates that brown fat can also attenuate energy intake (Li et al., 2018). In addition to positive effects on energy balance, chronic activation of BAT leads to improved glucose tolerance and the release of batokines that beneficially regulate metabolism in rodent models (Bartelt et al., 2011; Hondares et al., 2011). Several novel molecular mediators for the recruitment of BAT and/or the browning of WAT have been found (Bartelt and Heeren, 2014), but only few direct activators of respiration in brown adipocytes were reported, so far (Braun et al., 2018). The latter mostly are adrenergic receptor agonists which exhibit unwanted systemic side effects (Cypess et al., 2012, 2015; Vosselman et al., 2012; Carey and Kingwell, 2013). Therefore, the present study was designed to reveal novel non-adrenergic activators of brown adipocytes. As the activation of the G_s-coupled β_3-adrenergic receptor leads to increased lipolytic activity by the canonical cAMP-PKA pathway providing FFAs essential for the activation of UCP1-mediated respiration, we screened for

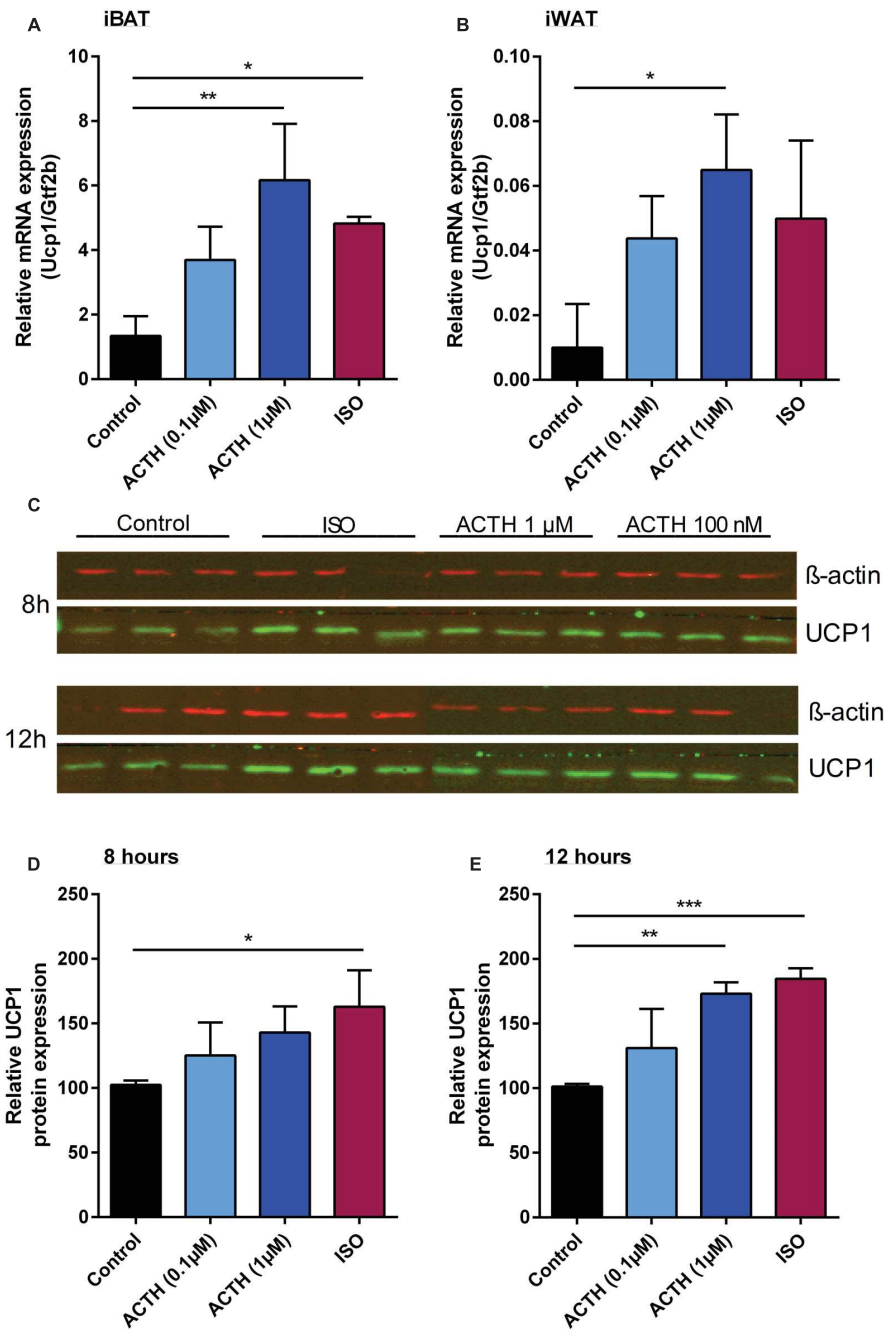

FIGURE 3 | ACTH increases Ucp1 expression in primary brown and white adipocytes. Relative expression of uncoupling protein 1 (*Ucp1*) normalized to transcription factor *Gtf2b* in primary adipocytes from both **(A)** interscapular brown (iBAT) and **(B)** inguinal white adipose tissue (iWAT) in response to isoproterenol (ISO) or adrenocorticotropic hormone (ACTH). **(C)** Western blot analysis of UCP1 and β-actin in primary inguinal adipocytes after stimulation with ISO or ACTH for 8 and 12 h. Relative UCP1 protein expression normalized to β-actin in primary inguinal white adipocytes after treatment with differentiation medium (control), ACTH (0.1 μM), ACTH (1 μM) or ISO (0.5 μM) for **(D)** 8 or **(E)** 12 h. Data are presented as means ± SD ($n = 4$). **(A,B,D,E)** were analyzed by one-way ANOVA (Tukey's test). $^{*}p < 0.05$, $^{**}p < 0.01$, $^{***}p < 0.001$.

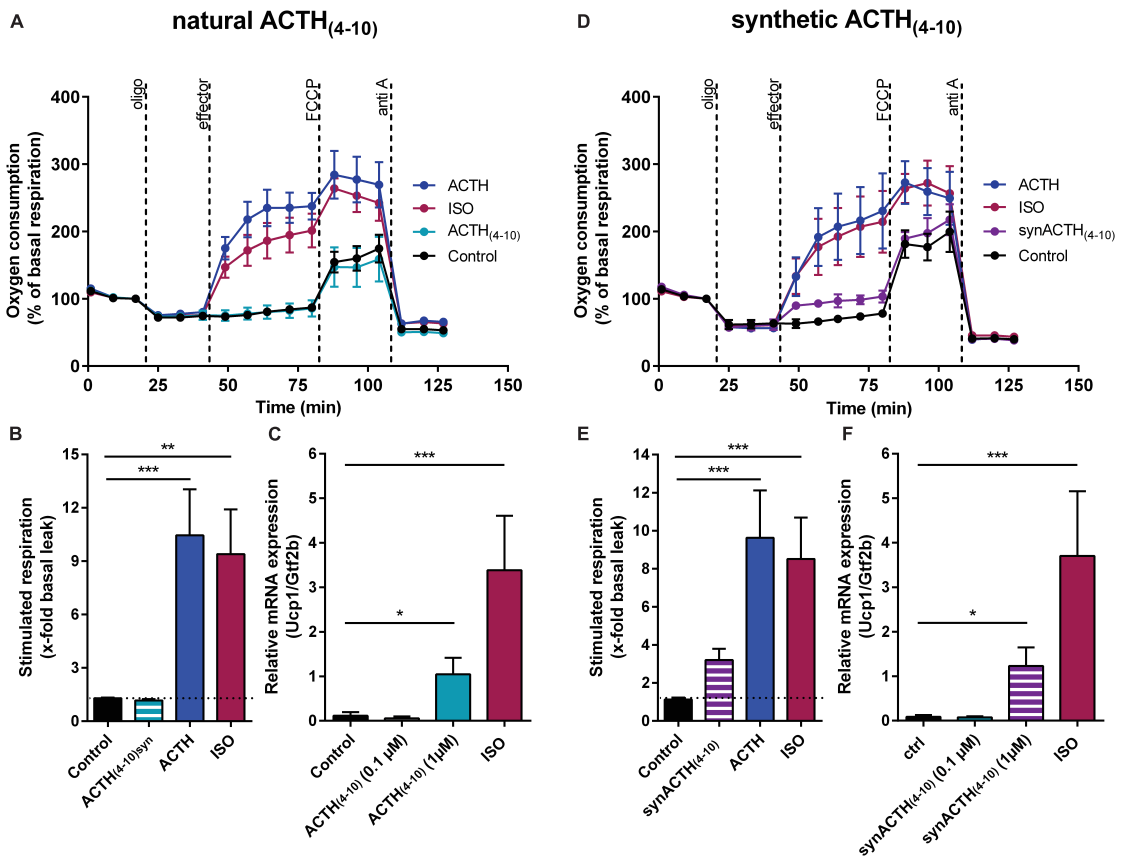

FIGURE 4 | A synthetic ACTH fragment (heptapeptide) slightly stimulates respiration and increases Ucp1 mRNA level in primary brown adipocytes. **(A–C)** Heptapeptide core sequence of adrenocorticotropic hormone [$ACTH_{(4-10)}$] and **(D–F)** a synthetic analog [$ACTH_{(4-10)}$] having an amino acid exchange from Arg to Glu were analyzed with regard to their ability to recruit and activate uncoupling protein 1 (UCP1) in primary brown adipocytes. **(A,D)** First, basal respiration was assessed. Subsequently, adenosine triphosphate (ATP) inhibitor oligomycin (oligo) was added to define basal leak respiration. Next, UCP1-dependant uncoupled respiration was measured in response to 0.5 µM isoproterenol (ISO), ACTH or the heptapeptide fragments of ACTH (all 1 µM). The chemical uncoupler carbonyl cyanide 4-(trifluoromethoxy) phenylhydrazone (FCCP) was added to determine maximal respiratory capacity. Lastly, non-mitochondrial background was determined by addition of complex III inhibitor antimycin A (anti A). **(B,E)** Stimulated respiration was calculated as fold increase of basal leak respiration. **(C,F)** Relative expression of uncoupled protein 1 (*Ucp1*) normalized to transcription factor *Gtf2b* assessed by qPCR. Data are presented as means ± SD ($n = 4$). **(B,C,E,F)** were analyzed by one-way ANOVA (Tukey's test). $^*p < 0.05$, $^{**}p < 0.01$, $^{***}p < 0.001$.

G_sPCR expressed in mature murine adipocytes and assessed their capability to trigger the same signaling cascade. In our screen, we identified six peptidergic ligands of non-adrenergic G_sPCR expressed in brown fat which acutely activated UCP1-mediated respiration in cultured brown adipocytes. Among these ligands, the glandotropic peptide hormone ACTH was one of the most potent activators of brown adipocyte respiration.

Some technical premises were of particular importance in our search for activators of UCP1-mediated respiration. Firstly, we tested the selected ligands for their acute effect on respiration. Secondly, by adding essentially fatty acid-free bovine serum into the respiration medium we prevented unspecific UCP1-independent uncoupling activity induced by uncontrolled high FFA levels (Li et al., 2014b). Thirdly, for ACTH we compared the effects in primary brown adipocytes from *wild-type* and *Ucp1* knockout mice. In previous studies identifying potential activators of brown adipocyte uncoupled respiration, either UCP1 specificity was uncertain due to the applied assay conditions, or the effects on respiration were due to mitochondrial biogenesis induced by long term stimulation with the putative activator.

Consistent with our recent report (Li et al., 2018), secretin was the strongest activator of UCP1-mediated uncoupled respiration, closely followed by ACTH. In comparison, the effects of PTH and PTHrP on respiration were rather minor, demonstrating some potential of these peptides to activate brown adipocytes, in addition to their demonstrated role in WAT browning (Kir et al., 2014). Furthermore, in line with the known pro-lipolytic activity

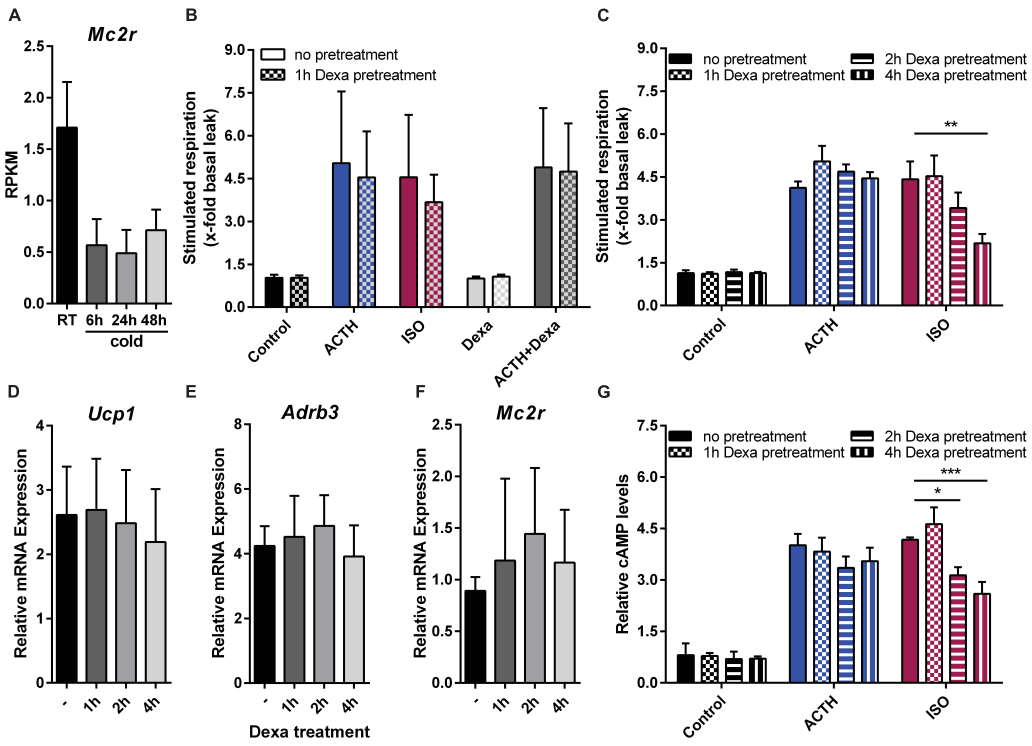

FIGURE 5 | Acute glucocorticoid treatment attenuates β3 adrenergic signaling but does not affect non-adrenergic ACTH-signaling. **(A)** Gene expression of melanocortin 2 receptor (*Mc2r*) in response to varying ambient temperatures obtained from RNA sequencing of murine brown adipose tissue. Data are shown as RPKM (reads per kilobase per million mapped reads) **(B)** Primary brown adipocytes were either not pretreated or with dexamethason (Dexa) for 1 h prior to microplate-based respirometry. Subsequently, stimulated respiration as fold increase of basal respiration was determined in response to adrenocorticotropic hormone (ACTH), isoproterenol (ISO), Dexa or a combination of ACTH and Dexa. After either no or 1, 2 or 4 h of pretreatment with Dexa **(C)** ACTH- and ISO-stimulated respiration, relative expression of **(D)** uncoupling protein 1 (*Ucp1*), **(E)** β3-adrenergic receptor (*Adrb3*) and **(F)** *Mc2r* or **(G)** relative cellular cyclic aenosine monophosphate (cAMP) was assessed in primary brown adipocytes. Data are presented as means ± SD ($n = 4$). **(B**,**C**,**G)** were analyzed by two-way ANOVA (Tukey's test). **(D–F)** were analyzed by one-way ANOVA. $*p < 0.05$, $**p < 0.01$, $***p < 0.001$.

of α-MSH and PACAP (Akesson et al., 2003; Lafontan, 2012), these peptides also showed low stimulation of brown adipocyte respiration.

Most peptides were about equipotent in stimulating respiration and gene expression, whereas secretin and ACTH showed a bias toward acute activation, thus resembling ISO (**Figure 1E**). Other than ACTH, the $ACTH_{(4-10)}$ fragment stimulated *Ucp1* gene expression but failed to activate UCP1-dependant respiration (**Figures 4B,C**). This discrepancy is unexpected as activation and recruitment of BAT share a common signaling pathway that furcates at the level of PKA. Upon cAMP binding, activated PKA phosphorylates the lipid droplet coating proteins perilipin and HSL which are essential for lipolysis and acute activation of thermogenesis (Li et al., 2014b), as well as the transcription factor cAMP response element binding protein (CREB). In concert with activating transcription factor 2 (ATF-2) and PPAR coactivator 1α (PCG1α), both downstream of PKA, CREB induces *Ucp1* expression (Klingenspor et al., 2017). On this background, one would assume a fixed ratio for the increase in *Ucp1* expression and UCP1 activity in response to the G_s-coupled activation of the canonical cAMP-PKA pathway. Alike isoproterenol, however, ACTH and secretin both prioritize acute activation of respiration over gene expression. This phenomenon, known as signaling bias, is due to a receptor's ability to selectively engage specific subsets of downstream signaling modules. Bias may have multiple causes, including variation of ligand concentration and selective G-protein activation. Depending on concentration, one ligand can trigger variable activation of multiple cellular pathways (Kenakin, 1995), and GPCRs can interact with different G-proteins, arrestins and accessory proteins (Wootten et al., 2018). The secretin receptor for example couples to both G_s- and G_q-protein with opposing downstream signaling effects (Siu et al., 2006), and ACTH stimulates arrestin-dependent internalization of MC2R and MC2R accessory protein 1 (MRAP1) in a concentration dependent manner (Roy et al., 2011). The molecular mechanisms responsible for biased signaling of ACTH and secretin in brown adipocytes merit

further investigation to identify signaling events that prioritize activation of UCP1.

In mice, ACTH increases thermogenic gene expression, hallmarked by *Ucp1*, in immortalized brown adipocytes (T37i) and in primary brown adipocytes, respectively (van den Beukel et al., 2014; Biswas, 2017). We here demonstrate acute activation of UCP1-dependent respiration in primary brown adipocytes by ACTH, as proven by the exclusion of unspecific uncoupling by fatty acids, the dose-dependent thermogenic response, and the knockout of UCP1. In combination, the pronounced acute stimulating effect on respiration and the induction of *Ucp1* gene expression qualify ACTH as a non-adrenergic effector candidate to boost activation of BAT thermogenesis *in vivo*. The discrepancy in the magnitude of ACTH effects on *Ucp1* expression assessed by either luciferase activity in our screening assay or *Ucp1* mRNA levels is probably due to strain differences of primary brown adipocytes, methodological differences and/or different duration of stimulation.

The melanocortins ACTH and α-MSH are known for their lipolytic action in rodent adipocytes, as first reported in 1958 (Lafontan, 2012; Braun et al., 2018). Cold exposure increased the plasma level of ACTH and in adipocytes it also progressively increased the responsiveness to this hormone (Rochon and Bukowiecki, 1990; van den Beukel et al., 2014). ACTH enhanced BAT function in obese rats (York and Al-Baker, 1984), and increased glucose transport and respiration in isolated brown adipocytes (Marette and Bukowiecki, 1990) via fatty acid activation of mitochondrial uncoupled respiration. In mouse strains with different stress reactivity, the physiological serum ACTH concentrations are variable, ranging from 12 to 27 pM at basal level (Ochedalski et al., 2001; Touma et al., 2008) and 133–246 pM after 15-min restraint stress (Heinzmann et al., 2010). In response to cold exposure (4°C for 24 h), serum ACTH levels rise up to 260 pM (van den Beukel et al., 2014). In cell culture, adipocytes respond to ACTH at concentrations ranging from 50 nM (T37i cells) to 100 nM (immortalized murine adipocytes) (Iwen et al., 2008; van den Beukel et al., 2014). We observed increased respiration rates at 200 nM, with most robust effects at 1 μM, with effective concentrations on *Ucp1* gene expression in a comparable range reported by others (Biswas, 2017). Thus, effective concentrations in cell culture are approximately 1,000-fold higher than the maximal physiological ACTH levels in response to restraint stress or cold exposure. To the best of our knowledge, no published studies are available that tested the effect of ACTH on brown adipocyte respiration at physiological doses. Treatment with a supraphysiological dose (15 μM ACTH, ∼50.000-fold above physiological levels), however, increased glucose uptake into BAT (van den Beukel et al., 2014). Pathophysiological chronic exposure to excessive concentrations of ACTH results in elevated glucocorticoid levels, as known for Cushing's syndrome, with symptoms like visceral obesity, growth retardation, hirsutism, acne and hypertension (Bista and Beck, 2014; Lacroix et al., 2015), but no evidence for increased BAT activity. Further analysis is necessary to evaluate the thermogenic effect of physiological concentrations of ACTH *in vivo*. In a physiological context, it has to be taken into account that the sensitivity and affinity of the receptor *in vivo* might be different, or increased by certain stimuli such as cold.

In the attempt to reduce side effects as well as to improve efficacy, alternative MC2R ligands could be of advantage to develop strategies for tissue-specific MC2R activation or selective intracellular signaling. We therefore compared an ACTH heptapeptide representing the core sequence of melanocortins (Draper et al., 1975) with an synthetic analog of this ACTH fragment carrying a mutation in position 5 (Arg > Glu). Despite the high lipolytic activity reported for the synthetic analog $ACTH_{(4-10)syn}$, it had only minor effects on brown adipocyte respiration, whereas the heptapeptide fragment was inactive. Thus, these alternative ligands are unsuitable to efficiently activate brown fat.

The glandotropic hormone ACTH induces the production and secretion of glucocorticoids (GCs) in the adrenal glands. The interplay between the murine GC corticosterone and ACTH has been previously studied (van den Beukel et al., 2014). Higher GC doses, and more chronic elevation of GC inhibit BAT activity, as concluded from cell culture data and clinical observations reporting a lower ^{18}FDG uptake by BAT in patients during chronic glucocorticoid therapy (Ramage et al., 2016). In rodents, GC exert inhibitory effects on BAT development and activity, most likely mediated via the glucocorticoid receptor (Soumano et al., 2000; Viengchareun et al., 2001; Armengol et al., 2012). Furthermore, in animal studies, adrenalectomy led to an increased BAT activity (Strack et al., 1995; Scarpace et al., 2000), while GC replacement normalized BAT activity (Scarpace et al., 1988, 2000). As these studies did not investigate a direct effect of ACTH on BAT activity, it remains elusive whether increased BAT activity can be attributed to the absence of GC or to increased ACTH levels as GC are strong negative regulators of ACTH secretion. Thus, the physiological relevance of ACTH in regulating BAT function may rather be indirect, depending on glucocorticoids. Notably, in obese rats the thermogenic effect of ACTH was attenuated by chronic increases in corticosterone (York and Al-Baker, 1984). However, no study so far addressed the immediate impact of GC on respiration in brown adipocytes. Therefore, we tested the thermogenic effects of ACTH and ISO after pretreatment of brown adipocytes with DEXA for up to 4 h. We found that DEXA had no effect on ACTH mediated respiration but attenuated the effect of ISO. We therefore conclude that the inhibitory action of DEXA occurs upstream of cAMP, as we observed an attenuation of the adrenergic signaling already at this level. For example, there might be an inhibition of G_s-mediated activation of adenylyl cyclase which is selective for ADRB3 signaling. Such selectivity would require that ARDB3 and MC2R couple to different isoforms of G-proteins and/or adenylyl cyclases expressed in brown adipocytes. Two hours of DEXA treatment was sufficient to obtain a significant downregulation of the thermogenic response to ISO. This effect was more pronounced after extended DEXA treatment for 4 h. This temporal increase of inhibitory action is compatible with the activation or repression of gene transcription mediated by DEXA via the glucocorticoid receptor. DEXA treatment for 1 h had no effect, thus excluding the involvement of rapid non-genomic effects of GC.

Pertaining to systemic demands and BAT functionality, cold exposure and restraint stress, both elevating circulating ACTH levels, fundamentally differ. In the cold, metabolic fuels need to be mobilized and delivered to BAT, whereas in a fight-or-flight situation, metabolic fuels must be channeled to brain, heart and skeletal muscle. Cold exposure (24 h) led to a strong rise in ACTH plasma levels (van den Beukel et al., 2014). It remains to be clarified whether this physiological rise in ACTH levels is sufficient to transiently activate BAT thermogenesis and contribute to the initial defense of body temperature in the cold. The lipolytic activity of ACTH in WAT may also indirectly support fuel supply to BAT in the cold by augmenting the release of fatty acids into circulation. As the ACTH receptor MC2R in BAT is down-regulated in chronic cold exposure, it seems less likely, that ACTH is involved in long term stimulation and maintenance of cold-induced thermogenesis. In restraint stress, extended activation of BAT thermogenesis by ACTH and the sympathetic neurotransmitter norepinephrine would be rather counterproductive. In this context, the observed attenuation of beta-adrenergic stimulation of thermogenesis by GC avoids excessive fuel wasting in BAT and limits stress-induced hyperthermia. However, pertaining to cold stress glucocorticoid levels rise as well as norepinephrine levels (Young et al., 1982; Sesti-Costa et al., 2010). Maximal activation of BAT thermogenesis can lead to a rapid depletion of lipid stores in brown adipocytes. Acute GC-mediated downregulation of beta-adrenergic signaling might transiently hinder the sequestration of lipid stores in brown adipocytes and promote the import of metabolic fuel from circulation, for example fatty acids from lipolysis in WAT depots or triglyceride-rich lipoproteins originating from intestine and liver.

Regarding long-term effects of the HPA-axis the bidirectional effect of stress on body weight might be explained by eating behavior and BAT recruitment and thermogenesis (Razzoli et al., 2016). Obesity is associated with chronic stress and low socio-economic status and stress induced thermogenesis has been repeatedly reported in mice and humans (Lkhagvasuren et al., 2011; Kataoka et al., 2014; Robinson et al., 2016). Thus, BAT function is a determinant of the vulnerability to stress-induced obesity (Razzoli et al., 2016). An attenuation of the beta-adrenergic stimulation of BAT thermogenesis by glucocorticoids could contribute to an amplification of the obese phenotype.

In summary, we identified several activators in cell culture which can serve as potential candidates to induce BAT thermogenesis *in vivo*. As a showcase, we demonstrated that ACTH activates the canonical pathway also targeted by β-adrenergic receptor signaling for activation of BAT thermogenesis. Furthermore, we add a synthetic ACTH peptide fragment to the expanding list of thermogenic compounds. As the ACTH receptor MC2R is down-regulated in response to cold, we hypothesize that its impact on cold-induced thermogenesis is rather transient. ACTH triggers the synthesis and release of GCs from the adrenal glands which have been reported to inhibit *Ucp1* expression in brown adipocytes. Additionally, in the present study we demonstrate that the GC dexamethasone attenuates β-adrenergic receptor signaling. We conclude that stress induced GC levels *in vivo* may limit extended energy dissipation in brown adipocytes and stress-induced hyperthermia, probably in a rather transient manner. Further studies *in vivo* are required to elucidate the effects of physiological cold- and stress-induced ACTH and glucocorticoid levels on BAT thermogenesis.

DATA AVAILABILITY STATEMENT

Publicly available datasets were analyzed in this study. This data can be found here: https://www.ncbi.nlm.nih.gov/geo/query/acc.cgi?acc=GSE119452.

AUTHOR CONTRIBUTIONS

KS and MK conceived and designed the study. KS and JW performed the experiments. YL helped with the luciferase assay. KS analyzed the data. KS and MK wrote the manuscript. All authors read and approved the manuscript.

FUNDING

This work was supported by grants to MK from the German Research Foundation (Deutsche Forschungsgemeinschaft, DFG KL973/12 and RTG1482) and the Else Kröner-Fresenius-Stiftung. KS was a fellow in the DFG Research Training Group RTG1482.

REFERENCES

Akesson, L., Ahren, B., Manganiello, V. C., Holst, L. S., Edgren, G., and Degerman, E. (2003). Dual effects of pituitary adenylate cyclase-activating polypeptide and isoproterenol on lipid metabolism and signaling in primary rat adipocytes. *Endocrinology* 144, 5293–5299. doi: 10.1210/en.2003-0364

Armengol, J., Villena, J. A., Hondares, E., Carmona, M. C., Sul, H. S., Iglesias, R., et al. (2012). Pref-1 in brown adipose tissue: specific involvement in brown adipocyte differentiation and regulatory role of C/EBPdelta. *Biochem. J.* 443, 799–810. doi: 10.1042/BJ20111714

Bartelt, A., Bruns, O. T., Reimer, R., Hohenberg, H., Ittrich, H., Peldschus, K., et al. (2011). Brown adipose tissue activity controls triglyceride clearance. *Nat. Med.* 17, 200–205. doi: 10.1038/nm.2297

Bartelt, A., and Heeren, J. (2014). Adipose tissue browning and metabolic health. *Nat. Rev. Endocrinol.* 10, 24–36. doi: 10.1038/nrendo.2013.204

Bista, B., and Beck, N. (2014). Cushing syndrome. *Indian J. Pediatr.* 81, 158–164. doi: 10.1007/s12098-013-1203-8

Biswas, H. M. (2017). Effect of adrenocorticotropic hormone on UCP1 gene expression in brown adipocytes. *J. Basic Clin. Physiol. Pharmacol.* 28, 267–274. doi: 10.1515/jbcpp-2016-0017

Bohnekamp, J., and Schoneberg, T. (2011). Cell adhesion receptor GPR133 couples to Gs protein. *J. Biol. Chem.* 286, 41912–41916. doi: 10.1074/jbc.C111.265934

Bouw, E., Huisman, M., Neggers, S. J., Themmen, A. P., van der Lely, A. J., and Delhanty, P. J. (2014). Development of potent selective competitive-antagonists of the melanocortin type 2 receptor. *Mol. Cell. Endocrinol.* 394, 99–104. doi: 10.1016/j.mce.2014.07.003

Braun, K., Oeckl, J., Westermeier, J., Li, Y., and Klingenspor, M. (2018). Non-adrenergic control of lipolysis and thermogenesis in adipose tissues. *J. Exp. Biol.* 221(Pt Suppl. 1):jeb165381. doi: 10.1242/jeb.165381

Buhl, A. M., Johnson, N. L., Dhanasekaran, N., and Johnson, G. L. (1995). G alpha 12 and G alpha 13 stimulate Rho-dependent stress fiber formation and focal adhesion assembly. *J. Biol. Chem.* 270, 24631–24634. doi: 10.1074/jbc.270.42.24631

Cannon, B., and Nedergaard, J. (2004). Brown adipose tissue: function and physiological significance. *Physiol. Rev.* 84, 277–359. doi: 10.1152/physrev.00015.2003

Carey, A. L., and Kingwell, B. A. (2013). Brown adipose tissue in humans: therapeutic potential to combat obesity. *Pharmacol. Ther.* 140, 26–33. doi: 10.1016/j.pharmthera.2013.05.009

Chang, C. L., Roh, J., and Hsu, S. Y. (2004). Intermedin, a novel calcitonin family peptide that exists in teleosts as well as in mammals: a comparison with other calcitonin/intermedin family peptides in vertebrates. *Peptides* 25, 1633–1642. doi: 10.1016/j.peptides.2004.05.021

Cho, K. J., Shim, J. H., Cho, M. C., Choe, Y. K., Hong, J. T., Moon, D. C., et al. (2005). Signaling pathways implicated in alpha-melanocyte stimulating hormone-induced lipolysis in 3T3-L1 adipocytes. *J. Cell Biochem.* 96, 869–878. doi: 10.1002/jcb.20561

Cypess, A. M., Chen, Y. C., Sze, C., Wang, K., English, J., Chan, O., et al. (2012). Cold but not sympathomimetics activates human brown adipose tissue *in vivo*. *Proc. Natl. Acad. Sci. U.S.A.* 109, 10001–10005. doi: 10.1073/pnas.1207911109

Cypess, A. M., Lehman, S., Williams, G., Tal, I., Rodman, D., Goldfine, A. B., et al. (2009). Identification and importance of brown adipose tissue in adult humans. *N. Engl. J. Med.* 360, 1509–1517. doi: 10.1056/NEJMoa0810780

Cypess, A. M., Weiner, L. S., Roberts-Toler, C., Franquet Elia, E., Kessler, S. H., Kahn, P. A., et al. (2015). Activation of human brown adipose tissue by a beta3-adrenergic receptor agonist. *Cell Metab.* 21, 33–38. doi: 10.1016/j.cmet.2014.12.009

Dean, T., Linglart, A., Mahon, M. J., Bastepe, M., Juppner, H., Potts, J. T., et al. (2006). Mechanisms of ligand binding to the parathyroid hormone (PTH)/PTH-related protein receptor: selectivity of a modified PTH(1-15) radioligand for GalphaS-coupled receptor conformations. *Mol. Endocrinol.* 20, 931–943. doi: 10.1210/me.2005-0349

Draper, M. W., Merrifield, R. B., and Rizack, M. A. (1973). Lipolytic activity of Met-Arg-His-Phe-Arg-Trp-Gly, a synthetic analog of the ACTH (4-10) core sequence. *J. Med. Chem.* 16, 1326–1330. doi: 10.1021/jm00270a003

Draper, M. W., Rizack, M. A., and Merrifield, R. B. (1975). Synthetic position 5 analogs of adrenocorticotropin fragments and their in vitro lipolytic activity. *Biochemistry* 14, 2933–2938. doi: 10.1021/bi00684a022

Galmozzi, A., Sonne, S. B., Altshuler-Keylin, S., Hasegawa, Y., Shinoda, K., Luijten, I. H. N., et al. (2014). ThermoMouse: an *in vivo* model to identify modulators of UCP1 expression in brown adipose tissue. *Cell Rep.* 9, 1584–1593. doi: 10.1016/j.celrep.2014.10.066

Gnad, T., Scheibler, S., von Kugelgen, I., Scheele, C., Kilic, A., Glode, A., et al. (2014). Adenosine activates brown adipose tissue and recruits beige adipocytes via A2A receptors. *Nature* 516, 395–399. doi: 10.1038/nature13816

Hauser, A. S., Attwood, M. M., Rask-Andersen, M., Schioth, H. B., and Gloriam, D. E. (2017). Trends in GPCR drug discovery: new agents, targets and indications. *Nat. Rev. Drug Discov.* 16, 829–842. doi: 10.1038/nrd.2017.178

Heinzmann, J. M., Thoeringer, C. K., Knapman, A., Palme, R., Holsboer, F., Uhr, M., et al. (2010). Intrahippocampal corticosterone response in mice selectively bred for extremes in stress reactivity: a microdialysis study. *J. Neuroendocrinol.* 22, 1187–1197. doi: 10.1111/j.1365-2826.2010.02062.x

Himms-Hagen, J. (1995). Role of brown adipose tissue thermogenesis in control of thermoregulatory feeding in rats: a new hypothesis that links thermostatic and glucostatic hypotheses for control of food intake. *Proc. Soc. Exp. Biol. Med.* 208, 159–169. doi: 10.3181/00379727-208-43847A

Hondares, E., Iglesias, R., Giralt, A., Gonzalez, F. J., Giralt, M., Mampel, T., et al. (2011). Thermogenic activation induces FGF21 expression and release in brown adipose tissue. *J. Biol. Chem.* 286, 12983–12990. doi: 10.1074/jbc.M110.215889

Ishibashi, J., and Seale, P. (2010). Medicine. Beige can be slimming. *Science* 328, 1113–1114. doi: 10.1126/science.1190816

Iwen, K. A., Senyaman, O., Schwartz, A., Drenckhan, M., Meier, B., Hadaschik, D., et al. (2008). Melanocortin crosstalk with adipose functions: ACTH directly induces insulin resistance, promotes a pro-inflammatory adipokine profile and stimulates UCP-1 in adipocytes. *J. Endocrinol.* 196, 465–472. doi: 10.1677/JOE-07-0299

Kataoka, N., Hioki, H., Kaneko, T., and Nakamura, K. (2014). Psychological stress activates a dorsomedial hypothalamus-medullary raphe circuit driving brown adipose tissue thermogenesis and hyperthermia. *Cell Metab.* 20, 346–358. doi: 10.1016/j.cmet.2014.05.018

Kenakin, T. (1995). Agonist-receptor efficacy. II. Agonist trafficking of receptor signals. *Trends Pharmacol. Sci.* 16, 232–238. doi: 10.1016/S0165-6147(00)89032-X

Kir, S., White, J. P., Kleiner, S., Kazak, L., Cohen, P., Baracos, V. E., et al. (2014). Tumour-derived PTH-related protein triggers adipose tissue browning and cancer cachexia. *Nature* 513, 100–104. doi: 10.1038/nature13528

Klepac, K., Kilic, A., Gnad, T., Brown, L. M., Herrmann, B., Wilderman, A., et al. (2016). The Gq signalling pathway inhibits brown and beige adipose tissue. *Nat. Commun.* 7:10895. doi: 10.1038/ncomms10895

Klingenspor, M. (2003). Cold-induced recruitment of brown adipose tissue thermogenesis. *Exp. Physiol.* 88, 141–148. doi: 10.1113/eph8802508

Klingenspor, M., Bast, A., Bolze, F., Li, Y., Maurer, S. F., Schweizer, S., et al. (2017). "Brown adipose tissue," in *Adipose Tissue Biology*, ed. M. E. Symonds (cham: Springer), 91–147. doi: 10.1007/978-3-319-52031-5_4

Kobilka, B. K. (2011). Structural insights into adrenergic receptor function and pharmacology. *Trends Pharmacol. Sci.* 32, 213–218. doi: 10.1016/j.tips.2011.02.005

Lacroix, A., Feelders, R. A., Stratakis, C. A., and Nieman, L. K. (2015). Cushing's syndrome. *Lancet* 386, 913–927. doi: 10.1016/S0140-6736(14)61375-1

Lafontan, M. (2012). Historical perspectives in fat cell biology: the fat cell as a model for the investigation of hormonal and metabolic pathways. *Am. J. Physiol. Cell Physiol.* 302, C327–C359. doi: 10.1152/ajpcell.00168.2011

Latek, D., Modzelewska, A., Trzaskowski, B., Palczewski, K., and Filipek, S. (2012). G protein-coupled receptors–recent advances. *Acta Biochim. Pol.* 59, 515–529.

Lefkowitz, R. J. (2007). Seven transmembrane receptors: something old, something new. *Acta Physiol.* 190, 9–19. doi: 10.1111/j.1365-201X.2007.01693.x

Li, Y., Bolze, F., Fromme, T., and Klingenspor, M. (2014a). Intrinsic differences in BRITE adipogenesis of primary adipocytes from two different mouse strains. *Biochim. Biophys. Acta* 1841, 1345–1352. doi: 10.1016/j.bbalip.2014.06.003

Li, Y., Fromme, T., Schweizer, S., Schottl, T., and Klingenspor, M. (2014b). Taking control over intracellular fatty acid levels is essential for the analysis of thermogenic function in cultured primary brown and brite/beige adipocytes. *EMBO Rep.* 15, 1069–1076. doi: 10.15252/embr.201438775

Li, Y., Schnabl, K., Gabler, S. M., Willershauser, M., Reber, J., Karlas, A., et al. (2018). Secretin-activated brown fat mediates prandial thermogenesis to induce satiation. *Cell* 175, 1561.e–1574.e. doi: 10.1016/j.cell.2018.10.016

Lkhagvasuren, B., Nakamura, Y., Oka, T., Sudo, N., and Nakamura, K. (2011). Social defeat stress induces hyperthermia through activation of thermoregulatory sympathetic premotor neurons in the medullary raphe region. *Eur. J. Neurosci.* 34, 1442–1452. doi: 10.1111/j.1460-9568.2011.07863.x

Ludwig, M. G., Vanek, M., Guerini, D., Gasser, J. A., Jones, C. E., Junker, U., et al. (2003). Proton-sensing G-protein-coupled receptors. *Nature* 425, 93–98. doi: 10.1038/nature01905

Marette, A., and Bukowiecki, L. J. (1990). Mechanism of norepinephrine stimulation of glucose transport in isolated rat brown adipocytes. *Int. J. Obes.* 14, 857–867.

Maurer, S. F., Fromme, T., Grossman, L. I., Huttemann, M., and Klingenspor, M. (2015). The brown and brite adipocyte marker Cox7a1 is not required for non-shivering thermogenesis in mice. *Sci. Rep.* 5:17704. doi: 10.1038/srep17704

Nahar, J., Rainville, J. R., Dohanich, G. P., and Tasker, J. G. (2016). Further evidence for a membrane receptor that binds glucocorticoids in the rodent hypothalamus. *Steroids* 114, 33–40. doi: 10.1016/j.steroids.2016.05.013

Neves, S. R., Ram, P. T., and Iyengar, R. (2002). G protein pathways. *Science* 296, 1636–1639. doi: 10.1126/science.1071550

Ochedalski, T., Zylinska, K., Laudanski, T., and Lachowicz, A. (2001). Corticotrophin-releasing hormone and ACTH levels in maternal and fetal blood during spontaneous and oxytocin-induced labour. *Eur. J. Endocrinol.* 144, 117–121. doi: 10.1530/eje.0.1440117

Ouellet, V., Routhier-Labadie, A., Bellemare, W., Lakhal-Chaieb, L., Turcotte, E., Carpentier, A. C., et al. (2011). Outdoor temperature, age, sex, body mass index, and diabetic status determine the prevalence, mass, and glucose-uptake activity

of 18F-FDG-detected BAT in humans. *J. Clin. Endocrinol. Metab.* 96, 192–199. doi: 10.1210/jc.2010-0989

Petrovic, N., Walden, T. B., Shabalina, I. G., Timmons, J. A., Cannon, B., and Nedergaard, J. (2010). Chronic peroxisome proliferator-activated receptor gamma (PPARgamma) activation of epididymally derived white adipocyte cultures reveals a population of thermogenically competent, UCP1-containing adipocytes molecularly distinct from classic brown adipocytes. *J. Biol. Chem.* 285, 7153–7164. doi: 10.1074/jbc.M109.053942

Ramage, L. E., Akyol, M., Fletcher, A. M., Forsythe, J., Nixon, M., Carter, R. N., et al. (2016). Glucocorticoids acutely increase brown adipose tissue activity in humans, revealing species-specific differences in UCP-1 regulation. *Cell Metab.* 24, 130–141. doi: 10.1016/j.cmet.2016.06.011

Razzoli, M., Frontini, A., Gurney, A., Mondini, E., Cubuk, C., Katz, L. S., et al. (2016). Stress-induced activation of brown adipose tissue prevents obesity in conditions of low adaptive thermogenesis. *Mol. Metab.* 5, 19–33. doi: 10.1016/j.molmet.2015.10.005

Robinson, L. J., Law, J. M., Symonds, M. E., and Budge, H. (2016). Brown adipose tissue activation as measured by infrared thermography by mild anticipatory psychological stress in lean healthy females. *Exp. Physiol.* 101, 549–557. doi: 10.1113/EP085642

Rochon, L., and Bukowiecki, L. J. (1990). Alterations in adipocyte response to lipolytic hormones during cold acclimation. *Am. J. Physiol.* 258, C835–C840. doi: 10.1152/ajpcell.1990.258.5.C835

Rosen, E. D., and Spiegelman, B. M. (2006). Adipocytes as regulators of energy balance and glucose homeostasis. *Nature* 444, 847–853. doi: 10.1038/nature05483

Roy, S., Roy, S. J., Pinard, S., Taillefer, L. D., Rached, M., Parent, J. L., et al. (2011). Mechanisms of melanocortin-2 receptor (MC2R) internalization and recycling in human embryonic kidney (hek) cells: identification of Key Ser/Thr (S/T) amino acids. *Mol. Endocrinol.* 25, 1961–1977. doi: 10.1210/me.2011-0018

Saito, M., Okamatsu-Ogura, Y., Matsushita, M., Watanabe, K., Yoneshiro, T., Nio-Kobayashi, J., et al. (2009). High incidence of metabolically active brown adipose tissue in healthy adult humans: effects of cold exposure and adiposity. *Diabetes* 58, 1526–1531. doi: 10.2337/db09-0530

Santos, R., Ursu, O., Gaulton, A., Bento, A. P., Donadi, R. S., Bologa, C. G., et al. (2017). A comprehensive map of molecular drug targets. *Nat. Rev. Drug Discov.* 16, 19–34. doi: 10.1038/nrd.2016.230

Scarpace, P. J., Baresi, L. A., and Morley, J. E. (1988). Glucocorticoids modulate beta-adrenoceptor subtypes and adenylate cyclase in brown fat. *Am. J. Physiol.* 255, E153–E158. doi: 10.1152/ajpendo.1988.255.2.E153

Scarpace, P. J., Kumar, M. V., Li, H., and Tumer, N. (2000). Uncoupling proteins 2 and 3 with age: regulation by fasting and beta3-adrenergic agonist treatment. *J. Gerontol. A Biol. Sci. Med. Sci.* 55, B588–B592. doi: 10.1093/gerona/55.12.B588

Sesti-Costa, R., Baccan, G. C., Chedraoui-Silva, S., and Mantovani, B. (2010). Effects of acute cold stress on phagocytosis of apoptotic cells: the role of corticosterone. *Neuroimmunomodulation* 17, 79–87. doi: 10.1159/000258690

Shaqura, M., Li, X., Al-Khrasani, M., Shakibaei, M., Tafelski, S., Furst, S., et al. (2016). Membrane-bound glucocorticoid receptors on distinct nociceptive neurons as potential targets for pain control through rapid non-genomic effects. *Neuropharmacology* 111, 1–13. doi: 10.1016/j.neuropharm.2016.08.019

Siu, F. K., Lam, I. P., Chu, J. Y., and Chow, B. K. (2006). Signaling mechanisms of secretin receptor. *Regul. Pept.* 137, 95–104. doi: 10.1016/j.regpep.2006.02.011

Soumano, K., Desbiens, S., Rabelo, R., Bakopanos, E., Camirand, A., and Silva, J. E. (2000). Glucocorticoids inhibit the transcriptional response of the uncoupling protein-1 gene to adrenergic stimulation in a brown adipose cell line. *Mol. Cell. Endocrinol.* 165, 7–15. doi: 10.1016/S0303-7207(00)00276-8

Strack, A. M., Horsley, C. J., Sebastian, R. J., Akana, S. F., and Dallman, M. F. (1995). Glucocorticoids and insulin: complex interaction on brown adipose tissue. *Am. J. Physiol.* 268, R1209–R1216. doi: 10.1152/ajpregu.1995.268.5.R1209

Touma, C., Bunck, M., Glasl, L., Nussbaumer, M., Palme, R., Stein, H., et al. (2008). Mice selected for high versus low stress reactivity: a new animal model for affective disorders. *Psychoneuroendocrinology* 33, 839–862. doi: 10.1016/j.psyneuen.2008.03.013

Tseng, Y. H., Cypess, A. M., and Kahn, C. R. (2010). Cellular bioenergetics as a target for obesity therapy. *Nat. Rev. Drug Discov.* 9, 465–482. doi: 10.1038/nrd3138

U Din, M., Saari, T., Raiko, J., Kudomi, N., Maurer, S. F., Lahesmaa, M., et al. (2018). Postprandial oxidative metabolism of human brown fat indicates thermogenesis. *Cell Metab.* 28, 207.e3–216.e3. doi: 10.1016/j.cmet.2018.05.020

van den Beukel, J. C., Grefhorst, A., Quarta, C., Steenbergen, J., Mastroberardino, P. G., Lombes, M., et al. (2014). Direct activating effects of adrenocorticotropic hormone (ACTH) on brown adipose tissue are attenuated by corticosterone. *FASEB J.* 28, 4857–4867. doi: 10.1096/fj.14-254839

van Marken Lichtenbelt, W. D., Vanhommerig, J. W., Smulders, N. M., Drossaerts, J. M., Kemerink, G. J., Bouvy, N. D., et al. (2009). Cold-activated brown adipose tissue in healthy men. *N. Engl. J. Med.* 360, 1500–1508. doi: 10.1056/NEJMoa0808718

Viengchareun, S., Penfornis, P., Zennaro, M. C., and Lombes, M. (2001). Mineralocorticoid and glucocorticoid receptors inhibit UCP expression and function in brown adipocytes. *Am. J. Physiol. Endocrinol. Metab.* 280, E640–E649. doi: 10.1152/ajpendo.2001.280.4.E640

Virtanen, K. A., Lidell, M. E., Orava, J., Heglind, M., Westergren, R., Niemi, T., et al. (2009). Functional brown adipose tissue in healthy adults. *N. Engl. J. Med.* 360, 1518–1525. doi: 10.1056/NEJMoa0808949

Vosselman, M. J., Brans, B., van der Lans, A. A., Wierts, R., van Baak, M. A., Mottaghy, F. M., et al. (2013). Brown adipose tissue activity after a high-calorie meal in humans. *Am. J. Clin. Nutr.* 98, 57–64. doi: 10.3945/ajcn.113.059022

Vosselman, M. J., van der Lans, A. A., Brans, B., Wierts, R., van Baak, M. A., Schrauwen, P., et al. (2012). Systemic beta-adrenergic stimulation of thermogenesis is not accompanied by brown adipose tissue activity in humans. *Diabetes* 61, 3106–3113. doi: 10.2337/db12-0288

Wang, H., Willershäuser, M., Karlas, A., Gorpas, D. Reber, J., et al. (2018). A dual *Ucp1* reporter mouse model for imaging and quantitation of brown and brite fat recruitment. *Mol. Metab.* doi: 10.1016/j.molmet.2018.11.009. [Epub ahead of print].

Wang, Y., Falting, J. M., Mattsson, C. L., Holmstrom, T. E., and Nedergaard, J. (2013). In brown adipocytes, adrenergically induced beta(1)-/beta(3)-(Gs)-, alpha(2)-(Gi)- and alpha(1)-(Gq)-signalling to Erk1/2 activation is not mediated via EGF receptor transactivation. *Exp. Cell Res.* 319, 2718–2727. doi: 10.1016/j.yexcr.2013.08.007

Wettschureck, N., and Offermanns, S. (2005). Mammalian G proteins and their cell type specific functions. *Physiol. Rev.* 85, 1159–1204. doi: 10.1152/physrev.00003.2005

WHO (2018). *Obesity and Overweight*. Available at: http://www.who.int/en/news-room/fact-sheets/detail/obesity-and-overweight

Wootten, D., Christopoulos, A., Marti-Solano, M., Babu, M. M., and Sexton, P. M. (2018). Mechanisms of signalling and biased agonism in G protein-coupled receptors. *Nat. Rev. Mol. Cell. Biol.* 19, 638–653. doi: 10.1038/s41580-018-0049-3

York, D. A., and Al-Baker, I. (1984). Effect of corticotropin on brown adipose tissue mitochondrial GDP binding in obese rats. *Biochem. J.* 223, 263–266. doi: 10.1042/bj2230263

Young, J. B., Saville, E., Rothwell, N. J., Stock, M. J., and Landsberg, L. (1982). Effect of diet and cold exposure on norepinephrine turnover in brown adipose tissue of the rat. *J. Clin. Invest.* 69, 1061–1071. doi: 10.1172/JCI110541

Conflict of Interest Statement: The authors declare that the research was conducted in the absence of any commercial or financial relationships that could be construed as a potential conflict of interest.

Article

Cell

Secretin-Activated Brown Fat Mediates Prandial Thermogenesis to Induce Satiation

Graphical Abstract

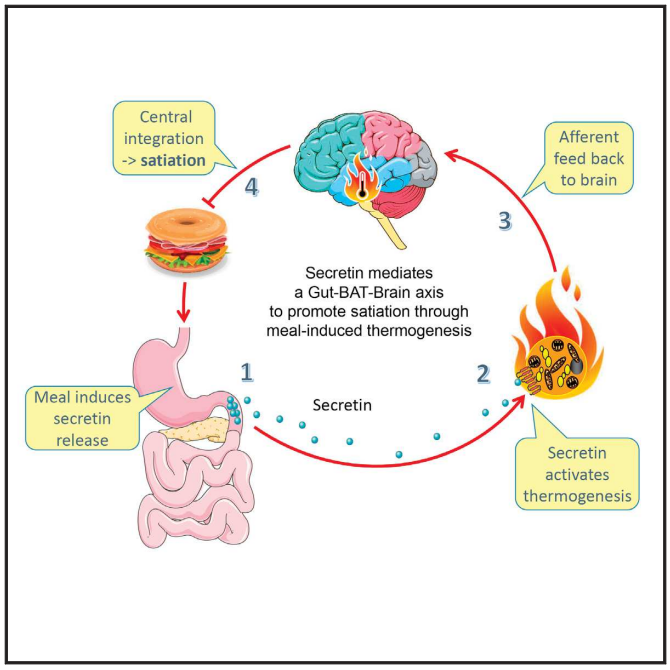

Authors

Yongguo Li, Katharina Schnabl, Sarah-Madeleine Gabler, ..., Vasilis Ntziachristos, Pirjo Nuutila, Martin Klingenspor

Correspondence

mk@tum.de

In Brief

Secretin, a gut hormone secreted while eating a meal, stimulates brown fat thermogenesis and induction of satiation in mice and humans.

Highlights

- Secretin receptor (SCTR) is highly expressed in BAT
- Secretin activates BAT thermogenesis through SCTR-PKA-ATGL/HSL pathway
- Secretin-activated BAT mediates prandial thermogenesis and induces satiation
- Secretin activates human BAT

Li et al., 2018, Cell *175*, 1–14
November 29, 2018
https://doi.org/10.1016/j.cell.2018.10.016

CellPress

Please cite this article in press as: Li et al., Secretin-Activated Brown Fat Mediates Prandial Thermogenesis to Induce Satiation, Cell (2018), https://doi.org/10.1016/j.cell.2018.10.016

Article

Cell

Secretin-Activated Brown Fat Mediates Prandial Thermogenesis to Induce Satiation

Yongguo Li,[1,2,9] Katharina Schnabl,[1,2,3,9] Sarah-Madeleine Gabler,[1,2,3] Monja Willershäuser,[1,2] Josefine Reber,[4,5] Angelos Karlas,[4,5] Sanna Laurila,[6] Minna Lahesmaa,[6] Mueez u Din,[6] Andrea Bast-Habersbrunner,[1,2] Kirsi A. Virtanen,[6] Tobias Fromme,[1,2,3] Florian Bolze,[1,2] Libbey S. O'Farrell,[7] Jorge Alsina-Fernandez,[7] Tamer Coskun,[7] Vasilis Ntziachristos,[4,5] Pirjo Nuutila,[6,8] and Martin Klingenspor[1,2,3,10,*]

[1]Chair for Molecular Nutritional Medicine, TUM School of Life Sciences, Technical University of Munich, Freising, Germany
[2]EKFZ – Else Kröner-Fresenius Center for Nutritional Medicine, Technical University of Munich, Freising, Germany
[3]ZIEL – Institute for Food & Health, Technical University of Munich, Freising, Germany
[4]Institute for Biological and Medical Imaging (IBMI), Helmholtz Zentrum München, Neuherberg
[5]Chair for Biological Imaging, Technical University of Munich, Munich, Germany
[6]Turku PET Centre, University of Turku, Turku, Finland
[7]Lilly Research Laboratories, Lilly Corporate Center, Indianapolis, IN, USA
[8]Department of Endocrinology, Turku University Hospital, Turku, Finland
[9]Theses authors contributed equally
[10]Lead Contact
*Correspondence: mk@tum.de
https://doi.org/10.1016/j.cell.2018.10.016

SUMMARY

The molecular mediator and functional significance of meal-associated brown fat (BAT) thermogenesis remains elusive. Here, we identified the gut hormone secretin as a non-sympathetic BAT activator mediating prandial thermogenesis, which consequentially induces satiation, thereby establishing a gut-secretin-BAT-brain axis in mammals with a physiological role of prandial thermogenesis in the control of satiation. Mechanistically, meal-associated rise in circulating secretin activates BAT thermogenesis by stimulating lipolysis upon binding to secretin receptors in brown adipocytes, which is sensed in the brain and promotes satiation. Chronic infusion of a modified human secretin transiently elevates energy expenditure in diet-induced obese mice. Clinical trials with human subjects showed that thermogenesis after a single-meal ingestion correlated with postprandial secretin levels and that secretin infusions increased glucose uptake in BAT. Collectively, our findings highlight the largely unappreciated function of BAT in the control of satiation and qualify BAT as an even more attractive target for treating obesity.

INTRODUCTION

In mammals, white adipose tissue (WAT) stores fat as the major energy backup for times of limited food supply, whereas brown adipose tissue (BAT) generates heat in response to cold exposure (Rosen and Spiegelman, 2006). Thermogenesis in BAT, known as non-shivering thermogenesis, dissipates chemical energy of nutrients by uncoupling oxygen consumption from ATP synthesis in mitochondria (Klingenspor, 2003). This mechanism depends on the uncoupling protein 1 (UCP1). Cold exposure activates BAT and leads to the recruitment of thermogenic capacity (Cannon and Nedergaard, 2004).

The discovery of cold-induced BAT activity in adult humans, attenuated with age, insulin resistance, diabetes, and obesity, has attained large interest (Sidossis and Kajimura, 2015). Cold acclimation recruits BAT activity (Blondin et al., 2014; van der Lans et al., 2013) and improves insulin sensitivity (Chondronikola et al., 2014; Hanssen et al., 2015), body fat mass (Yoneshiro et al., 2013), and hypercholesterinemia (Berbée et al., 2015). It is unclear, however, whether the total catabolic capacity of BAT is sufficient to account for these beneficial metabolic effects (Blondin et al., 2017; Hanssen et al., 2015).

BAT also contributes to meal-associated thermogenesis (Glick et al., 1981; Saito, 2013; U Din et al., 2018; Vosselman et al., 2013) and to long-term diet-induced thermogenesis (Rothwell and Stock, 1979). Meal-associated thermogenesis, when regarding a single meal, maybe divided into three phases: a pre-prandial, a prandial, and a postprandial phase. The contribution of BAT thermogenesis to these three phases is unclear. Furthermore, the molecular mediators and functional significance of meal-associated BAT thermogenesis are poorly understood. It is generally believed that an increased periprandial tone of the sympathetic nervous system (SNS) stimulates norepinephrine release from sympathetic nerves in BAT and activates canonical cAMP-PKA (cyclic AMP-protein kinase A) signaling via β3-adrenergic receptors (β3-ARs). This pathway activates lipolysis, UCP1, and non-shivering thermogenesis (Cannon and Nedergaard, 2004). Notably, meal-associated thermogenesis in BAT may promote central perception of satiation (Blessing et al., 2013; Brobeck, 1948; Glick, 1982; Himms-Hagen, 1995). In fasted mice, acute pharmacological BAT activation with a β3-AR agonist reduces cumulative food intake during refeeding (Grujic et al., 1997; Susulic et al., 1995).

Please cite this article in press as: Li et al., Secretin-Activated Brown Fat Mediates Prandial Thermogenesis to Induce Satiation, Cell (2018), https://doi.org/10.1016/j.cell.2018.10.016

Cell

All macronutrients elicit meal-associated thermogenesis, but only carbohydrate activates the SNS (Glick, 1982; Himms-Hagen, 1995; Welle et al., 1981). Notably, blockade of β-ARs with propranolol does not attenuate the early meal-associated rise in whole-body heat production caused by a carbohydrate meal or a mixed carbohydrate-rich meal (Astrup et al., 1989; Thörne and Wahren, 1989; Zwillich et al., 1981). We therefore hypothesized that not only catecholamines but also one of the gut hormones secreted into circulation during a meal may directly activate BAT. Secretion of gut hormones during a meal encodes information on the nutritional status and coordinates gastrointestinal motility and secretion for digestion and resorption, and it also controls the central perception of satiation and satiety in the brain via enteric neuronal afferent and endocrine feedback pathways (Chaudhri et al., 2006). In addition, periprandial secretion of gut hormones, like cholecystokinin (CCK) and glucagon-like peptide 1 (GLP-1), stimulates the central efferent tone of sympathetic innervation in BAT and thereby activates meal-associated non-shivering thermogenesis (Beiroa et al., 2014; Blouet and Schwartz, 2012). Furthermore, gut hormones directly modulate triglyceride metabolism in adipocytes. For example, the gut hormone peptide YY (PYY) inhibits lipolysis via Y2R coupled to G_i signaling (Valet et al., 1990), and secretin stimulates lipolysis through the secretin receptor (*Sctr*) coupled to G_s (Braun et al., 2018). As lipolysis is an essential prerequisite of BAT thermogenesis, we therefore set out to identify gut hormones that directly activate meal-associated thermogenesis in BAT and control satiation.

RESULTS

Abundant Expression of the Secretin Receptor in Brown Adipocytes

In a first step, we profiled gene expression of gut hormone receptors by inquiring transcriptome data obtained from interscapular BAT (iBAT) tissue of mice (GSE119452). Among the detectable transcripts of gut hormone receptor genes in iBAT, the secretin receptor (*Sctr*) stood out with the highest transcript abundance compared to other gut hormone receptors (Figure 1A). Our qPCR analyses revealed that *Sctr* is more abundantly expressed in iBAT compared to inguinal (iWAT) and epididymal (eWAT) white adipose tissue (Figure 1B). Preferential *Sctr* expression in brown adipocytes was also observed in primary cultures derived from these fat depots (Figure 1C). The Online Biology Gene Portal System (BioGPS) also detects *Sctr* as highly expressed in BAT (Figure S1).

Sctr gene expression predominated in mature brown adipocytes compared to undifferentiated stromal vascular cells (SVF) (Figure 1D), and differentiation of brown adipocytes was associated with an increase in *Sctr* at the transcript (Figure 1E) and at the protein level (Figure 1F). SCTR is a G_s protein-coupled GPCR (G-protein-coupled receptor) receptor of the class II receptor family (Afroze et al., 2013). Upon secretin binding, SCTR activates lipolysis by cAMP-PKA signaling in murine white adipocytes (Braun et al., 2018). In brown adipocytes, free fatty acids released by lipolysis serve as activators of UCP1 and substrates for thermogenesis. Moreover, secretin was reported to stimulate oxygen consumption in rat brown adipocytes (Dicker et al., 1998). Therefore, we postulated that SCTR in brown adipocytes may activate UCP1-mediated thermogenesis upon binding of secretin.

Secretin Activates Thermogenesis

To test whether secretin can activate thermogenesis, we measured UCP1-mediated thermogenesis in cultured adherent primary brown adipocytes (Li et al., 2014). We observed that secretin at a 50-fold lower concentration is as potent as isoproterenol (ISO), a β-AR agonist, in stimulating thermogenesis (Figures 2A and 2B). The minimal concentration to stimulate thermogenesis in brown adipocytes was 0.1 nM for secretin (Figure S2A) but at least 10 nM for ISO (Figure S2B). In dose-response experiments, EC_{50} values for secretin and ISO were 0.13 nM and 23.4 nM, respectively (Figure S2C). The thermogenic effect of secretin was independent of ARs, since pretreatment of brown adipocytes with propranolol, a nonselective β-AR antagonist, did not attenuate secretin-stimulated respiration while blocking the effect of ISO in a dose-dependent manner (Figure 2C). The thermogenic effect of secretin, however, depends on SCTR, as small interfering RNA (siRNA)-mediated downregulation of receptor expression (Figure S2G) blunted the effects of secretin on oxygen consumption (Figure 2D). Secretin stimulation resulted in a dose-dependent increase of relative cytosolic cAMP levels in brown adipocytes (Figure S2D). Pretreatment of cells with H89, a selective inhibitor of PKA (Figure 2E), or inhibitors targeting the two key lipases involved in lipolysis (adipose triglyceride lipase, ATGL; hormone-sensitive lipase, HSL), completely blocked the thermogenic effect of secretin (Figure 2F). This demonstrates that secretin-induced thermogenesis depends on the activation of lipolysis through the canonical cAMP-PKA pathway. Secretin also increased thermogenic gene expression in brown and white adipocytes (Figures S2E and S2F). Together, these data reveal a novel physiological role of secretin, serving as a non-adrenergic activator of thermogenesis.

We next tested whether secretin could induce thermogenesis *in vivo* using indirect calorimetry. A single intraperitoneal (i.p.) injection of secretin increased heat production in wild-type (WT) mice but not in UCP1 knockout (KO) mice (Figures 2G–2I). The thermogenic secretin effect in WT mice was maintained at thermoneutrality (TN, 30°C), and the magnitude is comparable to noradrenaline (Figures 2J and 2K), which was confirmed by a corresponding rise in iBAT temperature (Figure 2L). To further visualize BAT activation, we applied indirect calorimetry with multispectral optoacoustic tomography (MSOT) in nude mice, which detects the spectra of oxygenated and deoxygenated hemoglobin in high resolution deep in tissues and blood vessels (Reber et al., 2018). By monitoring the Sulzer's vein, the only venous drainage of iBAT, we found that total blood volume (TBV) was increased whereas relative oxygen saturation (SO_2) was dramatically decreased after secretin stimulation (Figures 2M–2P). Thus, secretin activates iBAT thermogenesis *in vivo*.

Secretin-Activated BAT Induces Satiation

Plasma secretin levels were decreased by fasting (18 hr) and increased significantly within 1 hr after refeeding (Figure 3A), which is congruent with changes of iBAT temperature (Figure 3B).

Please cite this article in press as: Li et al., Secretin-Activated Brown Fat Mediates Prandial Thermogenesis to Induce Satiation, Cell (2018), https://doi.org/10.1016/j.cell.2018.10.016

Cell

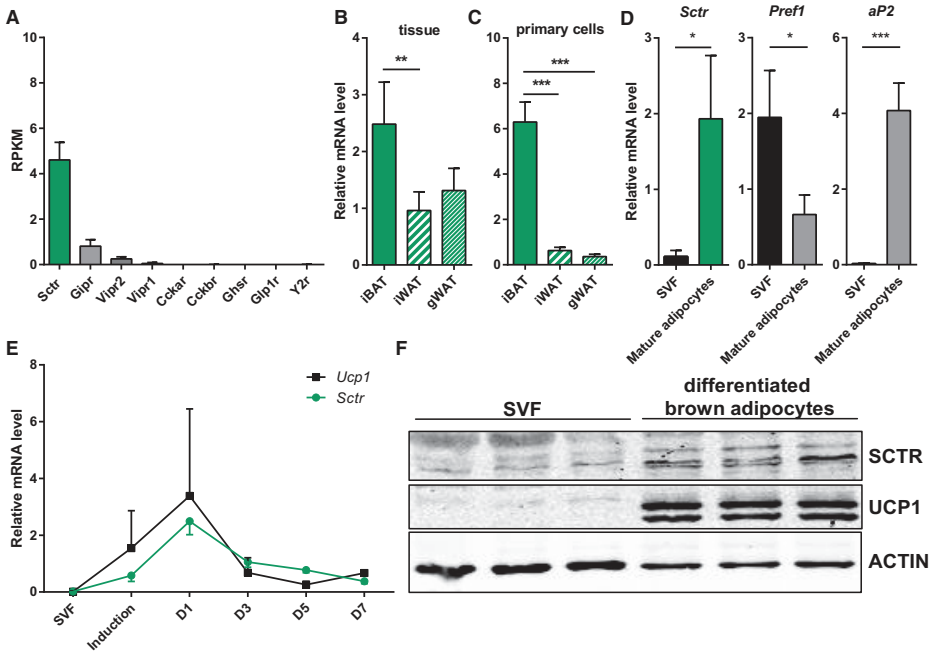

Figure 1. Secretin Receptor Is Highly Expressed in Murine BAT

(A) Profiling of gut hormone receptors expressed in murine brown adipose tissue (BAT) using RNA sequencing (RNA-seq) data. Data are shown as RPKM (reads per kilobase per million mapped reads). Secretin receptor (*Sctr*) stood out with the highest transcript abundance compared to other gut hormone receptors such as gastric inhibitory polypeptide receptor (*Gipr*), vasoactive intestinal peptide receptor1/2 (*Vipr1/2*), cholecystokinin A/B receptor (*Ccka/br*), ghrelin receptor (*Ghsr*), glucagon-like peptide 1 receptor (*Glp1r*), and the PYY_{3-36} receptor (*Npy2r*) (n = 4).

(B and C) Relative expression levels of *Sctr* in BAT and inguinal (iWAT) and epididymal (eWAT) white adipose tissues as well as primary cultures (C) derived from these fat depots assessed by qPCR (n = 5).

(D) Relative expression abundance of *Sctr*, *Pref1* (preadipocyte factor 1), and *aP2* (adipocyte protein 2) in stromal vascular fraction (SVF) and mature adipocytes (n = 3).

(E) Time course expression of uncoupling protein 1 (*Ucp1*) and *Sctr* mRNA during brown adipocyte differentiation (n = 3).

(F) Western blot analysis of SCTR, UCP1, and β-actin in both SVF and differentiated brown adipocytes. Data are presented as means ± SD.

(B) Repeated-measures one-way ANOVA (Tukey's test), (C) one-way ANOVA (Tukey's test), (D) unpaired t test. * = $p < 0.05$, ** = $p < 0.01$, *** = $p < 0.001$. See also Figure S1.

The periprandial rise of secretin may suppress food consumption, as peripheral and central administration of secretin reduces food intake in fasted mice depending on the presence of the SCTR (Cheng et al., 2011). Integrated with our present finding, we hypothesized that secretin inhibits food intake through activation of BAT. To test this hypothesis, fasted mice were injected with 5 nmol secretin before refeeding. Secretin reduced food intake compared with PBS-injected mice (Figure 3C) during the first 2–3 hr of refeeding, possibly due to the short half-life of secretin (Curtis et al., 1976).

To further explore whether the reduction in food intake was dependent on BAT thermogenesis, we compared the effect of secretin on food intake in UCP1 WT and KO mice. Remarkably, the inhibitory effect of secretin on food intake was attenuated in UCP1-KO mice (Figures 3D and 3E). Therefore, we conclude that secretin-induced thermogenesis in BAT accelerates satiation during the first bouts of refeeding. This satiation effect could be mediated either by direct activation of BAT or by central effects of secretin activating the sympathetic output to BAT. In contrast to the effect of β3-AR agonist CL-316,243 (CL), the effects of secretin on food intake (Figures 3F–3H) and BAT temperature (Figures 3I–3P), however, were retained in mice pretreated with propranolol. Therefore, secretin directly activates BAT independent of the efferent sympathetic innervation. Consistent with previous findings (Grujic et al., 1997; Susulic et al., 1995), BAT activation by adrenergic signaling (CL) also leads to a suppression of appetite, which indicates that satiation is a general consequence of BAT thermogenesis. Moreover, our data also demonstrate that BAT plays a negligible role in pre-prandial thermogenesis (Figure S3A). While prandial thermogenesis and early postprandial thermogenesis do not depend on adrenergic signaling, as propranolol failed to block the increase

Cell

Please cite this article in press as: Li et al., Secretin-Activated Brown Fat Mediates Prandial Thermogenesis to Induce Satiation, Cell (2018), https://doi.org/10.1016/j.cell.2018.10.016

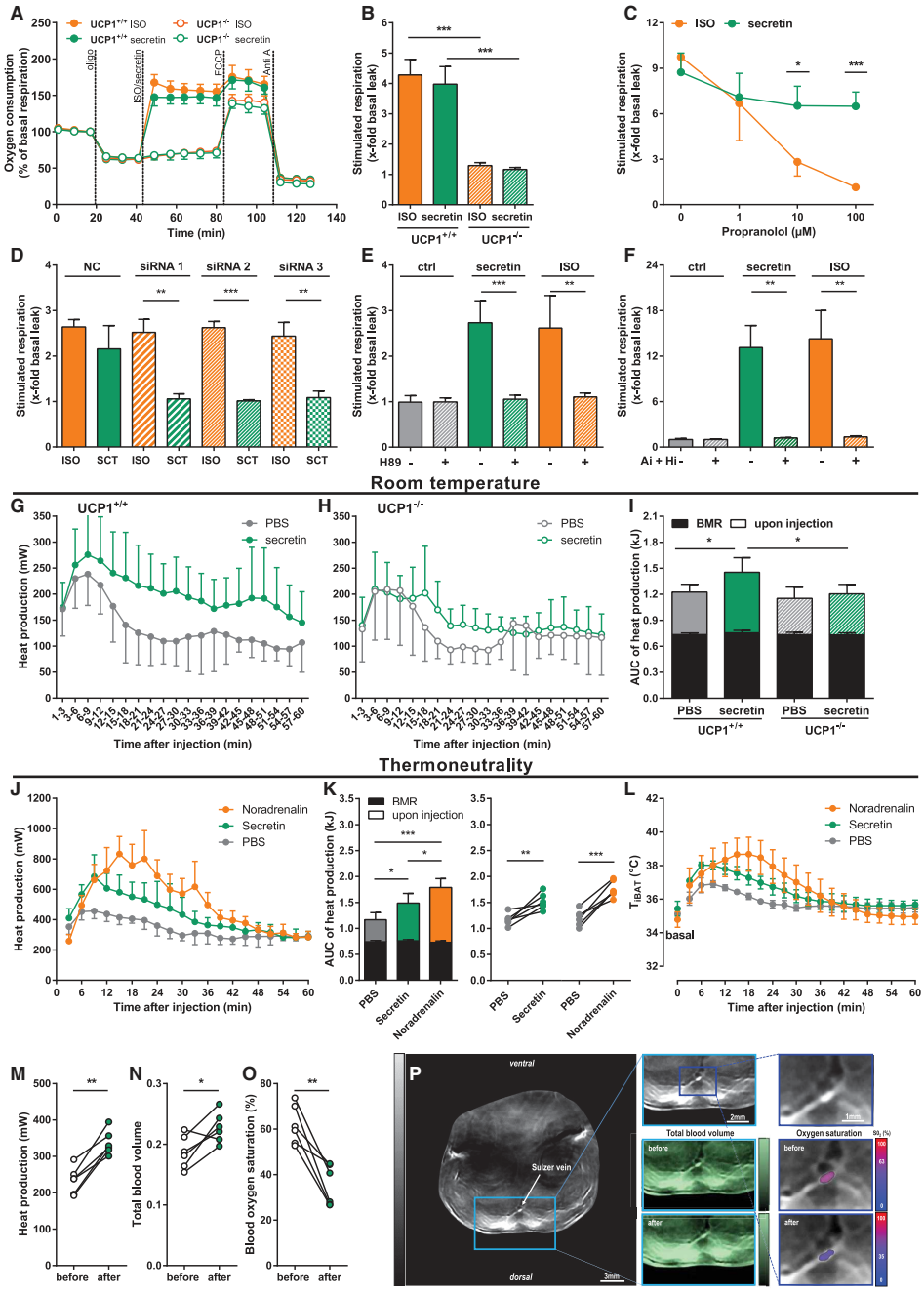

(legend on next page)

Please cite this article in press as: Li et al., Secretin-Activated Brown Fat Mediates Prandial Thermogenesis to Induce Satiation, Cell (2018), https://doi.org/10.1016/j.cell.2018.10.016

in BAT temperature induced by refeeding, late postprandial thermogenesis depends on adrenergic signaling (Figures S3A and S3B). This is consistent with the previous finding that the most pronounced effect of β-blockade on postprandial energy expenditure was found 3–4 hr after the meal (Astrup et al., 1989).

We next investigated the neurobiological basis of satiation induced by secretin-activated BAT. We found that secretin treatment elevated anorexigenic proopiomelanocortin (POMC) and repressed orexigenic agouti-related protein (AgRP) mRNA levels in the hypothalamus of fasted mice in an UCP1-dependent manner (Figures 3Q–3S). There was no effect of secretin on cocaine- and amphetamine-regulated transcript (CART) and neuropeptide Y (NPY) transcript levels (Figures S3C–S3E). Moreover, the expression of transient receptor potential vanilloid 1 (TRPV1), a temperature-sensitive ion channel expressed in POMC neurons, was upregulated by secretin treatment in the hypothalamus of WT but not in UCP1-KO mice (Figure 3T). Activation of TRPV1-like receptors in POMC neurons of the hypothalamic arcuate nucleus by warm temperature leads to appetite suppression (Jeong et al., 2018). Thus, our data support the idea that the TRPV1 receptor senses the rise in hypothalamic temperature due to BAT-mediated meal-associated prandial thermogenesis and activates the POMC neurons (Rampone and Reynolds, 1991). Congruently, we found that short-term heat exposure regulated neuropeptides and TRPV1 gene expression in a similar pattern as secretin treatment (Figures S3F and S3G). Together, these results suggest that the satiation signal emanating from secretin-activated BAT was sensed in the brain and promoted satiation, likely through perception of heat generated by BAT.

To further emphasize the strong relationship between BAT thermogenesis and food intake, we performed an analysis of around 2,000 food intake events in 23 mice during 70 hr (*ad libitum* feeding) when BAT temperature was recorded simultaneously using implanted transmitters. Our analysis showed that (1) the initiation of feeding is always accompanied by a rise in iBAT temperature and that (2) the peak of iBAT temperature is followed by termination of feeding (Figures S3H–S3K). Therefore, a rise in iBAT temperature was plausibly the consequence of food intake and subsequently could have caused the termination of feeding. In short, thermogenic BAT plays an important role in the acute control of food intake in mice. Consistently, UCP1-KO mice showed dramatic alterations in feeding behavior with decreased number of meals, increased meal size and meal duration, and decreased inter-meal bout length, whereas total food intake was similar to WT mice (Figures 3U–3Z and S4). Taken together, secretin inhibits food intake through directly activating BAT thermogenesis and thereby conveys an unappreciated function of BAT in the control of satiation.

Neutralizing Prandial Secretin Activity Blunts Meal-Associated Thermogenesis, Increases Food Intake, and Changes Meal Patterning

Based on the thermogenic effects of exogenous secretin, we reasoned that endogenous release of secretin during refeeding stimulates prandial thermogenesis in BAT. A polyclonal secretin antibody was applied to neutralize the endogenous activity of secretin. This antibody completely neutralized purified secretin as well as endogenous blood-borne secretin mediated activation of SCTR signaling when tested *in vitro* (Figure S5). Refeeding of fasted mice was associated with an immediate rise in iBAT temperature by ~2°C within 30 min (Figure 4A). Compared to mice treated with isotype-like anti-GFP antibody, this rise in iBAT temperature was largely attenuated in mice pretreated with the secretin antibody (Figures 4A and 4B). The antibody also increased food intake during the early phase of refeeding

Figure 2. Secretin Activates UCP1-Dependent Thermogenesis Both *In Vitro* and *In Vivo*

(A–F) Secretin activates UCP1-dependent thermogenesis through the SCTR-PKA-ATGL/HSL pathway in primary brown adipocytes. (A) Time course of oxygen consumption rate of UCP1 WT ($UCP1^{+/+}$) and KO ($UCP1^{-/-}$) brown adipocytes recorded by microplate-based respirometry (Seahorse XF96 Analyzer) under basal conditions and during successive addition of 5 μM oligomycin (oligo), 1 μM isoproterenol (ISO) or 10 nM secretin, 1 μM FCCP, and 5 μM antimycin A (Anti A). Data are expressed as percentage of basal respiration. (B) Quantitation of ISO- and secretin-stimulated UCP1-mediated uncoupled respiration in $UCP1^{+/+}$ and $UCP1^{-/-}$ brown adipocytes. Data are expressed as fold of basal leak respiration, 1-fold of basal leak indicating no stimulation of UCP1-mediated uncoupled respiration (n = 5). (C) Effects of various concentrations of propranolol, a non-selective blocker of β-adrenergic receptors, on secretin- and ISO-stimulated UCP1-mediated uncoupled respiration in brown adipocytes (n = 3). (D) SCT (secretin)- and ISO- stimulated respiration in primary brown adipocytes after siRNA-mediated knockdown of the secretin receptors in comparison to a non-targeting control (NC) (n = 3). (E) UCP1-mediated uncoupled respiration expressed as fold increase of basal leak respiration after stimulation with ISO, secretin, and vehicle (assay medium) without protein kinase A inhibitor H89 (50 μM), which was injected together with oligo prior to addition of stimulators (n = 3). (F) Respiration stimulated by ISO, secretin, or vehicle as fold increase of basal leak after 1 hr pre-treatment with both 40 μM A_i (Atglistatin, ATGL-inhibitor) and H_i (Hi76-0079, HSL-inhibitor) (n = 4).

(G–I) The thermogenic effect of secretin in $UCP1^{+/+}$ (G) and $UCP1^{-/-}$ (H) mice kept at room temperature. After determining the basal metabolic rate (BMR) at 30°C, respiration of mice treated with either 5 nmol secretin or equal volume PBS via intraperitoneal injection (i.p.) was measured by indirect calorimetry for 1 hr at 27°C. BMR and heat production upon stimulation were quantified as area under the curve (AUC) (I) (n = 6–9).

(J–L) The thermogenic effects of secretin (5 nmol), noradrenalin (1 mg/kg), and PBS on mice acclimatized for 1 week to thermoneutrality (30°C). Heat production was determined by the same procedure as for mice kept at room temperature. Additionally, the temperature of interscapular brown adipose tissue was recorded via implanted E-mitter (L).

(M–P) Direct visualization of BAT activation by secretin (5 nmol) in nude mice through indirect calorimetry coupled with multispectral optoacoustic tomography (MSOT) (n = 6). (M) Heat production before and after intravenous secretin injection (5 nmol). (N) Normalized MSOT image signal of total blood volume (TBV) in the Sulzer vein (SV) before and after intravenous (i.v.) injection of secretin. (O) Oxygen saturation (SO_2) calculated as MSOT signal ratio between oxygenated hemoglobin and TBV in the SV before and after i.v. injection of secretin. (P) Representative reconstructed anatomical MSOT image (800 nm) showing iBAT and the Sulzer vein *in vivo* in three different magnifications as well as TBV (green) and SO_2 (red/blue) before and after i.v. secretin injection. Data are presented as means ± SD or individual values.

(B, C, and I) Two-way ANOVA (Tukey's test), (D–F) unpaired t test, (M–O) paired t test. * = $p < 0.05$, ** = $p < 0.01$, *** = $p < 0.001$. See also Figure S2.

Cell

Please cite this article in press as: Li et al., Secretin-Activated Brown Fat Mediates Prandial Thermogenesis to Induce Satiation, Cell (2018), https://doi.org/10.1016/j.cell.2018.10.016

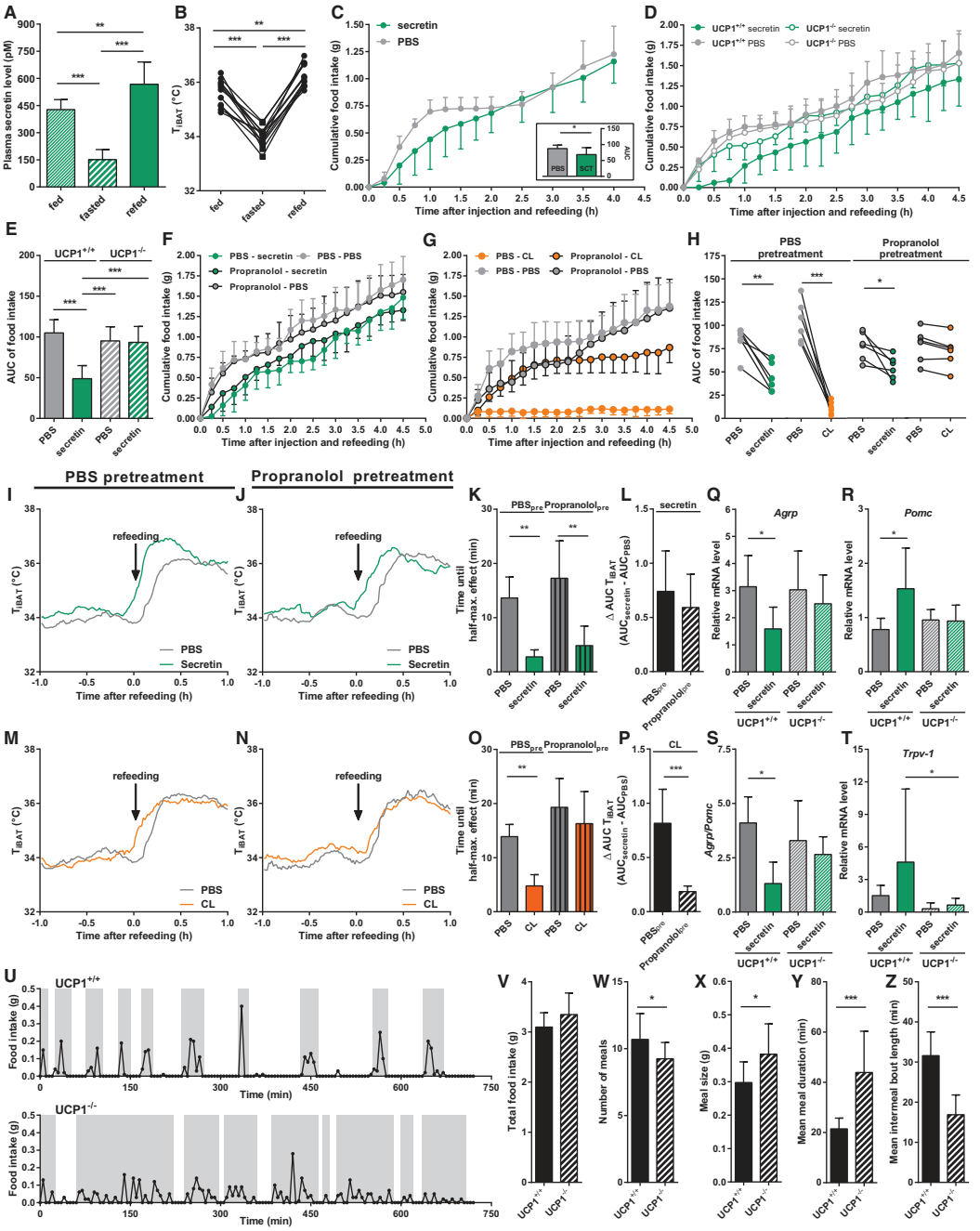

(legend on next page)

Please cite this article in press as: Li et al., Secretin-Activated Brown Fat Mediates Prandial Thermogenesis to Induce Satiation, Cell (2018), https://doi.org/10.1016/j.cell.2018.10.016

(Figures 4C–4E). Detailed analysis revealed a negative correlation between the rise in iBAT temperature and food intake (Figure 4F). Thus, secretin released endogenously in response to food intake is a physiological mediator of meal-associated thermogenesis in BAT, and the induction of BAT thermogenesis is necessary for the inhibitory effect of secretin on food intake. Our findings demonstrate a novel endocrine gut-secretin-BAT-brain axis in the acute control of food intake.

Analyzing the feeding behavior of WT mice treated with the secretin antibody under *ad libitum* feeding conditions, we found that these WT mice phenocopied the UCP1-KO mice by showing increased meal sizes as well as longer meal durations (Figures 4G–4K). Therefore, disruption of the gut-BAT-brain axis in the control of satiation by blocking endogenous secretin activity alters feeding behavior. We thereby recapitulate our findings in a WT mouse model with acute loss of secretin function that is not subject to long-term adaptive responses due to genetic ablation as may be prevalent in germline UCP1-KO.

Secretin Infusion Transiently Elevates Energy Expenditure in Diet-Induced Obese Mice

Secretin promoted negative energy balance through both increasing energy expenditure and decreasing energy intake and therefore may hold promise for developing novel obesity therapies. To clarify the potential therapeutic uses, we chronically infused diet-induced obese mice (DIO) with native human secretin (native secretin) and a modified human secretin analog (modified secretin), respectively. In a first experiment conducted with DIO mice kept at room temperature (RT), the modified secretin caused a small transient reduction in cumulative food intake (Figure S6A) and body weight gain (Figure S6B). After 2 weeks of treatment, body fat mass was slightly lower in modified-secretin-treated mice. This was not reflected by a lower body mass as the lean mass was slightly increased in these mice (Figure S6C). Compared to GLP-1 as a positive control, these effects were minor. Employing a linear mixed effects model to test whether secretin also affects metabolic rate, we found that the small effect of secretin on food intake was not alone explained by the starting body weight (which captures the metabolic requirements of the animal) and the change in body weight (which primarily captures the alternate fate of food: fat deposition loss), suggesting that the modified secretin modulated metabolic rate.

Effects on energy expenditure at RT may be masked, as this thermal environment already imposes a cold challenge on mice and activates thermoregulatory heat production, mainly in BAT, as exemplified by a nearly 2-fold increase of resting metabolic rate by transfer from 30°C to 20°C (Fischer et al., 2018). Therefore, we conducted a second experiment to directly measure whether chronic infusion of the modified secretin increases energy expenditure analyzed as heat production in DIO mice kept at TN. On days 1 and 2 after start of infusion, the modified secretin led to a transient increase in daily energy expenditure by 32% and 9%, respectively (Figures 5A–5C). No such effect on energy expenditure was observed in control mice infused with native secretin, or with the GLP-1 analog. The GLP-1 analog induced a pronounced decrease in food intake and body fatness, whereas the minor effects of the modified secretin on body composition observed at RT were not observed at TN (Figures 5D–5F). We conclude that the transient increase in energy expenditure after onset of chronic infusion of the human secretin analog strongly promoted negative energy balance in DIO mice even when kept at TN. Notably, mice infused with the modified secretin at TN showed a significant increase in water intake most likely to compensate for increased water secretion by the pancreas (Figure 5G).

These data demonstrate thermogenic activity of secretin also in DIO mice but rather discourage the application of chronically elevated secretin levels as a therapeutical option for the treatment of obesity.

Figure 3. Secretin Inhibits Food Intake through Direct Activation of BAT Thermogenesis in Mice

(A) Plasma secretin levels of mice fed *ad libitum*, fasted for 18 hr, and/or refed for 1 hr after 17 hr of fasting (n = 6).

(B) Temperature of iBAT (T_{iBAT}) of fed, fasted, and refed mice. T_{iBAT} was calculated as mean of 1 hr period (fed: random 1 hr; fasted: 1 hr before refeeding; refed: 1 hr after refeeding) (n = 12).

(C) Cumulative food intake of overnight fasted (18 hr) C57BL6/N mice upon refeeding. Mice were injected (i.p.) with either secretin or vehicle (PBS) before refeeding. For statistics, we calculated area under cumulative food intake−time curve (see inset: AUC 0–2.5 hr) (n = 11–12).

(D) The effects of secretin on acute food intake in overnight fasted (18 hr) $UCP1^{+/+}$ and $UCP1^{-/-}$ 129S1/SvEv mice upon refeeding.

(E) The area under cumulative food intake−time curve (AUC 0–2.5 hr) was calculated (n = 6).

(F–H) The effects of β-blocker propranolol (10 mg/kg BW) pre-treatment (20 min prior to secretin, CL, or PBS injection) on secretin (5 nmol) (F) and CL 316,243 (CL,1 mg/kg BW) (G) induced suppression of food intake in overnight (18 hr) fasted 129S6/SvEv mice, respectively. (H) Area under cumulative food intake curve (AUC 0–2.5 hr) was quantified (n = 6).

(I–P) The effects of β-blocker propranolol (10 mg/kg BW) pre-treatment (20 min prior to secretin, CL, or PBS injection) on refeeding-induced rise in iBAT temperature in overnight (18 hr) fasted mice without secretin and CL treatments. Propranolol delayed the rise of CL-induced T_{iBAT} but not refeeding- or secretin-induced T_{iBAT} as quantified by the required time to reach half-maximal iBAT temperature in response to refeeding/injection (K and O) as well as the calculated differences between the AUC of secretin- (L) or CL-induced (P) rise in iBAT temperature and their corresponding PBS controls (ΔAUC T_{iBAT}) under both PBS and propranolol pre-treatment conditions.

(Q–T) The neurobiological basis of satiation induced by secretin-activated BAT. Relative expression abundance of *Agrp* (agouti-related protein) (Q), *Pomc* (pro-opiomelanocortin) (R), and *Trpv-1* (transient receptor potential vanilloid 1) (T) in hypothalamus of fasted $UCP1^{+/+}$ and $UCP1^{-/-}$ mice in response to i.p. injection of PBS or secretin (hypothalamus was removed 4 hr after injection). (S) Ratio of *Agrp* and *Pomc* expression.

(U–Z) Feeding patterns of $UCP1^{+/+}$ and $UCP1^{-/-}$ 129S1/SvEv mice. (U) Representative food intake of one $UCP1^{+/+}$ and one $UCP1^{-/-}$ mouse during dark phase. Meals defined as food intake >0.005 g; inter-meal bout lengths ≥15 min are indicated in gray. Total food intake (V), number of meals (W), mean meal size (X), mean meal duration (Y), and mean inter-meal bout length (Z) during dark phase (n = 12) were quantified.

(A) One-way ANOVA (Tukey's test), (B) RM one-way ANOVA, (C, L, P–T, V, and X–Z) unpaired t test, (H, K, and O) paired t test, (E) two-way ANOVA (Tukey's test), (W) non-parametric t test as normality test failed. Data are presented as means ± SD. * = $p < 0.05$, ** = $p < 0.01$, *** = $p < 0.001$. See also Figures S3 and S4.

Please cite this article in press as: Li et al., Secretin-Activated Brown Fat Mediates Prandial Thermogenesis to Induce Satiation, Cell (2018), https://doi.org/10.1016/j.cell.2018.10.016

Cell

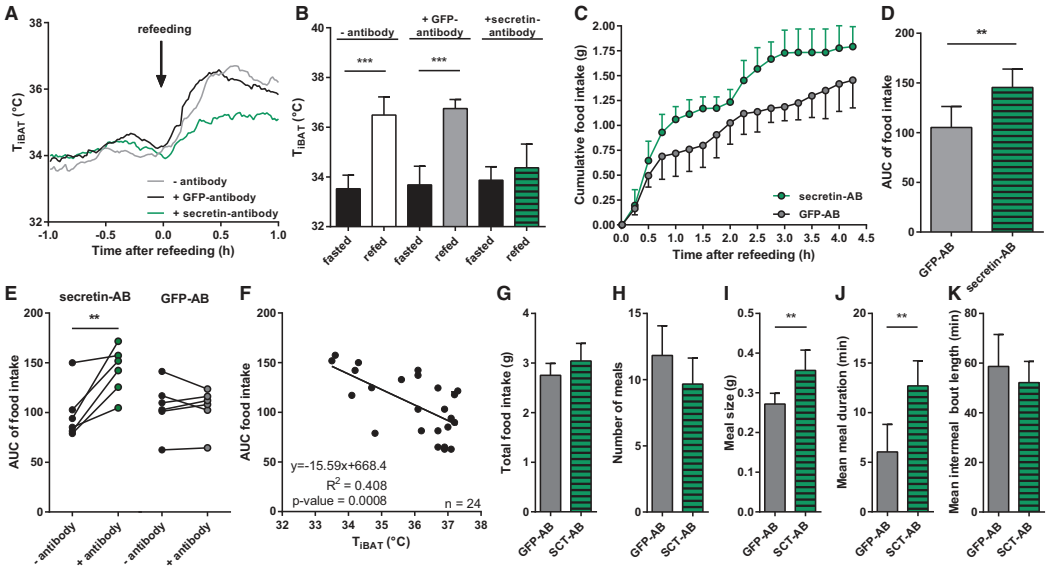

Figure 4. Neutralization of Endogenous Secretin Prevents Meal-Induced Increase in iBAT Temperature and Acutely Increases Food Intake

(A–F) Refeeding responses, in terms of rise in T_{iBAT} and increase in cumulative food intake, were recorded (1-min bins) in overnight fasted mice (18 hr) upon refeeding under control, GFP-antibody-, and secretin-antibody-treated conditions. In total, 12 mice were used for non-treated control characterization. After 1 week washout to minimize the potential previous effects of fasting, mice were divided into two groups (n = 6) and either injected with GFP or secretin antibody when fasted again. (A) Time course changes of T_{iBAT} in secretin-antibody-injected mice in comparison with GFP-antibody- and non-treated controls upon refeeding. (B) Minimal and maximal T_{iBAT} of control, GFP-, and secretin-antibody-injected mice compared to respective controls within 30 min before and 30 min after refeeding. (C) Cumulative food intake of mice pre-treated with GFP- or secretin-antibody within 4.5 hr of refeeding. (D) The area under cumulative food intake–time curve (AUC 0–2.5 hr) was calculated. (E) Paired comparison of individual $AUC_{0-2.5\ hr}$ of food intake before and after antibody treatment. (F) Negative correlation of $AUC_{0-2.5\ hr}$ of food intake and iBAT temperature.

(G–K) Feeding behavior of *ad libitum*-fed mice treated with either secretin antibody of GFP antibody. Total food intake (G), number of meals (H), mean meal size (I), mean meal duration (J), and mean inter-meal bout length (K) of GFP- or secretin-antibody-treated 129S6/SvEv mice during one dark phase. The analysis was performed 2 days after the antibody injection to minimize previous fasting effects (n = 6).

Data are presented as means ± SD or individual values. (D and G–K) Unpaired t test, (B and E) paired t test. * = $p < 0.05$, ** = $p < 0.01$, *** = $p < 0.001$. See also Figure S5.

Secretin Activates Human BAT

We addressed the biological significance of thermogenic action of secretin in humans. For this purpose, secretin concentrations were measured in serum samples from human subjects showing BAT activation in response to a single meal, as reported very recently (U Din et al., 2018). Consistent with our observations in mice, serum secretin levels increased after single-meal ingestion (Figure 6A). The increment of plasma secretin levels induced by a single meal positively correlated with postprandial oxygen consumption rates and fatty acid uptake rates in BAT (Figures 6B and 6C). Direct evidence for the thermogenic action of secretin in BAT was obtained by FDG-PET-CT scans after two secretin infusions that significantly increased serum secretin level (Figure S6D) and glucose uptake in human BAT compared to placebo control treatment (Figure 6D). Collectively, we propose that the satiation axis sparked by BAT activation through secretin is conserved from mouse to man.

DISCUSSION

Thermogenesis in brown adipose tissue, contributing to meal-associated thermogenesis (or diet-induced thermogenesis) and cold-induced non-shivering thermogenesis, is generally believed to be switched on by noradrenaline released from sympathetic nerve endings. In this study, we identified that the gut hormone secretin, upon release during eating, serves as a novel non-sympathetic BAT activator mediating prandial thermogenesis, which consequentially induces satiation. We thereby reveal a gut-secretin-BAT-brain axis in mammals that constitutes the physiological basis of prandial thermogenesis in the control of satiation. Establishing a largely unappreciated function of BAT in the control of hunger and satiation qualifies BAT as an even more attractive target for treating obesity. Demonstration of a non-canonical gut-secretin-BAT-brain axis beyond the canonical gut-brain-BAT axis uncovers

Please cite this article in press as: Li et al., Secretin-Activated Brown Fat Mediates Prandial Thermogenesis to Induce Satiation, Cell (2018), https://doi.org/10.1016/j.cell.2018.10.016

Cell

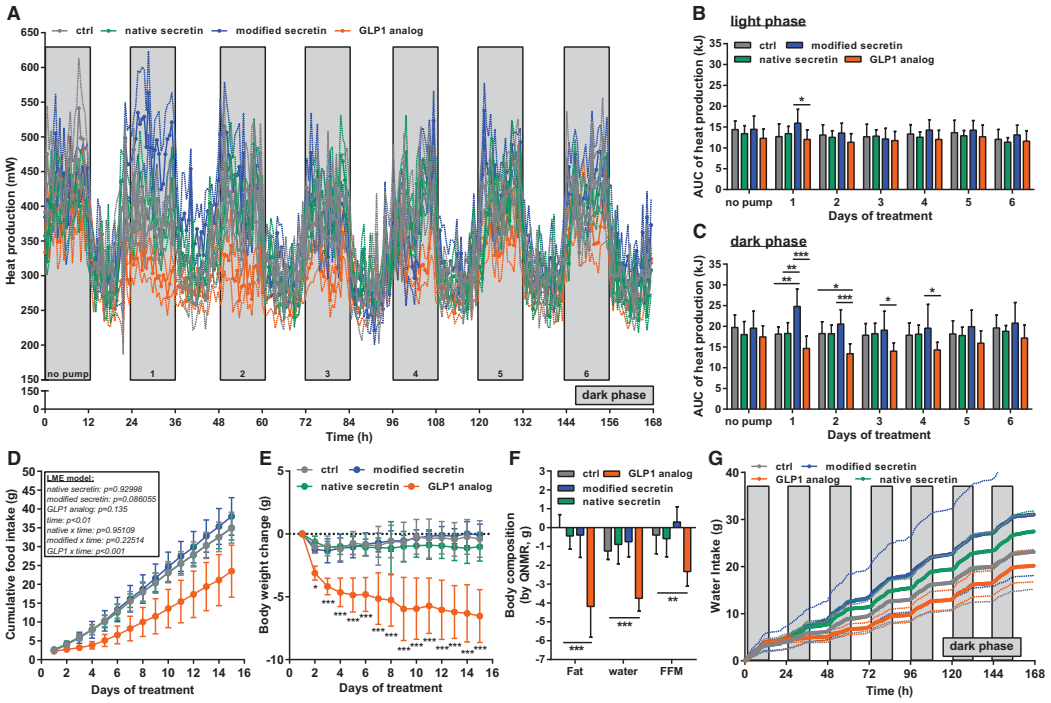

Figure 5. Secretin Infusion Transiently Increases Energy Expenditure in Diet-Induced Obese Mice at Thermoneutrality

(A–G) The effects of continuous infusion of native secretin (996 nmol/kg/day), modified secretin (326 nmol/kg/day), GLP1 analog (CEX51, 30 nmol/kg/day), or vehicle (20 mM Citrate) on metabolic parameters such as heat production (A–C), cumulative food intake (D), body weight changes (E), and changes in body composition from day 1 to day 14 (F) as well as water intake (G) in diet-induced obese (DIO) male C57BL6/N mice kept at thermoneutrality (30°C). The continuous infusion with subcutaneous miniosmotic-pumps (12 μl/mouse/day) lasted 2 weeks. Heat production data was only presented for the first 6 days as no differences were observed in the second experimental week. Area under the heat production time curve was calculated for light (B) and dark (C) phases separately. Dashed lines in (A) and (G) represent standard deviation of corresponding groups. (D) Linear mixed effects model with "treatment," "time" and their interaction as fixed effects, and "individual" as random factor. (F) One-way ANOVA (Tukey's test), (B, C, and E): repeated-measures two-way ANOVA (Tukey's test). * = $p < 0.05$; ** = $p < 0.01$, *** = $p < 0.001$. See also Figure S6.

a yet unknown facet of the complex regulatory system controlling energy balance.

Secretin, an Old Dog Playing a New Trick

Secretin was the first hormone discovered and laid grounds for the conceptual framework of endocrine regulation (Bayliss and Starling, 1902). It stimulates water and bicarbonate secretion from pancreas to ensure a proper milieu for digestion and absorption of macronutrients and inhibits gastric emptying. Beyond these well-characterized gastrointestinal functions, secretin exhibits metabolic control functions, such as stimulation of lipolysis in white adipocytes (Sekar and Chow, 2014b) and inhibition of food intake (Cheng et al., 2011). The latter anorexigenic action of secretin was reported to depend on the activation of secretin receptors in vagal sensory nerves and melanocortin signaling in the brain (Cheng et al., 2011; Chu et al., 2013). Our study demonstrates that secretin, upon release during eating, directly activates BAT thermogenesis. Secretin executes this thermogenic action by signaling via secretin receptors abundantly expressed in brown adipocytes. The BAT activation function of secretin is conserved in human. This BAT activation by secretin is essential for the acute satiating effect of secretin. This link between secretin-induced BAT thermogenesis and satiation is underlined by the observed negative correlation of food intake and meal-associated rise in iBAT temperature. We thereby assign a new metabolic control function to secretin as an endocrine activator of prandial thermogenesis in BAT. We propose that the nutritional status encoded by the meal-induced rise in blood secretin levels is directly transformed into thermogenic activity of BAT, which relays this information to the brain and promotes satiation. This establishes a yet unknown endocrine gut-secretin-BAT-brain axis with major implications for integrative energy balance physiology.

Please cite this article in press as: Li et al., Secretin-Activated Brown Fat Mediates Prandial Thermogenesis to Induce Satiation, Cell (2018), https://doi.org/10.1016/j.cell.2018.10.016

Cell

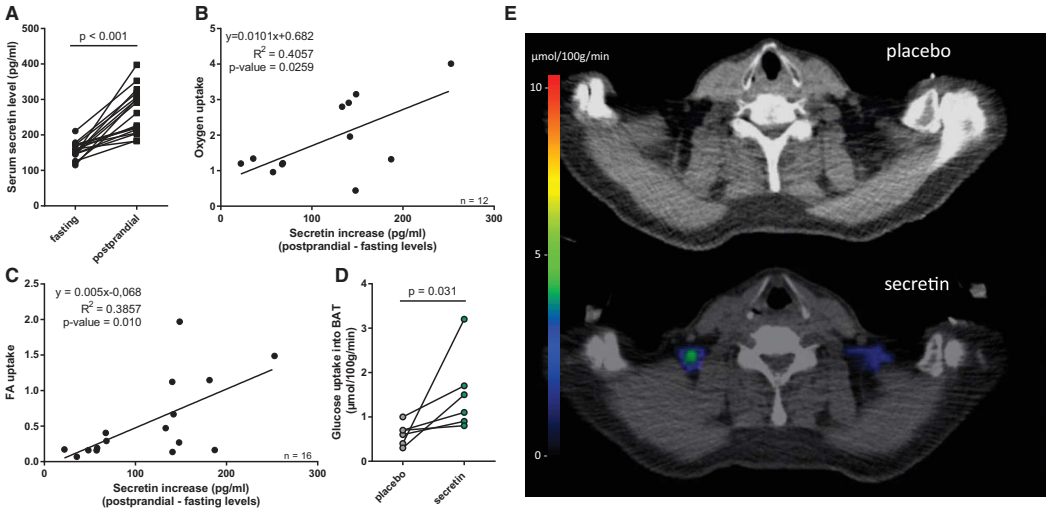

Figure 6. Secretin Increases Glucose Uptake in Human BAT

(A–C) Serum secretin level upon a single meal ingestion in humans (n = 17). Correlation upon meal ingestion of serum secretin levels and postprandial oxygen (B) and fatty acid uptake (C) in BAT, respectively.

(D) Effect of secretin infusion on glucose uptake in human BAT compared to placebo (n = 6).

(E) Representative parametric PET-CT image from supraclavicular BAT areas showing increased glucose uptake after secretin infusion.

(A) Parametric paired t test, (D) non-parametric paired t test. See also Figure S6.

Secretin as an Endocrine Mediator of Meal-Associated Thermogenesis

Meal-associated thermogenesis consists of two parts, the obligatory metabolic costs of food handling for ingestion, digestion and absorption (handling thermogenesis) and facultative thermogenesis. The existence of the latter is still debated, including source of thermogenesis (BAT dependent or not), functional significance and potential mediators (Cannon and Nedergaard, 2004; Kozak, 2010). BAT as a heater organ has been suggested as a source for facultative meal-associated thermogenesis (Cannon and Nedergaard, 2004; Kozak, 2010). The general concept of a gut – brain – BAT axis consisted of gastrointestinal hormones being sensed in the brain, either directly or via neural afferent projections increase SNS activity, and stimulate meal-associated thermogenesis by release of norepinephrine in BAT (Bachman et al., 2002). A contribution of such postprandial sympathetic activation to meal-associated thermogenesis is not always evident (Welle et al., 1981). Notably, β-blockade failed to reduce metabolic rate in man during the first 3 hours after a carbohydrate meal (Zwillich et al., 1981) or mixed meal (Thörne and Wahren, 1989), but exerted a significant effect in the period 3-4 hours after the meal (Astrup et al., 1989). It thus appears that while sympathetically mediated thermogenesis in the late postprandial phase cannot be ruled out, the prandial and early postprandial rise in energy expenditure is initiated by mechanisms independent of the SNS. Consistent with this notion, we found that secretin, as a non-sympathetic endocrine activator, mediates prandial thermogenesis, which may explain the non-sympathetically mediated meal-associated thermogenesis. In contrast to previous studies, focused on postprandial thermogenesis or diet-induced thermogenesis mediated by the SNS activation in animals exposed to long term cafeteria/high-fat diets, we here examined the prandial rise in thermogenesis by directly monitoring iBAT temperature. This physiological readout is unbiased by the animal activity as observed by indirect calorimetry. Recording BAT temperature demonstrated that onset of refeeding acutely activated BAT thermogenesis and this acute prandial BAT thermogenesis is largely independent of adrenergic signaling. Therefore, our study revealed a previously unappreciated BAT – derived thermogenesis during the prandial phase that functions as a signal to the brain to terminate a meal.

Secretin-Activated Brown Fat Controls Food Intake

Our findings elucidate a novel molecular mechanism for meal-associated thermogenesis with BAT acting as a peripheral communication hub between the gut and the brain. In a physiological context, one may question why BAT dissipates part of the energy ingested during a meal where no extra heat production is necessary for body-temperature regulation. Integrating thermostatic (Brobeck, 1948) and glucostatic (Mayer, 1953) hypotheses, meal-associated thermogenesis in BAT was suggested to play a key role in thermoregulatory feeding (Himms-Hagen, 1995). However, this concept was not further pursued mostly because the loss of thermogenic function in BAT does not cause hyperphagia in UCP1-KO mice, and the β-blocker propranolol does not increase meal sizes (Cannon and Nedergaard, 2004).

Please cite this article in press as: Li et al., Secretin-Activated Brown Fat Mediates Prandial Thermogenesis to Induce Satiation, Cell (2018), https://doi.org/10.1016/j.cell.2018.10.016

We here reveal that secretin-induced satiation in fasted mice during refeeding depends on the presence of UCP1 and thus on thermogenic BAT function. If BAT relays information on nutritional status to the brain, we suggest that the meal-associated wasting of nutrient energy in BAT, beyond its role in buffering the overwhelming caloric load during feeding, is an inevitable result of this relay function (the cost of a signal). We therefore propose a physiological function of secretin-mediated prandial thermogenesis in the control of satiation. Further evidence compatible with this proposal is provided by our observation that systemic blockade of secretin function not only attenuated the prandial rise in iBAT temperature but also increased food intake. The effect of secretin on thermogenesis and food intake were absent in UCP1-KO mice. In addition, these mice showed a drastic alteration in meal patterning, with longer bouts of feeding indicating a delayed perception of satiation compared to WT mice. These findings consolidate the existence of a gut-secretin-BAT-brain axis involved in the regulation of satiation. Similar to UCP1-KO mice, secretin and SCTR germline KO mice are not hyperphagic but display normal body weight and food intake (Cheng et al., 2011; Sekar and Chow, 2014a). Disruption of the proposed gut-secretin-BAT-brain axis in the control of satiation is apparently compensated by other anorexigenic pathways preventing long-term disturbances of energy balance, as exemplified by the mild metabolic phenotypes (eat normally and maintain the same body weight as WT mice) of several gut hormone and gut hormone receptor KO mice, such as ghrelin KO mice, CCK and its receptor KO mice, and GLP-1 and its receptor KO mice, highlighting the extensive compensatory mechanisms occurring *in vivo* (see review in Strader and Woods [2005]). However, meal patterning, which is altered in UCP1-KO mice, has not been studied in secretin- and SCTR-deficient mouse models so far. It is highly likely that these germline KO mouse models compensate for increased meal size by initiating fewer meals and thereby maintain body weight due to the interaction between long-term energy homeostasis and meal-related satiation signals. In this scenario, tissue-specific ablation of UCP1, secretin, and SCTR in the adult stage is required to further explore our hypothesis.

Brown Fat Relays Nutritional Status to the Brain

Gut hormones play a critical role in relaying signals of nutritional and energy status from the gut to the central nervous system in order to regulate food intake. Canonically, satiation signals reach the brain either directly via the blood (e.g., amylin and ghrelin) or indirectly by activation of vagal afferent nerves in the intestine (e.g., CCK and GLP-1). In our study, the common satiating effect evoked by secretin and CL indicates that meal termination by BAT-derived heat production is another alternative general mechanism. The hypothalamus and brainstem harbor metabolic sensors, which play a central role in the control of hunger and satiation. Therefore, the meal-termination signal that encodes the nutritional status must be relayed from BAT to the brain. Consistent with this notion, secretin treatment increases anorectic neuropeptide expression in hypothalamic nuclei (Cheng et al., 2011). Our study further demonstrated that the modulatory effects of secretin on feeding-related neuropeptides were UCP1 dependent, consolidating the essential role of BAT thermogenesis in mediating the satiation effect of secretin. Regarding communication between BAT and said brain regions, it is most likely that a rise in local brain temperature caused by BAT thermogenesis represents the key signal inducing satiation. This view is supported by a classical study demonstrating a rise in temperature in the preoptic hypothalamic area during feeding in rats, where a strong positive correlation was found between the maximal temperature rise in the hypothalamus and the duration of feeding (Abrams and Hammel, 1964). And there is further evidence that BAT thermogenesis contributes to increases in body and brain temperature under *ad libitum* condition (Blessing et al., 2013). A very recent report found a subpopulation of POMC neurons expressing the temperature-sensitive ion channel, TRPV1, which can directly sense local changes in brain temperature. Slight increases in body temperature in response to exercise caused a TRPV1-dependent increase in the activity of POMC neurons, which suppressed feeding in mice (Jeong et al., 2018). Consistent with this scenario, we discovered that secretin treatment altered *Trpv1* transcript abundance in the hypothalamus of WT but not UCP1-KO mice. Despite our data indicating heat as a signal, other possibilities such as neuronal or endocrine mechanisms cannot be excluded. Secretin-induced release of adipokines (batokines) or neuronal afferent signaling may alter melanocortin signaling in the hypothalamus. In fact, it has been postulated that afferent sensory nerves in BAT sense the thermal status, blood flow, or intracellular lipolytic products and hence regulate BAT thermogenesis via efferent SNS output (Bartness et al., 2010). Of note, several hypothalamic nuclei such as the paraventricular nucleus, dorsomedial hypothalamus, and lateral hypothalamus receive sensory inputs from fat depots, pointing toward a sensory feedback mechanism (Ryu et al., 2015). This alternative or complementary pathway of BAT-brain communication along the gut-secretin-BAT-brain axis is supported by the observation that the anorexigenic action of secretin depends on afferent sensory nerves (Chu et al., 2013). Further studies are warranted to dissect the contributions of these potential mechanisms. In any case, demonstration of a non-canonical role of BAT in relaying nutritional status to brain beyond the canonical gut-vagal nerve-brain axis uncovers a yet unknown facet of the complex regulatory system that contributes to the termination of feeding.

Meal-Related Satiation Signal and Long-Term Adiposity

Despite the ability of some gastrointestinal hormones such as CCK in previous studies and secretin in our study to reliably reduce meal size when administered prior to a meal, their repeated administration is largely ineffective in reducing food intake and body weight, mainly due to increased feeding frequency to compensate for the suppressed meal size. Thus, orchestration of gut-derived satiation and satiety signals contributes to the maintenance of a relatively constant level of body fat/weight, possibly through interaction with long-term adiposity-related signals (leptin and insulin). This accounted for the negligible effect of chronic secretin infusion to suppress body weight as compared to the pronounced effect of a GLP1 analog with its dual function of both satiation and satiety signal. Indeed, suppression of food intake induced by the GLP-1 analog arises from a combination of reduced meal size and

Please cite this article in press as: Li et al., Secretin-Activated Brown Fat Mediates Prandial Thermogenesis to Induce Satiation, Cell (2018), https://doi.org/10.1016/j.cell.2018.10.016

Cell

increased inter-meal interval (Williams et al., 2009). In murine model systems with *ad libitum* access to food, gut-hormone-based therapies require targeting both satiation and satiety in an effort to alter energy homeostasis. In a setting closer resembling the human meal pattern, however (i.e., three 30-min meals per day), laboratory rats could not compensate for the satiating effect of the peptide and consequently lost weight (West et al., 1982). Presence or absence of an altered systemic energy balance thus remains to be determined in man.

Together, these data demonstrate secretin-activated brown fat to be a hub for satiation signaling to reduce meal size and initiate meal termination. Brown adipose tissue thermogenesis thus constitutes a unique target mechanism to manipulate both energy expenditure and energy intake.

Future Perspectives

Research addressing the (patho-) physiological relevance of BAT is concentrating on thermogenesis and the capacity to increase resting metabolic rate. Based on the results of our study, however, the view of BAT as a mere catabolic heater organ must be revised, and more attention needs to be directed toward the function of BAT in the control of hunger and satiation. Several reports demonstrated that glucose and fatty acid uptake in BAT is increased in rodents and humans exposed to a single meal and that maximal thermogenesis coincides with meal termination (Blessing et al., 2013; Glick et al., 1981; U Din et al., 2018; Vosselman et al., 2013), but there has been a lack of experimental proof for a role of BAT thermogenesis in the control of food intake. According to our data, any stimulus that activates BAT thermogenesis could potentially induce satiation. Targeting this mechanism by nutritional or pharmacological interventions such as enforcing or stimulating the transient meal-associated surge of secretin secretion may provide novel treatment options. In conclusion, we demonstrate that BAT regulates energy intake. Activation of the gut-BAT-brain axis not only increases energy expenditure but also promotes satiation, therefore qualifying this physiological mechanism as an attractive, peripheral target for the treatment of obesity.

STAR★METHODS

Detailed methods are provided in the online version of this paper and include the following:

- KEY RESOURCES TABLE
- CONTACT FOR REAGENT AND RESOURCE SHARING
- EXPERIMENTAL MODEL AND SUBJECT DETAILS
  - Animals
  - Primary cell culture
  - Human study
- METHOD DETAILS
  - RNA-sequencing
  - Western Blot
  - Gene expression analysis (qRT–PCR)
  - Respiration assays
  - Surgical implantation of telemetry transmitters
  - Monitoring of food intake and iBAT temperature
  - Indirect calorimetry
  - Macroscopic multi-spectral optoacoustic tomography (MSOT) combined with indirect calorimetry
  - Analysis of food intake data
  - Measurement of plasma secretin concentrations
  - Hypothalamic neuropeptides gene expression analysis
  - Diet-induced obese mice study
  - Dual luciferase reporter assay
- QUANTIFICATION AND STATISTICAL ANALYSIS
- DATA AND SOFWARE AVAILABILITY

SUPPLEMENTAL INFORMATION

Supplemental Information includes six figures and can be found with this article online at https://doi.org/10.1016/j.cell.2018.10.016.

ACKNOWLEDGMENTS

This work was supported by grants to M.K. from the Deutsche Forschungsgemeinschaft (DFG) (KL973/11&12 and RTG1482) and the Else Kröner-Fresenius-Stiftung. K.S. and S.-M.G. were fellows in the DFG Research Training Group RTG1482. V.N. was funded by the DFG (Leibniz Prize 2013; NT 3/10-1) and the European Research Council (grant agreement 694968). PET studies were conducted at the Finnish CoE in Cardiovascular and Metabolic Diseases with support from Academy of Finland (259926, 265204, 292839, and 269977), University of Turku, Turku University Hospital, Åbo Akademi University, and European Union (EU FP7 project 278373; DIABAT). Thanks to Sabine Mocek (TUM), Uwe Klemm (IBMI), and Sarah Glasl (IBMI) for excellent technical assistance and Gael Diot for advice on data analysis. The images used for graphical abstract construction were purchased from Fotolia (© benchart, Alexander Pokusay, ychty/Fotolia.com).

AUTHOR CONTRIBUTIONS

Y.L. and K.S. contributed equally to this study. Y.L., K.S., F.B., and M.K. conceived and designed the study. Y.L. found UCP1 activation property of secretin and provided key visions of the study. K.S. established methods. K.S., S.-M.G., A.B.-H., and Y.L. performed experiments. K.S. analyzed data. M.W., J.R., A.K., and V.N. performed the MSOT analysis. S.L., M.L., M.D., K.A.V., and P.N. performed the human experiments. T.C., L.S.O., and J.A.-F. performed the DIO experiments. T.F. provided the RNA-seq data and helped with MATLAB analysis. Y.L., K.S., and M.K. wrote the manuscript. All authors read and approved the manuscript.

DECLARATION OF INTERESTS

The Technical University of Munich has applied for a patent. T.C., L.S.O., and J.A.-F. were employees from Eli Lilly and Company.

Received: March 14, 2018
Revised: August 6, 2018
Accepted: October 2, 2018
Published: November 15, 2018

REFERENCES

Abrams, R., and Hammel, H.T. (1964). Hypothalamic temperature in unanesthetized albino rats during feeding and sleeping. Am. J. Physiol. *206*, 641–646.

Afroze, S., Meng, F., Jensen, K., McDaniel, K., Rahal, K., Onori, P., Gaudio, E., Alpini, G., and Glaser, S.S. (2013). The physiological roles of secretin and its receptor. Ann. Transl. Med. *1*, 29.

Astrup, A., Simonsen, L., Bülow, J., Madsen, J., and Christensen, N.J. (1989). Epinephrine mediates facultative carbohydrate-induced thermogenesis in human skeletal muscle. Am. J. Physiol. *257*, E340–E345.

Please cite this article in press as: Li et al., Secretin-Activated Brown Fat Mediates Prandial Thermogenesis to Induce Satiation, Cell (2018), https://doi.org/10.1016/j.cell.2018.10.016

Bachman, E.S., Dhillon, H., Zhang, C.Y., Cinti, S., Bianco, A.C., Kobilka, B.K., and Lowell, B.B. (2002). betaAR signaling required for diet-induced thermogenesis and obesity resistance. Science *297*, 843–845.

Bartness, T.J., Vaughan, C.H., and Song, C.K. (2010). Sympathetic and sensory innervation of brown adipose tissue. Int. J. Obes. *34* (*Suppl 1*), S36–S42.

Bayliss, W.M., and Starling, E.H. (1902). The mechanism of pancreatic secretion. J. Physiol. *28*, 325–353.

Beiroa, D., Imbernon, M., Gallego, R., Senra, A., Herranz, D., Villarroya, F., Serrano, M., Fernø, J., Salvador, J., Escalada, J., et al. (2014). GLP-1 agonism stimulates brown adipose tissue thermogenesis and browning through hypothalamic AMPK. Diabetes *63*, 3346–3358.

Berbée, J.F., Boon, M.R., Khedoe, P.P., Bartelt, A., Schlein, C., Worthmann, A., Kooijman, S., Hoeke, G., Mol, I.M., John, C., et al. (2015). Brown fat activation reduces hypercholesterolaemia and protects from atherosclerosis development. Nat. Commun. *6*, 6356.

Blessing, W., Mohammed, M., and Ootsuka, Y. (2013). Brown adipose tissue thermogenesis, the basic rest-activity cycle, meal initiation, and bodily homeostasis in rats. Physiol. Behav. *121*, 61–69.

Blondin, D.P., Daoud, A., Taylor, T., Tingelstad, H.C., Bézaire, V., Richard, D., Carpentier, A.C., Taylor, A.W., Harper, M.E., Aguer, C., and Haman, F. (2017). Four-week cold acclimation in adult humans shifts uncoupling thermogenesis from skeletal muscles to brown adipose tissue. J. Physiol. *595*, 2099–2113.

Blondin, D.P., Labbé, S.M., Tingelstad, H.C., Noll, C., Kunach, M., Phoenix, S., Guérin, B., Turcotte, E.E., Carpentier, A.C., Richard, D., and Haman, F. (2014). Increased brown adipose tissue oxidative capacity in cold-acclimated humans. J. Clin. Endocrinol. Metab. *99*, E438–E446.

Blouet, C., and Schwartz, G.J. (2012). Duodenal lipid sensing activates vagal afferents to regulate non-shivering brown fat thermogenesis in rats. PLoS ONE *7*, e51898.

Braun, K., Oeckl, J., Westermeier, J., Li, Y., and Klingenspor, M. (2018). Non-adrenergic control of lipolysis and thermogenesis in adipose tissues. J. Exp. Biol. *221*. https://doi.org/10.1242/jeb165381.

Brobeck, J.R. (1948). Food intake as a mechanism of temperature regulation. Yale J. Biol. Med. *20*, 545–552.

Cannon, B., and Nedergaard, J. (2004). Brown adipose tissue: function and physiological significance. Physiol. Rev. *84*, 277–359.

Chaudhri, O., Small, C., and Bloom, S. (2006). Gastrointestinal hormones regulating appetite. Philos. Trans. R. Soc. Lond. B Biol. Sci. *361*, 1187–1209.

Cheng, C.Y., Chu, J.Y., and Chow, B.K. (2011). Central and peripheral administration of secretin inhibits food intake in mice through the activation of the melanocortin system. Neuropsychopharmacology *36*, 459–471.

Chondronikola, M., Volpi, E., Børsheim, E., Porter, C., Annamalai, P., Enerbäck, S., Lidell, M.E., Saraf, M.K., Labbe, S.M., Hurren, N.M., et al. (2014). Brown adipose tissue improves whole-body glucose homeostasis and insulin sensitivity in humans. Diabetes *63*, 4089–4099.

Chu, J.Y., Cheng, C.Y., Sekar, R., and Chow, B.K. (2013). Vagal afferent mediates the anorectic effect of peripheral secretin. PLoS ONE *8*, e64859.

Curtis, P.J., Fender, H.R., Rayford, P.L., and Thompson, J.C. (1976). Disappearance half-time of endogenous and exogenous secretin in dogs. Gut *17*, 595–599.

Dicker, A., Zhao, J., Cannon, B., and Nedergaard, J. (1998). Apparent thermogenic effect of injected glucagon is not due to a direct effect on brown fat cells. Am. J. Physiol. *275*, R1674–R1682.

Dong, M., Te, J.A., Xu, X., Wang, J., Pinon, D.I., Storjohann, L., Bordner, A.J., and Miller, L.J. (2011). Lactam constraints provide insights into the receptor-bound conformation of secretin and stabilize a receptor antagonist. Biochemistry *50*, 8181–8192.

Fischer, A.W., Cannon, B., and Nedergaard, J. (2018). Optimal housing temperatures for mice to mimic the thermal environment of humans: An experimental study. Mol. Metab. *7*, 161–170.

Glick, Z. (1982). Inverse relationship between brown fat thermogenesis and meal size: the thermostatic control of food intake revisited. Physiol. Behav. *29*, 1137–1140.

Glick, Z., Teague, R.J., and Bray, G.A. (1981). Brown adipose tissue: thermic response increased by a single low protein, high carbohydrate meal. Science *213*, 1125–1127.

Grujic, D., Susulic, V.S., Harper, M.E., Himms-Hagen, J., Cunningham, B.A., Corkey, B.E., and Lowell, B.B. (1997). Beta3-adrenergic receptors on white and brown adipocytes mediate beta3-selective agonist-induced effects on energy expenditure, insulin secretion, and food intake. A study using transgenic and gene knockout mice. J. Biol. Chem. *272*, 17686–17693.

Hanssen, M.J., Hoeks, J., Brans, B., van der Lans, A.A., Schaart, G., van den Driessche, J.J., Jörgensen, J.A., Boekschoten, M.V., Hesselink, M.K., Havekes, B., et al. (2015). Short-term cold acclimation improves insulin sensitivity in patients with type 2 diabetes mellitus. Nat. Med. *21*, 863–865.

Himms-Hagen, J. (1995). Role of brown adipose tissue thermogenesis in control of thermoregulatory feeding in rats: a new hypothesis that links thermostatic and glucostatic hypotheses for control of food intake. Proc. Soc. Exp. Biol. Med. *208*, 159–169.

Jeong, J.H., Lee, D.K., Liu, S.M., Chua, S.C., Jr., Schwartz, G.J., and Jo, Y.H. (2018). Activation of temperature-sensitive TRPV1-like receptors in ARC POMC neurons reduces food intake. PLoS Biol. *16*, e2004399.

Klingenspor, M. (2003). Cold-induced recruitment of brown adipose tissue thermogenesis. Exp. Physiol. *88*, 141–148.

Kozak, L.P. (2010). Brown fat and the myth of diet-induced thermogenesis. Cell Metab. *11*, 263–267.

Li, Y., Fromme, T., and Klingenspor, M. (2017). Meaningful respirometric measurements of UCP1-mediated thermogenesis. Biochimie *134*, 56–61.

Li, Y., Fromme, T., Schweizer, S., Schöttl, T., and Klingenspor, M. (2014). Taking control over intracellular fatty acid levels is essential for the analysis of thermogenic function in cultured primary brown and brite/beige adipocytes. EMBO Rep. *15*, 1069–1076.

Maurer, S.F., Fromme, T., Grossman, L.I., Hüttemann, M., and Klingenspor, M. (2015). The brown and brite adipocyte marker Cox7a1 is not required for non-shivering thermogenesis in mice. Sci. Rep. *5*, 17704.

Mayer, J. (1953). Glucostatic mechanism of regulation of food intake. N. Engl. J. Med. *249*, 13–16.

Rampone, A.J., and Reynolds, P.J. (1991). Food intake regulation by diet-induced thermogenesis. Med. Hypotheses *34*, 7–12.

Reber, J., Willershäuser, M., Karlas, A., Paul-Yuan, K., Diot, G., Franz, D., Fromme, T., Ovsepian, S.V., Bézière, N., Dubikovskaya, E., et al. (2018). Non-invasive Measurement of Brown Fat Metabolism Based on Optoacoustic Imaging of Hemoglobin Gradients. Cell Metab. *27*, 689–701.e4.

Rosen, E.D., and Spiegelman, B.M. (2006). Adipocytes as regulators of energy balance and glucose homeostasis. Nature *444*, 847–853.

Rothwell, N.J., and Stock, M.J. (1979). A role for brown adipose tissue in diet-induced thermogenesis. Nature *281*, 31–35.

Ryu, V., Garretson, J.T., Liu, Y., Vaughan, C.H., and Bartness, T.J. (2015). Brown adipose tissue has sympathetic-sensory feedback circuits. J. Neurosci. *35*, 2181–2190.

Saito, M. (2013). Brown adipose tissue as a regulator of energy expenditure and body fat in humans. Diabetes Metab. J. *37*, 22–29.

Sekar, R., and Chow, B.K. (2014a). Secretin receptor-knockout mice are resistant to high-fat diet-induced obesity and exhibit impaired intestinal lipid absorption. FASEB J. *28*, 3494–3505.

Sekar, R., and Chow, B.K.C. (2014b). Lipolytic actions of secretin in mouse adipocytes. J. Lipid Res. *55*, 190–200.

Sidossis, L., and Kajimura, S. (2015). Brown and beige fat in humans: thermogenic adipocytes that control energy and glucose homeostasis. J. Clin. Invest. *125*, 478–486.

Strader, A.D., and Woods, S.C. (2005). Gastrointestinal hormones and food intake. Gastroenterology *128*, 175–191.

Please cite this article in press as: Li et al., Secretin-Activated Brown Fat Mediates Prandial Thermogenesis to Induce Satiation, Cell (2018), https://doi.org/10.1016/j.cell.2018.10.016

Cell

Susulic, V.S., Frederich, R.C., Lawitts, J., Tozzo, E., Kahn, B.B., Harper, M.E., Himms-Hagen, J., Flier, J.S., and Lowell, B.B. (1995). Targeted disruption of the beta 3-adrenergic receptor gene. J. Biol. Chem. *270*, 29483–29492.

Thörne, A., and Wahren, J. (1989). Beta-adrenergic blockade does not influence the thermogenic response to a mixed meal in man. Clin. Physiol. *9*, 321–332.

U Din, M., Saari, T., Raiko, J., Kudomi, N., Maurer, S.F., Lahesmaa, M., Fromme, T., Amri, E.Z., Klingenspor, M., Solin, O., et al. (2018). Postprandial Oxidative Metabolism of Human Brown Fat Indicates Thermogenesis. Cell Metab. *28*, 207–216.e3.

Valet, P., Berlan, M., Beauville, M., Crampes, F., Montastruc, J.L., and Lafontan, M. (1990). Neuropeptide Y and peptide YY inhibit lipolysis in human and dog fat cells through a pertussis toxin-sensitive G protein. J. Clin. Invest. *85*, 291–295.

van der Lans, A.A., Hoeks, J., Brans, B., Vijgen, G.H., Visser, M.G., Vosselman, M.J., Hansen, J., Jörgensen, J.A., Wu, J., Mottaghy, F.M., et al. (2013). Cold acclimation recruits human brown fat and increases nonshivering thermogenesis. J. Clin. Invest. *123*, 3395–3403.

Virtanen, K.A., Lidell, M.E., Orava, J., Heglind, M., Westergren, R., Niemi, T., Taittonen, M., Laine, J., Savisto, N.J., Enerbäck, S., and Nuutila, P. (2009). Functional brown adipose tissue in healthy adults. N. Engl. J. Med. *360*, 1518–1525.

Vosselman, M.J., Brans, B., van der Lans, A.A., Wierts, R., van Baak, M.A., Mottaghy, F.M., Schrauwen, P., and van Marken Lichtenbelt, W.D. (2013). Brown adipose tissue activity after a high-calorie meal in humans. Am. J. Clin. Nutr. *98*, 57–64.

Welle, S., Lilavivat, U., and Campbell, R.G. (1981). Thermic effect of feeding in man: increased plasma norepinephrine levels following glucose but not protein or fat consumption. Metabolism *30*, 953–958.

West, D.B., Williams, R.H., Braget, D.J., and Woods, S.C. (1982). Bombesin reduces food intake of normal and hypothalamically obese rats and lowers body weight when given chronically. Peptides *3*, 61–67.

Williams, D.L., Baskin, D.G., and Schwartz, M.W. (2009). Evidence that intestinal glucagon-like peptide-1 plays a physiological role in satiety. Endocrinology *150*, 1680–1687.

Yoneshiro, T., Aita, S., Matsushita, M., Kayahara, T., Kameya, T., Kawai, Y., Iwanaga, T., and Saito, M. (2013). Recruited brown adipose tissue as an antiobesity agent in humans. J. Clin. Invest. *123*, 3404–3408.

Zwillich, C., Martin, B., Hofeldt, F., Charles, A., Subryan, V., and Burman, K. (1981). Lack of effects of beta sympathetic blockade on the metabolic and respiratory responses to carbohydrate feeding. Metabolism *30*, 451–456.

Please cite this article in press as: Li et al., Secretin-Activated Brown Fat Mediates Prandial Thermogenesis to Induce Satiation, Cell (2018), https://doi.org/10.1016/j.cell.2018.10.016

STAR★METHODS

KEY RESOURCES TABLE

REAGENT or RESOURCE	SOURCE	IDENTIFIER
Antibodies		
anti-Secretin	Phoenix Pharmaceuticals	Cat# G-067-04; RRID: AB_2650428
anti-UCP1	Custom made	N/A
anti-GFP	Thermofischer	Cat# A-11122; RRID: AB_221569
anti-ACTIN	Millipore	Cat# MAB1501; RRID: AB_2223041
anti-SCTR	Sigma-Aldrich	Cat# HPA007269-100UL; RRID: AB_1856640
Bacterial and Virus Strains		
NEB5α competent *E. coli*	NEB	Cat# C2988J
Chemicals, Peptides, and Recombinant Proteins		
Arterenol	Sanofi	1mg/ml
Isobutylmethylxanthine	Sigma-Aldrich	Cat# I5879
Indomethacin	Sigma-Aldrich	Cat# I7378
Dexamethasone	Sigma-Aldrich	Cat# D4902
Insulin	Sigma-Aldrich	Cat# I9278-5ML
T3	Sigma-Aldrich	Cat# T6397
Propranolol hydrochlorid	Sigma-Aldrich	Cat# P8688
Bovine serum albumin (BSA) Fatty Acid Free	Sigma-Aldrich	Cat# A3803-100G
Isoproterenol	Sigma-Aldrich	Cat# I6504-100MG
Oligomycin	Sigma-Aldrich	Cat# O4876-5mg
Antimycin A	Sigma-Aldrich	Cat# A8674
Collagenase A	Biochrom	Cat# C 1-22
FCCP	Sigma-Aldrich	Cat# C2920-10MG
Secretin	Tocris	Cat# No.1919
H89 dihydrochloride	Tocris	Cat# No.2910
Atglistatin	Gift from Robert Zimmermann (*University of Graz*)	N/A
Hi 76-0079	Gift from Robert Zimmermann (*University of Graz*)	N/A
SensiMix SYBR no Rox	BioLine	Cat# QT650-20
DMEM	Sigma-Aldrich	Cat# D5796
Fetal bovine serum (FBS)	Biochrom	Cat# S0615
TRISure	Bioline	Cat# BIO-38033
Human secretin	This study	N/A
Modified human secretin analog	This study	N/A
GLP1 analog (CEX51)	This study	N/A
Critical Commercial Assays		
SV Total RNA Isolation System	Promega	Cat# Z3105
Pierce BCA Protein Assay Kit	Pierce	Cat# PI-23225
SensiFast cDNA Synthesis Kit	BioLine	Cat# BIO-65054
SensiMix Sybr no Rox	BioLine	Cat# QT650-20
Secretin ELISA kit	Cloud-clone	Cat# CEB075Mu, CEB075Hu
Dual luciferase reporter assay	Promega	Cat# E1960
Seahorse XF96 fluxPak	Seahorse Bioscience	Cat# 102310-001
TruSeq Stranded Total RNA Library Prep Kit	Illumina	Cat# RS-122-2102

(*Continued on next page*)

Please cite this article in press as: Li et al., Secretin-Activated Brown Fat Mediates Prandial Thermogenesis to Induce Satiation, Cell (2018), https://doi.org/10.1016/j.cell.2018.10.016

Cell

Continued

REAGENT or RESOURCE	SOURCE	IDENTIFIER
Deposited Data		
Brown fat RNA-seq data	This paper	GEO: GSE119452, GSM3374837, GSM3374838, GSM3374839, GSM3374840
Experimental Models: Cell Lines		
HEK293	DSMZ	Cat# ACC 305
Primary murine brown and white cells	This paper	N/A
Experimental Models: Organisms/Strains		
Mouse: C57BL/6J	Jackson Laboratory	JAX Stock No:000664
Mouse: 129S-Ucp1^{tm1Kz}/J	Jackson Laboratory	JAX Stock No:017476
Mouse: 129S6/SvEVTac	Taconic Biosciences	129SVE
Mouse: Athymic Nude-Foxn1^{nu}	Envigo	Athymic Nude-*Foxn1*^{nu}
Oligonucleotides		
siRNA targeting sequence: SctR #1: CCUGCUGAUCCCUCUCUUU	This paper	N/A
siRNA targeting sequence: SctR #2: CCCUGUCCAACUUCAUCAA	This paper	N/A
siRNA targeting sequence: SctR #3: CCAUCGUGAUCAAUUUCAU	This paper	N/A
Primers for qPCR, see detailed methods	This paper	N/A
Recombinant DNA		
pCMV-murine SCTR expressing vector	This paper	N/A
pAD-CRE luciferase reporter vector	This paper	N/A
phRG-B-Renilla luciferase vector	Promega	Cat# E6281
Software and Algorithms		
GraphPad Prism 6	Graphpad Software	N/A
Genomatix Software Suite	Genomatix AG	N/A
MATLAB	Mathsworks	N/A
Other		
TSE LabMaster	TSE Systems	N/A
FoxBox	Sable Systems	N/A
G2 E-Mitter	Starr Life Sciences	N/A
MSOT imaging system inVision 256-TF	iThera Medical GmbH	N/A
XF96 Extracellular Flux Analyzer	Seahorse Bioscience	N/A
ER4000 Energizer/Receiver	Starr Life Sciences	N/A
Lightcycler II	Roche	N/A

CONTACT FOR REAGENT AND RESOURCE SHARING

Further information and requests for resources and reagents should be directed to and will be fulfilled by the Lead Contact, Martin Klingenspor (mk@tum.de).

EXPERIMENTAL MODEL AND SUBJECT DETAILS

Animals

Animal experiments were approved by the German animal welfare authorities at the district government (approval no. 55.2-1-54-2532-34-2016 and 55.2-1-54-2532-123-2013). Mice were bred at the specific-pathogen free animal facility of Technical University of Munich. They had *ad libitum* access to food and water and were maintained at 22 ± 1°C and 50%–60% relative humidity in a 12 h:12 h light:dark cycle. Male 129S6/SvEv mice, aged 5 to 6 wk were used for primary cultures of brown and white adipocytes. Male C57BL/6J, male C57BL6/N mice, male 129S1/SvImJ mice (UCP1-KO mice and wild-type littermates) and male 129S6/SvEV

Please cite this article in press as: Li et al., Secretin-Activated Brown Fat Mediates Prandial Thermogenesis to Induce Satiation, Cell (2018), https://doi.org/10.1016/j.cell.2018.10.016

were used for the *in vivo* experiments. Athymic female Nude-Foxn1^{nu} mice, aged 13 wk at the beginning of the experiments were obtained from Envigo and kept at 24 ± 1°C with *ad libitum* access to food and water at the Helmholtz Zentrum München.

Primary cell culture

Adipose tissues were dissected from 5 week-old 129S6/SvEV mice or 129S1/SvImJ mice (UCP1-KO mice and wild-type littermates) (n = 2 per experiment, pooled) and digested with collagenase as described previously (Li et al., 2014). Floating mature adipocytes were harvested for gene expression analysis. Stromal vascular fraction (SVF) cells were either harvested or plated in 12-well plates, and adherent cells were grown to confluence. Cells were differentiated into adipocytes as previously described. Briefly, cells were cultured for 2 days with 5 μg/ml insulin, 1 nM 3,3′,5-triiodo-l-thyronine (T3), 125 μM indomethacin, 0.5 mM isobutylmethylxanthine (IBMX) and 1 μM dexamethasone in adipocyte culture media (DMEM supplemented with 10% heat-inactivated FBS, penicillin/streptomycin). Cells were then maintained in adipocyte culture media supplemented with 5 μg/ml insulin and 1 nM T3 for 6 days, with fresh media replacement every 2 days. Cells were harvested on day 7 with or without 6h secretin (500nM) treatment in TRISure.

Human study

Human experiments were performed in Turku PET Centre in Finland as part of two separate PET/CT imaging study cohorts. The ethical committee of South-Western Finland Hospital District evaluated and approved the studies, and all participants gave their written informed consent before any study procedures (Clinical trial number: NCT03290846).

Serum secretin levels were measured in seventeen healthy volunteers (13 females and 4 males; 36.3 ± 9.5 years; BMI 27.2 ± 2.9), who participated in a study where post-prandial BAT oxygen consumption and fatty acid uptake were measured using 15O-O2 and 18F-FTHA PET/CT, respectively. Blood samples for secretin measurement were drawn at baseline (overnight fasting) and 30-40 minutes after completing a mixed meal consisting of 542 kcal (58% carbohydrates, 25% fat, 17% protein). Concurrent dynamic PET imaging of supraclavicular and upper thoracic region was performed during postprandial state.

Effects of secretin on BAT glucose metabolism was evaluated in a separate group of lean, healthy males (n = 7, mean age 46.6 ± 11.9 years; mean BMI 23.7 ± 2.0). Studies were done twice, after two short intravenous infusions of secretin hydrochloride (Secrelux, 1IU/kg each) or saline (placebo) using single-blinded randomization. Dynamic PET-CT scans of the neck area, were done using 18F-FDG and analyzed as described earlier (Virtanen et al., 2009).

METHOD DETAILS

RNA-sequencing

Total RNA isolated from BAT samples of male C57BL/6J mice (n = 4) housed under room temperature (23°C) was applied to transcriptome analysis by next generation sequencing (RNA-Seq) using Illumina HiSeq 2500 platform (Illumina). Sequencing libraries were prepared using the TruSeq RNA Sample Prep kit v2 (Illumina). Libraries from 4 samples were pooled into one sequencing lane and sequenced using a 50-cycle TruSeq SBS Kit v3-HS (Illumina), resulting in a depth of > 25 million reads/sample. Sequenced tags were aligned to the Ensembl 75 transcriptome annotation (NCBI38/mm10 mouse genome) using Genomatix Software Suite. All genes and transcripts were assigned relative coverage rates as measured in RPKM units ('reads per kilobase per million mapped reads').

Western Blot

For western blot analysis, cells were lysed in RIPA buffer. 30μg of total-cell lysates were separated on 12.5% SDS-PAGE gels, transferred to PVDF membrane (Millipore) by using a Trans-Blot SD. Semi-Dry Transfer Cell (Bio-Rad), and probed with anti-UCP1 (1:10,000), anti-ACTIN (Millipore, 1:10,000) and anti-SCTR (Sigma, 1:300). Secondary antibodies conjugated to IRDye 680 or IRDye 800 (Li-Cor Biosciences) were incubated at a dilution of 1:20,000. Fluorescent images were captured by an Odyssey fluorescent imager (Li-Cor Biosciences).

Gene expression analysis (qRT–PCR)

RNA was extracted from cultured cells or frozen tissue samples (129S6/SvEV) using TRIsure, purified with SV Total RNA Isolation System, Promega and reverse transcribed using SensiFAST cDNA Synthesis Kit (BIOLINE). The resultant cDNA was analyzed by qRT–PCR. Briefly, 1 μL of 1:10 diuluted cDNA and 400 nmol of each primer were mixed with SensiMix SYBR Master Mix No-ROX (Bioline). Reactions were performed in 384-well format using a lightcycler II instrument (Roche). Standard reactions containing serial diluted pooled cDNA of all samples (Pure, 1:2, 1:4, 1:8, 1:16, 1:32 and 1:64) as a template were used to establish a standard curve, from which gene expression levels of samples were calculated. The RNA abundance of each gene was normalized to a housekeeping gene *Gtf2b*. The following primers were used:

Ucp1 F: 5′-GTACACCAAGGAAGGACCGA-3′, R: 5′-TTTATTCGTGGTCTCCCAGC-3′;
Sctr F: 5′-ATGCACCTGTTTGTGTCCTT-3′, R: 5′-TAGTTGGCCATGATGCAGTA-3′;
Gtf2b F: 5′-TGGAGATTTGTCCACCATGA-3′, R: 5′-GAATTGCCAAACTCATCAAAACT-3′;
Pref1 F: 5′-AGTACGAATGCTCCTGCACAC-3′, R: 5′-CTGGCCCTCATCATCCAC-3′;
Fgf21 F: 5′-AGATCAGGGAGGATGGAACA-3′, R: 5′-TCAAAGTGAGGCGATCCATA-3′;

Please cite this article in press as: Li et al., Secretin-Activated Brown Fat Mediates Prandial Thermogenesis to Induce Satiation, Cell (2018), https://doi.org/10.1016/j.cell.2018.10.016

Fabp4 F: 5′-GATGGTGACAAGCTGGTGGT-3′, R: 5′-TTTATTTAATCAACATAACCATATCCA-3′;
PGC1a F: 5′-GGACGGAAGCAATTTTTCAA-3′, R: 5′-GAGTCTTGGGAAAGGACACG-3′;
Dio2 F: 5′-TGTCTGGAACAGCTTCCTCC-3′, R: 5′-AGTGAAAGGTGGTCAGGTGG-3′;
Pparg F: 5′-TCAGCTCTGTGGACCTCTCC −3′, R: 5′-ACCCTTGCATCCTTCACAAG-3′;
Agrp F: 5′-GTCTAAGTCTGAATGGCCTCAAG-3′, R: 5′-CATCCATTGGCTAGGTGCGAC-3′;
Pomc F: 5′-CCCTCCTGCTTCAGACCTC-3′, R: 5′-CGTTGCCAGGAAACACGG-3′;
Npy F: 5′-CTGACCCTCGCTCTATCTCTGC-3′ R: 5′-CCATCACCACATGGAAGGGTCT-3′
Cart F: 5′-CGAGCCCTGGACATCTACTCTG-3′ R: 5′-TCTTTGCACACACACCAACACC-3′
Bdnf F: 5′-TGGTATGACTGTGCATCCCAGG-3′ R: 5′-TCACCCGGGAAGTGTACAAGTC-3′
Pacap F: 5′-ACCAATGACCATGTGTAGCGGA-3′ R: 5′-CCATTTGTTTTCGGTAGCGGCT-3′
Trpv-1 F: 5′-ATCTTCACCACGGCTGCTTACT-3′ R: 5′-TCCTTGCGATGGCTGAAGTACA-3′

Respiration assays

The cellular oxygen consumption rate (OCR) of primary adipocytes was determined using an XF96 Extracellular Flux Analyzer (Seahorse Bioscience) as described previously (Li et al., 2014). Briefly, primary adipocytes were cultured and differentiated in XF96 microplates. At day 7 of differentiation, cells were washed once with prewarmed, unbuffered assay medium (DMEM basal medium supplemented with 25 mM glucose, 31 mM NaCl, 2 mM GlutaMax and 15 mg/l phenol red, pH 7.4) (basal assay medium) and then the medium was replaced with basal assay medium containing 1%–2% essentially fatty acid free bovine serum albumin (BSA), and incubated at 37°C in a room air incubator for 1 h. The drug injections ports of the sensor cartridges were loaded with the assay reagents at 10X in basal assay medium (no BSA). Basal respiration was measured in untreated cells. Coupled respiration was inhibited by oligomycin treatment (5 μM). UCP1 mediated uncoupled respiration was determined after isoproterenol or secretin stimulation. Maximum respiratory capacity was assessed after FCCP (Sigma-Aldrich) addition (1 μM). Finally, mitochondrial respiration was blocked by antimycin A (Sigma-Aldrich) (5 μM) treatment and the residual OCR was considered non-mitochondrial respiration. For some experiments, cells were pretreated with 50μM H89 (PKA inhibitor), 1 – 100 μM propranolol (β-adrenergic receptor antagonist), 40 μM Atglistatin (ATGL inhibitor) and 40 μM Hi76-0079 (HSL inhibitor), or reverse transfected with small interfering RNAs (siRNAs) targeting SctR (#1CCUGCUGAUCCCUCUCUUU; #2CCCUGUCCAACUUCAUCAA; #3CCAUCGUGAU CAAUUUCAU) and nontargeting control siRNA (UUUGUAAUCGUC GAUACCC) as described previously (Li et al., 2017) before bioenergetic profiling. Oxygen consumption rates were automatically calculated by the Seahorse XF-96 software. Each experiment was repeated at least 3 times with similar results.

Surgical implantation of telemetry transmitters

To monitor interscapular BAT temperature, telemetry transmitters (G2 E-Mitter, Starr Life Sciences Corp., Oakmont, PA, USA) were implanted above the interscapular BAT in 10-weeks-old 129S6/SvEv mice (n = 24). Mice were anesthetized by combined i.p. injection of medetomidine (0.5 mg/kg), midazolam (5 mg/kg) and fentanyl (0.05 mg/kg). The interscapular region was opened by a small incision and the transmitter was placed above the interscapular BAT pad. The incision was closed with surgical adhesive. Atipamezole (2.5 mg/kg), flumazenil (0.5 mg/kg) and naloxone (1.2 mg/kg) were injected subcutaneously to terminate anesthesia. In addition, mice received 10 mg/kg rimadyl and were singly housed in the post-operative recovery period for 4–5 days.

Monitoring of food intake and iBAT temperature

Food intake (FI) was recorded in individually housed mice using an automated monitoring system (TSE LabMaster Home Cage Activity, Bad Homburg, Germany). The food baskets were connected to high precision balances to record FI. A receiver plate (ER4000 Energizer/Receiver, Oakmont, PA, USA) underneath the cage recorded interscapular BAT temperature (T_{iBAT}) signals of the implanted transmitter. Food basket weight and T_{iBAT} were averaged in 5 min intervals. Mice were habituated to the cages with daily i.p. PBS injections for three days ahead of the experiment start, after which food was removed from the cages at 5pm and mice were fasted for overnight. In the next morning, mice were i.p. injected either PBS or secretin (5 nmol/mouse) and food intake was monitored during the following 72hs. For endogenous secretin blocking experiment, mice were s.c. injected with either anti-GFP or anti- secretin antibody at the time when food was removed. Postprandial secretin serum levels (Figure. 3a) as well as *in vitro* testing results for blocking efficiency of the anti-secretin antibody (Phoenix Pharmaceuticals, G-067-04) (Figure S5) were used to estimate the appropriate concentration of antibody to block endogenous secretin activity during refeeding. Assuming a total blood volume of 2 ml/mouse, 400 pmol anti-secretin antibody were injected per mouse. Propranolol (10mg/kg BW) or PBS was i.p. injected 20 min prior to secretin or PBS in the β-blockage experiment.

Indirect calorimetry

Indirect calorimetry was based on an open respirometer system (LabMaster System; TSE Systems, Bad Homburg, Germany) and was performed as described previously (Maurer et al., 2015). Mice were placed in metabolic cages (3L volume) without food and water, transferred to a climate cabinet (TPK 600, Feutron, Greiz/Germany) preconditioned to 30 °C and connected to the indirect calorimetry setup (Phenomaster, TSE Systems, Bad Homburg/Germany) to measure basal metabolic rate (BMR) during fasting (8:00 am–12:00 pm). The air from the cages was extracted over a period of 1 min every 7 min with a flow rate of 33 l/h, dried in a

Please cite this article in press as: Li et al., Secretin-Activated Brown Fat Mediates Prandial Thermogenesis to Induce Satiation, Cell (2018), https://doi.org/10.1016/j.cell.2018.10.016

cooling trap and analyzed for O_2 content. O_2 consumption [ml/h] was calculated via comparison of the air from the cages with the air from an empty reference cage. BMR [ml O_2/h] was calculated as the lowest mean of three consecutive oxygen consumption values. After BMR measurements, mice were i.p. injected either PBS or secretin (0.5mg/kg) and measured in the calorimetry chamber for about one hour with a high-resolution recording of 10 s intervals at 27 °C to avoid secretin induced hyperthermia. Metabolic rates were converted into heat production (HP [mW] = (4.44+1.43*respiratory exchange ratio)*oxygen consumption [ml/h])).

Macroscopic multi-spectral optoacoustic tomography (MSOT) combined with indirect calorimetry

Real-time multi-spectral optoacoustic tomography (MSOT) mouse measurements were conducted with an MSOT small animal imaging system (inVision 256-TF, iThera Medical GmbH, Munich, Germany) as described previously (Reber et al., 2018). Athymic female Nude-Foxn1^{nu} mice were anesthetized by i.p. injection of 75 mg/kg pentobarbital (Narcoren, Merial GmbH, Germany) and placed in the MSOT system. To induce and image BAT activation, secretin (5 nmol) was administered via a catheter inserted in the mouse tail vein. Before, during, and after the activation period images were acquired at 25 different wavelengths: from 700 nm to 900 nm, with a step increment of 10 nm providing multi-spectral anatomic and functional information in a real-time and label-free mode. In parallel O_2 and CO_2 were analyzed in 1 s intervals using a transportable indirect calorimetry system (FoxBox, Sable Systems International, USA) and later converted into HP. For this compressed air from a bottle was pulled through the MSOT mouse holder with a flow rate of 700ml/min using the pump of the FoxBox. After the mouse holder air was dried by a cooling trap and magnesium perchlorate (Merck KGaA, Germany) and passing a filter (Model 9922-11, Parker Balston) before entering gas analysis. Gas composition of the empty mouse holder was analyzed before and after measuring the mouse and used for drift correction. Drift correction and data analysis was performed with the software ExpeData (ExpeData version 1.1.22, Sable Systems International, USA). HP before reflects the mean of the 5 min interval before injection and HP after the mean maximum HP in a 1 min interval measured after injection. The data analysis for MSOT measurements consisted of the calculation of the total blood volume (TBV = oxygenated hemoglobin (HbO_2) + deoxygenated hemoglobin (Hb)) and the oxygen saturation (SO_2 = HbO_2/TBV).

Analysis of food intake data

Food intake was calculated as first derivative of cumulative food intake obtained from automated monitoring system (TSE LabMaster Home Cage Activity, Bad Homburg, Germany). Food intake greater than 0.005 g and separated by intermeal bout length greater or equal 15 min where defined as meal. Mean meal duration and mean intermeal bout length were calculated as mean of individual means.

Measurement of plasma secretin concentrations

Blood was collected at the time the mouse was killed. Plasma secretin levels were determined by ELISA using the kit purchased from Cloud-Clone following the manufacturer's instructions. Concentrations were calculated using a standard curve generated by secretin standards included in the kit.

Hypothalamic neuropeptides gene expression analysis

Male 129S1/SvImJ mice (UCP1 WT and KO) were fasted overnight and i.p. injected either PBS or secretin (5 nmol/mouse). After 4h of treatment, hypothalamic tissues were dissected, snap-frozen and later subjected to RNA extraction and gene expression analysis. In a second experiment, male 129S6/SvEV mice were fasted overnight and subsequently put into a climate chamber where they were exposed to room temperature or to moderate heat. In case of the heat exposure, environmental temperature has been raised from 34°C to 37°C with one degree per hour resulting in a total exposure time of 4 hours. Afterward hypothalamic tissue and preoptical region were separately dissected followed by the same procedure as in the previous experiment.

Diet-induced obese mice study

All diet-induced obese (DIO) mice studies have been approved by Eli Lilly and Company's Institutional Animal Care and Use Committee.

Human secretin (1-27 amide: HSDGTFTSELSRLREGARLQRLLQGLV-amide; native secretin) and modified human secretin analog (1-27 amide: HSDGTFTSELSRLREE*ARLK*RLLQGLV-amide; modified secretin) (Dong et al., 2011) that contains a lactam bridge between side chains of Glu16 and Lys20 were synthesized by solid-phase peptide synthesis using established chemical protocols. After cleavage from the solid support and purification using reversed-phase chromatography, the lyophilized powders as trifluoroacetate salts were formulated in aqueous buffer.

Diet-induced obese (DIO) male C57BL6/N mice (Taconic Biosciences, Cambridge City, IN) 30 to 31 weeks old, maintained on a calorie rich diet since arrival at Lilly (TD95217; Teklad, Madison, WI), were used in the study. Mice were individually housed in a temperature-controlled (24°C) facility with 12 hour light/dark cycle (lights on 2200) and free access to food (TD95217) and water. After a minimum of 2 weeks acclimation to the facility, the mice were randomized according to their body weight, so each experimental group of animals would have similar body weight. The body weights ranged from 46 to 54 g. Vehicle (20 mM Citrate at pH 5.5), native secretin (166 nmol/kg/day) or modified secretin (163 nmol/kg/day) dissolved in vehicle was administered by subcutaneous (SC) mini-osmotic pump (Alzet, Model 2002; Durect Corporation, Cupertino, CA) as a SC infusion (12 μl/mouse/day) to *ad libitum* fed DIO mice throughout the study period. Body weight and food intake were monitored daily. Absolute changes in body weight were

Please cite this article in press as: Li et al., Secretin-Activated Brown Fat Mediates Prandial Thermogenesis to Induce Satiation, Cell (2018), https://doi.org/10.1016/j.cell.2018.10.016

Cell

calculated by subtracting the body weight of the same animal on the first day of the treatment. On Days 1 and 14, total fat mass and total water mass were measured by quantitative nuclear magnetic resonance (QNMR) using an Echo Medical System (Houston, TX) instrument. Fat-free mass was calculated as body weight – fat mass. For the thermoneutral experiment, mice were acclimatized to 30°C one week before the experiment started. All other study conditions were kept, except the dosage. Native secretin was administered in a concentration of 996 nmol/kg/day and modified secretin of 326 nmol/kg/day. In addition to body weight and food intake, oxygen consumption was also measured.

Dual luciferase reporter assay

Blocking potential of the anti-secretin-antibody was determined by measuring secretin receptor activation in response to variable ratios of secretin and anti-secretin antibody. Secretin receptor activity was quantified using a dual luciferase reporter system based on cAMP response element (CRE) driven firefly luciferase (CRE-PLuc; *Photinus pyralis*) and constitutive Renilla luciferase (RLuc; *Renilla reniformis*). HEK293 cells were transiently transfected with CRE-PLuc, RLuc, and Sctr. Secretin receptor activity was quantified as the ratio of bioluminescence of firefly (PLuc) and renilla (RLuc) luciferase.

QUANTIFICATION AND STATISTICAL ANALYSIS

Two-tailed Student's t tests were used for single comparisons and analysis of variance (ANOVA) with Tukey's post hoc tests for multiple comparisons. PET/CT analysis was analyzed using paired one-tailed t test. P values below 0.05 were considered significant. Statistical analysis was performed with GraphPad prism 6 software. All data are represented as mean ± SD.

All linear mixed effect models were calculated with the *fitlme* function of MATLAB R2016b (Mathworks). Specifically, cumulative food intake was analyzed by means of linear mixed effect models with the fixed effects 'time' and 'treatment group', their interaction, and 'individual' as random effect. Additionally, we applied a more sophisticated model to specifically detect an effect of secretin on metabolic rate from cumulative food intake data by including the additional random factors 'initial body mass' (to capture the metabolic requirements of the mouse) and 'overall change in body mass' (to capture the alternate fate of food, i.e., fat deposition/loss).

DATA AND SOFWARE AVAILABILITY

The accession number for the RNA-Seq data presented in this article is GEO: GSE119452.

Cell

Supplemental Figures

Figure S1. BioGPS Data for *Sctr* Expression in 96 Mouse Tissues and Purified Mouse Cell Population, Related to Figure 1

Sctr (secretin receptor) expression data were retrieved from the BioGPS database (http://biogps.org/#goto=genereport&id=319229) and expressed as fold over the median (M). *Sctr* is most abundant in neuroblastoma cell line (Neuro2a), followed by brown adipose tissue, placenta and stomach.

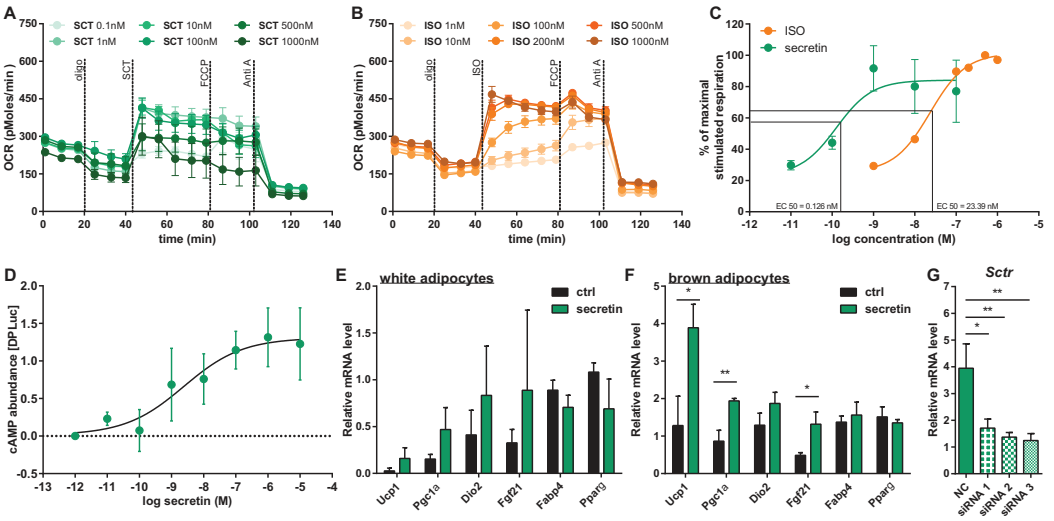

Figure S2. Effects of Secretin on Both Thermogenic Activity and Capacity in Primary Brown and White Adipocytes, Related to Figure 2

(A-C) Microplate-based respirometry of primary brown adipocytes according to the following protocol. After assessment of basal oxygen consumption oligo (oligomycin) was injected to determine basal leak respiration. Next, different doses of either ISO (isoproterenol, 1nM–1μM) or SCT (secretin, 0.1nM–1μM) were added to stimulate UCP1-mediated uncoupled respiration. By adding of FCCP maximal leak respiration was determined. Lastly, non-mitochondrial oxygen consumption was assessed by injecting Anti A (antimycin A). Representative time-course of oxygen consumption rates (OCR) of primary brown adipocytes stimulated with different doses of either (A) secretin (n = 3) or (B) ISO (n = 1). (C) EC_{50} values of secretin and ISO in stimulating the maximal UCP1-mediated uncoupled respiration. The maximal stimulated respiration was calculated as fold change over basal leak and was set to 100%. (D) Cytosolic cAMP abundance after stimulation with increasing secretin concentrations for 30 min (n = 3) inprimary brown adipocytes. (E+F) Effect of secretin (6h) on the expression of thermogenic genes in primary adipocytes derived from interscapular brown (E) and inguinal white (F) adipose tissue determined by qRT-PCR (n = 3). *Pgc1α*: Peroxisome proliferator-activated receptor γ coactivator 1α; *Dio-2*: Deiodinase, Iodothyronine Type II; Fgf21: Fibroblast growth factor 21; *Fabp4*: Fatty acid binding protein 4; *Pparγ*: Peroxisome proliferator-activated receptor γ. (G) Relative mRNA expression of *Sctr* (secretin receptor) normalized to *Gtf2b* (General transcription factor IIb) in primary brown adipocytes reverse transfected with either small interfering RNAs (siRNA) targeting *Sctr* or nontargeting controls (NC), respectively. Reverse transfection was performed at day 5 of differentiation (n = 3). Analysis was performed at day 8 of differentiation. Data are presented as mean ± SD (E+F+G) Statistical analysis was conducted using unpaired t test. *p < 0.05; **p < 0.01, compared with the control group.

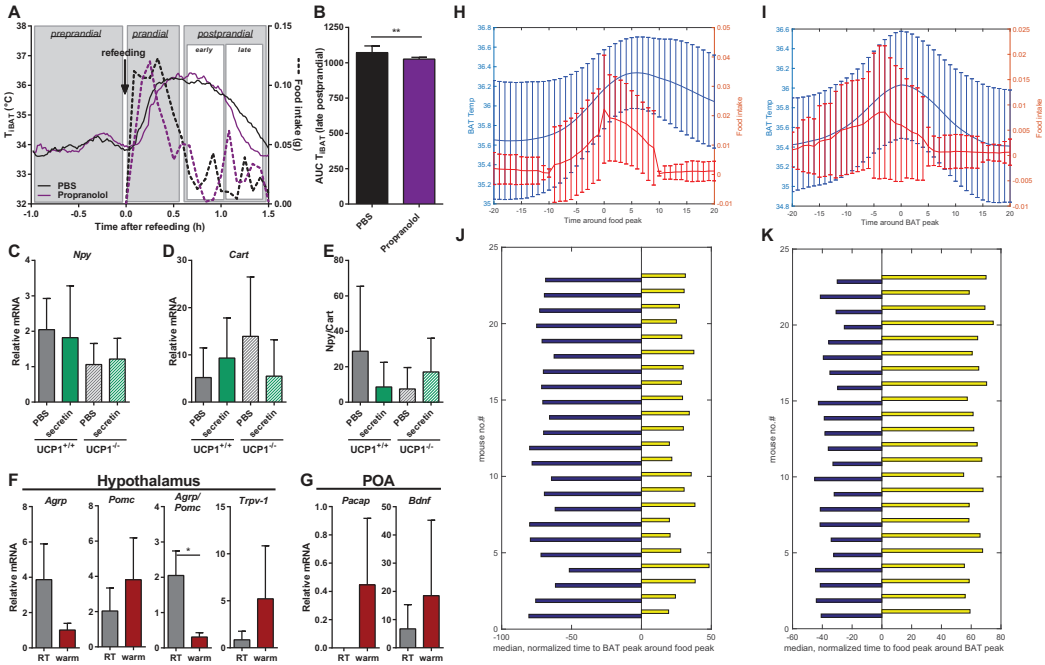

Figure S3. The Close Relationship between Food Intake and Thermogenesis as Evidenced by Hypothalamic Gene Expression and Food Intake Events Analyses, Related to Figure 3

(A+B) Three main different phases of single meal-associated thermogenesis: prepandial, prandial and postprandial (early and late) thermogenesis. Propranolol only decreased the late postprandial thermogenesis. (A) Mean iBAT temperature in response to refeeding after propranolol or PBS pre-treatment (20mins before refeeding). (B) The late postprandial thermogenesis was reduced in response to propranolol pre-treatment, as quantified as area under the curve (AUC) of iBAT temperature. (C-G) Anorexigenic and orexigenic hypothalamic gene expression was regulated by both secretin treatment and short exposure to ambient temperature above thermoneutrality. Relative mRNA level of *Npy* (neuropeptide y) (C) and *Cart* (cocaine and amphetamine regulated transcript) (D) in hypothalamus of fasted UCP1$^{+/+}$ and UCP1$^{-/-}$ mice in response to a single i.p. injection of PBS or secretin (4h) normalized to transcription factor Gtf2b. (E) Ratio of *Npy* and *Cart* expression. (F+G) Fasted mice (18h) were placed into a climate chamber and temperature was gradually increased from 34 to 37°C over 4 h and gene expression was analyzed in hypothalamus (F) and preoptic region (G). *Agrp* (agouti-related peptide), *Pomc* (pro-opiomelanocortin), *Trpv-1* (transient receptor potential cation channel subfamily V member 1), *Pacap* (pituitary adenylate cyclase-activating peptide), *Bdnf* (brain-derived neurotrophic factor). Ratio of *Agrp*/*Pomc* .

(H-K) Relationship between feeding behavior and brown fat thermogenesis during *ad libitum* feeding. In total, we detected 1919 feeding events and 1706 bouts of BAT activity during 70h of continuously monitoring food intake by automatic manger scales and recording iBAT temperature by implanted telemetry sensors on 23 mice in a 1-minute bins resolution. Feeding event and iBAT activity bout were defined based on a peak in the mean of ten consecutive minutes. (H) Mean food intake (red) and iBAT temperature (blue) during 20 minutes preceding and 20 minutes following a feeding event. The initiation of feeding is always accompanied by a rise in iBAT temperature. iBAT temperature reached its maximum approx. 5 minutes after the food intake peak. (I) Mean food intake (red) and iBAT temperature (blue) during 20 minutes preceding and 20 minutes following a BAT activity bout. Peaks in iBAT temperature are associated with a preceding feeding event peaking approx. 5 minutes earlier. (J) In every single mouse of 23 in total, during feeding events, the time span for iBAT temperature to reach a peak after the food peak (yellow bars) was generally shorter compared to the time span before the food peak (blue bars). Bars represent median time spans normalized to individual peak frequency (arbitrary units). This data indicated that a rise in iBAT temperature was plausibly the consequence of food intake. (K) In every single mouse, during BAT activity bouts, the time span preceding the BAT temperature peak to a food intake peak (blue bars) was generally shorter than time span after the BAT temperature peak to the next food peak (yellow bars). Bars represent median time spans normalized to individual peak frequency (arbitrary units).This data indicated that a rise in iBAT temperature could have caused the termination of feeding.

Cell

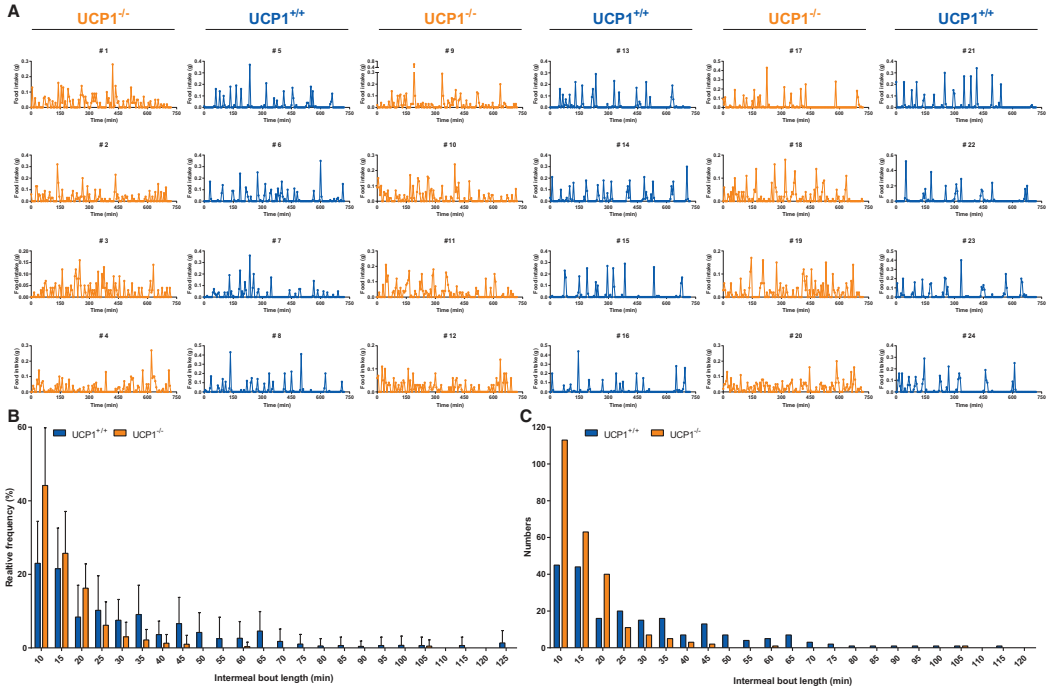

Figure S4. Altered Feeding Patterns in UCP1-KO Mice, Related to Figure 3

Food intake (FI) was recorded in 12 individually housed UCP1$^{+/+}$ (blue) and 12 UCP1$^{-/-}$ (orange) mice (129S1/SvImJ) using an automated monitoring system (TSE LabMaster Home Cage Activity, Bad Homburg, Germany) during one dark phase after acclimatization period of three days. The food baskets were connected to high precision balances to record FI in 5-min bins. (A) Individual eeding over 12 hours during dark phase. (B) Relative distribution frequency of intermeal bout length of UCP1$^{+/+}$ (blue) and UCP1$^{-/-}$ (orange) mice during one dark phase. (C) Numbers of variant intermeal bout length during one dark phase of UCP1$^{+/+}$ (blue) and UCP1$^{-/-}$ (orange) mice. Data are presented as mean ± SD (n = 12).

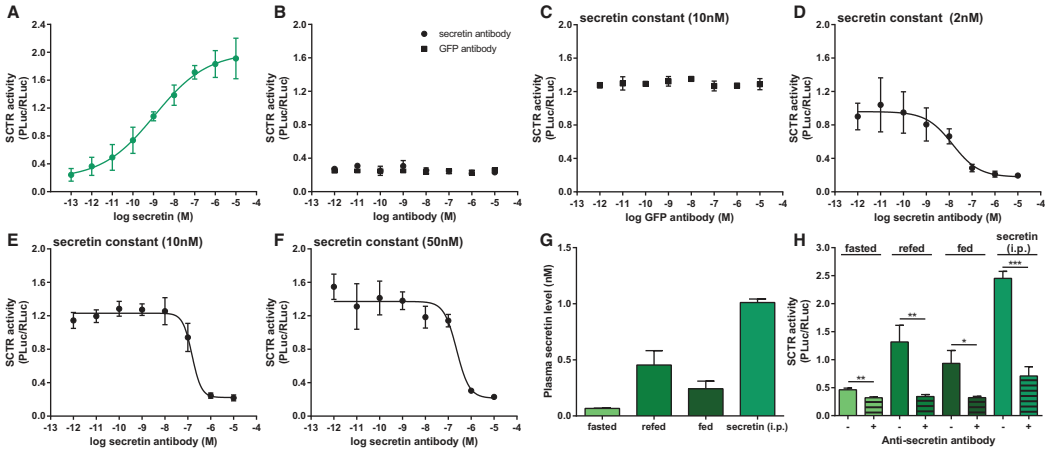

Figure S5. Anti-secretin Antibody Is Capable of Completely Inhibiting Secretin Activity *In Vitro*, Related to Figure 4

The blocking efficiency of anti-secretin antibody on secretin activity was characterized using HEK293 cells expressing triple vectors (SCTR, CRE-PLuc and RLuc). (A) Secretin increased SCTR activity in a dose-dependent manner as reflected by cAMP response element (CRE)-mediated luciferase activity. (B) Increasing concentrations of secretin- or GFP- (green-fluorescent protein) antibody had no effect on SCTR activity. (C) Increasing concentrations of GFP-antibody had no impact on secretin (10nM)-induced SCTR activity. (D–F) Increasing concentrations of secretin-antibody were capable to inhibit secretin-stimulated SCTR activity. A concentration ratio of 100 (antibody/secretin) was able to neutralize secretin activity in stimulating SCTR-cAMP pathway. (G) Secretin concentration was quantified in plasma from mice either fasted, 1h refed after fasting, fed *ad libitum* or 30 min after intraperitoneal injection of 5 nmol secretin based on their capacities in stimulating SCTR activity according to the standard curve in panel A. (H) 30 min incubation with secretin-antibody (630nM) was sufficient to completely inhibit plasma secretin activity. Data was analyzed by paired t test. Data are presented as mean ± SD (n = 3). ** = $p < 0.01$, *** = $p < 0.001$.

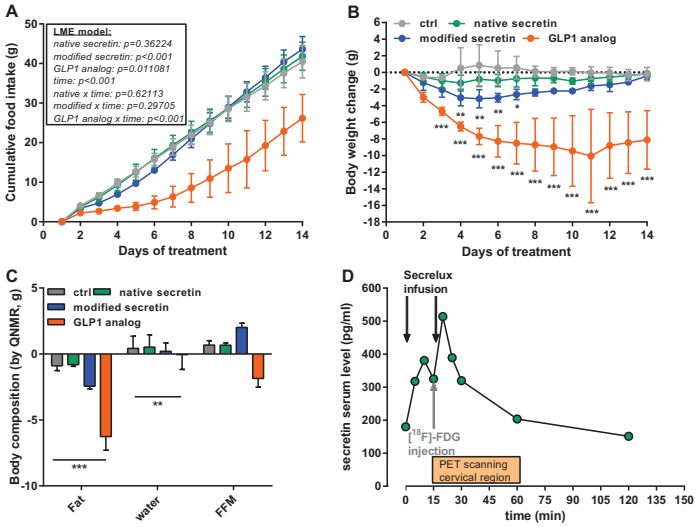

Figure S6. Chronic Infusion of Modified Secretin Transiently Slightly Decreases Food Intake and Body Weight in Diet-Induced Obese Mice at Room Temperature, Related to Figures 5 and 6

(A-C) Vehicle (20mM Citrate), native secretin (166 nmol/kg/day), modified secretin (163 nmol/kg/day) or GLP1 analog (CEX51, 30 nmol/kg/day) dissolved in vehicle was administered by subcutaneous (s.c.) miniosmotic pumps as a s.c. infusion (12µl/mouse/day) to *ad libitum* fed diet-induced obese (DIO) male C57BL6/N mice throughout the study period (n = 6). Mice were kept at room temperature. (A) Food intake and (B) body weight were monitored daily. Absolute changes in body weight were calculated by subtracting the body weight of the same animal on the first day of treatment. (C) On day 1 and 14, total fat mass and total water mass were measured by quantitative nuclear magnetic resonance (QNMR). Fat-free mass was calculated as body weight minus fat mass. (D) Two-bolus Secrelux infusion increases serum secretin level in humans. Representative time course of serum secretin level after two-bolus Secrelux infusion (0 min and 15 min). The second Secrelux bolus was administered right after [^{18}F]-FDG injection. Subsequently, PET scanning of the cervical region was initiated and glucose uptake was measured for approximately 40 min. (A) was analyzed by linear mixed effects model with fixed effects "treatment," "time" and interaction between both and with random factor "individual." (B) was analyzed by two-way ANOVA RM (Tukey's test). (C) was analyzed by one-way ANOVA (Tukey's test). * = $p < 0.05$; ** = $p < 0.01$, *** = $p < 0.001$.

6.2 LETTERS OF APPROVAL

6.2.1 Letter of approval – Journal of Experimental Biology, 2018 March

Permission Request

permissions <permissions@biologists.com>
Mi 20.03, 09:20
Schnabl, Katharina; permissions <permissions@biologists.com>

Allen antworten

Dear Katharina,

Thank you for your request. Permission is granted for the use that you describe.

To continue to build data on the use of your paper it is important to drive users back to the journal website. So whilst we do not object to your paper being placed in a repository, the acknowledgement should state "reproduced/ adapted with permission" and give the source journal name - the acknowledgement should either provide full citation details or refer to the relevant citation in the article reference list - the full citation details should include authors, journal, year, volume, issue and page citation.

Where appearing online or in other electronic media, a link should be provided to the original article (e.g. via DOI). Your article DOI is https://doi.org/10.1242/jeb.165381

Journal of Experimental Biology: http://www.biologists.com/journal-of-experimental-biology

We wish you the best of luck with your dissertation.

Kind regards

Richard

Richard Grove
Commercial Manager
The Company of Biologists Ltd
Bidder Building, Station Road, Histon, Cambridge, CB24 9LF, UK
T: +44 (0) 1223 632 850 | richard.grove@biologists.com | www.biologists.com

6.2.2 Letter of approval – Frontiers in Physiology, 2019 January

Permission request

Frontiers Editorial Office <editorial.office@frontiersin.org>
Di 19.03, 17:40
Schnabl, Katharina

Allen antworten

Dear Mr Schnabl,

Thank you for your email.

Under the Frontiers Terms and Conditions, authors retain the copyright to their work. Furthermore, all Frontiers articles are Open Access and distributed under the terms of the Creative Commons Attribution License (CC-BY 3,0), which permits the use, distribution and reproduction of material from published articles, provided the original authors and source are credited, and subject to any copyright notices concerning any third-party content.

You can therefore freely reuse this article published at Frontiers as part of your thesis without having to ask for permission. More information about CC-BY can be found here: http://creativecommons.org/licenses/by/4.0/

Best regards,

Gearóid

Senior Manager, Research Integrity: Gearóid Ó Faoleán, PhD

Frontiers

www.frontiersin.org
Avenue du Tribunal-Fédéral 34
1005 Lausanne, Switzerland

6.2.3 Letter of approval – Cell, 2018 November

Permission Request

Lingayath, Roopa (ELS-CHN) <r.lingayath@elsevier.com>
Do 04.04, 09:33
Schnabl, Katharina

Allen antworten

Dear Katharina Schnabl,

You retain the right to submit your article in electronic format, and formal permission is not required to reuse your article in your thesis.

You are permitted to post this Elsevier article online if it is embedded within your thesis. You are also permitted to post your Author Accepted Manuscript online. However, posting of the final published article separately from your thesis is prohibited.

Please refer to Elsevier's Sharing Policy for further information:
https://www.elsevier.com/about/our-business/policies/sharing

Let me know if you have any questions.

Thanks & Regards,
Roopa Lingayath
Sr Copyrights Coordinator – Global Rights
Elsevier | Health Content Operations
(A division of Reed Elsevier India Pvt. Ltd.)

International Tech Park | Crest – 5th Floor | CSIR Road | Taramani | Chennai 600 113 | India
Tel: +91 44 3378 4167 | Fax: +91 44 4299 4568
E-mail: r.lingayath@elsevier.com | url: www.elsevier.com

6.3 KEY RESOURCES TABLE

REAGENT or RESOURCE	SOURCE	IDENTIFIER
Antibodies		
anti-Secretin	Phoenix Pharmaceuticals	Cat# G-067-04
anti-UCP1	Custom made	N/A
anti-GFP	Thermofischer	Cat# A-11122
anti-ACTIN	Millipore	Cat# MAB1501
anti-SCTR	Sigma-Aldrich	Cat# HPA007269-100UL
IRDye 800CW Goat Anti-Rabbit	Li-Cor	Cat# 926-32211
IRDye 680CW Donkey Anti-Mouse	Li-Cor	Cat# 926-68072
Bacterial and Virus Strains		
NEB5α competent E. coli	NEB	Cat# C2988J
Chemicals, Peptides, and Recombinant Proteins		
100 bp-DNA Ladder	Carl Roth	Cat# T833
1k bp-DNA Ladder	Carl Roth	Cat# Y014
Aceton	Carl Roth	Cat# 9372
ACTH (1-39) trifluoroacetate salt	Bachem	Cat# H-4998
ACTH (4-10)	Abcam	Cat# ab142255
Antimycin A	Sigma-Aldrich	Cat# A8674
Arterenol	Sanofi	1mg/ml
Atglistatin	Gift from Robert Zimmermann (*University of Graz)*	N/A
Bocine serum albumin (BSA) fraction V	Carl Roth	Cat# 8076
Bovine serum albumin (BSA) Fatty Acid Free	Sigma-Aldrich	Cat# A3803-100G
Chloroform p.a.	Carl Roth	Cat# Y015.1
Collagenase A	Biochrom	Cat# C 1-22
Dexamethasone	Sigma-Aldrich	Cat# D4902
DMEM	Sigma-Aldrich	Cat# D5796
DMSO	Carl Roth	Cat# 4720
Ethanol 70%, denatured	Carl Roth	Cat# T913
Ethanol 96%, denatured	Carl Roth	Cat# T171
Ethanol 99.8% p.a.	Carl Roth	Cat# 9065
FCCP	Sigma-Aldrich	Cat# C2920-10MG
Fetal bovine serum (FBS)	Biochrom	Cat# S0615
Fungizone (Amphotericin B)	Biochrom	Cat# A2612
Gentamycin	Biochrom	Cat# A2712
GLP1 analog (CEX51)	Eli Lilly and Company	N/A
Glucose	Biochrom	Cat# HN06
Glutamax	Life Technologies	Cat# 35050-061
GPS1573	Abbiotech	Cat# 350595
H89 dihydrochloride	Tocris	Cat# No.2910
Hank's balanced salt solution (HBSS) w/Mg;Ca	Invitrogen	Cat# 14025-050

Hi 76-0079	Gift from Robert Zimmermann (*University of Graz)*	N/A
Human secretin	Eli Lilly and Company	N/A
Indomethacin	Sigma-Aldrich	Cat# I7378
Insulin	Sigma-Aldrich	Cat# I9278-5ML
Isobutylmethylxanthine	Sigma-Aldrich	Cat# I5879
Isoproterenol	Sigma-Aldrich	Cat# I6504-100MG
Modified human secretin analog	Eli Lilly and Company	N/A
Nitrocellulose	Li-Cor	Cat# 926-31092
Nuclease-free water	Qiagen	Cat# 129114
Oligomycin	Sigma-Aldrich	Cat# O4876-5mg
Penecillin/Strptomycin	Biochrom	Cat# A2212
Phosphate Buffered Saline (PBS) Tablets	Gibco	Cat# 18912-014
Propranolol hydrochlorid	Sigma-Aldrich	Cat# P8688
Secretin	Tocris	Cat# No.1919
SensiMix SYBR no Rox	BioLine	Cat# QT650-20
Sodium chloride	Carl Roth	Cat# 3957
Sodium pyruvate solution 100 mM	Gibco	Cat# 11360-070
synthetic ACTH (4-10)	JPT Peptide Technologies GmbH	synthesized peptide
T3	Sigma-Aldrich	Cat# T6397
TEMED	Carl Roth	Cat# 2367
TRISure	Bioline	Cat# BIO-38033
XF calibrant buffer	Agilent technologies	Cat# 100840-000
Critical Commercial Assays		
SV Total RNA Isolation System	Promega	Cat# Z3105
Pierce BCA Protein Assay Kit	Pierce	Cat# PI-23225
SensiFast cDNA Synthesis Kit	BioLine	Cat# BIO-65054
SensiMix Sybr no Rox	BioLine	Cat# QT650-20
Secretin ELISA kit	Cloud-clone	Cat# CEB075Mu, CEB075Hu
Dual luciferase reporter assay	Promega	Cat# E1960
Seahorse XF96 fluxPak	Agilent	Cat# 102310-001
TruSeq Stranded Total RNA Library Prep Kit	Illumina	Cat# RS-122-2102
Deposited Data		
Brown fat RNA-seq data	This study	GEO: GSE119452, GSM3374837, GSM3374838, GSM3374839, GSM3374840
Experimental Models: Cell Lines		
HEK293	DSMZ	Cat# ACC 305
Primary murine brown and white cells	This study	N/A
Experimental Models: Organisms/Strains		
Mouse: C57BL/6J	Jackson Laboratory	JAX Stock No:000664
Mouse: 129S-Ucp1^{tm1Kz}/J	Jackson Laboratory	JAX Stock No:017476

Mouse: 129S6/SvEVTac		Taconic Biosciences	129SVE
Mouse: C57BL/6NTac-Ucp1tm3588 *(LUC-T2A-iRFP713-T2A-Ucp1)Arte*		Taconic Biosciences	N/A
Mouse: Athymic Nude-Foxn1^{nu}		Envigo	Athymic Nude-*Foxn1^{nu}*
Oligonucleotides			
siRNA targeting sequence: SctR #1: CCUGCUGAUCCCUCUCUUU			Eurofins Genomics
siRNA targeting sequence: SctR #2: CCCUGUCCAACUUCAUCAA			Eurofins Genomics
siRNA targeting sequence: SctR #3: CCAUCGUGAUCAAUUUCAU			Eurofins Genomics
Ucp1	forward	5'-GTACACCAAGGAAGGACCGA-3'	Eurofins Genomics
	reverse	5'-TTTATTCGTGGTCTCCCAGC-3'	Eurofins Genomics
Sctr	forward	5'-ATGCACCTGTTTGTGTCCTT-3'	Eurofins Genomics
	reverse	5'-TAGTTGGCCATGATGCAGTA-3'	Eurofins Genomics
Gtf2b	forward	5'-TGGAGATTTGTCCACCATGA-3'	Eurofins Genomics
	reverse	5'-GAATTGCCAAACTCATCAAAACT-3'	Eurofins Genomics
Pref1	forward	5'-AGTACGAATGCTCCTGCACAC-3'	Eurofins Genomics
	reverse	5'-CTGGCCCTCATCATCCAC-3'	Eurofins Genomics
Fgf21	forward	5'-AGATCAGGGAGGATGGAACA-3'	Eurofins Genomics
	reverse	5'-TCAAAGTGAGGCGATCCATA-3'	Eurofins Genomics
Fabp4	forward	5'-GATGGTGACAAGCTGGTGGT-3'	Eurofins Genomics
	reverse	5'-TTTATTTAATCAACATAACCATATCCA-3'	Eurofins Genomics
Pgc1α	forward	5'-GGACGGAAGCAATTTTTCAA-3'	Eurofins Genomics
	reverse	5'-GAGTCTTGGGAAAGGACACG-3'	Eurofins Genomics
Dio2	forward	5'-TGTCTGGAACAGCTTCCTCC-3'	Eurofins Genomics
	reverse	5'-AGTGAAAGGTGGTCAGGTGG-3'	Eurofins Genomics
Pparγ	forward	5'-TCAGCTCTGTGGACCTCTCC-3'	Eurofins Genomics
	reverse	5'-ACCCTTGCATCCTTCACAAG-3'	Eurofins Genomics
Agrp	forward	5'-GTCTAAGTCTGAATGGCCTCAAG-3'	Eurofins Genomics
	reverse	5'-CATCCATTGGCTAGGTGCGAC-3'	Eurofins Genomics
Pomc	forward	5'-CCCTCCTGCTTCAGACCTC-3'	Eurofins Genomics
	reverse	5'-CGTTGCCAGGAAACACGG-3'	Eurofins Genomics
Npy	forward	5'-CTGACCCTCGCTCTATCTCTGC-3'	Eurofins Genomics
	reverse	5'-CCATCACCACATGGAAGGGTCT-3'	Eurofins Genomics
Cart	forward	5'-CGAGCCCTGGACATCTACTCTG-3'	Eurofins Genomics
	reverse	5'-TCTTTGCACACACACCAACACC-3'	Eurofins Genomics
Bdnf	forward	5'-TGGTATGACTGTGCATCCCAGG-3'	Eurofins Genomics
	reverse	5'-TCACCCGGGAAGTGTACAAGTC-3'	Eurofins Genomics
Pacap	forward	5'-ACCAATGACCATGTGTAGCGGA-3'	Eurofins Genomics
	reverse	5'-CCATTTGTTTTCGGTAGCGGCT-3'	Eurofins Genomics
Trpv-1	forward	5'-ATCTTCACCACGGCTGCTTACT-3'	Eurofins Genomics
	reverse	5'-TCCTTGCGATGGCTGAAGTACA-3'	Eurofins Genomics
Recombinant DNA			
pCMV-murine SCTR expressing vector		Gift from Professor B.K.C. Chow (*University of Hong Kong*)	N/A
pAD-CRE luciferase reporter vector		This study	N/A
phRG-B-Renilla luciferase vector		Promega	Cat# E6281

Software and Algorithms		
GraphPad Prism 6	Graphpad Software	N/A
Genomatix Software Suite	Genomatix AG	N/A
MATLAB	Mathsworks	N/A
Equipment, devices and disposables		
Cell strainer, 40 µM	BD Biosciences	Cat# 352340
ER4000 Energizer/Receiver	Starr Life Sciences	20'' x 10'' x 2.5''
Falcon tube (10 ml)	Sarstedt	Cat# 62.547.254
Falcon tube (15 ml)	Sarstedt	Cat# 62.554.502
Climate cabinet	Feutron	TPK600
Climate cabinet	Memmert	HPP750life
FoxBox	Sable Systems	N/A
G2 E-Mitter	Starr Life Sciences	15.5 mm x 6.5 mm
Infinite M200 Microplate reader	Tecan	Cat# 30016056
LI-COR Odyssey Infrared Imaging System	Li-Cor	Ody-2197
Lightcycler 480 (384 well)	Roche	5015243001
Matix Electronic 384 Equalizer Pipette	Thermo Scientific	Cat# 2139-11
Micro 96 well plate nunc	VWR	Cat# 260895
Microvettes coated with lithium heparin	Sarstedt	Cat# 16.443
MSOT imaging system inVision 256-TF	iThera Medical GmbH	N/A
neoVortex® Vortex Mixer	neoLAB®	Cat# D-6012
Nitrocellulose membrane	Li-Cor	Cat# 926-31092
Nylon Mesh	Schwegmann Filtrationstechnik	250 µm
PCR tubes	Sarstedt	Cat# 72.991.992
Pipette tips (0.5-10, 10-100, 100-1000 µl)	Sarstedt	Cat# 70.1130, 70.760.002, 70.762
Precise shaking incubator	WiseCube®WIS-20	N/A
Thermomixer comfort	Eppendorf	Cat# 926-31092
Trans-Blot SD Semi-Dry Transfer Cell	BioRad	170-3940
TSE LabMaster System	TSE Systems	N/A
Tubes (1.5 ml, 2 ml)	Sarstedt	Cat# 72.690.001, 72.691
XF96 Extracellular Flux Analyzer	Agilent	N/A

6.4 RESPIROMETRY PROTOCOL

The following table was used to program the Mix, Wait, Measure and Injection protocol.

Protocol for UCP1 activity
1 - Calibrate probes
2 - Equilibrate 12 min*
3 - Loop 3 times **4** - (1-2-3)Mix 2min **5** - Time Delay of 2 min **6** - (1-2-3)Measure 3 min
7 - Loop end
8 - Inject A (20µl) - *oligomycin*
9 - Loop 3 times **10** - (4-5-6)Mix 2min **11** - Time Delay of 2 min **12** - (4-5-6)Measure 3 min
13 - Loop end
14 - Inject B (22µl) – *effector of interest*
15 - Loop 5 times **16** - (7-8-9-10-11) Mix 2min **17** - Time Delay of 2 min **18** - (7-8-9-10-11) Measure 3 min
19 - Loop end
20 - Inject C (24µl) - *FCCP*
21 - Loop 3 times **22** - (12-13-14)Mix 2min **23** - Time Delay of 2 min **24** - (12-13-14)Measure 3 min
25 - Loop end
26 - Inject D (26µl) – *antimycin A*
27 - Loop 3 times **28** - (15-16-17)Mix 2min **29** - Time Delay of 2 min **30** - (15-16-17)Measure 3 min
31 - Loop end
32 - Program end
*Default Equilibrate command consists of 2 min Mix, 2 min Wait repeated 3X.

7 ACKNOWLEDGMENT

At this point, I would like to thank all those who made it possible to carry out and complete this work on a scientific and personal level.

My first and greatest **Thank You** goes to my doctoral supervisor Martin Klingenspor. I thank you for your trust, your support and your numerous ideas, constructive suggestions and thought-provoking impulses, which have contributed to the success of this work. **Thank You** for your continuous support and encouragement.

A very big **Thank You** goes to Yongguo, who has been and continues to be an unprecedented source of ideas for my projects. **Thank You** for the productive and successful team work, I still have a lot to learn from you. I would also like to thank Tobi for answering every single question. Whether on a scientific or personal level, you have always been a great help to me. And of course a big **Thank You** to Flo. From the beginning you believed in me, supported me and were the best mentor I could have wished for. I hope it will stay that way even after my PhD. **Thank You** Theresa, you gave me the self-confidence I needed to start this PhD. Through my master thesis with you, I discovered my joy for research.

Of course, I would like to thank all my colleagues in the lab with whom I have worked over the years. **Thank You** for the pleasant working atmosphere and the great willingness to help. It's great to have colleagues who build you up in times of frustration and who celebrate with you in times of success. At this point I want to explicitly mention Andrea and Sebastian, who have always volunteered to help me to solve various problems and supported me a lot during last-minute editing. I especially want to say **Thank You** to our technicians Sabine, Samira and Anika, not only for their technical assistance, but also for their efforts in keeping the lab running.

Special thanks go to all our collaboration partners. Sanna (Turku Finland), it is a pleasure to work with you and Tamer (Eli Lilly), we share the passion for Secretin. **Thank You** Monja and Josefine for the MSOT measurements. These collaborations have contributed enormously to the success of this work.

Furthermore, I would also like to acknowledge the German Research Foundation (DFG) and the Else-Kröner-Fresenius Foundation for the financing of this work and various conference visits.

Furthermore I would like to thank my examination committee, Prof. Harald Luksch as chairman and Prof. Martin Klingenspor as well as Prof. Hannelore Daniel as examiners.

Last but not least, I would like to thank my family for their support and unlimited trust. Even though it was not always easy for you to understand what I do, you never doubted that I would find my way. That gave me a lot of strength. With all my heart, a great **Thank You** to my husband Christof! **Thank You** for your support, your backing, your feedback on scientific and personal issues and your tremendous interest in my work. It really means a lot to me. Finally, I would like to thank all my friends who provided the necessary distraction.

Thank You!